MORPHOMETRY OF HUMAN LUNG WITH PHYSIOLOGICAL CORRELATIONS

ALEXANDER McLEAN

Ph.D.
University of Edinburgh
1987

DECLARATION

The composition of this thesis and the investigations described were designed and performed by the author except where otherwise acknowledged.

ACKNOWLEDGEMENTS

During my time in the Department of Pathology I have received both friendship and assistance from many of my colleagues. Unfortunately, I am unable to acknowledge everyone individually. Nevertheless, I am grateful to them.

I would like to register my particular appreciation to the following people.

Firstly to Dr David Lamb. This thesis is indebted to his considerable knowledge and experience in the fields of pulmonary pathology and research.

Being a clinico-pathological study I offer my thanks to Professor David Flenley and the rest of my respiratory colleagues. In particular I acknowledge their generosity in allowing me to use the respiratory and CT data and for their friendship, help and advice throughout this project.

I am also obliged to Professor Sir Alastair Currie and Professor Colin Bird for the opportunity to work in their department.

Numerous individuals of the technical staff have been of considerable help during this study. The following are acknowledged for their assistance in the preparation of histological material, Craig Walker, John Lauder, Ross Shepard, Alan Dishington and John Shiels.

On a personal basis I thank my wife Aileen for her patience and for sharing the burden of this thesis.

Last, but by no means least I am greatly indebted to Diane McGiffen for proof reading this thesis. Any errors which remain are mine and not hers.

Abstract

Resected lobes from patients having pre-operative pulmonary function tests were fixed by inflation with formal saline and cut into 1cm parasagittal slices. Randomly selected tissue, from the lateral two slices, was plastic embedded and sections prepared for microscopic analysis.

A semi-automatic image analysis system was used to quantitate bronchiolar calibre and shape and peribronchiolar attachment number, inter-alveolar attachment distance and the amount of macroscopic emphysema. An automatic image analyser (IBAS2) was used to measure alveolar surface area *per* unit volume (AWUV).

Measured bronchiolar calibre (minimum diameter and measured lumen area) was not related to patient height, lung volume, pulmonary function or other morphometric variables.

AWUV, mean inter-alveolar attachment distance, theoretical lumen area and bronchiolar shape were independent of patient size and lung volume, but were inter-related. A combination of low AWUV and loss of attachments profoundly affected bronchiolar shape. However, AWUV and alveolar attachment loss were not always in proportion and demonstrated different functional effects: AWUV affects carbon monoxide transfer factor whereas attachments affect the slope of phase III and forced expiratory volume with bronchiolar shape affecting closing volume.

Macroscopic emphysema did not accurately reflect the extent of alveolar wall loss as identified by AWUV and showed poor correlations with pulmonary

function tests.

Computerised axial tomography (CT scan) exhibited a strong correlation with AWUV and can be used to assess lung density in life.

TABLE OF CONTENTS

CHAPTER 1

INTRODUCTION

This thesis is concerned with detailed morphometry of the lung. As little is known of the detailed structure of the lung in relation to the pathological basis of pulmonary function accurate measurements were required of bronchioles and alveoli. The objective of the thesis was to investigate the interaction and association of these structures with each other and on the function of the lung.

The study is based on a group of patients who had peripheral tumours that could be surgically removed. Suitable patients underwent a battery of pulmonary function tests 48–72 hours prior to thoracotomy. Immediately after surgery the resected lung tissue was prepared for morphometric analysis. Structure *vs* structure and structure *vs* function analysis was carried out on the data obtained.

The introduction is subdivided into a number of sections. These deal with relevant aspects of lung structure, chronic airflow obstruction (concentrating primarily on emphysema), smoking and its consequences and lastly morphometry. The last of these is the largest section reflecting its importance in this thesis as recent technical and computing advances, especially in image analysis, have given rise to a number of new morphometric techniques. A major part of this study has entailed assessing the appropriateness and accuracy of established and new methodologies.

1.1. RELEVANT ASPECTS OF LUNG STRUCTURE

1.1.1. Position of the Lung

The lungs are situated within the thoracic cavity and are separated from one another by the contents of the mediastinum. They almost completely fill the pleural cavities and are lined by the visceral pleura which is separated from the parietal pleura by a thin film of fluid. This acts as a lubricant and allows the pleura to glide over one another during respiration and at the same time maintains their close association. Anatomically the base of both lungs rests on their respective halves of the diaphragm, while the apices extend up to the root of the neck.

1.1.2. Division of the Lung

The largest division of the lungs is that of the lobes which are demarcated by fissures of pulmonary pleura running up towards the hilum. The division of the lungs into lobes is dissimilar. The right lung is divided into three lobes (upper, middle and lower) whereas the left lung is divided into two lobes (upper and lower) and the lingula. The lingula is analagous to the right middle lobe but has an arrested development due to the position of the heart and the pericardium (Spencer 1985).

Each lobe is further subdivided into segments. Importantly, each segment is ventilated by its own segmental bronchus and therefore constitutes a discrete area of lung tissue. The right lung has ten segments, the left lung nine. The division of the lobes into segments is as follows: both upper lobes have three segments; the right middle lobe and the left lingula have two; the right lower lobe has five, but the left lower has only four, the lower medial

basal segment being absent in the left lung.

1.1.3. The Bronchial Tree

The bronchial tree is a highly complex structure exhibiting detailed and intricate inter- and intra-relationships between airway and alveolar branching, distribution and size, alterations in the latter being associated with chronic obstructive pulmonary disease. This complexity has rendered it a very difficult organ to study morphometricallly, both *in vivo* and *in vitro*.

Before studying the changes brought about by disease it is helpful to understand where possible the "normal" structure of the lung. For this reason, various aspects of lung structure are outlined below and their possible influence or role on airflow discussed.

1.1.3.1. Description of Airway Types

The bronchial tree consists of two types of conductive airway: the larger airways (bronchi), and the smaller airways (bronchioli). This study adopts Weibel's definition of an airway (Weibel 1963), that is a unit airway of the conductive and transitory airways begins at the bifurcation of its parent and stretches to the production of two conjugate branches.

Bronchi

Bronchi in general possess a lumen larger than two millimetres in diameter and are lined by a pseudostratified respiratory epithelium. Goblet cell frequency in these airways is relatively high. Seromucous glands are present within the wall as is cartilage which maintains the patency of the airway. The

cartilage, below the trachea, is arranged circumferentially and its content within the wall decreases with bronchial size. Smooth muscle is present, but constitutes a relatively thin layer.

Bronchioles

In contrast to bronchi, bronchioles have a lumen that is generally smaller than two millimetres in diameter. Their walls contain neither mucous glands nor cartilage, but smooth muscle reaches its maximum development. The epithelium of the last generation is cuboidal there being a gradual change from the epithelial type within the larger airways. Goblet cell frequency decreases with bronchial calibre while that of Clara cells increases (Lumsden *et al* 1984).

1.1.3.2. Organisation of the Bronchial Tree

Von Hayek (1960), Boyden (1949), Boyden *et al* (1946) and Boyden and Hartmann (1948) give a detailed description of the large airways and both note the great variability in division and presence of the major named bronchi. In general, the trachea gives rise to the two main bronchi. The left main bronchus is smaller, longer and deviates from the trachea at a greater angle than that of the right . The main bronchi further subdivide to produce the lobar (and lingular) bronchi which in turn branch, giving rise to segmental then subsegmental bronchi. The number of branches arising from each segmental bronchus varies from ten to twenty five (Cotes 1975).

Bronchi eventually give way to bronchioli –the number of divisions required varying from four to fourteen. An important difference between these two

airway types is that bronchioles, in lacking cartilage, rely much more on surrounding peribronchiolar alveolar attachments to maintain their cylindricality and patency (Dayman 1951).

The last purely conductive airways of the bronchial tree are the terminal bronchioles (TBs), which are also the last airways to be completely lined by a non-respiratory epithelium and a continuous layer of smooth muscle. Each terminal bronchiole supplies a discrete area of lung tissue known as the acinus. The acinus is defined as the "the respiratory unit of lung tissue in man" (Spencer 1985) as it is the smallest repeating structural unit.

The acinus contains both conductive and respiratory structures. Each terminal bronchiole gives rise to, on average, three orders of respiratory bronchioles (Brewer 1968 and Hansen *et al* 1975). These each supply two to three alveolar ducts, which in turn give rise to two or more air sacs. The vast majority of alveoli arise from alveolar ducts and air sacs.

Respiratory bronchioles (RBs) differ from the more proximal airways in that they have an incomplete muscle layer and alveoli in their walls. Unlike other airways RBs have two functions, gas transport and mixing, and gaseous exchange. For this reason they have often been labelled the respiratory zone of the lung (Horsfield 1978). The frequency of alveoli increases with both the generation of RB (Thurlbeck 1976) and distance from the terminal bronchiole (Brewer 1968 and Horsfield 1978).

Alveolar ducts are produced by progressive alveolation of the walls of RBs (Weibel 1963). Structurally, the walls are reduced to a fine meshwork of elastic and collagen, with a few single smooth muscle fibres. These components form the entrance of alveolar sacs, which have a similar structure to that of ducts

except that the resultant alveoli constitute the terminal end of the bronchial tree.

1.1.3.3. Branching Properties of Airways within the Bronchial Tree

Conductive Airways: Pathway Types

The system of branching within the bronchial tree is one of predominantly asymmetrical dichotomy (Horsfield and Cummings 1968). The degree of asymmetry is greatest in the larger airways from trachea to lobular bronchioli with branching approximating symmetrical dichotomy occuring below this down to the level of the most distal respiratory bronchioles (Parker *et al* 1971). The shape of the lung and position of the hilum has produced two distinct pathway types, axial and lateral. These pathway types exhibit important differences which are relevant to this project.

Lateral pathways supply areas of the lung close to the hilum (Bucher and Reid 1961) whereas axial pathways supply areas distal to it (Hayward and Reid 1952). The branching of axial pathways is much more prolific than that of lateral ones (Thurlbeck 1976 and Bucher and Reid 1961). In lateral pathways a terminal bronchiole can be reached after nine divisions from the trachea. As many as twenty seven are necessary in the longer axial pathways. In distance terms this is a range of approximately eight to twenty two centimetres (Horsfield and Cummings 1968).

Von Hayek (1960) and Weibel (1963) have both demonstrated that the angle at which a conjugate branch deviates from the parent airway is inversely proportional to the ratio of their sizes. To ventilate areas close to the hilum,

airways of lateral pathways always arise from considerably larger intrasegmantal bronchi (Horsfield and Cummings 1968). The angle at which they deviate from the parent bronchus is obviously large. This contrasts to the branching of axial pathways. In the latter there is little appreciable reduction in the calibre of conjugate branches and the angle at which they deviate from the parent airway is small.

After branching, lateral pathway airways always follow a reflex course turning through 180 degrees to supply areas of parenchyma proximal to the site of bifurcation (Horsfield and Cummings 1968). However, axial pathway airways follow a more direct route to the area of parenchyma they supply and run perpendicular to the pleura in the immediately subpleural region.

The distribution and size of acini within proximal areas of the lung are greatly affected by the position of large structures eg bronchi and vessels, located in this area. This means that the supplying non-respiratory bronchioles (NRBs) have an uneven distribution. Conversely, acini in the outer peripheral areas have an isotropic or regular distribution, especially so in the immediately subpleural regions where they reach their maximum density. NRBs are similarly more evenly distributed and at their maximum density in this location. Correspondingly there is an absence of large airways and other large lung structures.

Branching within the acinus

Although disagreeing on the nature of branching of RBs, both Parker *et al* (1971) and Schreider *et al* (1981) found branching within acini to be very irregular, comprising monopody, dichotomy and trichotomy, with the degree of

asymmetry being most pronounced in the production of alveolar sacs (Parker *et al* 1971 and Hansen *et al* 1975). This increase in asymmetry has been hypothesised by Parker and Hansen and Ampaya to be a "space filling" phenomenon. The angle of branching is similarly variable (Schreider *et al* 1981) with alveolar duct diameter and length gradually decreasing with each generation (Hansen and Ampaya 1975). The majority of sacs arise from the lateral, as opposed to the distal, aspect of alveolar ducts (Hansen *et al* 1975).

1.1.4. Summary and Consequences of Branching Patterns

1.1.4.1. Anatomical Influences on Branching Patterns

The anatomy of the lung, as discussed above, dictates that small airways must branch off larger bronchi to ventilate areas close to the hilum. This obviously accounts for at least some of the asymmetry of branching observed in the larger airways. The degree of asymmetry is such that with each generation the number of airways increases by a factor of 1.38 (Parker *et al* 1971) as opposed to a doubling with true symmetrical dichotomy.

1.1.4.2. Functional Influences on Branching Patterns

Parker *et al* (1971) hypothesised that the mode of branching changes from asymmetry to symmetry within bronchioles as the method of gas transport changes from convection to diffusion. This seems unlikely for a number of reasons. Firstly, convection persists down into the respiratory bronchioles. Secondly, in alveolar ducts and sacs, where diffusion is the sole method of gas transport, division is irregular (Wilson 1922, Schreider *et al* 1981, Hansen *et al* 1975 and Hansen and Ampaya 1975). Lastly, Spencer (1985) indicates that symmetrical dichotomy occurs within the conducting airways of animals with a

centrally located heart, thereby infering that lung anatomy is the major influence on branching patterns.

1.1.4.3. Functional Influences on Branching Ratios

The two main methods of gas transport within the lung are convection and diffusion. In general, convection occurs within the conducting airways and diffusion within the alveolar ducts and sacs. Convection transports gas far more rapidly than diffusion. The speed of flow within conducting airways decreases proportionately with their size. To compensate for this, airway length becomes progressively shorter and the branching ratio of daughter to parent airways decreases in a similar fashion, ie parent-daughter airways become increasingly similar in calibre (Wilson 1922, Horsfield and Cummings 1968 and Parker *et al* 1971). The less efficient process of diffusion is similarly compensated.

The overall effects of these factors is that as the velocity of gas transport steadily decreases it has, *per* airway generation, a smaller distance over which to travel compensated with a larger cross sectional area.

1.1.5. Summary Models of Branching

Weibel (1963) and Horsfield and Cummings (1968) have constructed models that summarise both branching patterns and ratios. Weibel's model (model A) is trumpet shaped in outline, reflecting the progressive increase in combined cross sectional area of airways similar in size with distance from the carina. This particular model of Weibel's is inappropriate as it assumes symmetrical dichotomy to be the normal branching type, but it does accurately reflect the compensatory increase in combined cross sectional area with decrease in rate

of flow.

Horsfield and Cummings' model is turnip shaped in outline and more accurately reflects the *in vivo* situation. From this model it can be seen that airways of similar size differ greatly in their distance from the carina.

The most important features of branching, some of which are illustrated in Horsfield and Cummings' composite model, are listed below:

- The number of airways increases with each division. This is affected by a change from asymmetrical to symmetrical dichotomy, thereby bringing about a proportionately greater increase in number at each division especially in the region of the smaller conducting airways.
- Conjugate branches become steadily more comparable in size to their parents in proportion with decrease in airway calibre.
- Airway length decreases in line with calibre. This is true of conducting airways (Weibel 1963 and Horsfield 1974) and respiratory airways (Weibel 1963 and Hansen and Ampaya 1975).
- Changes in length, branching patterns and ratios of airways compensate for the progressive decrease in flow (ie unit distance over unit time) by providing a greater area over which to act.
- Finally, the least efficient methods of gas transport have increasingly less distance over which to function ie convection on average operates over 25cm (trachea to acinus), molecular diffusion 2.6mm (proximal alveolar ducts to alveolar walls) and diffusion through tissue 1µm (alveolar-capillary membrane).

1.2. VARIATIONS IN LUNG STRUCTURES

A number of pulmonary structures and volumes vary with parameters such as age, sex and height. The influence of these is discussed below.

1.2.1. Variability Attributable to Stature

Tracheobronchial Dimensions

Numerous aspects of lung function -vital capacity, residual volume, and forced expiratory volume- all correlate with height (Cotes 1975). Such relationships of stature with airway calibre are less obvious and not well established. Jesseph and Merendino (1957) found no relationship between any tracheobronchial dimension and height or body weight. Green *et al* (1974), Knudson *et al* (1976) and Hanna *et al* (1985) suggest that airway size and lung volume are relatively independent or "dysanaptic". Mead (1980) found even greater independence between those two variables. All these latter studies (listwise from Green) assessed airway size indirectly assuming it to be proportion to $V_{max}50$.

The most convincing evidence that stature and airway calibre covary comes from Thurlbeck and Haines (1975) who found that the cross sectional area of major bronchi correlates with body length (r=0.54) and from Niewhoehner *et al* (1974), as quoted by Thurlbeck and Haines, who found summed bronchial dimensions and lung volume to be related. Although physiological studies have been unable to elucidate any relationships between tracheal and lower airway size (Osmanliev *et al* 1982), morphometrically Jesseph and Merendino (1957), Fraser (1961), Weibel (1963), Horsfield and Cummings (1968), and Thurlbeck and Haines (1975) have all shown a close association between the trachea and its proximal ramifications while Weibel (1963) Horsfield and Cummings (1968) and Hansen and Ampaya (1975) have shown an association between airway calibres throughout the lung. The last three studies although highly intricate are based on very small sample sizes.

In summary, evidence suggests that there is an association between airway dimensions within the lung, albeit non-linear or linear, if airways are subdivided into three zones (Horsfield and Cummings 1968). Furthermore, there is morphometric evidence that these dimensions, in the larger bronchi at least, relate to indices of body stature. Lastly, airway calibre may be genetically predetermined (Green *et al* 1974) with enviromental factors producing variable phenotypes.

1.2.1.1. Alveolar Number and Surface Area

Weibel (1963) originally hypothesised that the total number of alveoli was constant irrespective of lung size. He further proposed that mean linear intercept (Lm or mean inter-alveolar distance) and alveolar surface area varied proportionately with lung size. The more recent studies of Thurlbeck (1967b), Hasleton (1972) and Angus and Thurlbeck (1972) disagree with most of those findings. Thurlbeck, using a larger sample size, found Lm to be unrelated to body length. The implication of this was that taller people have larger surface areas within larger lungs, embodying a greater number of alveoli. The results of Angus and Thurlbeck confirmed this. Lm was not related to body length nor lung size but alveolar number was; r=0.578 for body length and r=0.569 for body length cubed. Hasleton's results are in general agreement with those of Thurlbeck and Angus with the exception of Lm. He found this to regress inversely with height. That does not contradict the findings of Angus, but reinforces the findings of increased alveolar number with height.

In summary, it is thought that the number of NRBs and hence acini is constant. This means that acini are disimilar in that they are larger in taller people and have more alveoli. From their regressions, Angus proposes that

alveolar number is genotypically predetermined, but enviromental parameters give more variable phenotypes thus producing a large degree of variation.

1.2.2. Variability Attributable to Age

Airway Calibre

Bronchiolar calibre exhibits a parabolic relationship with age, increasing rapidly and peaking in the third and fourth decade, and thereafter decreasing at a similar rate. Contrastingly, bronchial calibre shows no covariance with age (Niewoehner and Kleinerman 1974).

Alveolar Number and Surface Area

Alveolar number was originally considered to be complete by the age of eight (Dunnill 1962a and Weibel 1963) with increases in alveolar surface area being brought about by enlargement of existing units. This has since been revised by Angus and Thurlbeck (1972) and Dunnill (1982a) who now consider that alveolar multiplication continues until somatic growth ceases. In numerical terms alveoli increase from 24 to 300 million from birth to age eight with alveolar air rising from 24% to 60% of lung volume from birth to age 25 (Dunnill 1962a).

Internal surface area likewise varies with age, increasing from birth until the age of 25, but thereafter (when standardised to a volume of 5 litres) regresses on average by 2.7 square metres *per* decade (r=0.57, Thurlbeck 1967b).

Many changes in the internal geometry and structure of the lung are

commonly associated with ageing. Such changes are not universal (Leopold and Gough 1957, Thurlbeck 1976 and Heppleston and Leopold 1961). One of the major changes is a loss of intra-alveolar elastin, the functional consequences of which are a reduction in elastic recoil pressure and an increase in compliance. This dimunition in elastic recoil is manifest topographically as a gradual rounding of the lungs (Anderson *et al* 1964).

Internally, there is an increase in Lm, but a decrease in alveolar surface area and surface-to-volume ratio (Hasleton 1972 and Thurlbeck 1983). These alterations are a result of changes in the geometry of alveoli which become thinner, shallower and flatter (Thurlbeck 1976). Alveolar ducts and RBs are preferentially affected by this process whereby the proportion of alveolar duct air regresses with age while that within alveoli exhibits the opposite relationship (Weibel 1963).

1.2.3. Variability Attributable to Sex

It has long been established that sex is an important factor in determining aspects of lung physiology (Cotes 1975). For example, the lung volume of females is know to be smaller than that of males of similar stature. More information is required on the structural variability between the sexes before extrapolations based on these differences in volume can be made.

1.3. CHRONIC AIRFLOW OBSTRUCTION

The preceding information summarised aspects of lung morphology relevant to this project, describing its basic structure and dimensions while also trying to take into account variations due to parameters such as stature and age. This section deals mainly with emphysema. Latterly, (section 1.5.5.)

data on small airways disease is reviewed. Small airways disease is a term similar to chronic airflow obstruction in that it encompasses the affects of more than one disease process (Thurlbeck 1976). A lengthy historical background to these disease states is not necessary as this has already been completed by for example Thurlbeck (1976).

Chronic Airflow Obstruction

Chronic airflow obstruction (CAO) is a blanket term comprising emphysema, chronic bronchitis, asthma, pneumoconiosis and bronchiectasis. The term chronic obstructive lung disease (COLD) is synonymous with CAO, the former being slightly more aposite in its emphasis on obstruction to airflow. The need for these terms has arisen as a result of the poor clinical diagnosis of these conditions, and has been confounded by their high level of coexistence, often multiple (Burrows 1981 and Thurlbeck 1976). Although emphasised in the title, airflow obstruction neither has to be constant (Snider 1983) nor detectable (Thurlbeck 1976).

1.3.1. Emphysema

1.3.1.1. Definition of Emphysema

Emphysema is a condition that primarily affects the acinus, a point made obvious by its definition: "Emphysema is a condition of the lung characterised by increases beyond normal in the size of air spaces distal to the terminal bronchiole arising either from dilatation or destruction of their walls" (CIBA 1959).

Emphysema is therefore defined in anatomical terms, and to date,

pathological assessment is the only accurate method for its diagnosis and quantification (Flenley and Warren 1980). Strong clinico-pathological correlations will have to be established before reliable clinical diagnosis can be made. At present, clinical diagnosis is poor, even on occasions when the affliction is severe (Thurlbeck and Simon 1978).

1.3.1.2. Types of emphysema

There are four main types of emphysema centriacinar, panacinar, paracicatricial and paraseptal (Thurlbeck 1976). These types vary in their distribution within the acinus and also to a degree within the lung. Pure examples of any type are rare (Dunnill 1982b) and can usually be only definitively distinguished when present in mild or moderate degrees. The individual types are defined and discussed below.

CENTRIACINAR EMPHYSEMA (CAE)

Distribution

Centriacinar or "central lobular emphysema" (Gough 1952) affects the proximal portion of the acinus, characteristically involving second and third order respiratory bronchioles, ie the central portion of the acinus. Its distribution is patchy and irregular both within lobules and lobes (Leopold and Gough 1957), requiring whole lung sections to ascertain its true involvement (Gough 1952). Having said this, it is more commonly associated with upper than lower zones of the lung, being more frequent in the posterior and apical segments of upper lobes and superior segments of lower lobes (Thurlbeck 1962 and Snider 1983). Like all forms of emphysema it is a predominantly

smoking related condition.

Progression of CAE

The early stages of this condition bring about the dilatation of RBs (Duguid and Lambert 1964) with associated inflammation and fibrosis of the peribronchiolar alveoli, eventually leading to their dilatation and destruction (Snider 1983). Classically, respiratory bronchioles that have been destroyed coalesce with neighbouring affected RBs (Leopold and Gough 1957). This pattern of destruction produces a "typical" centriacinar lesion, often pigmented, well demarcated, centrally located and separated from the surrounding non-parenchyma by a buffer of normal intact alveolar ducts and sacs. CAE is often found in conjunction with other forms of emphysema. Lesions classified as predominantly centriacinar in type vary in their destruction of the acinus and in the pathological changes observed, both within and between cases.

Heppleston and Leopold (1961), taking acinar structure into account, gives an excellent summary of the possible pathogenesis of CAE. They hypothesise that destruction is more notable in the distal orders of RBs for two reasons. Firstly, progressive alveolation of distal orders enhances their susceptibility to destruction following inflammation. Secondly, destruction may be aggravated by overstretching caused by the inability of the supplying airway to expand during inspiration. Such airway inertia or stiffness is attributable to inflammation or stenosis, a feature common in CAE (Leopold and Gough 1957 and Heppleston and Leopold 1961).

PANACINAR EMPHYSEMA (PAE)

Distribution

Like centriacinar and centrilobular, the terms panacinar and panlobular are synonymous. The former term was adopted by the 1958 CIBA symposium (CIBA 1959) being more descriptive of the site of the lesion, and in general has superceeded the use of the latter. As its name suggests, PAE is distributed uniformly throughout the acinus, thereby differing from the more restricted distribution of CAE. The lung bases are preferentially affected when the condition is severe (Thurlbeck 1962), isolated lesions are similarly more frequent in these zones and in the anterior margins (Snider 1983).

Progression of PAE

In normal lungs, the alveolar pattern can be envisaged as a honeycomb network organised around the cylindrical outline of alveolar ducts. This arrangement is evident on sectioning of the lungs -the smooth rounded profiles of the ducts and RBs contrasting with the sharp polyhedral configuration of the alveoli. Progressive affliction of PAE gradually erodes this highly organised arrangement, dilating and destroying alveoli throughout the acinus, eventually rendering them indistinguishable from the larger cylindrical ducts. If severe, all semblance of organisation within the acinus is lost, leaving strands of non-parenchymatous tissue as the sole remnants.

SCAR EMPHYSEMA

Distribution

The CIBA symposium (CIBA 1959) proposed the term "irregular emphysema" for this condition, as, unlike the other main types of emphysema, no particular part of the acinus or lung is preferentially affected. The lesions are found in association with scar tissue or areas of inflammation that have not properly resolved. This association has given rise to the term paracicatricial or scar emphysema, which, being more descriptive of the condition, has gained general acceptance.

Progression of Scar Emphysema

Paracicatricial emphysema is thought to come about through the weakening of alveoli adjacent to areas of inflammation, possibly aggravated by overdistension attributable to the contractile and rigid properties of adjacent scar tissue (Heppleston and Leopold 1961). Prolongation or poor resolution of the inflammatory process enhances alveolar destruction. Destruction is typically patchy, producing abnormal air spaces around such areas, most bordered by elongated and ruptured alveoli, some by fibrous tissue. Although the most common form of emphysema, alteration to airflow is typically minimal, with alveolar disruption being limited to the locality of scar tissue (Thurlbeck 1976). Often, isolated lesions of paracicatricial emphysema can be the sole location of tissue damage in otherwise unremarkable lungs, while ultimately, severity relates to the amount of lung damage and scarring.

PARASEPTAL EMPHYSEMA

Paraseptal, or distal acinar emphysema (Thurlbeck 1976), is so called because of its selective destruction of the more distal ducts and sacs of the acinus. Within the lungs, the anterior and posterior zones of the lungs are more frequently affected. It has been suggested that bullous emphysema may be an extension of this type, (Dunnill 1982b). However, the aetiology of both conditions is poorly understood.

Progression of Paraseptal Emphysema

This condition progresses through the gradual dilatation and loss of alveolar attachments to lobular septae, vessels, airways and the enveloping pluera. It is often found in conjunction with fibrosis, sometimes in the form of cysts lined by fibrous tissue as opposed to bullae lined by enlarged alveolar walls. Its archetypal appearance is one of enlarged, adjacent bullae or cysts, variable in size, located along the boundary of non-parenchymal structures, most typically the pluera. Many incidences of spontaneous pneumothorax can most probably be attributed to advanced stages of this condition (Thurlbeck 1976).

1.4. SMOKING AND LUNG DISEASE

1.4.1. Historical Review of Smoking

Pipe smoking came to Europe via Spain in the early 16th century from America and by the late 16th century had been brought to England. In the 17th century it became fashionable to inhale snuff, although pipe smoking remained the norm for the wider population. Although cigars preceded the introduction of cigarettes, in Britain at least it was not until the latter were readily available that smoking habits moved significantly away from pipe smoking. Mass produced cigarettes originated in Brazil, but were succeeded in popularity by cigarettes produced with Virginian tobacco (RCP 1971).

These events, in conjunction with the development of the briar pipe, saw the popularity and consumption of tobacco in Britain increase dramatically during the first half of the 20th century. The 1950s seem to have been a pivotal decade when this upward trend stopped and thereafter the over all proportion of people smoking manufactured cigarettes decreased, as has the number of ex-smokers (Van Reek 1984). The number of cigarettes consumed *per* person and the number of packets sold has also decreased (Kunze 1983). These decreases have been brought about by an increasing number of professional people giving up the habit. However, the proportion of working class smokers has remained more or less constant (RCP 1977).

In the first half of this century, the sexes showed similar trends, although females took up the habit in significant numbers later than males, *circa* 1920s as opposed to 1890s. Throughout this period, although growth trends were very similar, there was always a smaller proportion of female smokers and,

irrespective of age, women always smoked less *per* day than men (RCP 1971).

Since the 1950s, differences in the smoking habits of the sexes have diminished. During the period 1958-1972 when the percentage of male smokers dropped, that of women increased. Since that time, although the proportion of smokers has fallen for both sexes, the decrease in male smokers is greater than that of females smokers (Van Reek 1984 and Kunze 1983). These trends have served to minimise the differences between the sexes to a few percentage points, and in younger smokers to almost insignificant levels (Van Reek 1984).

Steinfield (1984), Van Reek and the RCP, consider increased medical awareness to be an important factor in the cessation of smoking. Currently, around 36% of the population are cigarette smokers. Doctors must be among the most medically aware yet 13% of them are smokers. Even if the number of smokers fell to that level, Britain would still have around one million smokers (Russel 1983). Therefore the health problems associated with smoking would appear to be with us for some considerable time.

Filter cigarettes are now the norm and are used by the vast majority of smokers. However, only 1% of cigarettes smoked were filtered prior to the 1966 report on smoking -published by the Royal College of Physicians (RCP 1971 and 1977). The increased popularity of cigarette smoking witnessed this century has eclipsed all other modes of tobacco consumption (pipes, cigars, snuff and chewing) to such an extent that when combined, these other modes now account for less than 5% of all tobacco users. This is despite the fact that health risks associated with these other modes of tobacco use are less than those for cigarette smoking (Russel 1983). For these reasons the discussion below on health risks and constituents of tobacco smoke in general

pertain to cigarettes and, in view of the objectives of this study, will relate to lung disease alone.

1.4.2. Harmful Constituents of Cigarette Smoke

Tobacco smoke is a highly heterogeneous mixture of over 3000 different substances (Loeb *et al* 1984) the precise composition of which varies with different factors; the type of tobacco used, its method of curing, the way in which it is inhaled, the temperature of combustion and the cigarette paper in which it is wrapped (Horsfield 1981). As revealed in the review of Loeb *et al* (1984) Lefcoe and Ashley (1984) and Campbell (1983) the components of cigarette smoke are sufficiently toxic to deleteriously affect the health of passive non-smokers.

While recognising that cigarette smoke of varying compositions will have differing effects on the lung, it is still possible to analyse the general composition of cigarette smoke and identify the most important compounds that affect the lung.

In general, the mixture of substances can be subdivided into 4 separate groups:

1. Gases.
2. Nicotine.
3. Irritants.
4. Carcinogens.

1. GASES

These include carbon monoxide, oxygen, nitrogen dioxide, ammonia, cyanides, aldehydes, ketones and acids. The most important of these is carbon monoxide (CO) which constitutes up to 5% of tobacco smoke (RCP 1977) and is a product of incomplete combustion. On being inhaled the concentration of CO in the lung is diluted to 40 parts *per* million. This may appear to be a minute proportion but Haemoglobins (Hb) affinity for CO is 20 times that of oxygen. Hence, where there is a mixture of these two gases, CO will out-compete oxygen to bind to haemoglobin. Thus levels of carboxyhaemoglobin in heavy smokers are typically as high a 10-15%. Reductions of this magnitude in the oxygen carrying capacity of blood have been found to restrict the exercise levels of individuals (Horsfield 1981 and RCP 1971).

2. NICOTINE

Nicotine was named after Jean Nicot, former french ambassador to Lisbon, who recommended pipe smoking for medicinal purposes (RCP 1971). His opinion has since been repudiated on many occasions and by many authors including King James I (Campbell 1983).

Russel (1983) is of the opinion that 90% of deaths from lung cancer (30,000 *per* year) and chronic bronchitis (20,000 *per* year) are directly attributable to smoking. Russel and the RCP also argue that people smoke tobacco for nicotine, but die mainly from inhalation of tar, CO and other harmful components of cigarette smoke. He therefore advocates the use of other

nicotine containing products such as snuff, chewing gum contain nicotine, cigars (which in general are not inhaled) and low yield cigarettes. Russel's paper highlights the point that smokers are nicotine addicts who find it very difficult to break the habit. 70% of smokers would like to break the habit while 50% have made a least two attempts. The reasons for this powerful addiction can be traced to the many pharmacological actions of nicotine, especially those which affect the nervous system.

Nicotine enters the blood stream via the lungs with "intravenous-like" rapidity and is quickly metabolised (Russel 1983). The amount inhaled varies with the type of cigarette and how it is inhaled. It has a biphasic effect on brain cells, first stimulating and then depressing the action of acetyl choline and noradrenalin. It can also mimic the function of these neurotransmitters.

Summarising its effects, nicotine reduces the tension of voluntary muscles, increases the pulse rate and blood pressure, platlete stickiness and invokes peripheral vasoconstriction -although reduced levels of blood pressure have been found in smokers between cigarettes. Horsfield (1981) and RCP reports (1971 1977 and 1983) give a fuller account of the effects of nicotine.

3. IRRITANT SUBSTANCES

Airways of the bronchial tree are lined by a ciliated epithelium. The cilia have a very important cleaning function in that, by constantly beating, they move the thin layer of mucus which overlies the epithelium toward the larynx. By doing this, foreign particles which have become trapped within the mucus are removed from the lung. Walker and Keiffer (1966) have identified a number of agents, the most important of which is acrolein, which impair this

clearing mechanism by inhibiting the action of cilia (ciliostasis). Substances within both the gas and particulate phase of cigarette smoke can induce ciliostasis. The effects of these agents is potent enough to cause measurable impedence of particle clearance from the lung within one year of starting to smoke. This implies that ciliostatic effects precede decreases in pulmonary function and may in fact play an important role in the pathogenesis of future lung disorders (Horsfield 1981 and RCP 1977).

Fletcher and co-worker (1976) have demonstrated a good linear correlation between hypersecretion of mucus and smoking. Cigarette smoke is also known to induce coughing and bronchoconstriction. This latter property is measurable, in that increases in airway resistance can by detected after smoking.

Qualitative proof that mucus hypersecretion is caused by irritants in cigarette smoke is given by the observation that in people who give up the habit mucus secretion eventually regresses to levels within non-smokers (Horsfield 1981).

4. CARCINOGENS

Many carcinogens are present within tobacco smoke some -eg polycyclic aromatic hydrocarbons and N-nitroso compounds -in quantifiably dangerous amounts, others, although potential carcinogens, at lower concentrations. Additionally, the enzymatic breakdown of otherwise innocuous substances can produce short-lived, but potent intermediate products. Enzymes involved in such metabolic pathways have been identified (Loeb *et al* 1984) and have been found to exist in greater quantities in smokers who go on to develop lung

cancer (Horsfield 1981). This association provides evidence to support the hypothesis that there may be a genetic link in the pathogenesis of lung cancer.

As noted earlier, Russel estimates 90% of all lung deaths to be caused by smoking. In their 1977 report, the Royal College of Physicians considered 50% of all cancer deaths to involve lung cancer. Combining these two statistics gives an estimated lung cancer death rate of 36% attributable to smoking. This agrees with the figure given by Loeb *et al* (1984) who furnishes a thorough review on the association between lung cancer and smoking. Most of the evidence is taken from epidemiological studies, and as the review concludes, "Without exception epidemiological studies have demonstrated a consistent association between lung cancer and smoking". Their list of major chemical carcinogens and tumour promoters make this association hardly surprising. Corroborating this, the RCP report of 1977 found the rise of lung cancer to be proportional to the number of cigarettes smoked and the age of starting.

1.4.3. Smoking and Chronic Bronchitis

Chronic bronchitis is defined in clinical terms (Ciba 1959) as being cough and sputum "occurring on most days for at least three months in the year for at least two consecutive years (other causes being excluded)". As stated above, cigarette smoke contains irritants that initiate hypersecretion of mucus as well as delaying the natural clearance of mucus from the airways of the lung –with tar levels perhaps being incidental to this response (Rimpela and Rimpela 1985 and Pride 1983). Therefore, although atmospheric pollution, workplace dust and poor economic status are associated with chronic

bronchitis, for smokers the most common source of such irritants is inhaled tobacco smoke (Pride 1983) making it "the chief cause of chronic bronchitis" (Thurlbeck 1976). Indeed cigarette smoke is such an irritant that the frequency of bronchitis, asthma and pneumonitis in children is related to their exposure to the cigarette smoke of their parents (Loeb *et al* 1984 and Lefcoe and Ashley 1984).

Numerous reviews have been carried out including those of Horsfield (1981), RCP (1971, 1977 and 1983), Thurlbeck (1976) and Fletcher *et al* (1976) which clearly substantiate the strong link between chronic bronchitis and smoking.

1.4.4. Smoking and Emphysema

Cigarette smoking promotes levels of macrophage and neutrophil derived elastolytic enzymes, decreased levels of alpha-1-antitrypsin (A1AT) and can increase the sensitivity of polymorphs (Campbell 1983). Given that a protease-antiprotease balance must by maintained within the lung, effects such as these could seriously undermine the delicate structure of lung parenchyma. This is discussed in greater detail immediately below.

Emphysema assessed macroscopically relates to the number of cigarettes smoked (Thurlbeck *et al* 1974). Indeed "cigarette smoking is the most important determinant of emphysema" (Thurlbeck 1976). In non-smokers, emphysema is uncommon except in people with the rare homozygous Pi genotype. Accepting that antiprotease levels may by reduced in heterozygous Pi genotypes (Pride 1983), Sutinen *et al* (1985) found "an expected link between smoking and emphysema", but not between Pi genotypes and emphysema. Cigarette smoke is therefore clearly linked with destructive loss

of lung parenchyma and over all is the most important factor causing such loss. Sobonya and Burrows (1983) in their review article reinforce this link reporting Auerbach to have found that 10% of smokers (taking more than 20 cigarettes a day) had emphysema.

It must be noted that only a minority of smokers develop chronic airflow obstruction (CAO). Pride (1983) gives a range of 10-20%. There is a significant, but weak link between cigarette consumption (as packyears) and annual decline in FEV, but the strength of this association is insufficient to explain which smokers do and do not develop CAO. Data on smoking has to be treated with caution. Peach *et al* (1986) have shown, in a longitudinal study, that less than half of smokers can correctly identify the brand of cigarette they smoked 12 years previously. They also show that current information on smoking habits can be contrary to previous smoking habits. This will all add considerable error to correlation statistics when smoking data is related to other parameters. Additionally, as stated above, tar levels may not be an important factor in the development of CAO.

Fletcher and colleagues (1976), in their large follow up study, found symptomatic smokers to have a greater annual decline in FEV while death from COPD is associated with the degree of airflow obstruction but not mucus hypersecretion (Peto *et al* 1983). However, although it has been recognised that some smokers are more susceptible to the harmful effects of cigarette smoke, the cause of this susceptiblity and the precise location of airflow restriction have yet to be agreed.

1.4.4.1. The Enzyme-Inhibitor Hypothesis

As documented by Sobonya and Burrows (1983), and discussed above, the incidence of macroscopic emphysema is considerably higher in smokers. The enzyme-inhibitor hypothesis (Idell and Cohen 1983), proposed to explain this phenomenon, arose from the observations of Laurell and Erikson (1963). These investigators noticed that individuals homozygous for alpha-1-antitrypsin (A1AT) deficiency were more prone to develop emphysema. By chance an experimental model supporting this observation arose when Gross *et al* (1963), who was interested in quartz induced fibrosis, observed that intrabronchial administration of papain (a plant derived protease) produced emphysema in rats. Numerous workers have since managed to repeat this work using different reagents and animal models. This experimental work was reviewed by Karlinsky and Snider (1978) and more recently by Lucey (1983). The bulk of evidence supporting the enzyme-inhibitor hypothesis is still circumstantial (Janoff 1983). One major criticism of it is that the emphysema produced by these models is panacinar in type, whereas that produced in human smokers is typically centriacinar.

The enzyme-inhibitor hypothesis has since grown to encompass three main arguments, advanced to explain smoking related emphysema. These arguments are that cigarette smoke:

1. Sequestors "elastase-vector cells" to the lung (Janoff 1983).
2. Interferes with protease-inhibitory capacity (Idell and Cohen 1983).
3. Deleteriously affects elastin-repair mechanisms.

1. SEQUESTRATION OF ELASTASE-VECTOR CELLS

There is, within the lung, a balance between proteolytic and antiproteolytic agents. The following observations provide data which suggest that this balance may by disturbed or removed in the lungs of smokers.

Neutrophils, pulmonary alveolar macrophages (PAMs) and monocytes have been cited as the main source of endogenous elastases (Stone 1983). More than five times the number of neutrophils can be obtained from the bronchial alveolar lavage fluid (BALF) of smokers than non-smokers (Stone 1983). This observation is important, as neutrophil elastase has superior elastin binding properties than either PAMs or monocytes and they also contains more elastases. PAM and monocyte numbers exhibit a 5 to 10 fold increase in the BALF of smokers, and have the ability to phagocytose neutrophil derived elastases (Campbell *et al* 1979) which may be re-released "with an appropriate stimulus or upon the cells death" (Stone 1983). Polymorphonuclear leucocyte chemoattractant (PAM derived) and C3, the third component of complement, levels are also increased in smokers (Janoff 1983).

Observations like these appear to indicate that the lungs of smokers have to contend with a greater protease burden. Animal experiments attempting to produce smoking induced emphysema have had little success (Lucey 1983). However, as human emphysema develops over many decades, animal models may be inappropriate.

2. PROTEASE-INHIBITION REDUCTION

A number of antiproteases have been identified within the lung. A1AT has already been mentioned and is probably the most important constituting more

than 70% of elastase inhibitory potential in alveolar fluid (Janoff 1983). In addition to A1AT, there are a number of local protease inhibitors which characteristically have a low molecular weight, are acid stable, but are not found in plasma, eg bronchial mucus protease inhibitor (BMPI) which is located in the upper airways (Janoff 1983). Clearly their homeostatic role is to regulate the effects of proteolytic agents. The sequestration of elastase-vector cells by cigarette smoke, with its potential to alter the protease-antiprotease balance, has been discussed. In conjunction with this, *in vitro* evidence has been produced by Carp *et al* (1982) which suggests that the active site on A1AT may undergo oxidisation in smokers reducing its elastolytic-inhibition capacity (EIC).

Active A1AT forms very stable protease-antiprotease complexes, but in its oxidised form its affinity for elastases is reduced by 2000 fold, the complexes it forms are less stable and A1AT itself may by prone to degradation (Idell and Cohen 1983). BMPI is similarly inactivated by oxidants.

Cigarette smoke is rich in oxidants and activated neutrophils, PAMs and monocytes can release oxygen radicals (H_2O_2 and superoxides). There is then the potential within the lung of smokers for large scale inactivation of A1AT. Indeed, Janoff and Carp (1977) found that the crude tar fraction from cigarette smoke was sufficient to inactivate A1AT.

Neiwoehner *et al* (1974), documented the clustering of inflammatory cells round the membranous airways of smokers. Accepting that A1AT inactivation in smokers may by short lived, focal accumulations such as these may produce high focal concentrations of proteases which could damage the lung.

3. ELASTIN-REPAIR INTERFERENCE

The arguments given above, on A1AT inactivation and enhanced recruitment of elastase-vector cells, indicates that cigarette smoke may promote the catabolic side of the protease-antiprotease equilibrium. If these observations occur *in vivo* then the architecture on the lungs of smokers may by compromised unless there is a compensatory increase in elastin repair. However, Osman *et al* (1982) and Laurent *et al* (1983) have obtained experimental data that suggests that elastin formation is impaired by exposure to cigarette smoke. Osman *et al* found the incorporation of lysine to be inhibited by unfiltered cigarette smoke. These results were verified by Laurent *et al* who also observed the action on lysl oxidase -a catalytic enzyme necessary for the proper production of elastin cross links and the conversion of tropoelastin to elastin- to be retarded by the water soluble components of cigarette smoke. Hence, as well as promoting catabolism of the lung, cigarette smoking may also impair anabolic repair.

Drawing these observations together, the enzyme-inhibitor hypothesis originated from the observation that people deficient in A1AT have a higher and earlier incidence of macroscopic emphysema. Since the antiproteases like A1AT have shown to be inactivated by oxidising agents derived both from cigarette smoke and immunological cells. Elastases, derived most notably from neutrophils, but also PAMs and monocytes, have been indicted as the most probable agents responsible for collagen and elastin degradation in the lung. This argument proposes that, in response to an appropriate stimulus, neutrophils will migrate to and through the interstitium where they may degranulate releasing elastases. Verificatory evidence supporting this scenario has been provided recently by Damiano *et al* (1986) who was able to locate

neutrophil derived elastase attached to elastin within the interstitium. Importantly, this work was carried out on resected human lung tissue.

The number of elastase-vector cells are increased as a result of exposure to cigarette smoke and structural damage inflicted by elastases, released by these cells, may not be properly repaired. However, it must be concluded that most of the evidence produced to back these arguments is circumstantial (Janoff 1985).

In summary, cigarette smoking is a phenomenon of the 19th century which, although still popular, is on the wane, probably as a result of increased medical awareness. Cigarette smoke contains a plethora of substances, its deleterious effects on the lung are multifactorial and it can cause, amongst other things, lung cancer, chronic bronchitis and emphysema. However, only a minority of smokers develop CAO, the reasons for this and the pathological changes which cause airflow obstruction have still to be defined.

1.5. MORPHOMETRY REVIEW

1.5.1. Introduction

The latter half of this century has seen a plethora of "measuring" techniques applied to the lung. These range from the completely subjective to the truly quantitative. This section deals with developments of techniques and principles which are relevant to or preceeded those used in this study. Reflecting the importance of stereological/morphometric methods this section begins with a summary on their introduction and development.

1.5.2. Historical Review of Morphometry

The most important axiom in morphometry (stereology) is that in any multiphase solid -whether mineral or tissue based- the average area fractions of randomly distributed components, measured on two dimensional transections, are representative of their volume fractions.

This principle was first demonstrated experimentally but, without mathematical proof, by the French geologist Dellesse in 1847 (Aherne and Dunnill 1982) and in recognition has been named after him. Although this principle supplied a powerful mathematical tool the absence of quick and accurate methods for the planimetric assessment of area limited its more widespread use.

Delesse's principle of assessing (3-D) volumetric proportions from (2-D) area profiles was reduced by a further dimension in 1898 by Rosiwall (Aherne and Dunnill). Rosiwall, another geologist, again using experimental proof, demonstrated that the average fraction of a line passing through a randomly

distributed component contained within a multiphase solid was representative of the volumetric fraction of that component. This technique has been termed lineal or Rosiwall analysis. In practice this method, even after the advent of integrated stages, was lengthy and tedious.

It was only with the introduction of point counting, pioneered by Glagolev in 1933 (this reference is in Russian, but is available in English (Glagolev 1934)), that a quick and accurate morphometric method for measuring area fractions was available. The theoretical basis of point counting simply states that the probability of a single point landing on a given component, distributed within a multiphase solid, is equal to the proportion of that solid constituted by the "target" component.

Point counting obviously adheres to the Delesse principle in that the one assesses area fractions to gain an unbiased estimate of volume fractions. Hennig (1959) Weibel *et al* (1966) and Weibel and Gomez (1962) realised the potential of the technique and produced point counting grids which were more complex and useful than the initially simple grid of Glagolev.

The Delesse principle is fundemental to morphometry, however, equally fundemental is the use of geometric probability. Aherne and Dunnill (1982) relate how in 1777 the Comte de Bouffon by solving his "needle problem" (accidentally) pioneered the field of geometric probability. Although the principles of Delesse, Rosiwall and Glagolev had long been put into practice it was not until much later that they were formally proven mathematically. Aherne and Dunnill (1982) furnish a chapter at the end of their book which credits various scholars with these proofs and gives a fuller historical account of morphometry than exists above. Williams (1977), Oosthuyzen (1980) and Weibel (1963) are likewise very informative.

Although not the originals the following authors provide proofs of the various principles; Delesse's principle- Weibel (1963, p12) and Aherne and Dunnill (1982, p170-171), Rosiwall analysis- Weibel (1963, p17) and point counting- again by Weibel (1963, p19-20).

As well as being used to formally prove existing principles geometric probability linked to existing principles has been used to derive new techniques and also calculate the inherent error of these methods. Doing precisely this both Saltykov and Tomkeieff (Aherne and Dunnill) proved that surface areas could be reliably measured using the mean linear intercept procedure. Tomkeieff's rational can be gleaned from his original paper in Nature (1945) and is discussed by Aherne and Dunnill who trace its links back to Bouffon.

Hally (1964) and Hennig (1959) furnish formulae which anticipate the number of points required to achieve a given relative standard error where the volume fraction of the component is iteratively estimated. Similarly, Gladman and Woodhead (1960) provide a formula which relates to the standard deviation. All these formulae are based on geometric probability.

As noted above, the factor that initially limited the use of Delesse's principle was the absence of quick and trusted planimetric methods. Modern technology, especially the advent of computer linked digitiser tablets, has solved this problem. These systems, usually software driven, consist of a digitiser tablet which is linked to a desktop computer via a cursor. The *modus operandi* of the one used in this study is discussed in a later section. Suffice to say that the location of the cursor on the tablet is "known" to the computer thereby enabling the profiles -as x,y coordinates- of objects to be defined. Parameters such as shape, area, perimeter, etc. can therefore be determined.

Digitiser tablets have not replaced but supplement the techniques discussed above, "offering distinct advantages in accuracy and analysis where individual object profiles or field values are of interest" (Aherne and Dunnill). Procedures which ensure the accuracy of these systems are given by Frolov and Maling (1969), Williams (1977) and Fleege *et al* (1986 and 1987).

The current drive to fully automate image analysis has seen the development of third generation image analysers (Joyce Loebl 1985). These systems, only very recently available, have the ability to capture images by converting them to digital information (typically 6 or 8 bit) and can via a large software library enhance the image, identify and measure objects or fields and execute detailed statistical analysis.

Where the boundaries of an object where input manually in older systems, modern analysers execute a procedure known as boundary chain encoding. This identifies a particular coordinate on the boundary of an object (usually the lowermost projection) and thereafter represents the profile of the object as a series of vectors -numbers from 0 to 7- which equate to the eight major points on a compass (Joyce Loebl 1985). It is worth noting that the founding principles of Delesse, Rosiwal and Glagolev are included in the measuring logic of these systems (Joyce Loebl 1985).

An indication of their accuracy is given indirectly by Gladman and Woodhead (1960). They show that a total of 19600 points are required to give a standard deviation of 0.01% for a component with a volume fraction of 2%. Each image stored by the IBAS2 system comprises over 250,000 individual points. Reverting to the formula give by Hally ie

$$\text{Relative Standard Error} = (1-Vv)^{0.5} / n^{0.5}$$

and assume we are measuring a component with a negligible volume fraction (ie almost 0%) then the relative standard error of the measurement will be less than 0.002%.

The *modus operandi* of the IBAS2 system used in this study and the software procedures applied are discussed in later sections.

1.5.3. Measurement Procedures Applied to the Lung

1.5.3.1. Point Counting

Chalkey (1943) modified Glagolev's point counting technique and in its new format applied it to biological material. In his treatise Chalkey demonstrated the technique, by experiment, to be accurate and reproducible. In turn his method was taken up and adapted by Dunnill (1962b) who applied it to human lung to macroscopically assess the proportions of non-parenchyma, normal parenchyma and abnormal air spaces. Its potential application for microscopic quantitation of alveolar air, alveolar duct air, abnormal air space, tissue and vessels is discussed in the same paper and Weibel (1984) furnishes a coherent system to this end.

The methodology devised by Dunnill has become a standard not only for the macroscopic assessment of emphysema (eg Dunnill 1964, Thurlbeck 1967a and 1967c and Thurlbeck *et al* 1970a and 1970b) but also -in adapted forms- for the assessment of area and volume fractions of components within other pulmonary structures (cf Bignon *et al* 1970, Langston *et al* 1979, Dunnill *et al* 1969, Matsuba and Thurlbeck 1971, 1972 and 1973 and Dalquen and Oberholzer 1983).

1.5.3.2. Mean Linear Intercept (Lm)

Tomkeieff's original and very brief description of mean linear intecept for assessment of surface areas was elaborated on in a further paper by Campbell and Tomkeieff (1952). The technique was first applied to human lungs by Dunnill (1962b) -in the same paper which introduced point counting- and a practical application was presented (Dunnill 1962a) in the same edition of Thorax concerning "Postnatal Growth of the Lung".

As with point counting, mean linear intercept has become a standard technique in lung morphometry (eg Dunnill 1964, Thurlbeck 1967a, 1967b and, 1967c, Thurlbeck *et al* 1970b, Bignon *et al* 1970 and Nagai *et al* 1985a). Its popularity is related to its quick and easy execution along with the limited qualities demanded of the component to be measured. In particular, the shape of the component (in this case air spaces) can vary but must be randomly distributed within the containing volume. Having said this specialised grids have been devised to measure the surface area of components which have an anisotropic distribution (Aherne and Dunnill).

Modifications, similar to those devised by Duguid *et al* (1964), were added to the Lm measure by Thurlbeck (1967b) who corrected Lm (re-expressed as internal surfaces area or ISA) for formalin inflated lungs to that for ISA at a predicted total lung capacity. Having calculated this corrected internal surface area (ISAc) Thurlbeck then expressed ISA at an arbitrary lung volume of 5 litres (ISA_5). This data transformation is still applied today (Nagai *et al* 1985a).

1.5.3.3. Subjective Measures of Emphysema

A number of these techniques have been formulated and include those of Ciba (1959), Cromie (1961), Heard (1969), Ryder *et al* (1969) and Thurlbeck *et al* (1969). All the above require the preparation of Gough-Wentworth sections (cf Gough and Wentworth 1949) and all but the Heard technique utilise a panel of standards against which unknowns can be compared and thence graded.

Comrie devised eight "arbitrary" grades which represent progressively severe emphysema. These standards and pictures were all of 1cm areas of lung parenchyma which made the application of his technique very laborious as it requires the assessment of every 1cm square of Gough-Wentworth whole lung slices.

The picture grading technique of Ryder divides the lung slice into ten segments. Each individual segment is then graded for emphysema from 0 to 3 (corresponding to none, mild, moderate or severe) against a set of standard grading pictures adapted from originals initially proposed by the Ciba symposium of 1959. Lung slices are graded separately for both panacinar and centriacinar emphysema. A composite score is then calculated for each of the emphysema types by summing the grades of the segments giving a possible range of scores from 0 to 30. These composite scores are often converted to percentages.

This type of assessment is similar to that of picture grading (described immediately below) but is more detailed in its scoring while also giving some impression of the distribution of emphysema in the lung.

The panel method (Thurlbeck *et al* 1969) initially established the following

grades.

- GRADE 100: "the most severe example of emphysema that one observer had seen".
- Grade 80: severe.
- Grade 50: moderate.
- Grade 20: mild.
- Grade 0: none.

Intervening standards were filled from a collection of 500 paper mounted sections to allow observers to match whole lung sections against the "panel" of pictures. As stated by the authors these grades "represented arbitrary, intuitive milestones in the spectrum of the severity of various types of emphysema".

The methodology of Heard divided the lung slice into six zones each of which was then subdivided into five parts, thereby ultimately dividing the slice into 30 parts. The number of parts and thence the percentage of each zone with emphysema was then assessed.

Following reviews of these and other techniques (Thurlbeck 1967a and Thurlbeck *et al* 1969 and 1970a) panel grading was recommended as the best ranking technique, principally for its speed of application and reproducibility, although its limitations were acknowledged, "It is important to stress that the range of 0 to 100 used does not imply that the method measures a percentage of anything" (Thurlbeck *et al* 1970a). This comment points to an important difference between the ranking and morphometric techniques ie point counting, Lm and planimetry, in that the former are subjective whereas

the latter are objective measures based on a true arithmetic scale. Emphysema assessed using any of the above ranking techniques belong to the ordinal scale of measurement (Siegel 1956 and Sokal and Rohlf 1981) and hence are not suitable for analysis with parametric statistical tests. Siegel in particular makes this point quite clearly, "tests which use means and standard deviations ought not to be used with data on an ordinal scale".

The originators of both the Ryder and the Thurlbeck techniques point out that their scales are arbitrary. A lung with moderate emphysema (grade 50 on the Thurlbeck scale) does not necessarily have 30 less units of emphysema than one with severe emphysema (grade 80) or 30 more units than one graded as mild (grade 20), as the distances on their measurement scale are unknown as are the units of measurement themselves as they have no known reference to a true scale. The calculation of means for statistical comparisons is clearly meaningless rendering parametric test like Pearson's correlation coefficient and least squares linear regression inappropriate as calculations of individual differences from means are required. Most morphometric studies, however, have utilised these and other parametric statistical tests whereas for example Nagai *et al* (1985a and 1985b) use more appropriate non-parametric statistics.

1.5.3.4. Techniques Relevant to Small Airways

MEASUREMENT OF SMALL AIRWAY CALIBRE

Assuming small airways are cylindrical their outlines will be elliptical in cross section. The lesser diameters of these ellipses will represent the true diameter of the sectioned airways (Nagai *et al* 1985a). Using this assumption small airway calibre, initially measured as the lesser elliptical diameter, can and has been measured with relative ease using a calibrated eyepiece (eg

Berend *et al* 1979a and 1979b and Mitchell *et al* 1976).

This technique has in some studies (eg Bignon *et al* 1969 and 1970 and Depiere *et al* 1972) been further simplified by using an eyepiece marked out in eight concentric circles each representing airways of predetermined sizes. Although this technique does not accurately measure individual airway sizes, it enables rapid analysis of the distribution of small airway sizes. A number of more recent studies have employed computerised planimeters to assess airway diameter (eg Berend *et al* 1981, Carlile and Edwards 1983, Nagai *et al* 1985a, Petty *et al* 1984 and 1986).

The basic assumption that small airways are always cylindrical has been questioned both theoretically and experimentally (Anderson and Foraker 1962 and Linhartova *et al* 1971, 1973, 1974 and 1982). Likewise Nagai *et al* (1985a) have shown that airway deformity is associated with loss of alveolar walls. This work has demonstrated that considerable bronchiolar deformity exists in patients with emphysema. Three dimensional reconstructions assembled by Linhartova *et al*, of small airways sampled from emphysematous patients, revealed them to deviate markedly from the tapered cylindrical model that small airways from normal lungs adhere to (Horsfield 1974 and 1978 and Horsfield and Cummings 1968). These findings call into question the assumption, and morphometric practice, that measurements of small airway diameter reliably estimates (spherical) cross sectional area in anything but "normal" lungs.

Berend *et al* (1979b) proposed a technique which compares the measurements of bronchiolar calibre against those of the external adventitia in the accompanying pulmonary artery to assess whether the airway is narrowed. Such a technique assumes arteries to be disease free, an assumption which

may not be valid. Nevertheless, this technique has found favour with other studies (Berend *et al* 1979b and Petty *et al* 1984).

MEASUREMENT OF SMALL AIRWAY COMPONENTS

Whereas components of large airways have been quantified by objective morphometric methods (eg Dunnill *et al* 1969, Dalquen and Oberholzer 1983 and Carlile and Edwards 1983) assessment in small airways has tended to be qualitative or semi-quantitative (Fulmer *et al* 1977, Mitchell *et al* 1976, Niewoehner and Kleinerman 1974 and Cosio *et al* 1977). The usage of the last technique -which ranks the presence of a number of parameters (eg goblet cells, luminal mucous etc.) from zero to three summing them to give a total pathology score- has been the most widespread (eg Petty *et al* 1984 and 1986, Pare *et al* 1985, Churg *et al* 1985, Wright *et al* 1983 and 1984, Berend *et al* 1981 and Nagai *et al* 1985a) and the reference standards used have been published by Wright *et al* (1985).. As with panel and picture grading of emphysema this is a ranking system based upon arbitrarily chosen grades. The criticism levelled at the statistical analysis of emphysema, scored on a ranking scale, must also be levelled at this system of ranking of small airways pathology. This is not to say that the techniques themselves are inappropriate, but the statistical analysis applied, in most cases, makes assumptions of the data which are not met. Where this occurs the relevance of the probabilities are unknown (Siegel 1956). Again, some studies eg Nagai *et al* (1985a and 1985b) are excepted from this criticism as is Niewoehner and Kleinerman (1974) who used non-parametric 'U' tests and were one of the first studies to develop a comprehensive ranking system for small airways.

1.5.4. Factors Affecting Lung Morphometry

1.5.4.1. Inflation and Fixation of Lungs

Lacking the support provided *in vivo* by the chest wall, lungs removed from the thoracic cavity revert to a collapsed state. Meaningful morphometry cannot be achieved from lungs in this condition. That this is true even for the macroscopic diagnosis of emphysema was noted by Gough (1952) and the point is put quite forcibly by Dunnill (1982b) who states "It cannot be stressed to strongly that emphysema cannot be reliably diagnosed from examination of unfixed uninflated lungs". It is clear then that where more detailed morphometry is to be carried out eg point counting, alveolar surface area and bronchiolar calibre quantitation, lungs must fixed and inflated.

A number of techniques has been devised to achieve this and the methodology and merits of these are discussed in a later section. Although there are differences between these techniques they all share a common principle of fixing the lungs with formal saline which is applied under pressure either in vapour or liquid phase. All three techniques provide a standard method by which lungs can be inflated and fixed. This is important as the dimensions of structures within the lung vary in proportion to lung volume. Pascall's principle states that fluids applied under pressure transmit this pressure equally and in all directions (Anderson *et al* 1964). Hence, all structures within the lung will expand proportionately with increases in lung volume. The term proportionately is important as 2D area and surface area changes and 1D linear changes (eg diameters) are not as large as 3D volume changes. In general, area changes vary to the two thirds power of volume changes with linear changes varying to the one third power of volume

changes. This has been shown to be true for large, medium and small airways, in dog lungs, over a large range of lung volumes ie 50% to 100% total lung capacity (TLC) (Hughes *et al* 1972 and Hahn *et al* 1976) and for cat alveoli during inflation and deflation (Storey and Staub 1962).

Another salient point with respect to lung volume is that as lungs approach TLC changes in transpulmonary pressure produce progressively smaller increments in lung volume. This is represented graphically by Netter *et al* (1979) and Cotes (1985). Interpolating from their graphic presentations of pressure-volume curves the following approximations can be gleaned. 10cm H_2O produces 60% TLC, 20cm H_2O 92% TLC and 25cm H_2O 98% TLC with 30cm H_2O producing TLC.

From the linear/volume relationship equation given above it would be expected that this range of transpulmonary pressures would have less effect on airway diameter. This has been confirmed by Hughes *et al* (1972) and by interpolating from the airway diameter vs transpulmonary pressure graph provided by these authors, (where airway diameter measured at TLC is expressed as 100%) 10cm H_2O gave 90% airway diameter, 20cm H_2O 95% airway diameter and 25cm H_2O gave airway diameters almost indiscernable from that obtained at TLC ie 30cm H_20. Viewing things from the other angle, Anderson *et al* (1964) by applying inflation pressures up to 120cm H_2O could only produce a 7% increase above TLC.

These studies demonstrate that; in the initial part of the pressure-volume curve relatively small increments in transpulmonary pressure produce marked changes in lung volume whereas subsequent increases in applied inflation pressure produce progressively smaller increases in lung volume, lungs reach a fairly definite end-point (ie TLC) and thereafter resist increasing changes of

volume even where there are substantial increases in the inflation pressure applied.

Another conclusion which can be taken from these studies is that areas and diameters measured in lungs which are inflated close to TLC should be relatively comparable. This has already been noted by Anderson *et al* (1964) who consider that "10% differences between final and 'true' inspiratory dimensions", produce variation in measurements that are comparitively small.

1.5.4.2. Embedding Media

Where measurements are to be made from histological sections, tissue blocks have to be sampled from the lung and embedded in an appropriate medium whereby sections of suitable size and thickness can be taken and stained to demonstrate the stuctures which are to be measured.

Paraffin has almost exclusively been the embedding medium of choice for lung morphometrists. Care has to be taken as there are a number of well known artefacts associated with paraffin embedding. These are dehydration, shrinkage and compression.

Dehydration occurs as tissue blocks are taken through and ascending series of alcohols. With the established procedures in use today, dehydration is not considered to be a source of significant tissue loss.

Shrinkage occurs as the paraffin wax in which the tissue is eventually embedded cools to room temperature. Shrinkage correction factors can be calculated by measuring the pre-embedded dimensions of a tissue block and then the post-embedded dimensions of the cut section. The ratio of these areas provides the area correction factor and the square root of this the linear

correction factor. Multiplying measurements made on the histological sections by the reciprocals of these correction factors corrects them to fixed tissue equivalents.

Most morphometric studies have calculated correction factors (eg Petty *et al* 1984 and 1986, Berend *et al* 1979a and 1981 and Nagai 1985a) while others appear to have assumed a certain loss attributable to processing (Mitchell *et al* 1976).

Where relative measurements are required and the embedding procedure provides reproducible changes it is not necessary to calculate correction factors (Aherne and Dunnill 1982). This was recognised by Berend *et al* (1979b) who set out to compare relative bronchial and pulmonary artery measurements and was possibly assumed by Linhartova *et al* (1971) who again were interested only in relative measures.

Calculation of shrinkage factors is appropriate where the embedding procedure may provide variable degrees of fixed tissue loss or where comparisons with work done in other laboratories is desirable.

It may appear at the first instance that the calculation of shrinkage factors would be unnecessary in studies where grading as opposed to true measurements was the principle aim (eg Cosio *et al* 1977 and Wright *et al* 1983), but as recognised by Mitchell *et al* (1976) where these studies set out to grade airways within a certain size limit ie internal diameter less than or equal to 2mm, then allowances must be made for processing loss or the sample measured will not be that which was intended.

Compression of paraffin embedded material arises when sections are taken from the blocks of tissue. As the microtome blade acts on only one side of

the tissue block compression differs from shrinkage in that it occurs only in that plane. Paraffin wax is a soft material and the amount of compression obtained relates to the density of the tissue. As lung is a "low density" tissue it offers very little resistance to the ingress of the microtome blade and is more prone to compression than for example sections of heart.

The calculation of shrinkage correction factors, as it is assessed on the cut sections, contains within them loss of fixed tissue due to both shrinkage and compression. This may appear to be a reasonable compromise, but will only be so if the effects of compression are evenly distributed. It is obvious that this cannot strictly be true as compression occurs in only one plane of the tissue section. Therefore airway diameter, area and shape will be anisotropically effected. This becomes clear where circular airways are considered, no matter where they lie in the tissue block (with respect to the plane of section) they will appear oval on histological sections. If compression is slight and distributed evenly throughout the section or perhaps abolished to some degree by floating the sections in a wax bath, then these changes may be assumed to be negligible or at least even themselves out. However, if compression is zonal eg arising when the microtome blade first encounters the tissue block or as a result of its increasing momentum through the block as it meets progressively less resistance, then the effects of compression will for most measurements be impossible to correct.

Dunnill (1962b) realising the possible effects of compression while assessing mean linear intercept recommends the use of a cross hair graticule to compensate for the possible differences in intersection counts between the two planes of the section. Niewoehner and Kleinerman (1974) adopted a less rigorous solution and simply stated that "Parenchymal sections with significant

artefact were excluded". Most morphometric studies though confront only the problem of shrinkage and possibly assume that compression is an insignificant artefact.

Conclusions on shrinkage and compression relevant to this study are made in a later section. The above discussion is an acknowledgement that these two factors have to be assessed if the variability inherent in measurement is to be controlled.

1.5.5. Review of Morphometric Studies

The work of Hogg, Macklem and Thurlbeck (1968) was fundemental in the development of the concept of "small airways disease" in man. This arose from their findings that peripheral airway resistance was low in normal lungs but increased from four to forty times in patients with emphysema and chronic bronchitis. From these results, Ranga and Kleinerman (1978) speculated that total airway resistance would only increase by around 10% were half the small airways destroyed by disease as the major component of airway resistance in normal lungs lay in the upper respiratory tree (Thurlbeck 1976). If this were true it meant that considerable damage to small airways may exist but remain clinically undetected.

The conclusion made by Hogg *et al*, that small airways were "the major site of resistance in obstructive lung disease", generated a lot of interest in small airways morphometry. The findings of these studies though have often been contradictory. Work on a series of related papers, by essentially the same research group, (Linhartova *et al* 1971, 1973, 1974, 1977, 1982 and 1983 and Anderson and Foraker 1962) provides a large body of evidence, both morphometric and diagramatic, which depicts an association between the

distortion of small airways and the presence of emphysema. Summarising their work, they found bronchioles in severe emphysema to be smaller, more tortuous, more stenotic, have thicker walls, fewer radial septae, aspherical (2-D) and non-cylindrical (3-D) and more prone to collapse. These changes were found to be irregularly distributed along a longitudinal axis.

This, and other work, has therefore demonstrated the coexistence of small airway distortion and emphysema, however, the functional contribution of small airway narrowing has been questioned. Contrasting the number and dimensions of small airways in emphysematous and non-emphysematous lungs Matsuba and Thurlbeck (1971 and 1972) found there to be insufficient change in small airways to account for the measured increase in airway resistance. From their work they opined that airflow resistance in emphysema was probably increased as a result of loss of elastic recoil, central flow limitation and associated chronic bronchitis (eg mucus plugging).

Niewoehner and Kleinerman (1974) contradict not only the latters findings but also the background assumptions made by Hogg and coworkers and Matsuba and Thurlbeck. These authors obtained a high and strikingly linear correlation (r=0.9) between inspiratory conductance and mean bronchiolar diameter while the correlation with segmental diameter was weak. Contrary to Hogg *et al*, Niewhoener and Kleinerman found airway resistance of small airways to be "considerably higher than previously thought" and to substantially increase with age. They therefore condidered that the Poiseuille flow model used by Matsuba and Thurlbeck to interpret their results ie that a halving of mean bronchiolar diameter was necessary to account for their observed increases in airway resistance, to be inappropriate. From their correlation, between inspiratory conductance and bronchiolar diameter, the

small decrease in bronchiolar diameter observed by Matsuba and Thurlbeck would be sufficient to account for the measured increase in airway resistance especially as the mean age of their sample was so high (mean age was 64 years old).

A large and extensive semiquantitative study (sample size 242) by Mitchell *et al* (1977) reported the severity of destructive emphysema (as assessed by panel grading technique) to be highly associated with the severity of chronic airway obstruction. Their analysis utilised contingency tables. From their tables it is clear that emphysema and CAO can be present without the other. It is therefore unlikely that there was a linear relationship between these variables for their cases. Measures of small airway calibre and density were included as were semiquantitative assessments of airways pathology including fibrosis, chronic inflammation, goblet cell metaplasia and mucous gland enlargement. These correlated poorly with the presence of CAO.

As outlined above, methods of scoring airways have been developed by other workers most notably by Cosio *et al* (1977). Other developments have seen the use of test specifically devised to assess small airway function eg the single breath nitrogen test. Relating small airway pathology scores to certain small airways tests Cosio and coworkers (1977) found that closing capacity, $V_{iso}V$ and the slope of phase III were associated with higher total pathology scores. A major criticism of this paper must be that the baseline group against which all others were compared were younger and had smoked less than the remaining groups.

In two papers (Niewoehner *et al* 1974 and Cosio *et al* 1980) comparing the small airways of smokers and non-smokers the authors hypothesised that small airways disease preceded and predisposed lungs to centriacinar

emphysema. This appeared to be substantiated by the finding that small airways were more diseased in upper than lower lobes (Cosio *et al* 1980). This latter finding has not been confirmed by other studies (Berend 1981 and Wright *et al* 1984). The former found small airway inflammation to be greater in lower lobes even where emphysema was predominant in upper lobes, whereas the latter group, excluding slightly increased inflammation of respiratory bronchioles, found no difference in small airway inflammation between upper and lower lobes and found no association with the presence of CAE.

Comparing bronchiolar pathology scores Cosio *et al* (1980), found goblet cell metaplasia, smooth muscle hypertrophy and mural inflammation to be higher in smokers than non-smokers. A similar study Wright *et al* (1983), reported few differences in graded membranous bronchiolar pathology with only goblet cell metaplasia being significantly increased. In contrast, they found significant differences in respiratory bronchiolar inflammation, pigment and fibrosis. An important observation made by Wright in this study was that although lung function was demonstrably better in ex- as opposed to current smokers there was no differences in small airway pathology including inflammation.

Petty *et al* (1984) using autopsy lungs demonstrated a weak ($r=-0.3$), but significant correlation between mean bronchiolar diameter and total pathology score. This is perhaps surprising in that other studies have failed to show differences in bronchiolar diameter between emphysematous and non-emphysematous lungs (Matsuba and Thurlbeck 1971 and 1972, Petty *et al* 1986 and Hale *et al* 1984) and smokers and non-smokers (Cosio *et al* 1980), yet the variables included in the pathology score are smoking related (Cosio *et*

al 1980). Also surprising was Petty's finding that fibrosis was correlated with mean bronchiolar diameter as this had failed to be a discriminating factor in other studies (Niewoehner *et al* 1974, Mitchell *et al* 1976, Wright *et al* 1983 and Cosio *et al* 1980).

A recent and extensive study has been carried out by Nagai, West and Thurlbeck (1985a and 1985b). Appreciating that the majority of previous studies had set out to measure either central airways, peripheral airways or emphysema in detail, these authors set out to complete detailed measurements on all three. Their study group consisted of patients with moderate to severe chronic airflow obstruction most of whom had severe emphysema. An age controlled group of non-smokers was assembled to provide baseline data.

The following morphologic features were found to differ between the two groups, bronchiolar muscle proportion, internal diameter, volume proportion of bronchioles, bronchiolar shape and the proportion of bronchioles with an internal diameter less than 400μm (P400). However, inter-relationships between morphometric variables were poor. These findings led the authors to conclude that all the changes were "smoking related".

Relationships with function (Nagai *et al* 1985b) were similarly poor, notably bronchiolar inflammation, fibrosis and the total pathology score as assessed by the Cosio technique were found to be unimportant. The degree of emphysema did correlate with tests of expiratory flow, the slope of phase III and residual volume. P400 and bronchiolar shape also correlated with these variables and also with dyspnea and PaO_2. These latter findings are interesting in that dyspnea and PaO_2 correlate with bronchiolar parameters but not with the extent of emphysema itself. Further analysis revealed that increased

bronchiolar muscle and fibrosis were beneficial possibly enhancing bronchiolar integrity where radial traction may have been compromised.

1.5.6. CT Scanning

Wegener *et al* (1978) proposed CT scanning to detect the presence of emphysema. Rosenblum *et al* (1980) quote, as a potential use of CT scanning, the diagnosis of early emphysema. This potential ability is based upon the following advantages that CT scanning has over conventional radiography: greater sensitivity, the ability to present a transaxial view of structures internal to the lung free from the overlying pleura and a greater dynamic range. Their group, in a preliminary publication, had already reported differences in mean lung density between emphysematous and non-emphysematous cases (Rosenblum *et al*, 1978). Supporting this Bergin *et al* (1986) reported qualitative differences between the CT scan of cases with mild as opposed to moderate macroscopic emphysema. A preliminary report involving eleven of the cases in this present study, found similar results in that cases with CAE lesions had proportionately more pixels with a lower lung density than those with no apparent macroscopic emphysema (Hayhurst *et al*, 1984) although there was no straight forward linear relationship.

Over all loss of alveolar walls in this study is measured as the amount of macroscopic emphysema present in the mid-sagittal slice and as alveolar surface area *per* unit volume of lung tissue. The opportunity then arises to investigate whether decreases in lung density, measured by CT scan, correlates with any of these two parameters. (This being a more stringent analysis than testing for differences between the group means of cases with and without emphysema).

CHAPTER 2

MATERIAL AND METHODS

2.1. METHODOLOGY

2.1.1. Sample Population

The sample population consists of patients diagnosed as having a probable peripheral carcinoma of the lung and who were suitable for both surgery and physiological assessment of lung function. Just over 120 such cases were obtained, forty four of whom were suitable for morphometry the details of which (age sex height etc.) are given in the appendix.

2.1.1.1. Criteria for Inclusion

Pneumonectomies were used where one lobe was uninvolved by tumour, and, in particular, where there was no involvement of any of the proximal airways that ventilated the unaffected lobe. In three cases, complete lungs were suitable for sampling, as, not only was there an uninvolved lobe, but the lesion was limited to a discrete segment in the affected lobe. Lobectomy specimens were accepted where there was a small peripheral lesion or where the lesion was clearly limited to one segment.

The assistance of an experienced consultant lung pathologist (cf acknowledgements) must be noted here, as expert advice was required at this stage to decide which specimens were suitable for morphometry.

Of the suitable specimens, 28 were lobectomies and 16 were pneumonectomies. The lobe or lung sampled in each case is noted in the appendix.

2.1.1.2. Criteria for Exclusion

Cases with a central tumour with or without distal pneumonia, or extensive tumour within a lobectomy were excluded from the sample. In particular, cases were excluded where there was involvement of the proximal airways. Also excluded were cases where other specific disease states existed eg asthma, fibrosis etc or where part of their treatment had involved chemotherapy. In practice, the latter conditions involved only a handful of cases. Most cases were excluded on the basis of tumour location.

2.1.2. Collection of Tissue

Fresh tissue was obtained by being present as surgery was performed at the Thoracic Theatre, City Hospital, Edinburgh. Immediately after resection specimens were taken to the Pathology Department, Edinburgh University Medical School.

2.1.3. Fixation of tissue

Specimens were fixed at inflation using Millonig's buffered phosphate paraformaldehyde solution. This formaldehyde based fixative was prepared using the following constituents.

- Cold water (10 litres).
- Sodium hydroxide (84g).
- Sodium dihydrogen orthophosphate (372g).
- 40% formaldehyde (2 litres).

The above solution is made up to a capacity of 20 litres using cold water.

This, like most other fixatives, acts on the proteins within the tissue, rendering them insoluble and thereby preserving the most important tissue components. This has the same properties as formalin and as such is a non-coagulant fixative (Baker 1966), in that it forms additions with proteins within the tissue. It has good penetration and causes little tissue hardening or shrinkage (Disbrey and Rack 1970) and is well buffered. Histologically, it gives good sub-cellular preservation providing material which is suitable for electron microscopy (Carson *et al* 1973).

2.1.3.1. Inflation/Fixation of tissue

ATS "NATURAL CONTOUR" INFLATION TECHNIQUE

This technique was recommended by the American Thoracic Society's committee on the preparation of lungs for macroscopic and microscopic study (1959). This study follows the same basic procedure, accepting that the preparation is simpler when applied to resected specimens.

A catheter is manually positioned and held in the largest available airway(s). This is connected to a head of fixative situated 25 to 30 cm H_20 above the lung. Formalin is then allowed to flow at pressure down into the lungs, which are inflated until the the "natural contours" of the pleura are established ie until pleura is completely smooth and firm. Once this situation is obtained the lungs are floated in a basin containing fixative, covered by wet toweling to prevent drying, and left for a minimum of three days to fix.

CONSTANT PRESSURE INFLATION

The principle of this technique is to inflate lungs at a transpulmonary pressure of 25 to 30cm H_2O, ie that required *in vivo* to obtain TLC, and to maintain this pressure for a given period of time. The method used here is an adaptation of that described by Heard in 1958 and later revised in further methodology paper in 1960. The apparatus (depicted in figure 2.1) consists of a large holding tank over which a formalin reservoir is placed. Both contain fixative: the larger some forty litres while the reservoir has sufficient to raise the level within it to a height of between 25 to 30 centimetres above that within the larger tank. A system of silicone tubing runs down from the reservoir to two catheters suspended immediately above the large holding tank. The return system consists of a glass tube, succeeded by more silicone tubing that runs back to the reservoir via a peristaltic pump.

Initial inflation is achieved using the natural contour technique described immediately above. Following this lungs are floated in the large holding tank with the main bronchus attached to one of the catheters. Formalin flows down and enters the lungs via the catheters at the predetermined pressure. The peristaltic pump removes any excess fixative (leaked from vessels etc.) back to the formalin reservoir via the glass tube preset at the initial level of fixative within the large holding tank. This maintains the height of fixative within the desired range of 25–30 centimetres.

Figure 2.1. Constant Pressure Inflation Apparatus. After being inflated using the natural contour technique lungs are placed in the large holding tank and connected to the inflation apparatus by the main bronchi using catheters. Formalin flows into the lungs at a pressure of 25 to 30cm H_2O for three days.

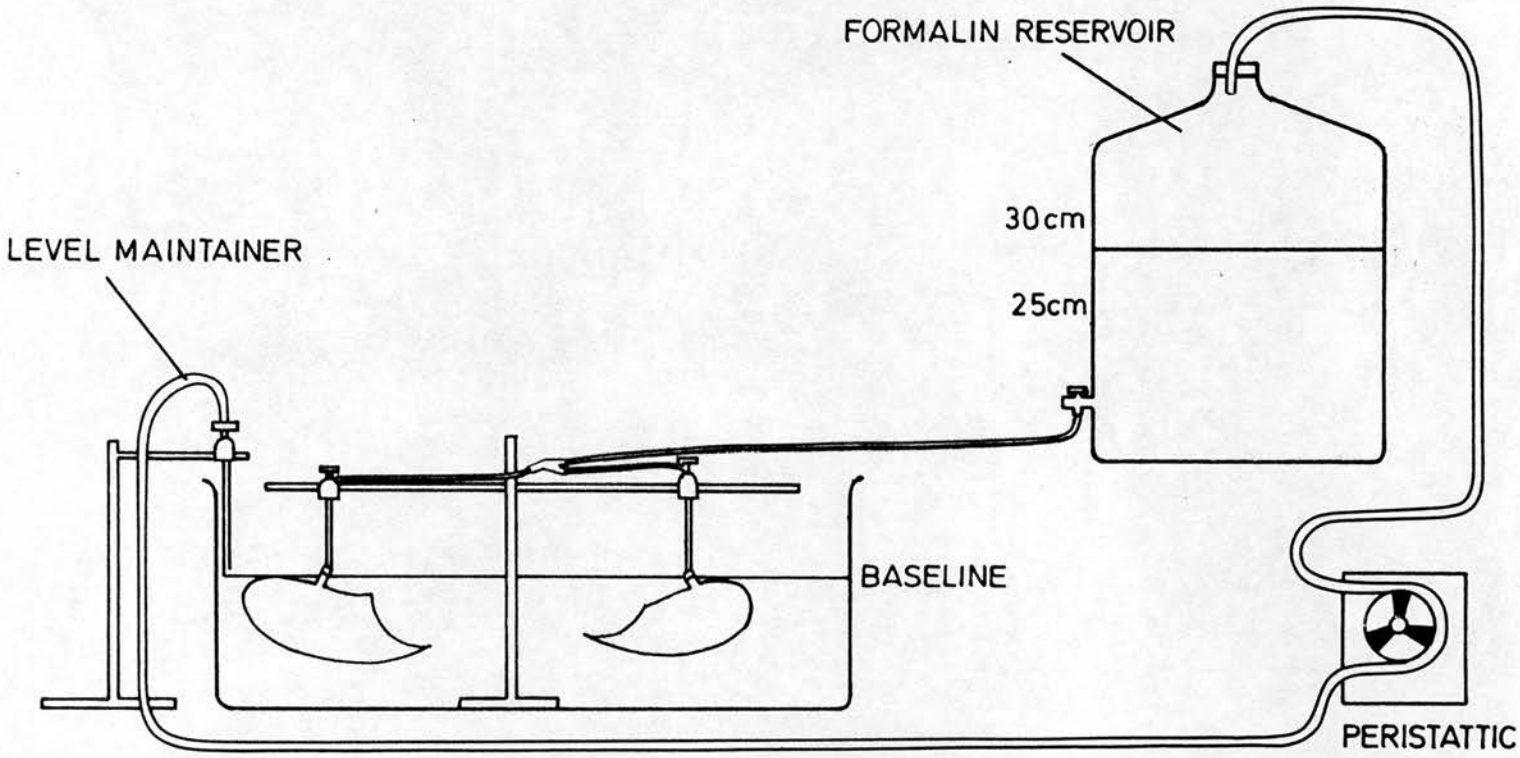

INFLATION APPARATUS

2.1.4. Specimen trimming technique

The lungs or lobes are placed on a cutting board with their hilar aspect uppermost. This board has 1 centimetre high raised edges. By sliding a large carving knife with an even force along these edges the specimens were cut into 1cm parasagittal slices. These slices were numbered P1 to Pn from the lateral to the hilar aspect. As these specimens were required for clinical diagnosis this trimming was carried out by a lung pathologist.

2.1.5. Tissue Sampling

In practice, most specimens were cut into 5 x 1cm slices. The two most hilar slices were utilised for the unimpeded sampling of large airways, (large airways were sampled from these cases as part of another on-going project) while the mid-sagittal slice was left intact for the macroscopic assessment of emphysema. A total of twelve blocks, measuring 1.9cm by 1.9 cm (ie 3/4 of an inch), were sampled from each case for the quantitation of small airways and alveolar parenchyma. Sampling was from the two most immediately lateral subpleural slices (p1 and p2) with 6 blocks being taken from each.

These blocks were sampled randomly by first placing a polythene sheet, marked out in 1.9cm squares, over the lung slices. Computer generated random numbers were then used to select six areas from each slice. A square was accepted only if it completely overlapped an area of the lung slice. Where there was a local disorder of lung tissue (eg tumour) selection was restricted to tissue at least one complete square from the zone where normal tissue architecture was seen to be restored.

Once selected, the lung tissue was trimmed using a scalpel blade in

conjunction with a template precisely machined to the required size. Blocks were kept to a depth of less than 0.5cm to facilitate optimum penetration of processing fluids, as suggested by Aherne and Dunnill (1982).

2.1.6. Tissue Embedding

2.1.6.1. Tissue Embedded in Paraffin Wax

This is an exceedingly common and well-established procedure easily obtained from any histological textbook eg Carleton's Histological Technique (Drury and Wellington 1967). A brief summary of the method should therefore suffice. Tissue is dehydrated prior to embedding by taking it through an ascending alcohol series into xylene. The tissue is then embedded in paraffin wax with a melting point of 56 degrees centigrade and placed in a vacuum oven.

2.1.6.2. Tissue Embedded in GMA

Once trimmed, the blocks were embedded in the acrylic resin glycol methacrylate (GMA) the constituents of which are:

Reagents for glycol methacrylate embedding

Solution A (Infiltrating solution)

- 2 Hydroxyethyl methacrylate 400ml.
- 2 Butoxyethyl methacrylate 35ml.
- Benzoyl peroxide.

(The benzoyl peroxide is added last and stirred continuously for two hours).

Solution B (Promoter solution)

- Polyethylene glycol 8ml.
- N,N dimethylaniline 1ml.

The final GMA mixture is achieved by adding the two solutions in the amounts (or proportions) given below.

- Solution A 42ml.
- Solution B 1ml.

The technique described below for GMA embedding is a variation of that described by Simms (1974) with the tissue being placed in each solution for a period of 2 hours.

Dehydration

- 10% ethanol
- 20% ethanol
- 30% ethanol
- 50% ethanol
- 80% ethanol
- 64 O.P. spirit
- 64 O.P. spirit
- 74 O.P. spirit

- 74 O.P. spirit
- Acetone
- Absolute alcohol

The alcohol within the tissue is gradually replaced with solution A of GMA. This impregnation is achieved by standing the tissue, immersed in solution A, inside a vacuum at a pressure of 15lbs. Two to three days are required for complete impregnation with fresh solution A being added every twenty four hours.

The final solution of GMA is obtained by adding solution B. A homogeneous mixture is assured by rotating the promoter and infiltrating solutions on a roller for five minutes. After rotation, the blocks of tissue are placed in small plastic moulds and orientated within the GMA. Addition of solution B causes an exothermic polymerisation reaction. To slow this reaction and prevent "bubbling" of the GMA the moulds are placed on crushed ice for one hour. The moulds are then peeled off and the blocks hardened in an oven at sixty degrees centigrade.

2.1.7. Tissue Sectioning

Blocks embedded in GMA were sectioned at 3um using a Reichart Jung Autocut with a tungsten carbide knife.

2.1.8. Staining of Tissue Sections

Haematoxylin and eosin (H&E) dyes were used. These gave good definition between epithelium, airway wall and the background unstained lumen.

Similarly, they gave staining of alveoli suitable for automatic image analysis. The method used here -to stain the sections with H&E- is similar to that outlined by Disbrey and Rack (1970).

2.2. TECHNIQUES USED IN QUANTITATION

2.2.1. Image analysers

2.2.1.1. Introduction

All measurements of area, surface area, diameters, ellipticality etc. were made using image analysers. The components and *modus operandi* of these are described below. The actual measurements carried out and the precise use of the image analysers to that end are described in the next section.

2.2.1.2. Semi-Automatic Image Analyser

The semi-automatic image analyser was purchased as a complete unit from Graphic Information Systems Ltd (GIS), Blairgowrie, Scotland and comprises the following (please refer to figure 2.2):

- Tektronix 4050 series programmable microprocessor.
- Digitiser tablet (52cm x 52cm).
- Cursor with light emitting diode (LED) and 4 flag input.
- General purpose interface bus.
- Line printer: Epsom MX-80F/T.

The Tektronix can be viewed as the host computer of the GIS unit. It is

programmable in BASIC and has a single 7 inch tape drive. It interfaces with the line printer, hard copy unit and the digitising tablet.

Used together the digitiser tablet and the LED constitute an x/y-co-ordinate measuring system. The digitising tablet defines the location of the LED as polar coordinates within the range 0-5200 for both the x- and y-axis and to an accuracy of 0.1mm. The LED is activated by pressing one of its 4 input keys. This relays x and y coordinates to the computer along with a "flag" identifying the activated key. Coordinates can be relayed in "point" or "stream" mode. The former relays a single point or locus whereas the latter allows a stream of points to be input.

Point mode is used to measure simple parameters such as diameters. Stream mode enables the manual recording of objects by tracing their profiles with the LED thereby allowing more complex parameters such as area, perimeter and shape to be quantified. To aid digitising, programmes were written so that the profiles of objects being defined were displayed upon the screen thereby allowing the user to monitor their progressive delineation.

USE IN LIGHT MICROSCOPY

Used simply, photographs, drawings or X-rays can be placed upon the tablet and objects of interest digitised. Where measurements from histological sections are to be made a light microscope with a *camera lucida* attachment is necessary. In this study a Leitz zoom *camera lucida* with x12.5 in-line eyepiece used in conjunction with a Leitz SM-Lux microscope (Leitz, Luton, England) was used with the GIS unit. The function of the *camera lucida* is to superimpose the LED upon the section thereby allowing the coordinates of the desired structure to be defined. As the computer is programmable calibration

factors can be calculated for different magnifications using a suitable micrometer slide. Two micrometer slides were used, one was 1cm in length and was marked out in 10 x 1mm and 100 x 0.1mm divisions (Graticules Ltd, Tonbridge, Kent, England) and was used to calibrate for the x2.5 objective, the other was 2mm in length and was marked out in 2 x 1mm divisions and 20 x 0.1mm divisions (Graticules Ltd.). The latter slide was used to calibrate the GIS for the other objectives. The input keys on the cursor allow calibration factors for four objective lenses to be stored at any one time.

Lastly a limited range, or digitising window, of the tablet is covered by the *camera lucida*. In practice this window was 2500 x-axis by 2500 y-axis board units.

Figure 2.2. GIS Semi-Automatic Image Analyser. This figure is a schematic representation of the GIS unit. Its main components and *modus operandi* are fully described in section 2.2.1.2. (The transducer is the cursor which comes with an LED.)

Figure 2.3. IBAS-2 Automatic Image Analyser. Section 2.2.1.3. has a full description of the components and *modus operandi* of this machine. The labelled components are A, the IBAS-1 semi-automatic evaluation unit; B, the IBAS-2 image processing unit; C, Bosch black and white camera; D, program and data monitor; E, image monitor and F, the digitising tablet with cursor.

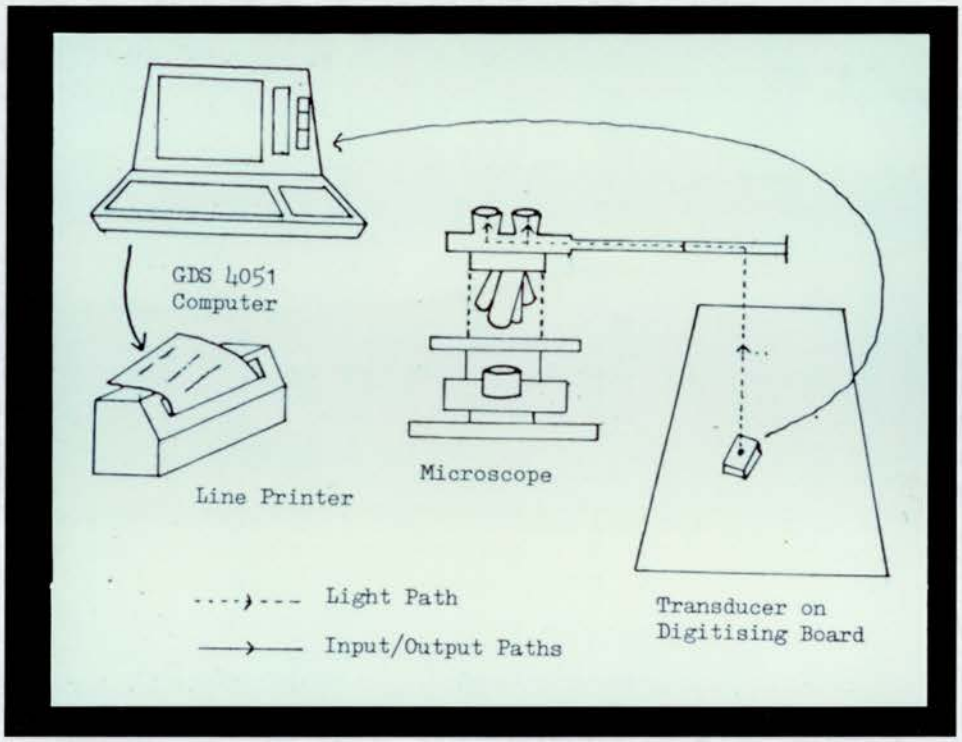
GDS 4051
Computer
Line Printer
Microscope
Transducer on
Digitising Board
Light Path
Input/Output Paths


A
B
C
D
E
F
BOSCH
IBAS

2.2.1.3. Automatic Image Analyser

An IBAS2 image analyser (Kontron Ltd, Watford, England) was used. This comprises the following units (refer to diagram 2.3):

IBAS-1 SEMI AUTOMATIC EVALUATION UNIT AND HOST COMPUTER

This consist of:

- Z80A CPU.
- 64K RAM.
- 16K graphic memory.
- Digitiser tablet (28cm x 28cm).
- Keyboard.
- Data monitor.
- Twin 8.5 inch disc drive units.

IBAS-2 Image processing unit

This consists of:

- TV frame grabber.
- Array processor.
- Video controller.
- Image memory.
- Black and white monitor.
- TV camera with chalnicon tube (Bosch type TYK 9A).
- Line printer (OKI U93 microline).

As outlined above, this system consists of two potentially separate units IBAS1 and IBAS2. IBAS1 is analagous to the GIS system while IBAS2 supplies the automatic image processing facilities.

IBAS1 Semi-Automatic Evaluation Unit

IBAS1 is similar to the Tektronix in that, with 64K bytes of RAM, it is the host computer for the complete IBAS system. The function and operation of this unit is virtually identical to that of the GIS and the description and *modus operandi* given above for the latter almost fully matches that for the IBAS1, with a few exceptions. The IBAS1 has two 8.5 inch floppy disc drives which give quicker data and program retrieval. The digitiser tablet of the IBAS1 is smaller but has the same accuracy ie 0.1mm. Lastly although programmable, IBAS1 measuring programmes are assembled from options displayed on a digitiser menufield. In this way programmes are progressively constructed in a piecemeal and stepwise fashion. This makes IBAS1 programmes more rigid and in practice programmes written (by the author) for the GIS were more user friendly and simpler and quicker to use. Hence, where semi-automatic image analysis tasks alone were required the GIS system was used.

IBAS2 Image Processing Unit

The main components of the IBAS2 are the Video Input/Output Board (VIOB), Video Matrix Board (VMB), Microprogrammable Image Array Processor (MIAP) and Memory Address Controller (MAC).

The function of the VIOB is to provide analogue-to-digital conversion of images input to the monitor via the TV camera. These images are converted to grey levels within the range 0 (black) to 255 (white) and stored as digital grey-tone images in the VMB (or 'Frame Grabber'). In practise, around 15

images measuring 512 by 512 pixels can be stored at one time. The MIAP facilitates a variety of manipulations to be carried out on the stored images including image multiplication, subtraction, addition and digital filtering. Lastly, the MAC organises the addressing of image memory sections as well as translating and displaying the position of the cursor on the digitiser tablet onto both the data and television monitors. This latter function permits cursor-based interactive image editing as well as program construction and execution.

Using IBAS as an automatic image analyser

The operating system of IBAS2 offers a number of commands - displayed along the top of the monitor -which assist in program construction and execution. These facilities are invoked by either single character inputs from the keyboard or by using the cursor. The latter is achieved by pressing the input key on the cursor when it is located over one of the command functions (as outlined in the section immediately above, one of the functions of the MAC is to display the digitiser location of the cursor onto both monitors). When a command is invoked it is highlighted on the screen and it's function is made available to the operator. The operating commands available to the user act upon either single statements or the complete program. Single statement operators include statement insertion (INS), deletion (DEL), and stepwise execution (STEP). Commands operating on the complete program include program listing (PRINT), execution (EXEC) paging (PAGE) and (PUP) and exit (EXIT).

IBAS has it's own high level language for program construction with approximately 150 program statements to choose from. These statements identify subroutines which carry out specific computer functions eg image

subtraction. Automatic image analysis programmes are therefore constructed by selecting and arranging a number of these functions to solve a particular quantitation problem. For ease-of-use the 150 program subroutines available are divided into 8 main categories which are displayed along the left hand side of the data monitor. All the subroutines held under any one category can be displayed in the centre of the monitor by activating the category with the cursor. Most subroutines have a selection of parameters which direct or modify their application. On selecting a particular subroutine, again using the cursor, the parameters relevant to it are displayed in the lower centre portion of the monitor. Once the desired controlling parameters are selected the subroutine is inserted into the program which is listed at the right hand side of the screen.

The structure and execution of the IBAS programme written to quantitate alveolar surface area is given in the next in section.

2.2.2. Computerised Axial Tomography

2.2.2.1. Introduction

Computerised axial tomography (CT) scanners measure density by comparing the X-ray attenuation of various structures with that of water, the latter being rated as zero to provide a standard against which all materials can be compared (Hayhurst *et al* (1984). The unit of measurement of attenuation is either the Hounsfield Unit (HU) or for EMI scanners the EMI unit. These two units are directly comparable in that 2HUs = 1EMI. Being a computer based device the reference area is a pixel (picture element). For the scanner used in this study -this being an EMI CT 5005 whole body scanner- each pixel refers to an area 1.25mm square and 13mm thick. Hence, all measurements are

average attenuations of tissue of this unit volume.

EMI units of attenuation for various structures are presented in figure 2.4. This illustrates the standardised score of water as zero, bone as +500 and air as -500.

2.2.2.2. Cases Used

Twenty eight cases had CT scans. These are identified in the appendix.

2.2.2.3. CT Scan Procedure

To ensure accuracy between measurements, the CT scanner was recalibrated each day using a water phantom. Each scan was carried out with the patient holding his breadth, within 500ml of total lung capacity, for 17 seconds. Frequency distributions of the pixel values (as EMI units) were obtained for each case -having excluded readings obtained from the hilar region of the lung and, if present, any solid mass or tumour. Data from the 6cm and 10cm slices (measured from the sternal notch) were pooled. This method has previously been documented by Hayhurst *et al* and has since been updated by Gould *et al* (1987).

Figure 2.4. Standard reference units for the EMI 5005 scanner. The density of structures is compared to that of water which is rated as 0 EMI units. Using the EMI scale bone is rated as 500 EMI units while air obtains a value of -500 EMI units.

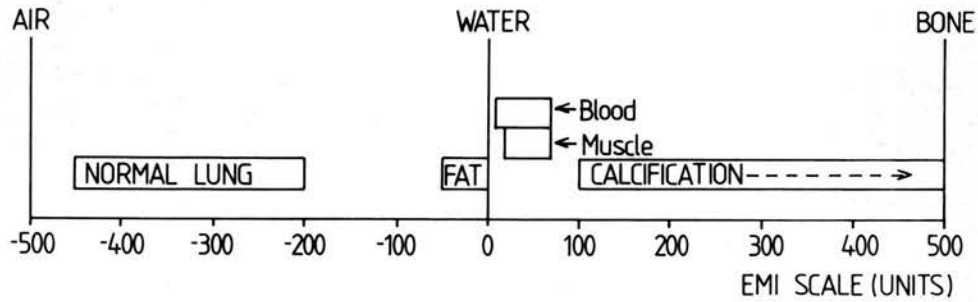

Adapted from EMI Medical Chart 1979

2.3. STATISTICAL ANALYSIS

SPSSx (Statistical Package for Social Studies -version x) package was used for both bivariate and multivariate correlation and regression analysis.

As more than one type of regression analysis is available it is pertinent at this point to describe the model used in this study along with any other relevant parameters involved. The BACKWARD regression method (SPSSX Users Guide) was used to input data into the regression equation. This entails inputing all the potentially independent (causative) variables into the regression equation at the start of the regression analysis. The predictive value of each variable is then assessed as the partial regression coefficient. This indicates the magnitude of change brought about in the dependent or effected variable, by each of the independent or causative variables. The significance of each partial regression line is tested by a t-test. This entails dividing the slope of each line by its standard error. If there are any independent variables which provide non-significant partial regression slopes, the one which has the least significance (probability) is removed. The regression equation and partial regression coefficients are then recalculated. This sequence is repeated until the regression equation contains only those independent variables which have significant partial regression slopes.

Multiple regression as a tool is used to identify those variables which have a significant predictive effect on a given dependent variable. However, it is also a compromise between increasing the amount of variation explained in the dependent variable while identifying only those independent variables which have significant predictive value. To balance this objective (of explaining as much of the variation as possible while identifying only those independent

variables which have a significant predictive effect) those independent variables whose slope has an associated probability of 0.1 or less are maintained within the regression equation. This is a standard guideline (SPSSx Users Guide and Sokal and Rohlf 1980).

Two null hypotheses were tested for each multiple regression equation. The first of these was that the coefficient of multiple determination (R^2) was zero. That is, that the variation of the dependent variable explained by the combination of independent variables is zero. The second is that all the slopes of the partial regression coefficients are zero, ie $b_1 = b_2 = b_n = 0$. (Sokal and Rohlf).

Partial regression coefficients express the rate of change (in the dependent variable) as a combination of the original units in which the dependent and independent variables are measured eg litres *per* year. As these make comparisons between independent variables very difficult to assess standardised partial regression coefficients are quoted. These give the rate of change in the dependent variable *per* one standard deviation change in the independent variables. Hence, the relative magnitude of independent or predictive variables can be assessed.

It should be noted that regression analysis assumes a model of cause-and-effect. This model makes the assumption that changes in the dependent variables directly cause changes in the independent variable. This model will only be tenable in certain instances, for example where there is published data indicating that such a cause-and-effect relationship exists. Elsewhere it may be less plausible to propose cause-and-effect arguments.

Where cause-and-effect models are inappropriate, partial correlation

coefficients are calculated. These assume a simpler model than regression analysis and represent the degree of covariance between two variables. As with standardised partial regression coefficients, where 3 or more variables are analysed, partial correlation coefficients are calculated for two variables with the others held constant. Sokal and Rohlf and Schroeder *et al* (1986) document this type of multivariate analysis and discuss the appropriateness of correlation as opposed to regression analysis.

Schroeder summarises the difference between the models of regression and correlation thus:

> "While this general relationship between r and b will always hold, one might ask if one of these two measures provides more information than the other. The answer is that the regression coefficient is more informative since it indicates by how much the dependent variable changes as the independent variable changes, whereas the correlation coefficient indicates only whether or not the two variables move in the same or opposite directions and the degree of linear association. This additional information from regression is obtained, however, only at the cost of a more restrictive assumption -namely, that the dependent variable is a function of the independent variable. It is not necessary to designate which is the dependent and which is the independent variable when a correlation coefficient is obtained."

Hartwigg and Dearing (1978) recommend exploratory analysis of bivariate correlations as outliers on plots can often mask the over all strength of otherwise important and valid correlations. Their examples demonstrate that there are often unique factors which make points outliers, factors that when identified may add to the understanding of the original relationship. Similarly, outliers may suggest significant relationships where in fact there is little association between the variables. Exploratory data analysis of the type recommended by Hartwigg and Dearing is carried out prior to the use of more

complicated multivariate analysis.

2.4. PARAMETERS MEASURED

2.4.1. Quantitation of Airspace Surface Area *per* Unit Volume (AWUV)

2.4.1.1. Source of Tissue

The cases used are identified in the appendix.

2.4.1.2. Summary of Tissue Handling

Lungs/lobes were inflated and fixed using the ATS natural contour technique (section 2.3.1.1.) and cut into 1cm parasagittal slices (section 2.1.4.). Twelve random blocks were taken *per* case using the procedure given above (section 2.1.5.), these were embedded in GMA (section 2.1.6.2.), sections cut at 3µm (section 2.1.7.) and stained with H&E (section 2.1.8.).

2.4.1.3. Quantitation of AWUV

Airspace surface area *per* unit lung volume (AWUV) is obtained by first measuring alveolar perimeter *per* unit area (APUA). APUA itself is measured directly -using the IBAS image analyser- from randomly selected fields.

The technique employed was to treat all twelve sections *per case* as the one sample unit. That is, a mean alveolar perimeter value was obtained for the twelve sections as a whole not for each individual section. Sample size was determined by constructing a running mean for each case (Aherne and Dunnill 1982) using the criteria that the mean must not vary by more than 3% for 5 consecutive fields and must not exhibit a constant upwards or downwards

trend. A minimum of 20 fields were analysed *per* case.

AWUV is obtained by mathematically transforming this mean value using the formula given below :

$$AWUV = APUA \times 4/\pi$$

and was taken to be representative for the case from which the twelve blocks were sampled.

A justification for this mathematical transformation is given in the appendix.

2.4.1.4. Random Selection of Fields

RANDOM SELECTION OF SECTIONS

Successive fields were chosen by first randomly selecting one of the 12 sections and then randomly selecting a field from that particular section. In practice random numbers from 1 to 12 -generated by the Tektronix- were used to select the order in which sections were chosen. Once APUA had been quantified for that field the section was returned to the sample "pool" from whence it could again be selected.

SELECTING A RANDOM FIELD FROM WITHIN A SECTION

The main tool used for the selection of random fields is the England Finder (Graticules Ltd, Tonbridge, Kent), cf Figure 2.5. This is a glass slide of standard dimensions (3.5 inches by 2.0 inches) marked out in squares which are labelled

from 1 to 75 along the X-axis and from A to Z along the Y-axis. This gives the England Finder the same properties as the grid reference system (rectangular coordinates) used in cartography in that any area or structure upon a glass slide can be located as an X-axis numeric-coordinate and a Y-axis alpha-coordinate.

As the sections are square two England Finder reference coordinates are sufficient to define all the England Finder coordinates which correspond to areas of a glass slide occupied by a stained section.

That is, by locating the upper left and lower right vertices, as England Finder reference coordinates, the location of an entire section on a glass slide is known. A computer program was devised to calculate the total number of England Finder squares covered by the section, to generate random numbers within this range and to then translate these random numbers back into England Finder coordinates within the boundaries established by the upper and lower vertex coordinates.

The reference coordinates of the two vertices were identified using the following procedure. Each mounted section was placed on the microscope stage and viewed with a x2.5 objective. The stage was manoeuvred until the upper left hand side of the section was located. The section was then replaced by the England Finder and the coordinate noted. This procedure was repeated to find the coordinate for the lower right hand side of the section. A summary of stage 1 and stage 2 sampling for the measurement of AWUV is given in figure 2.6.

Figure 2.5. England Finder. This is a low power photomicrograph of the England Finder as viewed on the image monitor of the IBAS (x2.5 objective with x10.0 eyepieces) which illustrates its alphanumeric grid reference system.

Figure 2.6. Schematic summary of the sampling regime used in the quantitation of AWUV. Random blocks are taken from the first two lateral sub-pleural slices. Random areas on the processed section are located using random numbers and the grid reference system of the England Finder.

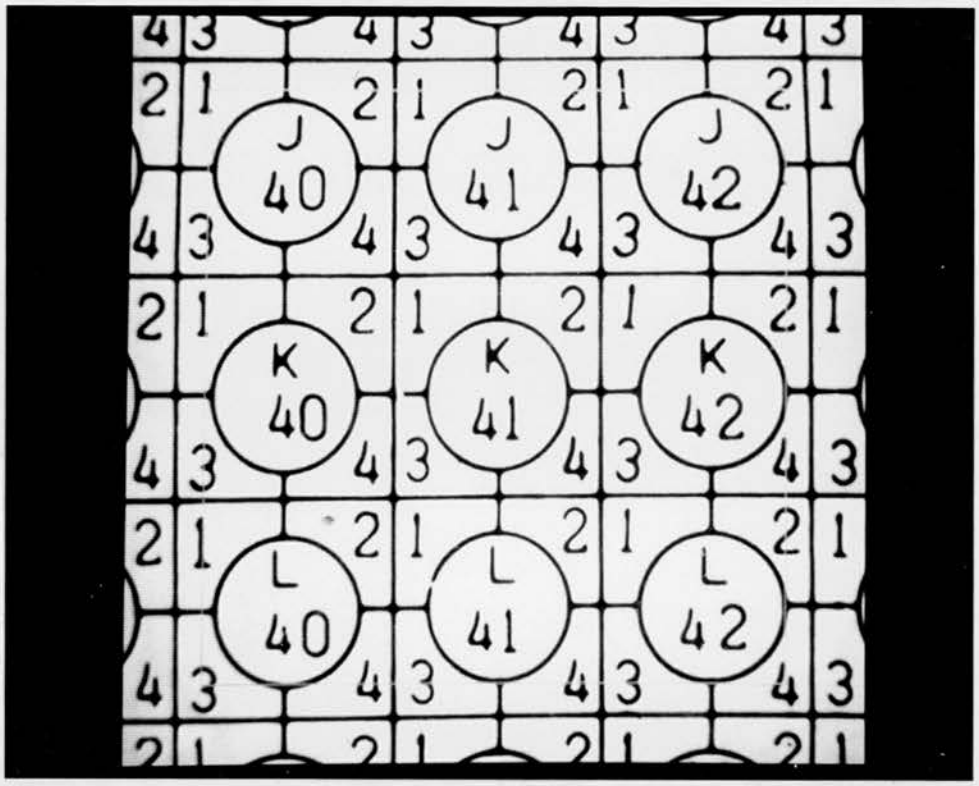
J 40
J 41
J 42
K 40
K 41
K 42
L 40
L 41
L 42

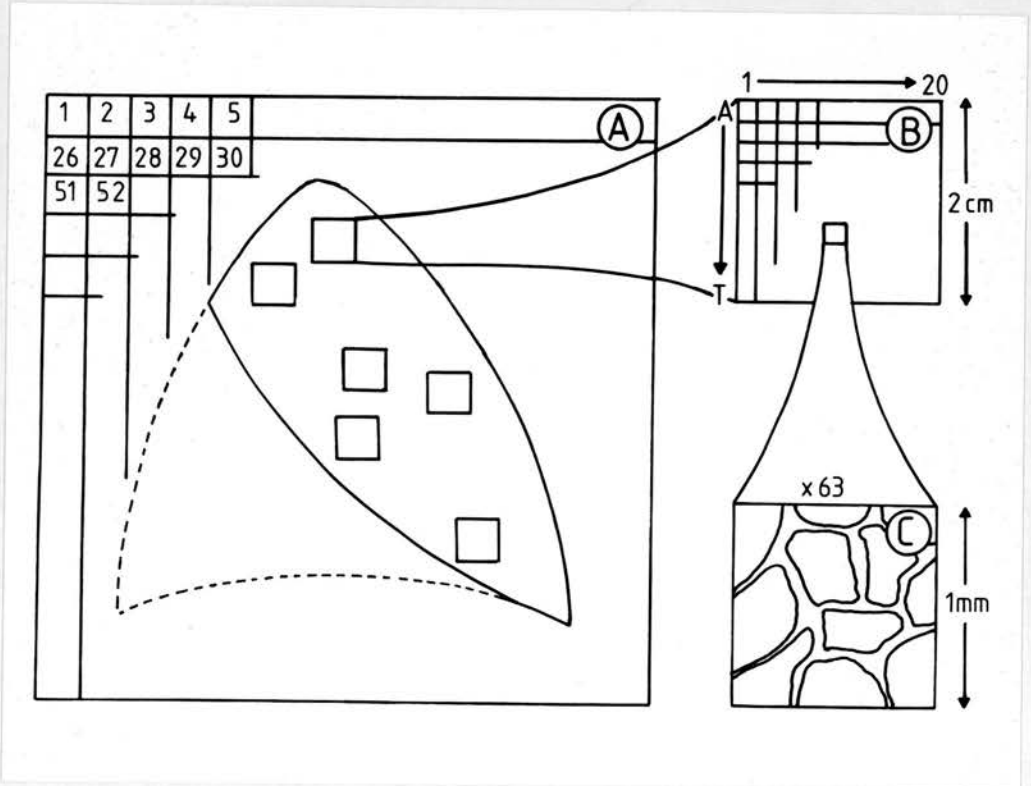
1 2 3 4 5
26 27 28 29 30
51 52
A
1
20
A
B
T
2 cm
x 63
C
1mm

This sampling procedure is not within current literature, but provides a cheap and simple alternative to other devices such as an automatic stage.

2.4.1.5. Quantitation of APUA using the IBAS image analyser

The IBAS image analyser is depicted in figure 2.3. and its components and *modus operandi* are described in section 2.2.1.3.

In the following pages (figure 2.7) the main image manipulations executed by the program are described and illustrated, while the tasks mainly involving "machine" functions eg file handling operations, are kept to a minimum.

Figure 2.7. Joint textual and illustrational description of the IBAS quantitation of AWUV.

File Handle.

A distinctive file handle, based upon the routine biopsy code, is established for each case to facilitate disc storage and retrieval of data.

CALIBRATION

Calibration.

IBAS is calibrated for the magnification being used (x6.3). This is done "on-line" by placing a micrometer slide onto the microscope stage, the image of which appears on the screen. Two points of the micrometer scale are input using the cursor. The distance between these two points is then input via the keyboard and the calibration factor calculated automatically by IBAS (see opposite). The square represents the $1mm^2$ measuring area and there is a thin line drawn between the two reference points used for in the calibration (in this case from 0.5mm to 1.5mm).

LOCATING AND STORING IMAGES

Location of a Random Field.

A section is randomly chosen from the sample of 12 and a randomly selected England Finder coordinate -from within the desired range- located and centred using a x10 objective (L38 in this example). The England Finder is the replaced by the relevant section and the x10 objective replaced by a x6.3 objective.

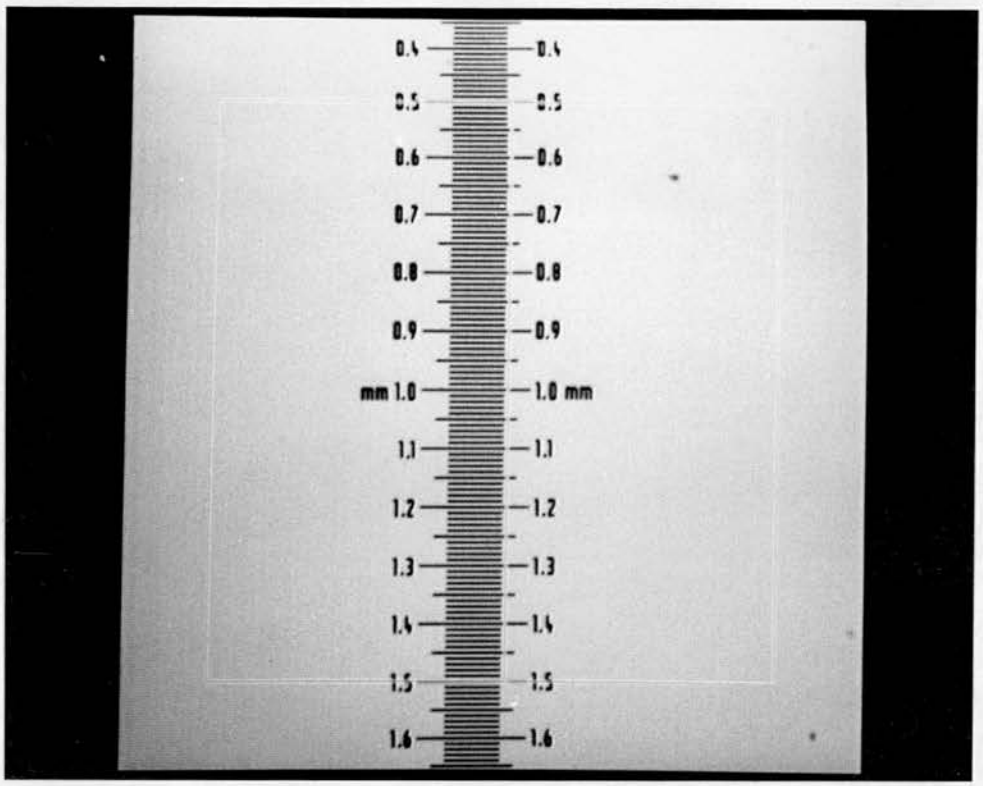
0.5
0.6
0.7
0.8
0.9
mm 1.0
1.1
1.2
1.3
1.4
1.5
1.6
1.0 mm

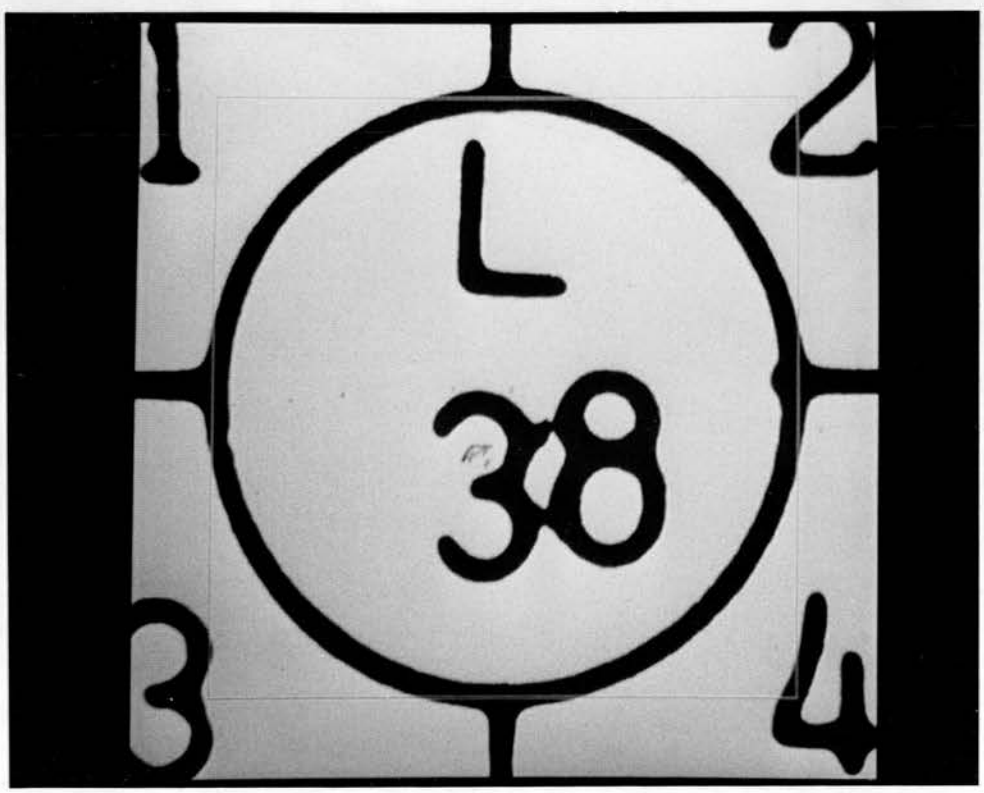
1
2
L
38
3
4

Image Input.

Each randomly selected field is located and it's image stored. To reduce the level of noise within the stored image 12 images were fed in consecutively, the final stored image being an average of these images.

IMAGE CLEANING

Shading Definition.

This function allows a reference image of the background illumination to be stored. These images were stored under the same conditions as those of the original image *vis a vis* focus, illumination and image averaging. Reference images were created by placing a clean glass slide upon the microscope stage and storing the image obtained.

Shading Correction. This function, using the reference image established above, executes a shading correction on the original image. In practice, the reference image should have a restricted grey level range. Extreme grey level values found within the reference image (due to uneven illumination, dust or dirt) can be compensated for or removed from the original image giving the image opposite.

Normalisation of Grey Level Histogram. The net effect of the above two functions is to supply an image with even background illumination. However, shading corrected images often lack contrast in that they do not occupy the full 256 grey level range. Excluding noise values (0.001% of the grey level distribution of the corrected image) the present function -by linearly expanding the grey level distribution- re-establishes the full grey level range thereby enhancing the contrast of the image.

Image Cleaning Summary. The effects of the image cleaning functions can be viewed in summary format. The four images displayed opposite correspond to the images shown above with each image being represented on a quarter of the screen (ie 128 by 128 pixels). Image 1 is the background illumination, Image 2 the original image, Image 4 the shading corrected image and Image 3 represents the final process of normalisation of the grey level distribution.

IMAGE ENHANCEMENT

Median Filter. The objective of image enhancement is to optimise the accuracy of later object discrimination (see below) in this case that of the alveolar walls. Enhancement using a median filter is a simple technique. A small median filter, as used here, highlights darker areas while altering little else within the image. In this application the result obtained using a median filter is such that no further image enhancement is required.

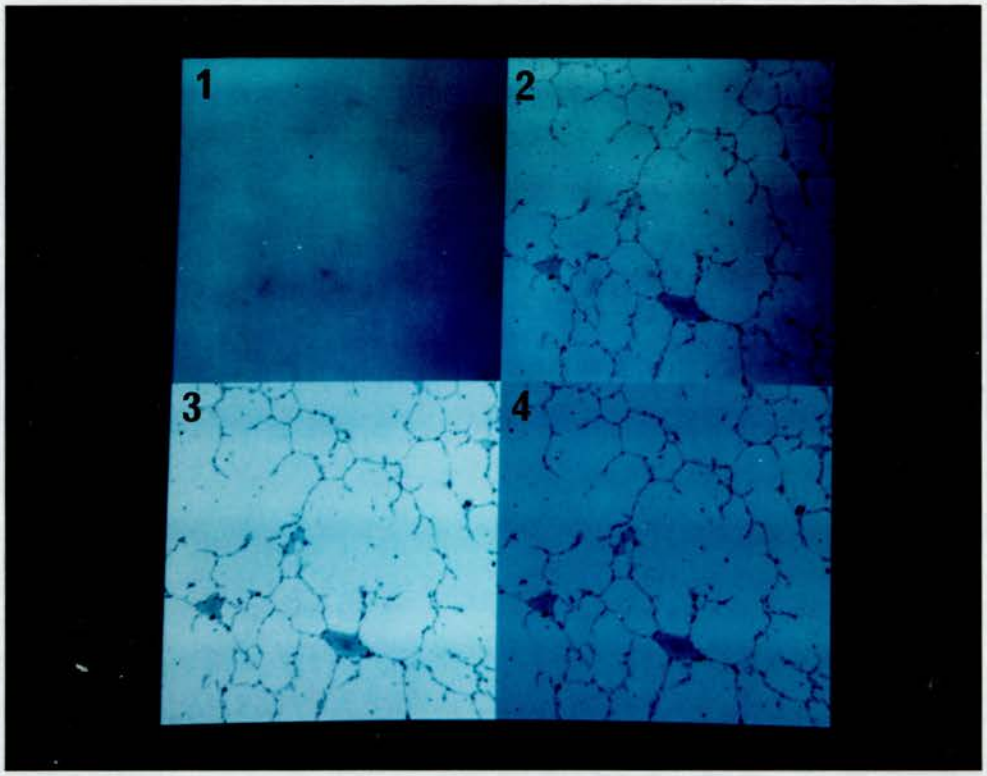
1
2
3
4

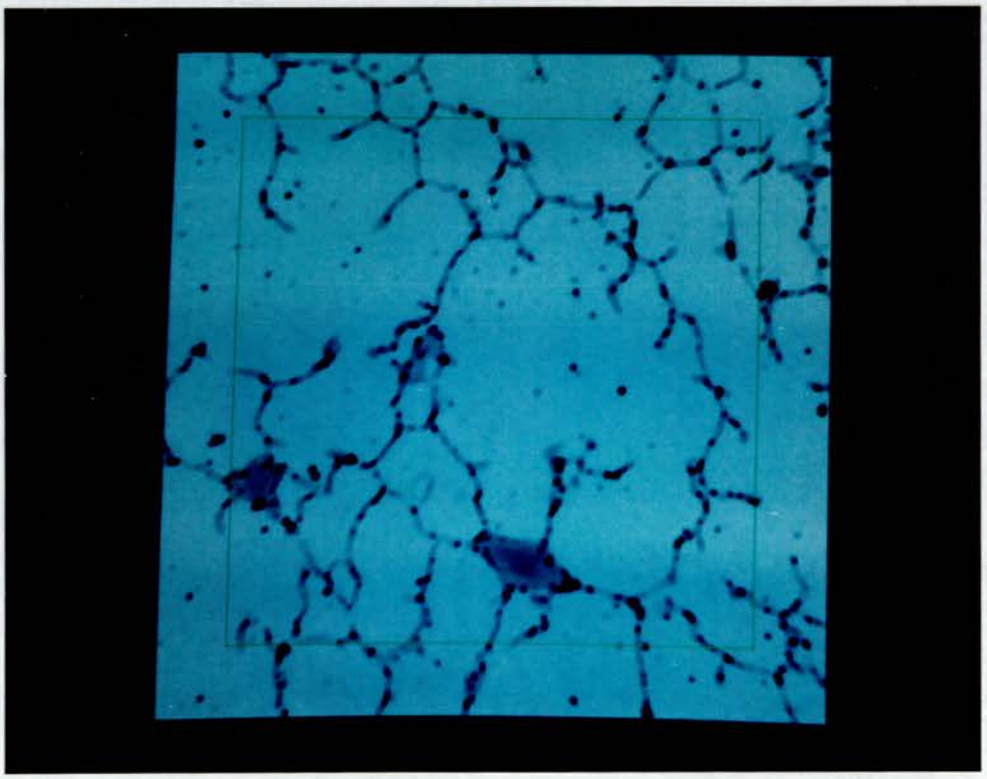

IMAGE DISCRIMINATION

Image Discrimination. A segmented image is produced by this process whereby objects of interest can either be selected for (+ve images) or selected against (-ve image) depending upon their grey levels. For this particular problem this function was carried out interactively (see below) to create a positive image. This requires two grey levels to be set that identify the grey level range which corresponds to the objects of interest ie in this case the alveolar walls.

Under Discriminated Image. As an aid to interactive discrimination IBAS overlays with green all areas which have grey levels between the current lower and upper limits. Additionally, areas with the current upper grey level are overlaid red. This latter facility helps the user to achieve an accurate end point discrimination. The figure opposite represents an under discriminated image. The lower grey level has been set at zero (black), but the upper limit does not include all the grey levels corresponding to the alveolar walls.

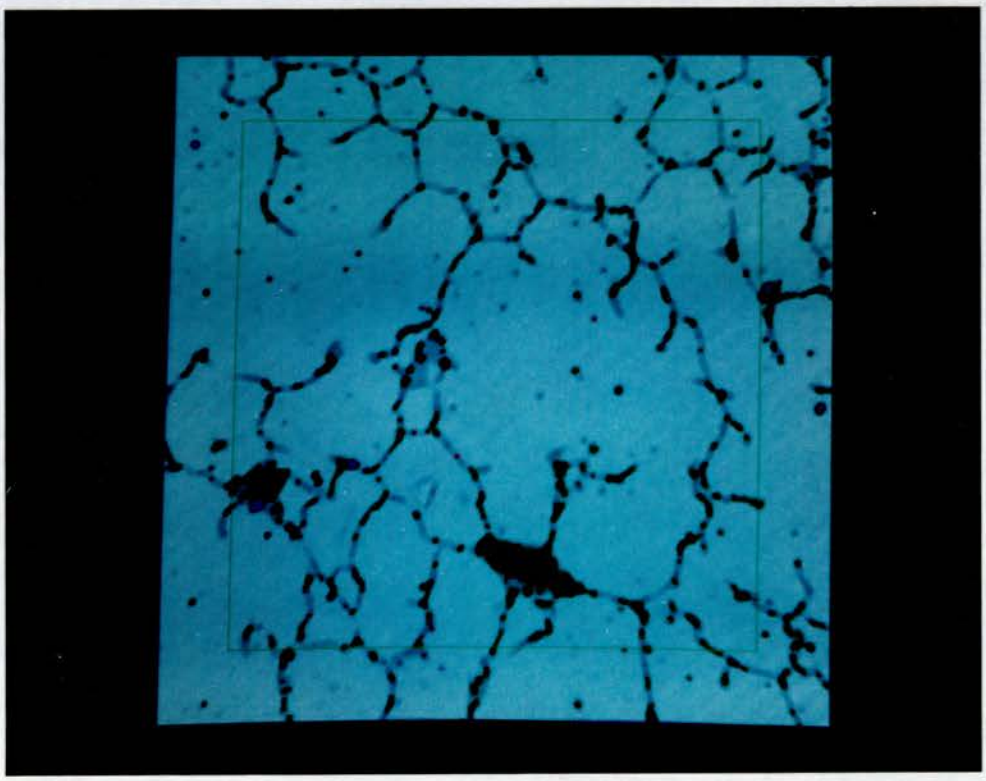

Over Discriminated Image. Clearly all the alveolar walls are recognised within the existing grey level range. However, background areas also lie within this range indicating that the upper grey level value has to be reduced to give an accurate discrimination.

Well Discriminated Image. The sparse appearance of areas overlaid with red is indicative of a clear division (in grey level terms) between the alveolar walls and the rest of the image. At this point the grey levels are finalised and a segmented image created.

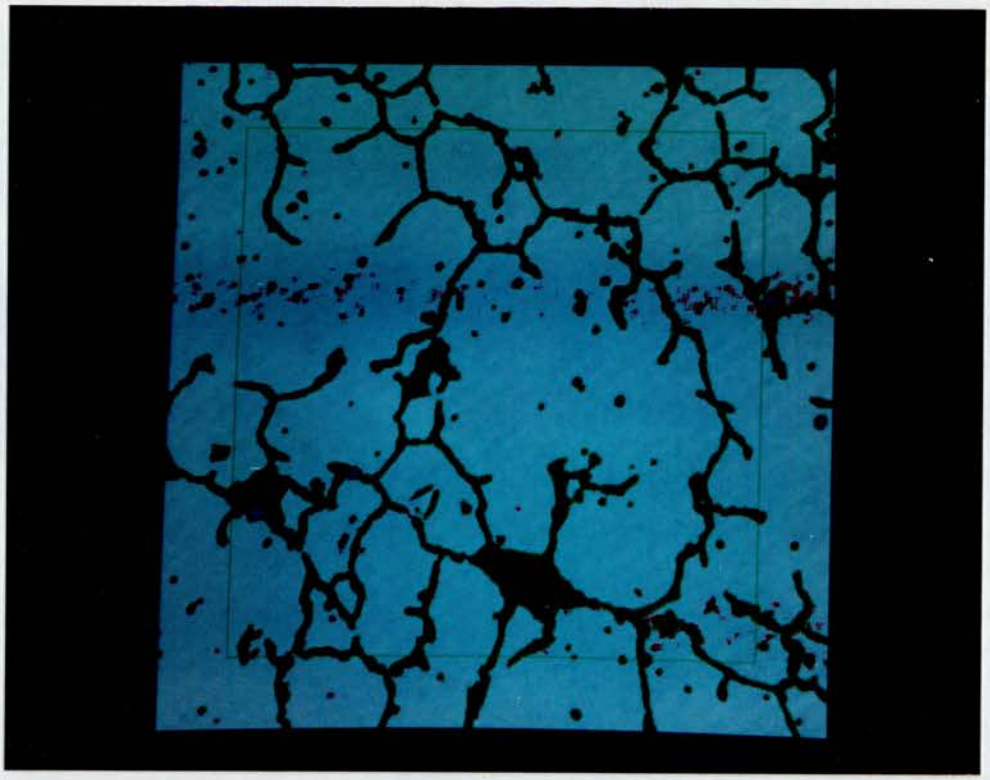

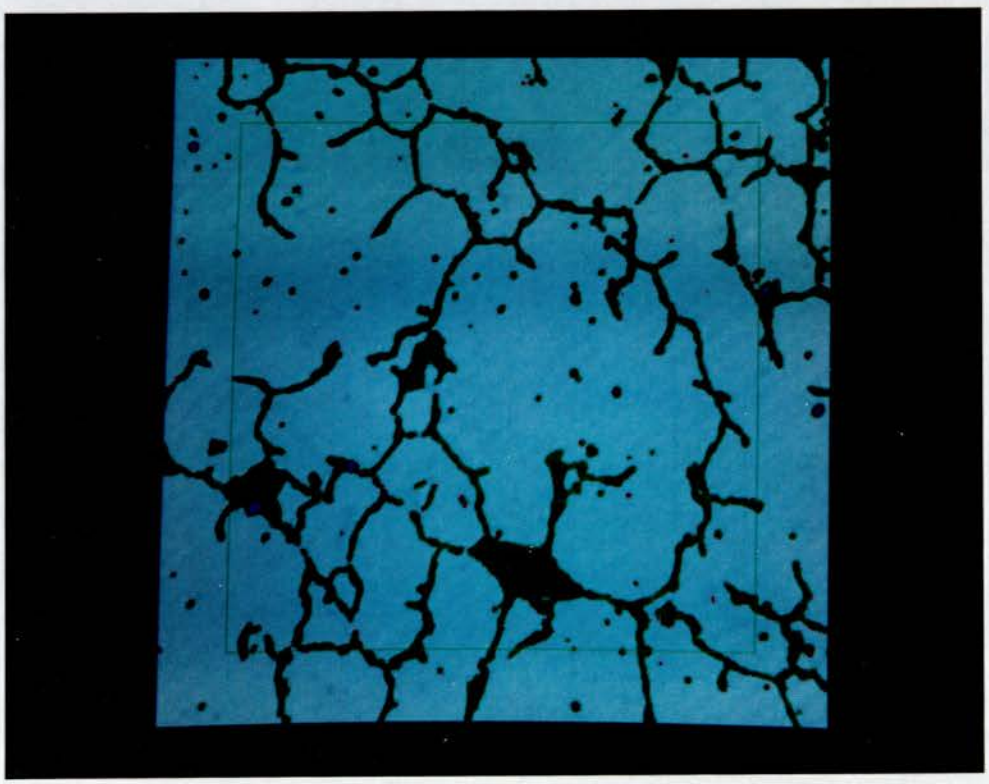

Segmented Image.

This is the segmented image produced by IBAS after setting the appropriate grey levels. It is a positive image in that all the objects within the selected grey level range are shaded white whereas all other areas including the unstained background default to black.

IMAGE EDITING

Small Object Detection.

Along with the alveolar walls various other small objects are also represented in the segmented image. These may be a variety of things such as macrophages or may be due to dust within the optics of the system. Particles within a certain size range can be identified and then subtracted from the segmented image.

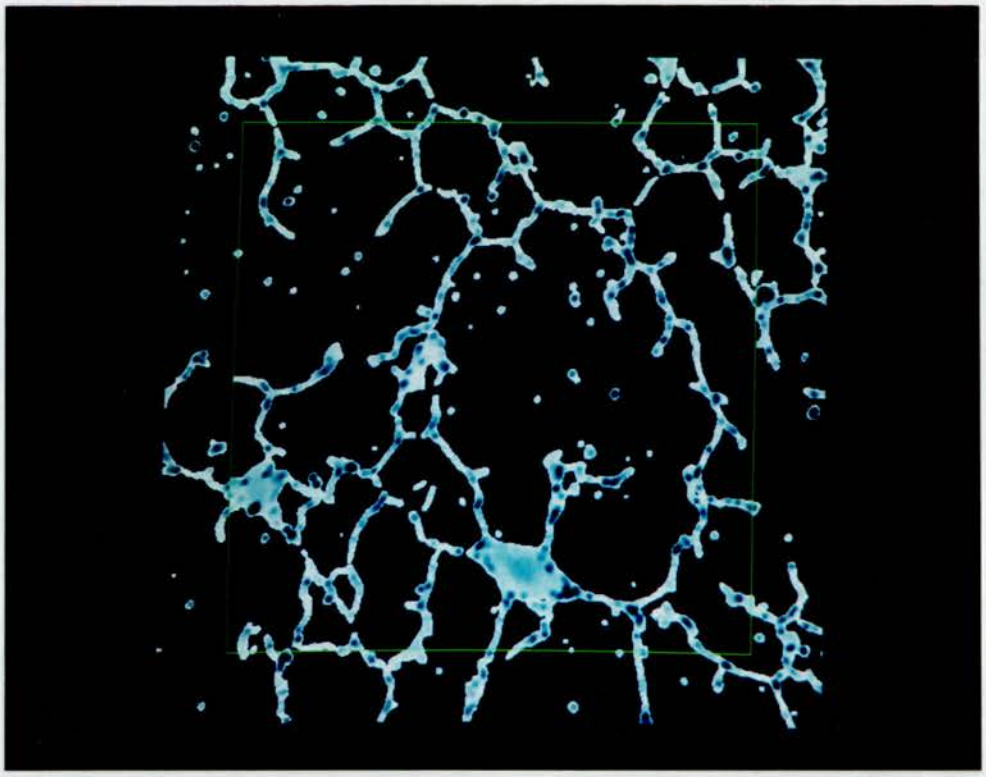

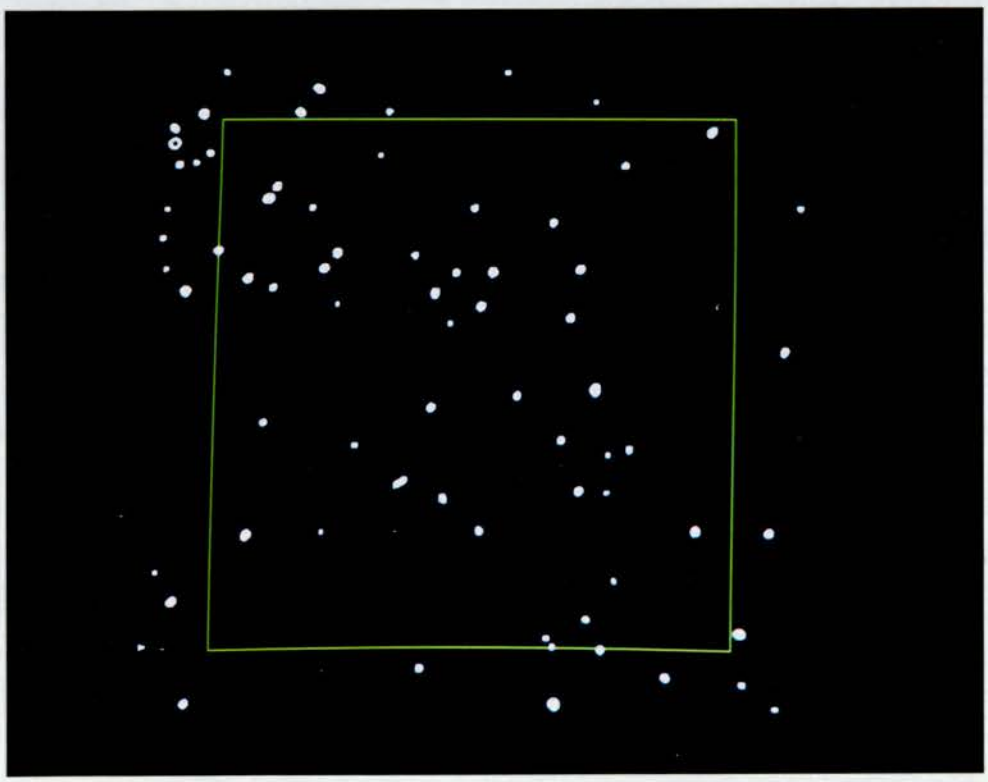

Interactive Editing.

A number of larger objects are still apparent within the image. These have to be edited interactively. The nature of these objects is determined by first viewing the section down the microscope and then taking the appropriate editing action (as described immediately below).

Image Editing - Deletion and Insertion.

The cursor (centre of picture) can be used like a paint brush in that it can be "loaded" with any grey level and used in a range of sizes depending on the required accuracy of the task. Where black is selected (grey level 0) the object can be removed from the image to become part of the background (deletion). Alternatively, by selecting a grey level greater than zero or pseudocolour (see below) areas such as those with a small vessel can be filled in, or where staining may have been light alveolar walls can be joined (insertion).

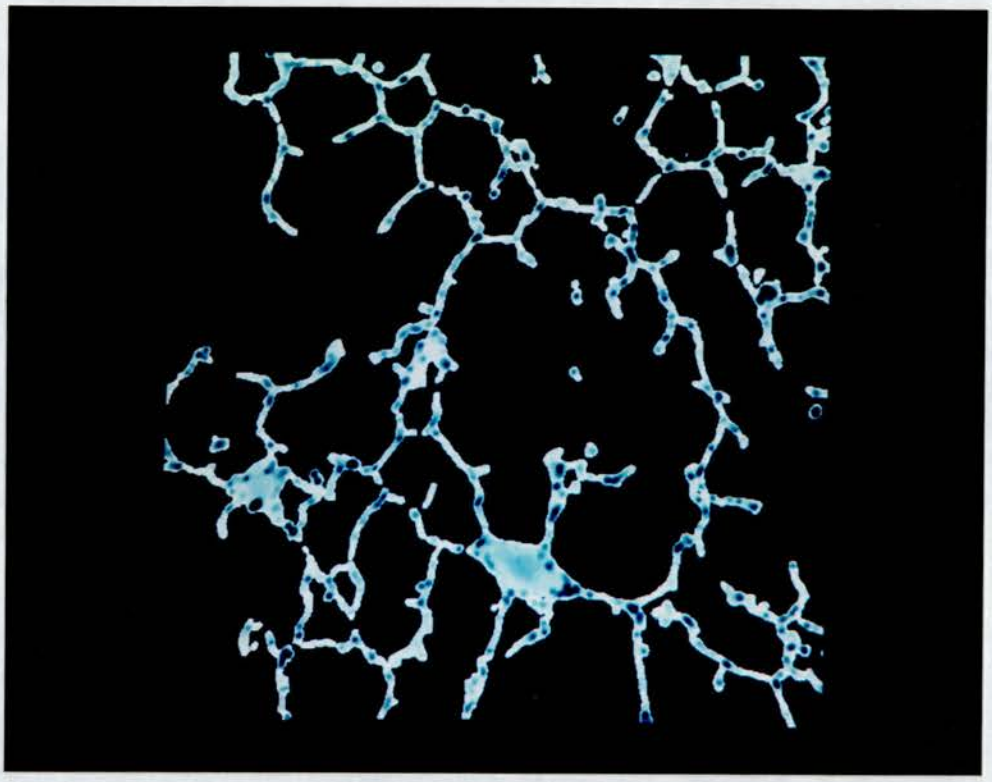

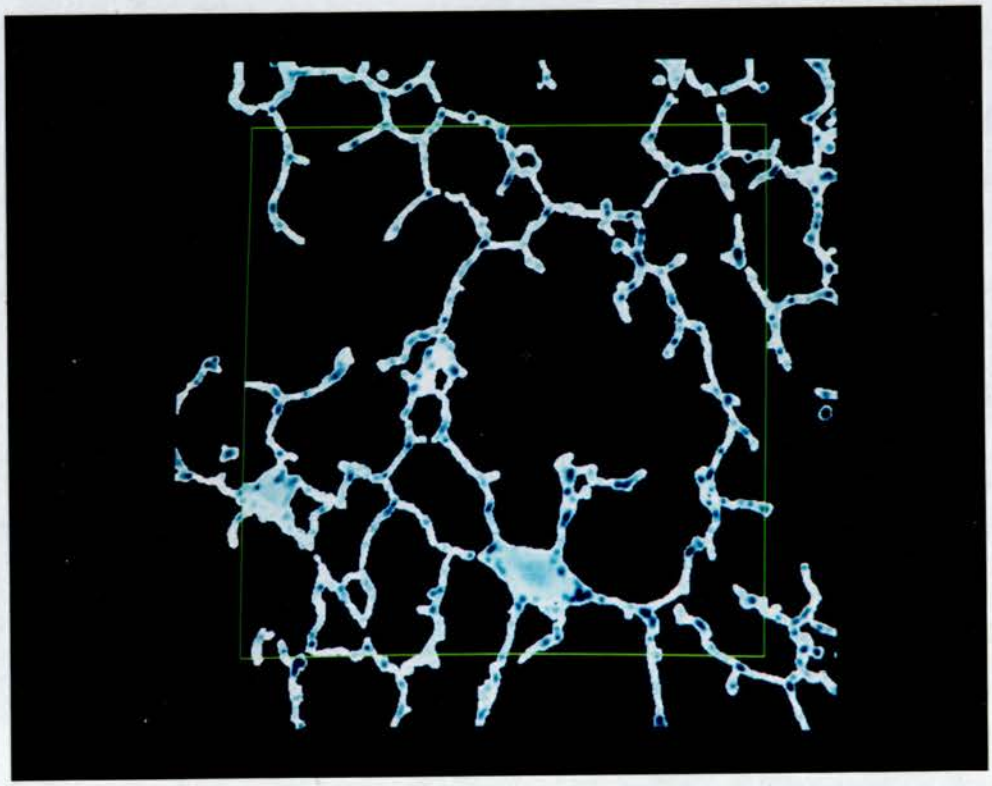

OBJECT IDENTIFICATION AND QUANTITATION

Image Identification.

Before IBAS can measure object parameters images must undergo a machine function known as IDENTIFICATION. A by product of this function is pseudocolouring. Here objects which IBAS will measure are "identified" and overlaid with one of seven colours. Where objects are not touching they obtain (where possible) different colours. This function is useful for identifying gaps in alveolar walls and objects which are not completely filled are more easily recognisable. These images can be edited in exactly the same way as segmented or binary images (see above).

Image Quantitation.

Alveolar wall perimeter *per* unit area is quantified within the predefined measuring square. The outline of all objects included within the measurement are overlaid with white.

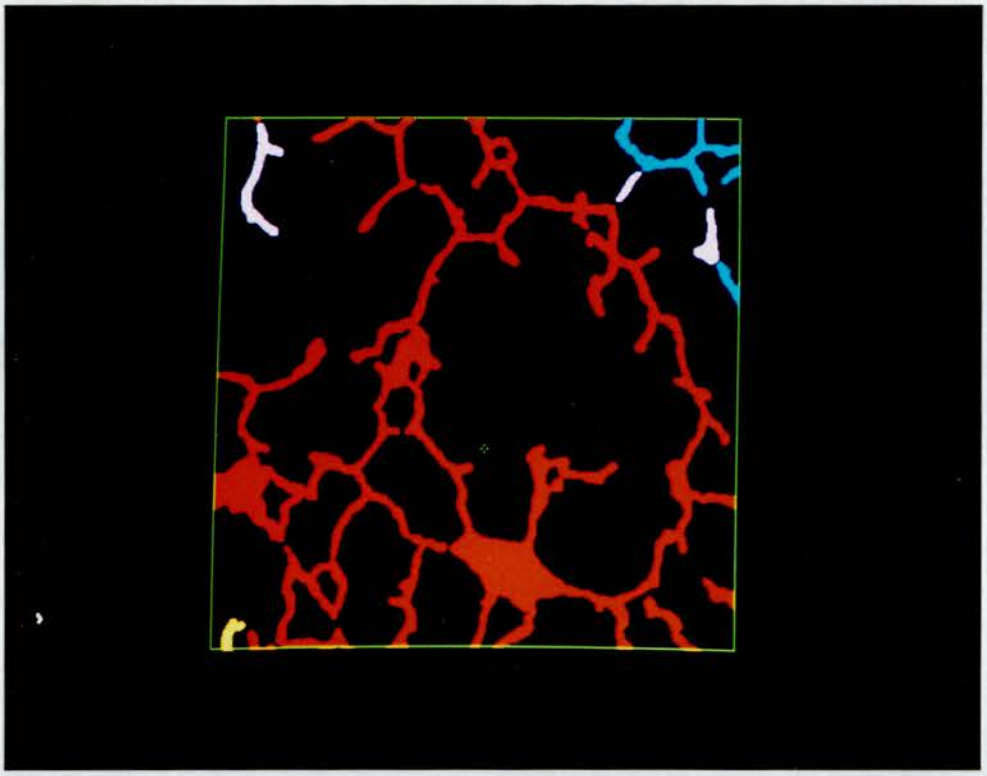

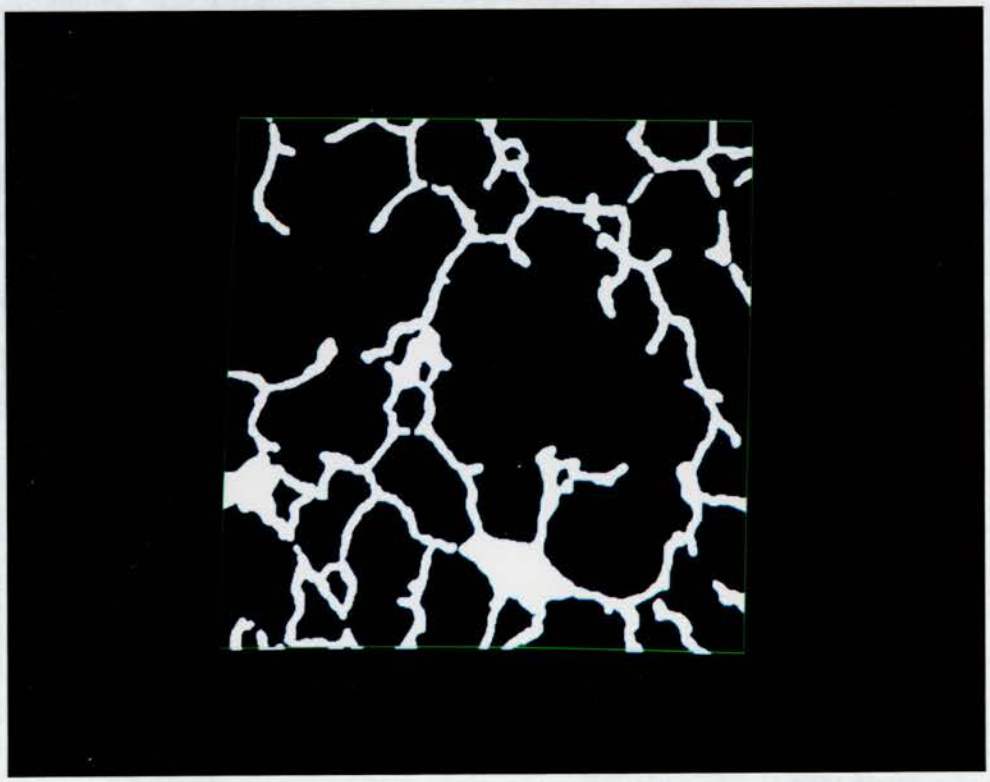

Contoured Image.

This image represents the measurements made by IBAS on the objects present. In this process IBAS detects and outlines all the contours present within an image. In this case this equates to the total length of alveolar wall. Note that only the areas of the image which fall within the $1mm^2$ measuring square are measured and that only the outer aspect of the small marked vessel is contoured and therefore measured.

Three examples of AWUV measurements. Case 13 (upper) has a mean AWUV value of $24.7mm^2/mm^3$. This particular field has a value of $24.5mm^2/mm^3$. Case 40 (middle) has a mean AWUV value of $14.3mm^2/mm^3$. The illustrated field has an AWUV value of $13.7mm^2/mm^3$. Case 11 (lower) has the lowest mean AWUV value for the study group ($8.8mm^2/mm^3$). The value obtained for this particular field is $7.3mm^2/mm^3$.

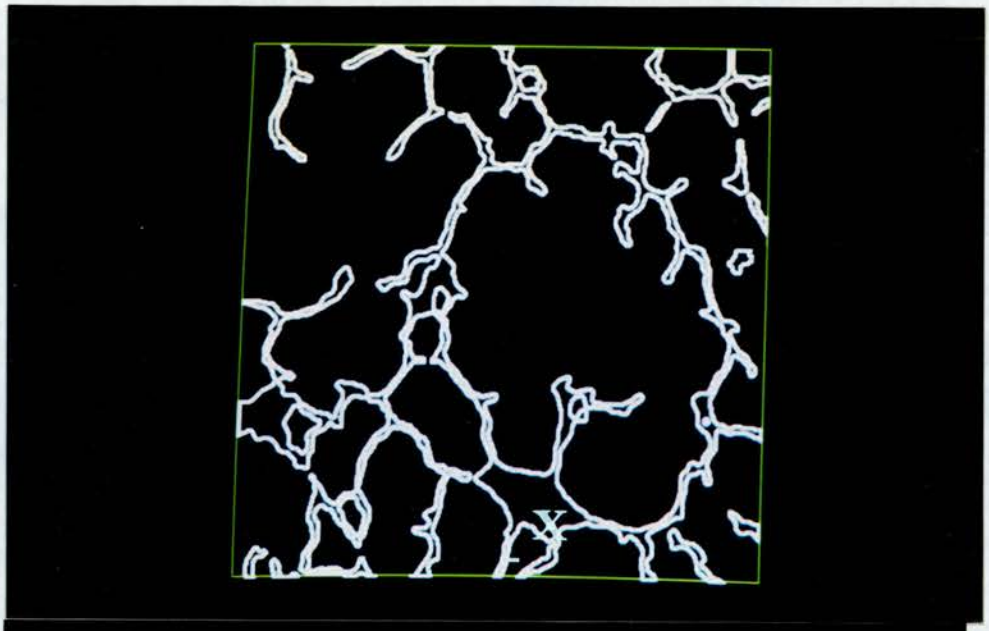

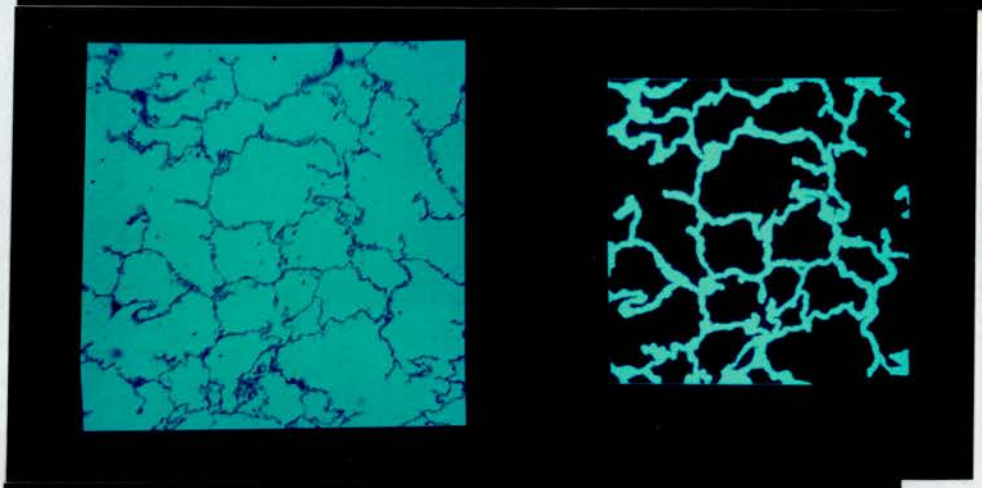

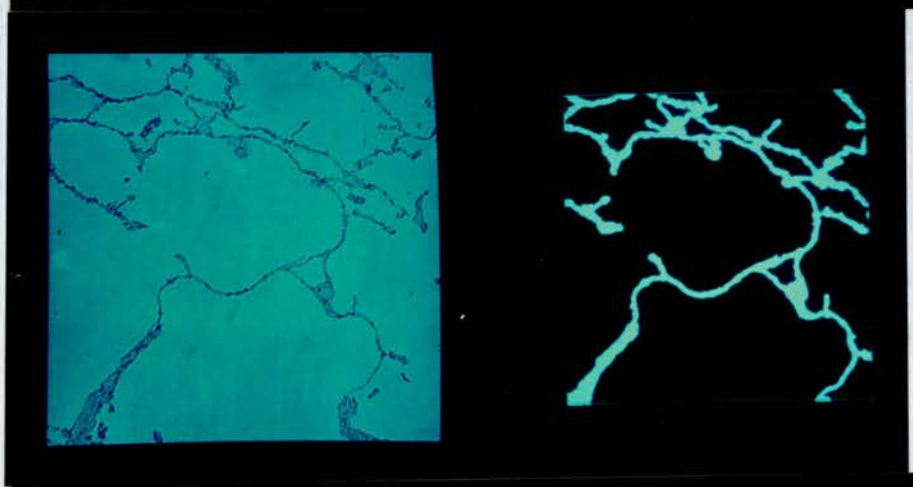

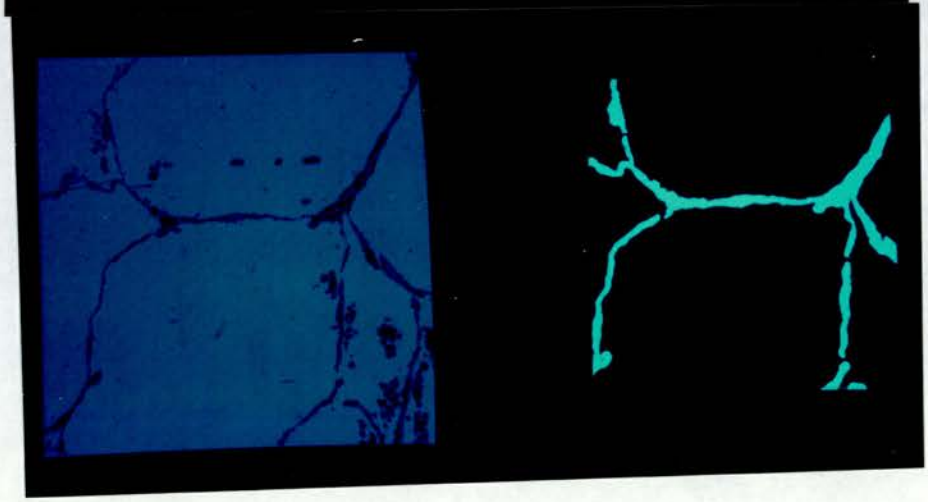

2.4.2. Non-Respiratory Bronchiolar Measurements

The objective of this part of the study was to measure -directly from histological sections- a number of parameters from suitably sectioned small airways. As these measurements included area, circumference, diameter and ellipticality, the angle at which each small airway was sectioned was obviously important as were any artefacts that would be introduced through tissue handling procedures. To minimise the effect of the former a number of sampling procedures were developed which increased the likelihood of obtaining transversely sectioned small airways. The rational behind these procedures are discussed in the chapter dealing with the assessment of techniques as are the techniques developed to minimise artefacts brought about through tissue handling procedures.

2.4.2.1. Cases Used

The cases used are identified within the appendix.

2.4.2.2. Tissue Handling and Selection of Blocks

The tissue handling procedures are the same as those described in section 2.1. In summary, twelve blocks were selected from each case and embedded in GMA, cut at µm and stained with H&E.

2.4.2.3. Selection of NRBs from Histological Sections

Initially all 12 sections *per* case were scanned to locate every NRB. Once located the minimum diameter (maximum diameter in the shortest plane) and then the maximum diameter (maximum diameter in the longest plane)

perpendicular to the minimum diameter were measured (see figure 2.8.). A 10mm cross haired graticule (Graticules Ltd) -situated within the right hand side eyepiece of the microscope- was used to ensure that the diameters measured were indeed perpendicular to each other. The ratio of these two diameters was then calculated (max to min) and the England Finder coordinates noted to facilitate future relocation. After all twelve sections had been fully scanned the diameter ratio which excluded the 30% most elliptical airways was identified as these were excluded from any further analysis (cf chapter 3 which deals with the assessment of techniques).

The minimum and maximum diameters of small airways were only measured if the airway satisfied the following criteria.

1. All three compartments (ie lumen, epithelium and outer wall) were represented on the section.
2. The airway was not bifurcating.
3. The walls of the airway were not alveolated.
4. The airway, using the description given in section 1.1.3, was deemed to be a bronchiole.

2.4.2.4. NRB Parameters Measured

All measurements were made using the GIS image analysis system whose components and *modus operandi* have been described previously (section 2.2.1.2). The parameters measured from each small airway can be subdivided into three categories.

1. Directly Measured Parameters: These parameters are illustrated in figure 2.8 and include the area and

circumference of the lumen, epithelium and outer wall. The maximum and minimum diameters are also included under this category.

2. Ellipticality: This parameter is calculated by expressing the maximum diameter as a ratio of the minimum diameter.

3. Derived Parameters: Using data stored on magnetic tape theoretical lumen area (TLA) was calculated for each airway. The formula used to obtain this parameter is:

$$TLA = \text{Lumen Circ.}^2/4\pi$$

The derivation of this formula is given in the appendix. This formula takes the measured lumen circumference and calculates the area it would bound if the luminal profile was smooth and spherical.

2.4.3. NRB Density

NRB density was calculated as the total number of digitised airways divided by the total cross section area of sampled parenchyma (ie 12 x 1.9cm x 1.9cm) this being the same for all cases.

Figure 2.8 Schematic representation of Measured Bronchiolar Parameters. D1 is the maximum diameter; D2 the minimum diameter; A1, A2 and A3 lumen, epithelial and wall areas respectively and C1, C2 and C3 the respective circumferences.

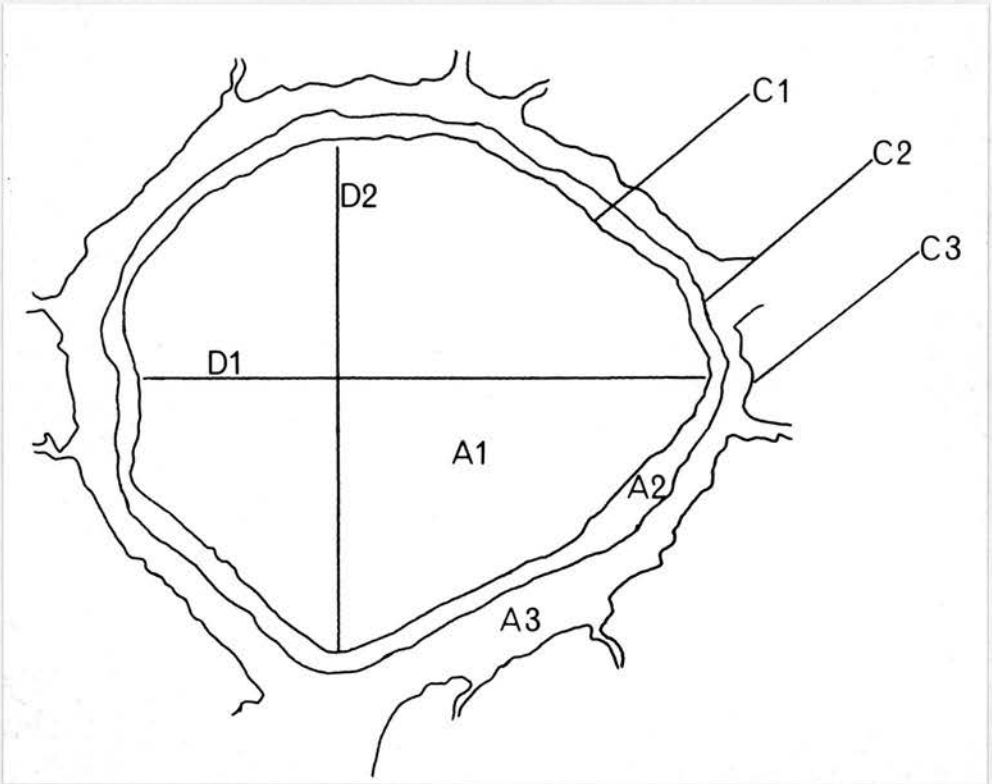
C1
C2
C3
D2
D1
A1
A2
A3

2.4.3.1. Quantitation of NRBs using the GIS System

The accuracy of planimetry is related to the area of the digitiser tablet covered by the profiles being measured, in this case small airways. Frolov and Maling (1969) and Williams (1977) quote a figure of $3cm^2$ to maintain a high degree of accuracy (0.2 to 0.5% as claimed by the manufacturers). However, the planimeters mentioned by these authors have been superceded by more modern and accurate digitiser tablets. In the more recent work of Fleege *et al* (1986 and 1987) a minimum figure of $1.5cm^2$ for area profiles has been calculated to give a coefficient less than 1.5%. For diameters Williams recommends that profiles should be larger than 1cm as represented on the digitiser tablets.

The GIS system used in this study makes use of a *camera lucida* attachment. This transposes the light emitting diode (LED) of the cursor onto the section being viewed under the light microscope. The area of the digitiser tablet occupied by the image is therefore dependent on the magnification of the objective lens being used.

The usable area of the digitiser tablet "seen" by the *camera lucida* measures 25cm by 25cm (2500 by 2500 board units) giving a total area of $625cm^2$. The range of objectives were chosen such that where the longest axis of an airway occupied around half of the field in view the magnification of the next objective increased this to three quarters of the field. The range of objective lenses used were thus chosen to optimise the accuracy of the analysis system. It may at first seem more sensible to have the airway fill an even greater proportion of the field than 0.75, however, it was felt that -even though flat field objectives were used- limiting the airway to 0.75 of the field

avoided all possible edge affect errors.

The minimal accuracy of this system was offered when the longest axis of an airway filled just over half of the field. Thus the corresponding length covered on the digitising tablet would be 12.5cm (ie 25cm x 0.5 = 12.5cm). Given that the most elliptical airway measured in the study had a maximum diameter *circa* 2.5 times that of the minimum diameter, the minimum diameter in this situation would measure 5cm on the digitiser tablet. Such an elliptical airway would cover approximately $49cm^2$ with the smallest measured component, the epithelium, occupying just under $5cm^2$. Therefore, even under the worst possible conditions, which would arise only once if at all, the conditions stipulated by Fleege *et al*, Williams and by Frolov and Maling have been met, with respect to accuracy of area (2-D) and diameter (1-D) measurements.

In practice, the majority of airways were measured using the x6.3 and x10.0 objectives. Each airway was relocated using its stored England Finder coordinate. The user was then prompted to input the minimum and maximum diameters. Three values were input for each of these with the computer program identifying the largest value for each diameter. The user was further prompted to draw round the contours of the lumen. As the lumen is being digitised the outline is represented on the monitor. Once the user gets to within 2.5mm of his starting point the "loop" is closed by the program and the user notified by a single bleep. After the lumen the user delineates the epithelium and outer wall which are likewise depicted on the monitor. When all three compartments have been completed the result is overlaid on to the screen and the user prompted to accept or reject the result. If the result is accepted a textual description of the airway is appended and the result output

to the printer and then written to the magnetic tape.

The series of objectives used -along with their serial linear and area magnifications- are given in table 2.1.

Objective Magnifications					
x2.5	x4.0	x6.3	x10.0	x16.0*	x25.0*
1.0	1.60	1.58	1.59	1.60	1.56
1.0	2.56	2.48	2.52	2.56	2.44

Table 2.1. Objectives used with the GIS image analysis system complete with (in series) linear and area magnification factors. Four magnifications were standardly programmed for in each computer run. (*)The program was designed such that if required the *16.0 or *25.0 lenses could input.

2.4.3.2. Expression of Results

For each case the total number of complete airways was stored and the mean value for each parameter calculated.

2.4.4. Quantitation of Alveolar Attachments

2.4.4.1. Introduction

In chapter 1 section 1.5.5 a number of studies were reviewed which indicated that small airway shape and size were related to the loss of lung parenchyma, both as measurements of over all loss (macroscopic assessments and Lm) and as loss of peribronchiolar alveolar attachments (Linhartova *et al* 1971 and Petty *et al* 1986). As measurements of airway size and ellipticality were being made in this study it was pertinent to assess the effect of such peribronchiolar alveolar loss for these cases.

To do this both the mean number of attachments *per* airway and a number of indices of mean inter-alveolar attachment distance were calculated. The latter calculations were carried out as it was reasoned that such measures would be independent of airway size *per se* whereas the mean number of attachments *per* airway would not.

2.4.4.2. Tissue Selection and Handling

The tissue sections used for the study of NRBs and alveolar surface area were used to count the mean number and inter-attachment distances of peribronchiolar alveoli.

2.4.4.3. Selection of Airways

Ten airways were randomly selected from each case for assessment. Having identified the 70% most circular NRBs along with their England Finder locations the total number of airways in each case was known. It was then a simple matter, using random numbers generated by the Tektronix, to randomly select and locate ten airways *per* case.

2.4.4.4. Counting Peribronchiolar Alveolar Attachments

Peribronchiolar attachments were counted using the method of Linhartova *et al* 1971 which has been used more recently by Petty *et al* 1986. Using this method attachments are counted on bronchioles where less than 25% of the outer circumference of the wall is free from sheaths of accompanying pulmonary arteries.

The mean number of attachments *per* airway was calculated for each case.

Having measured the luminal, epithelial and wall circumferences, the average inter-alveolar attachment distance could be calculated for each airway. By doing this the mean inter-alveolar attachment distance *per* case could also be calculated.

2.4.5. Quantitation of Macroscopic Emphysema

Macroscopic emphysema was assessed in each resected specimen as the percentage of the area of the midsagittal slice which was involved by macroscopically evident emphysema. This was defined as airspaces greater than 1mm in diameter. To make this measurement each slice was immersed in water and examined with a hand lens. Areas involved with either macroscopic panacinar, centriacinar or paraseptal emphysema were traced on to a clear polythene sheet. The combined area of these emphysematous areas was then measured using the GIS semi-automatic image analyser. Where smaller centriacinar lesions were hard to define Vernier calipers were used to measure their diameter. Assuming a spherical outline for these air spaces, their combined cross sectional area was calculated and added to the digitised figure. In practice the figure calculated for the smaller centriacinar lesions was very small and contributed very little to the total figure -never more than 1 or 2 percentage points. The total figure was expressed as a percentage of the cross sectional area of the midsagittal slice.

2.4.6. Pulmonary Function Tests

Total lung capacity (TLC) was measured by body plethysmography (Pulmorex, Fenyves and Gut, Basel, Switzerland). Values for TLC percent predicted were obtained from Grimby and Soderholm (1963). Forced expiratory

volume (FEV) was measured using a 7 litre dry spirometer (Vitalograph Ltd, UK). Kory *et al* (1961) was used to obtain percent predicted values for men, while those for women were taken from Ferris *et al* (1965). Single breath carbon monoxide diffusion capacity was measured by the technique of Ogilvie *et al* (1957) (Automatic transfer test model A system, PK Morgan Ltd, Chalham, UK). Time of breath holding was calculated by a modification of the Jones and Meade technique (Jones and Meade 1961). Alveolar volume was assessed from the dilution of helium during the single breath manoeuvre and was used to calculate K_{co}. Percent predicted values were taken from Billiet *et al* (1963) for T_{co} and Cotes and Hall for K_{co}. Single breath nitrogen washout test was measured using a wedge spirometer (Model 570, Medical Science Electronics Inc., St Louis, Missouri, USA) and a Nitrogen analyser (Ohio Medical Products, PK Morgan Ltd, Chalham, UK).

CHAPTER 3

ASSESSMENT OF TECHNIQUES

3.1. SELECTION OF NON-RESPIRATORY BRONCHIOLES FOR QUANTITATION

The objectives of this study entailed measuring a number of non-respiratory bronchiolar parameters. As these included areas, circumferences and ellipticality, the angle at which bronchioles had been sectioned was going to be important. Ideally, one would wish to section every airway transversely. In practice this is very difficult to achieve.

Linhartova *et al* (1973) have discussed this problem and diagramatically depict the range of angles at which small airways can be sectioned. Although some studies have limited their analysis of peripheral airways to those which are transversely sectioned (Linhartova *et al* 1971, Anderson and Foraker 1968, Bignon *et al* 1969 and Matsuba and Thurlbeck 1971) none have presented their criteria for defining such airways. Matsuba and Thurlbeck simply state that "airways sectioned obliquely or longitudinally were excluded". Appearance and/or possibly a set diameter ratio may have been applied.

Most studies have represented small airway size as minimum diameter. The rational behind this is based on the assumption that small airways are cylindrical tubes. As such, minimum diameter measured on any transection will represent the diameter of that small airway irrespective of the angle at which it has been cut.

This assumption contains some potential errors. These are:

- It is not true of cylinders that are tangentially sectioned.

- Bronchioles are only trully cylindrical between bifurcations (Linhartova *et al* 1974), the incidence of which increase with decreasing bronchiolar calibre.

- Loss of alveolar walls affects airway shape (Anderson and Foraker 1968, Linhartova *et al* 1971, 1973 and 1982 and Nagai *et al* 1985a).

Severe instances of the latter have been demonstrated very neatly by Linhartova and coworkers (1974). By painstakingly reconstructing three dimensional profiles of airways from normal and emphysematous lungs they showed that airways in the latter could be severely mishapen and tortuous.

This means that a set diameter ratio cannot be applied to determine which airways have been transversely sectioned as diseased lungs will have more mishapen airways. A set diameter ratio in such cases will select airways which are less mishapen (ie less diseased) and will also select fewer airways. However, the three dimensional reconstructions of diseased airways, presented by Linhartova *et al* illustrate the difficulties which must arise in deciding, arbitrarily, whether or not airways have been transversely sectioned.

Therefore, where one is studying diseased lungs it is not possible to tell diseased from irregularly sectioned airways on the basis of their histological appearance. Additionally, as airways may be mishapen minimum diameter may not necessarily represent cross-sectional area. Thus, comparisons between cases may be inaccurate where minimum diameter is used to represent airway size.

The approach taken in this study was to create a sampling regime which would minimise between case differences in the sampling of bronchioles with respect to the angle at which they had been cut and at the same time

optimise the efficiency of sampling the largest number of bronchioles possible. To achieve this sampling of bronchioles was from the first two immediately sub-pleural slices. The benefits obtained by applying such a sampling regime are (cf section 1.1.3.3):

- Bronchiolar density is at its greatest in the immediately sub-pleural zones as there are no larger non-parenchymatous structures (eg arteries, bronchi etc) due to the structural gradient which exists in lungs.

- The airways sampled will belong to axial pathways which tend to run perpendicular to the pleura. There is therefore a greater likelihood of obtaining more transversely sectioned small airways.

- The frequency of tangentially sectioned conducting airways will be less as the airways of axial pathways do not follow a reflex course after bifurcating and deviate very little from the course of their parent airway. This differs from the branching pattern of airways of lateral pathways which always follow a reflex course after they branch from their larger parent airway, which is invariably a bronchus.

- RBs branching off of TBs of axial pathways always follow a reflex course ventilating airways proximal to their bifurcation. Intuitively, these RBs have a greater chance of being longitudinally sectioned.

Using shared histological material, in a project measuring various aspects of pulmonary arteries, Fernie (1985) contrasted this sampling regime to that of sampling throughout the lung. Significantly more pulmonary arteries are transversely sectioned in tissue blocks taken from the lateral two sub-pleural slices. Wright *et al* (1983), Matsuba and Thurlbeck (1971 and 1972) and Nagai *et al* (1985a) utilise similar sampling regimes when looking at inflammatory and other changes associated with small airways.

This sampling regime will not completely eliminate airways whose histological profile is due as much to the angle at which they have been

sectioned as their true calibres. However, Linhartova *et al* (1973) were able to show that 70% of bronchioles from normal and minimally diseased lungs were either spherical or close to spherical in cross-section. This indicated that, for each case, bronchiolar shape may follow a distribution whereby a certain proportion of small airways may exhibit, in histological profile, a lumen area which is representative of their true *in vivo* lumen area. Thus the possibility arose that there may be criteria which objectively exclude airways which are more longitudinally as opposed to transversely sectioned.

To investigate whether this was true, for this study population the distribution of the maximum to minimum diameters, for the first ten cases were plotted as cumulative frequency distributions. From these plots it was observed that for every case the cumulative frequency distribution profiles presented two similar qualities (see figure 3.1). These were that:

1. The majority of airways lay on the initial steep slope of the curve and were included by a small part of the total range for airway ellipticality.

2. The slope of the curve lessened reaching a plateau. This second part of the curve, although long, incorporated only a minority of the airway population.

From these curves it could be discerned that in all cases the second part of the curve always included less than 30% of the total airway population and that these airways could be grossly elliptical irrespective of the nature of the rest of the distribution. It was concluded that this subset represented airways which had been sectioned at extreme angles. A criterion was therefore adopted which excluded the 30% most elliptical airways from further morphometric analysis. It is appreciated that the remaining 70% of airways

included by this ratio are not completely transversely sectioned as all are influenced to a certain degree by the angle at which they have been cut. However, the similarity of the distributions indicates that all cases are equally affected and that observed cross-sectional lumen area is proportional and representative of "true" cross-sectional lumen area.

To ensure that this result was not peculiar to the first group of ten cases, cumulative frequency distributions for airway ellipticality were completed for every case. This did not involve any extra work as all airways had to be analysed initially to identify the ratio which defined the 30% most elliptical airways.

Figure 3.1: This depicts the cumulative frequency distributions for three cases. These include one case with relatively circular airways, one close to the average for airway ellipticality and one with (relatively) very elliptical airways. In practice, the 70th percentile ratio is slightly conservative in that it occurs just before the slope of the curve lessens. This was probably advantageous in that it excludes "noise" from the analysis of airway area, circumference and ellipticality data.

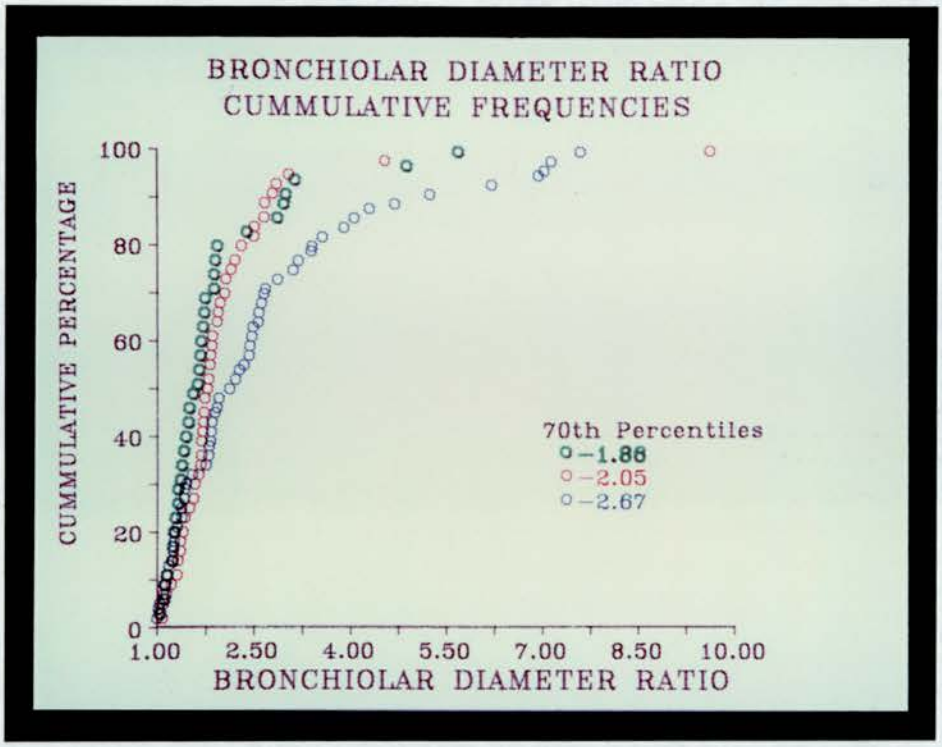
BRONCHIOLAR DIAMETER RATIO
CUMMULATIVE FREQUENCIES
CUMMULATIVE PERCENTAGE
100
80
60
40
20
0
1.00
2.50
4.00
5.50
7.00
8.50
10.00
BRONCHIOLAR DIAMETER RATIO
70th Percentiles
1.86
2.05
2.67

3.2. Comparison of Inflation Techniques

3.2.1. Introduction

In chapter one the problems of adequate fixation and inflation were mentioned. This section discusses the merits of the three main techniques that have been applied to lung morphometry ie those of Weibel and Vidone (1961), Heard (1958) and that recommended by the American Thoracic Society (1959). The reasons for selecting the technique used in this study are given and the results obtained by this technique are compared to that of constant pressure inflation.

3.2.2. Review of Inflation Techniques

The technique of Weibel and Vidone differs from the others in that formalin steam, under a negative pressure, is applied to inflate lungs. Formalin steam induces a gradual shrinkage of the lung giving on average specimens that are inflated to around three quarters of total lung capacity. This is not necessarily a disadvantage as relative comparisons can be made if tissue loss occurs evenly between and throughout lungs. Furthermore -assuming relationships between volume loss and area and linear loss hold (cf section 1.5.4)- relevant corrections can be made and results expressed corrected to total lung capacity.

Some aspects of this technique have been criticised by Wright *et al* (1974). Their three major criticisms are that:

- Injured lungs allow the passage of gas through perforations.
- Formalin steam drawn into the lungs condenses to give an

accumulation of aqueous formalin. This gives in most areas predominantly wet fixation. Other areas, in particular apices of the lung, remain relatively free of liquid resulting from drainage to dependant areas.

- Where lungs are fixed at room temperature the outer areas may decompose before the are perfused by fixative.

A further observation reported by Wright *et al* is that fixation within the lung is sometimes incomplete with sampled blocks requiring further fixation. Wright and coworkers furnish solutions to these problems with the aim of providing fixed and inflated lungs that are suitable for comparison with X-rays.

The Heard technique advocates applying liquid formalin into lungs at a pressure of 25 to 30 cm H_20 via a main bronchus usually for a period of at least 24 hours. To achieve this a stout cannula has to be attached to the main bronchus. This technique is described in greater detail in section 2.1.3.1.

The technique recommended by the American Thoracic Society is very similar to that of the Heard technique. This, or a similar technique, has been used by CIBA (1959), Ryder *et al* (1969) and Thurlbeck *et al* (1967a) to establish standard reference pictures and to test methods for assessing macroscopic emphysema. It differs form the other techniques in that lungs are not constant pressure inflated, but inflated until the "natural contours" of the pleura have been established.

The selection of the most appropriate inflation technique was greatly influenced by the stipulation placed upon the study that the bronchi and surrounding parenchyma must survive the inflation and fixation procedure undamaged. This condition was imposed as the proximal resection margin was considered to be diagnostically important both by surgeons and pathologists.

As both the Heard and the Weibel and Vidone techniques require the attachment of at least one, durable, catheter *per* lung the use of these techniques could not be gauranteed to meet this *a priori* condition. This meant that the ATS or "natural contour" technique was the most appropriate for this study as it is simple to apply and can be gauranteed not to damage any lung tissue.

Other advantages gained by using the ATS method include:

- In a number of cases more than a single bronchus required catheterisation. In general, it is more difficult to attach reliable catheters to smaller bronchi that will remain in position without maintenance for at least 24 hours.

- The technical aspects of the Weibel and Vidone technique are more difficult to maintain and gaurantee; especially if the adaptations recommended by Wright are put into effect. This is probably especially true where a relatively large number of specimens are to be inflated and fixed.

- *In vivo*, specimens with emphysema reach TLC at applied pressures as low as 10cm H_2O (Heard 1958). These may have reduce compliance and may be over inflated to varying degrees if a constant pressure is applied.

- The ATS technique allowed specimens to be fixed rapidly and could be applied to more cases than either the Heard or Weibel and Vidone techniques. This meant that more cases could be studied while using only one inflation technique.

Having decided that the ATS technique was the most appropriate it was of interest to investigate the possible magnitude of difference between this and the frequently used Heard constant-pressure technique on non-respiratory bronchiolar size and ellipticality.

3.2.3. Material and Methods

3.2.3.1. Source of material

Two post mortem subjects were obtained both of whom had died of ischaemic heart disease. These were examined by a consultant lung pathologist who considered them appropriate for lung morphometry. Subjects A and B were both male, subject A was 80 years old and subject B 79 years old.

3.2.3.2. Fixation/Inflation of the lungs

The right lungs were inflated using the ATS technique whereas the left lungs were constant-pressure inflated. The precise methodology has previously been described (section 2.1.3.1).

3.2.3.3. Slicing the lungs

After being allowed to fix for 3 days the lungs were cut into 1cm parasagittal slices and numbered using the method outlined in section 2.1.4.

3.2.3.4. Tissue sampling

Sampling was from P1 and P2 (lateral sub-plueral slices). Six blocks were taken from each slice for each embedding medium thus providing twelve blocks from each lung. These blocks were randomly sampled using the technique outlined in methods section 2.1.5. These blocks were all 1.9cm by 1.9cm (3/4" x 3/4") square and were taken using a template specifically manufactured for this study.

3.2.3.5. Tissue Processing

Selected blocks were embedded in GMA (section 2.1.6) cut at 3µm and stained with H&E (section 2.1.8).

3.2.3.6. Quantitation of Non-Respiratory Bronchioles

All non-respiratory bronchioles (NRBs) on the tissue sections were located and their minimum and maximum diameters measured using the GIS semi-automatic image analysis system (section 2.4.3.1).

3.2.3.7. Statistical Analysis

Given the non-Gaussian distribution of bronchiolar/small airway sizes (Salmon *et al* 1982) the Mann-Whitney U test was used to analyse the results. This is a non-parametric equivalent of the t-test. In general non-parametric tests are weaker than their parametric equivalents. With the sample sizes obtained the Mann-Whitney U test has >95% of the strength of the t-test.

As recommended by Siegel the U statistic obtained was converted to a z value (Siegel page 123 equation 6.8.) as this gives more accurate probabilities for larger samples (ie where at least one group is greater than 20).

3.2.4. RESULTS

3.2.4.1. Bronchiolar Size

In section 3.1 it is argued that the observed histological profile of NRBs is influenced by the angle at which they have been cut and that this artefact can

be controlled to a certain extent by excluding the 30% most elliptical airways. Analysis relates to the remaining 70% of airways.

The numbers and mean diameters of NRBs measured for each lung are given in table 3.1 as are the z values and associated probabilities. The probabilities are for the more powerful one-tailed test as the alternative hypothesis proposes that internal diameters of NRBs in left lungs (constant pressure inflated) are greater than that of right lungs.

For both cases A and B the null hypothesis, that there is no difference in internal diameters of small airways, was accepted.

Ho: There is no difference in bronchiolar diameters between lungs which are inflated using the ATS or constant-pressure techniques.

Hi: Bronchioles are larger in lungs inflated using the constant-pressure inflation technique (one-tailed).

	Bronchiolar Diameter(mm)			
Inflation Technique	Case A	(n)	Case B	(n)
Constant Pressure	0.78	(16)	0.67	(18)
ATS	0.84	(22)	0.60	(29)
z	0.01		0.53	
p	0.5		0.3	

Table 3.1: Mann-Whitney U test of the above null hypothesis. The test statistic U is converted to z to obtain more accurate probabilities. In both cases the null hypothesis is accepted.

3.2.5. Discussion

Accepting that only two lungs were analysed, comparisons suggest that the two inflation techniques produce insignificant differences in airway size.

There are two reasons which may account for these findings. Firstly, lungs removed from the body do not have to overcome the *in vivo* restrictions placed upon them by the chest wall when being inflated to TLC. Heard (1958) noted that in this situation 10cm H_20 is sufficient pressure to achieve TLC. The pressure range of of 25 to 30cm H_20 is recommended to overcome potential problems associated with mucous plugging of large airways. This problem is less common in surgical lungs. Having obtained TLC the extra applied pressure has little effect (cf section 1.5.4.1). This points to the fact that TLC is quite easy to obtain especially with surgical lungs.

Secondly, as mentioned previously (section 1.5.4.1), area and linear losses are only a proportion of volume ones. This being so, considerable differences in volume are required to produce significant differences in area and linear dimensions. Additionally, pressure-volume curves for lungs indicate that increases in volume become increasing difficult to obtain as one approaches TLC (again, cf section 1.5.4.1).

These effects combine to minimise any differences in one or two dimensional measures between different inflation techniques.

The above analysis was carried out to obtain an estimate of the potential differences between the Heard and ATS techniques for inflating lungs. However, the decision to use the ATS technique related to the following factors. Lobectomies and pneumonectomies were the source of tissue for this

study. These, especially the proximal resection margin, had to survive the tissue inflation and fixation procedure undamaged. The simplicity of the ATS technique meant that it could be applied to more specimens than either of the other two possible inflation techniques. Rather than employ more than one inflation technique, which always has the potential of increasing experimental variability, it was decided to use routinely the ATS technique.

3.3. ASSESSMENT OF EMBEDDING TECHNIQUES

3.3.1. Introduction

Accurate morphometry demands that embedding media either optimally preserve the morphology of parametwrs being quantified, or alter them in such a way that correction factors can be calculated.

The use of paraffin in histomorphometry is well established (Matsuba and Thurlbeck 1971 and 1972, Bignon *et al* 1969, Cosio *et al* 1977 and 1980, Depiere *et al* 1972, Linhartova *et al* 1973, Niewhoener and Kleinerman 1974 and Petty *et al* 1982) to name but a few. The occurence of shrinkage is acknowledged, but the effect and occurence of compression, as a rule, is not.

During an initial pilot project carried out prior to any quantitation a number of lung tissue blocks were embedded in paraffin to assess qualitatively the potential extent of shrinkage and compression artefacts. For comparison, a number of tissue blocks were also embedded in in glycol methacrylate (GMA) which, being a plastic, should be more resistant to compression. From this it was observed that there were notable differences in the sections produced by the two embedding media. Paraffin sections were distinctly smaller and bands of compressed tissue could be seen. As accurate measurements of airway size and ellipticality were to be made a study was initiated to quantitate the magnitude of these changes. This involved selecting a number of tissue blocks, randomly assigning them to either paraffin or GMA and then measuring the dimensions of the sections obtained. Bronchiolar size and ellipticality was also measured.

3.3.2. Material and Methods

3.3.2.1. Tissue Source Sampling and Processing

The source, sampling and preparation of tissue blocks is the same as that outlined in the previous section. In summary, a total of 96 blocks were taken with half being processed in each embedding medium; using the techniques previously described (section 2.1.6.1 and 2.1.6.2). Sampling was from P1 and P2 (lateral sub-plueral slices) with six blocks being randomly sampled from each slice for each embedding medium, giving a total of twelve blocks *per* lung. All blocks were of standard size 1.9cm by 1.9cm (3/4" x 3/4").

When the processed tissue blocks are sectioned compression can only occur in the plane of the block traversed by the microtome blade. Therefore, one plane of the block will be susceptible to shrinkage artefact alone while the other will be susceptible to the combined effects of shrinkage and compression.

To facilitate the assessment of compression, sections were placed so that the plane of the block traversed by the knife always lay parallel with the longer aspect of the glass slide (Figure 3.2). That is, viewed as x and y axes, the x-axis of the section represents shrinkage and compression effects whereas the y-axis represents shrinkage alone.

3.3.2.2. Quantitation of Shrinkage and Compression

The GIS image analyser used with a stereomicroscope (Wild Heerbrugg, Luton, England) and *camera lucida* (Wild type 256575) was used to measure the dimensions of the processed lung sections. The maximum dimensions of

the sections in the x-axis (shrinkage and compression) and y-axis (shrinkage) were measured as was total section area. Maximum dimensions were quantified as the processed sections (especially those embedded in paraffin) invariably had an uneven outline making average length extremely difficult and time consuming to measure accurately. Such measures obviously over estimate the true dimensions of the sections and therefore underestimate linear shrinkage and compression factors.

As the blocks were trimmed with a template of known size (1.9cm) the average shrinkage component for each medium was defined as any y-axis shortfall in mean section length. Average compression was defined as any x-axis shortfall in mean section length over and above that of the y-axis measure.

By measuring total section area over all tissue loss for each embedding medium was also quantified.

3.3.2.3. Quantification of NRB Size and Ellipticality

Using the GIS image analyser the maximum and minimum diameters of each small airway were quantified. Bronchiolar ellipticality was defined as the ratio of the maximum to minimum diameter.

3.3.2.4. Statistical Analysis

The Wilcoxon signed ranks test was used where paired data were available, ie on data relating to the dimensions of processed sections. The T statistic obtained is transformed to a z value using the formula given by Siegel (page 79 equation 5.5) as z provides more accurate probabilities for combined

sample sizes greater than 25. The Mann-Whitney U test was used for non-paired data, ie bronchiolar size and ellipticality. Again the U value is converted to z as described in the previous section. Where whole distributions, as opposed to the location of median values, were to be tested the Kolmogorov-Smirnov test was used. This test identifies the largest discrepancy between two cumulative frequency distributions. The magnitude of this discrepancy, or gap, is then tested to see if it is small enough for the two samples to belong to the same population. D, the test statistic, is converted to X^2 with two degrees of freedom for a one-tailed test (Siegel p131 equation 6.11).

3.3.2.5. Correcting for Shrinkage

Area loss incurred from fixed to processed tissue was measured. From this a linear correction factor (L.C.F.) is calculated.

$$L.C.F. = (Fixed\ Area / Processed\ Area)^{0.5}$$

The internal diameters of NRBs measured on the processed sections were multiplied by this correction factor to give values for fixed tissue. In practice, the area change of sections processed in GMA was so slight that this correction was not carried out.

Figure 3.2. To facilitate the assessment of compression and shrinkage, the plane of the section traversed by the microtome blade was always placed parallel with the longer aspect of the glass slide. Thus the x-axis represents shrinkage and compression while the y-axis represents shrinkage alone.

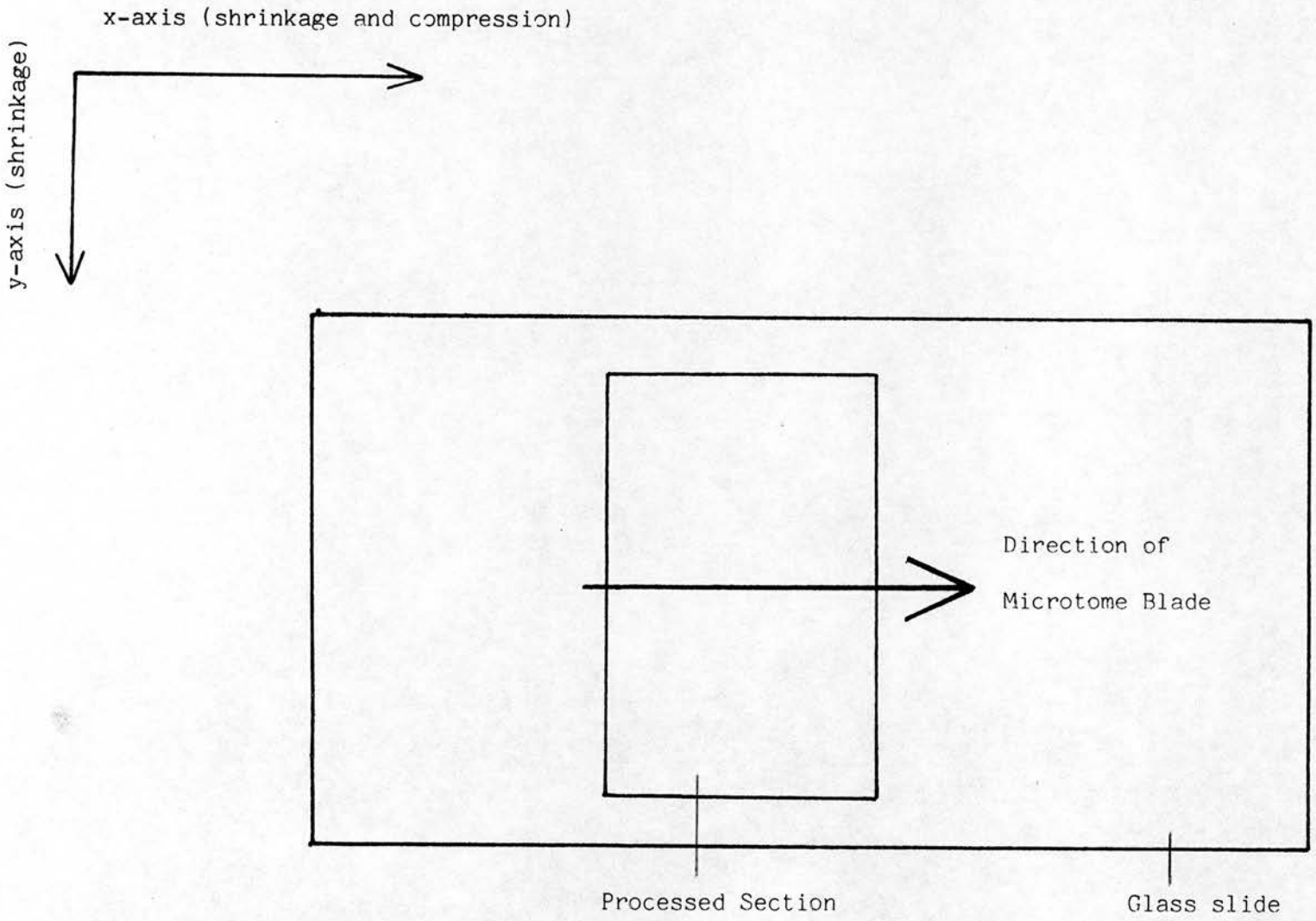
x-axis (shrinkage and compression)
y-axis (shrinkage)
Direction of
Microtome Blade
Processed Section
Glass slide

3.3.3. Results

3.3.3.1. Paraffin Embedded Blocks

The mean linear dimensions, with ranges, for tissue processed in paraffin and GMA are given in table 3.2.

Shrinkage artefact associated with paraffin embedded tissue accounts for at least 15% linear loss (Table 3.4). Using a Wilcoxon signed-ranks test compression was similarly shown to be a significant artefact (Table 3.5) causing a further 6% linear loss in the plane of section (Table 3.4).

Over all area loss of the paraffin sections was 39% (Table 3.3). The theoretical area of the sections, in the absence of any compression, was calculated by squaring the mean y-axis length (plane affected by shrinkage alone). The percentage area loss attributable to shrinkage alone was then calculated using the formula below. Shrinkage area loss=

$$100-(T^2/\text{Expected Area} \times 100)$$

where T^2 is the mean y-axis length squared.

Percentage area loss due to compression was assessed as:

Compression area loss=

$$100-(T^2-P/\text{Expected Area} \times 100)$$

where P is the value obtained for the mean processed section area.

3.3.3.2. GMA Embedded Blocks

The results of table 3.2 suggest that tissue embedded in GMA expands by a factor of roughly 6%, with no compression being evident (Table 3.5). The technique used to assess the linear dimensions of the sections is one which over estimates their average size. That is, if a zero percent increase had been found this would have indicated that the true average length of each section was in fact smaller.

A more accurate estimate of tissue gain or loss is obtained from the mean processed area figure. Tissue embedded in GMA shows an average area gain of 2%. This suggests a linear gain of 1.4% which in terms of the size of the original block (1.9cm by 1.9cm) represents an increase of 0.27mm. Error of this magnitude is negligible and indeed is within the realm of experimental error incurred in the trimming of the original blocks.

3.3.3.3. Qualitative Observations on the Embedding Media

Qualitatively, using paraffin wax, compression was observed to be unevenly distributed throughout the sections, being particularly prominent at the edges ie where the microtome blade had entered and left the blocks (figures 3.3 and 3.4). This artefact was observed even though particular care was taken to float the sections in a water bath before mounting on glass slides. This was not observed for sections embedded in GMA.

3.3.3.4. Quantitative Observations on NRB Size and Ellipticality

NRB SIZE

Comparing paraffin and GMA embedded lung tissue Case B has significantly larger paraffin embedded airways from the right lung and differences approaching conventional levels of significance from the left lung (Table 3.6). There were no significant differences observed from case A.

NRB ELLIPTICALITY

Average bronchiolar ellipticality is similar in all cases except that of paraffin embedded airways from the right lung of case B which are more elliptical than those embedded in GMA (Table 3.7).

As compression has been observed to occur unevenly throughout tissue sections airways in such "zones" will be disproportionately affected. This may affect the distributions of airway ellipticality. This is a potentially important factor as ellipticality is used as the criterion to define which airways are acceptable for the full range of measurements. To test for this possibility the distributions for bronchiolar ellipticality were compared between GMA and paraffin embedded airways. Data from all NRBs were used in this analysis.

Table 3.8 shows there are significant differences in the distributions for airway ellipticality in the right lung of case B and the left lung of case A. In both cases there is an excess of elliptical airways in paraffin embedded tissue.

Airway ellipticality was defined as the ratio of the maximum to minimum bronchiolar diameters, and for reasons outlined in section 3.1 the 30% most elliptical airways were excluded from further morphometric analysis. Table 3.9 shows that in all cases this critical ratio was always more elliptical in the

paraffin embedded sections.

Linear Dimensions of Processed Sections		
Embedding Medium	Y-axis(cm) (Shrinkage)	X-axis(cm) (Shrinkage and Compression)
Paraffin	1.62 (1.44-1.92)	1.50 (1.35-1.68)
GMA	2.02 (1.83-2.29)	2.02 (1.78-2.02)

Table 3.2: Mean linear dimensions with ranges for sections embedded in paraffin and GMA.

Area Dimensions of Processed Sections		
Embedding Medium	Mean Area(cm^2)	Deviation from Expected Area
Paraffin	2.22 (1.80-2.48)	-39%
GMA	3.71 (3.11-4.37)	+2%

Table 3.3: Mean area values -with ranges and deviations from expected values- for sections embedded in paraffin and GMA.

	Paraffin Embedded Tissue	
	Shrinkage	Compression
Linear Loss	15%	6%
Area Loss	28%	11%

Table 3.4: Mean linear and area loss attributable to shrinkage and compression for tissue embedded in paraffin.

Ho: There is no difference between the x and y axis dimensions (table 3.2) for sections embedded in paraffin (repeated for GMA).

Hi: X-axis dimensions < Y-axis dimensions due to the effect of compression (one tailed).

	z-value	probability	decision
Paraffin	5.62	0.0000	Ho rejected
GMA	0.06	0.4721	Ho accepted

Table 3.5: Wilcoxon signed-rank test of the the above null hypothesis.

Ho: There is no difference in NRB minimum diameter between airways processed in paraffin or GMA.

Hi: NRB internal diameter differs between the two embedding media

Subject A; Right Lung

Embedding Medium	Sample Size	Bronchiolar Diameters(cm) Minimum	Maximum	Median
GMA	22	0.48	1.75	0.84
Paraffin	17	0.51	1.85	0.93

z = 0.91 p = 0.363 Decision: Ho accepted

Subject A; Left Lung

Embedding Medium	Sample Size	Bronchiolar Diameters(cm) Minimum	Maximum	Median
GMA	16	0.62	2.34	0.78
Paraffin	22	0.51	2.87	0.85

z = 0.178 p = 0.857 Decision: Ho accepted

Subject B; Right Lung

Embedding Medium	Sample Size	Bronchiolar Diameters(cm) Minimum	Maximum	Median
GMA	29	0.36	1.55	0.60
Paraffin	29	0.48	2.20	0.82

z = 2.25 p = 0.012 Decision: Ho rejected

Subject B; Left Lung

Embedding Medium	Sample Size	Bronchiolar Diameters(cm) Minimum	Maximum	Median
GMA	18	0.34	2.24	0.67
Paraffin	24	0.45	2.64	0.86

z = 1.78 p = 0.075 Decision: Ho accepted

Table 3.6: Mann-Whitney U Tests of the above null hypotheses.

Ho: There is no difference in airway ellipticality between those embedded in paraffin or GMA.

Hi: Airways embedded in GMA are less elliptical than those embedded in paraffin due to the effects of compression on paraffin embedded tissue (one tailed).

Subject A; Right Lung

Embedding Medium	Sample Size	Bronchiolar Ellipticality Minimum	Maximum	Median
GMA	22	1.05	1.49	1.21
Paraffin	17	1.04	1.58	1.18

z = 0.241 p = 0.405 Decision: Ho accepted

Subject A; Left Lung

Embedding Medium	Sample Size	Bronchiolar Ellipticality Minimum	Maximum	Median
GMA	16	1.07	1.43	1.28
Paraffin	22	1.04	2.04	1.31

z = 0.917 p = 0.179 Decision: Ho accepted

Subject B; Right Lung

Embedding Medium	Sample Size	Bronchiolar Ellipticality Minimum	Maximum	Median
GMA	29	1.02	1.60	1.21
Paraffin	29	1.01	1.78	1.45

z = 2.372 p = 0.009 Decision: Ho rejected

Subject B; Left Lung

Embedding Medium	Sample Size	Bronchiolar Ellipticality Minimum	Maximum	Median
GMA	18	1.02	1.81	1.39
Paraffin	24	1.07	1.88	1.33

z = 0.127 p = 0.448 Decision: Ho accepted

Table 3.7: Mann-Whitney U Tests of the above null hypothesis.

Ho: There is no difference in the distributions of airway ellipticality between airways embedded in paraffin and GMA.

Hi: Airways embedded in paraffin are are more elliptical due to the effects of compression (one-tailed).

		Right Lung	Left Lung
Case A	(D)	0.15	0.33
	(X^2)	1.22	5.61
	(p)	NS	0.01
Case B	(D)	0.28	0.17
	(X^2)	5.89	1.64
	(p)	0.01	NS

Table 3.8: Kolmogorov-Smirnov Test of the above null hypothesis. D is the test statistic. This represents the largest gap between the two cumulative frequency distributions and is converted to X^2 with two degrees of freedom for a one-tailed test.

		Embedding Medium	
		GMA	Paraffin
Subject A	Right Lung	1.49	1.58
	Left Lung	1.43	2.04
Subject B	Right Lung	1.60	1.78
	Left Lung	1.81	1.88

Table 3.9: Ratio defining the 30% most elliptical airways for tissue embedded in GMA and paraffin. Ellipticality is defined as the ratio of the maximum to minimum bronchiolar diameters.

Figure 3.3. This figure shows a zone of compression in paraffin embedded tissue. Compression can be seen to occur along the acinar duct (AD).

Figure 3.4. Compression commonly occurs unevenly throughout the sections being more predominant at the top and bottom where the microtome blade enters and leaves the section. An example of this is presented in this figure. The left hand size of the figure shows a zone of obvious compression. The right hand size shows an area within the same section which appears to be unaffected by compression.

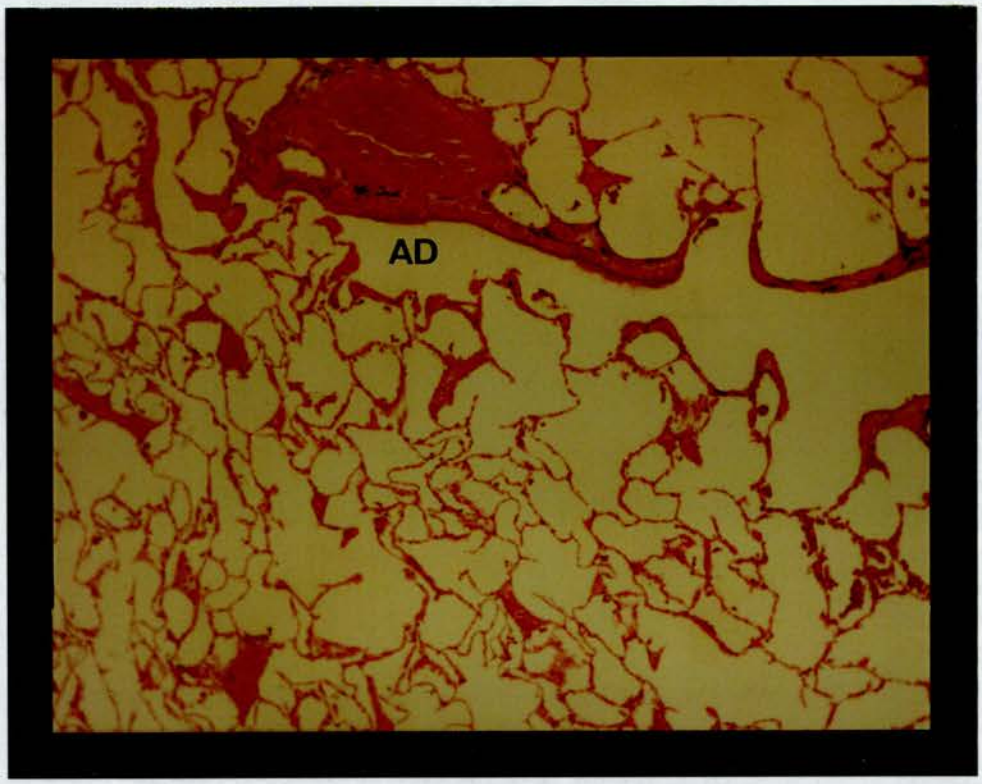
AD

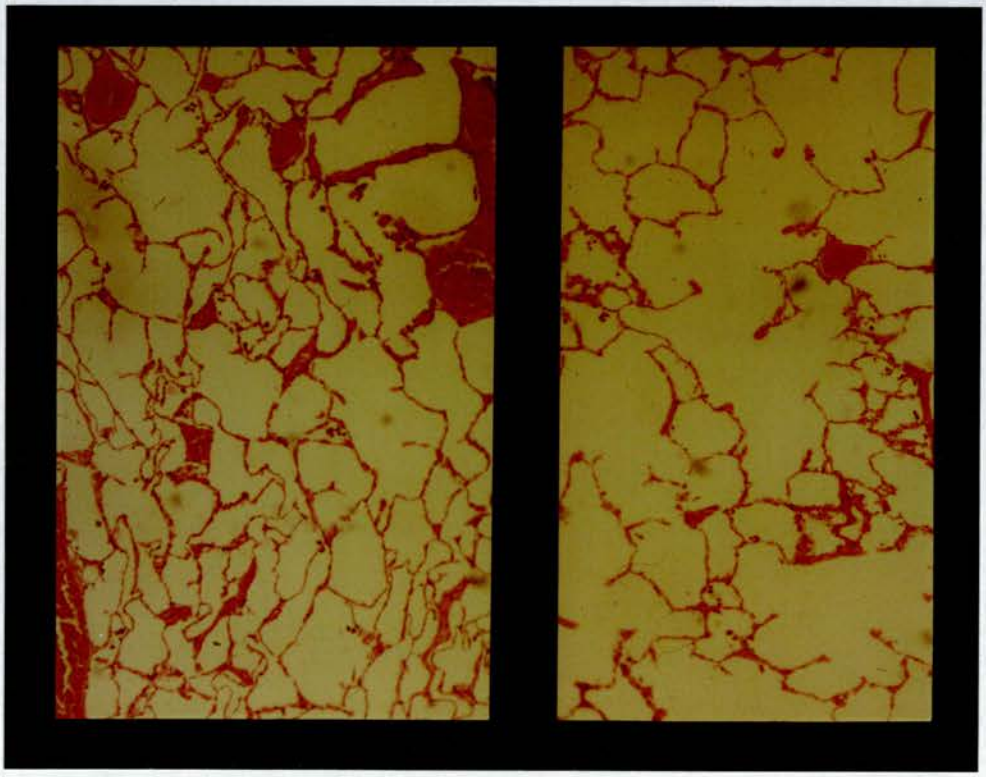

3.3.4. Discussion

The qualitative observations themselves, ie that compression in paraffin embedded sections is unevenly distributed or zonal, negates the proper use of linear shrinkage factors as structures in these zones will be disproportionately affected. These observations are verified by the quantitative analysis of airway ellipticality and size which revealed variable differences between the paraffin and GMA embedded material along with differences in the distribution of airway ellipticality. In addition to this, the upper values for airway size are larger for airways embedded in paraffin. The zonal distribution of compression may account for this. Airways outside the zonal areas of compression will be less affected than those within such zones. The calculated linear correction factors do not discriminate between these and as such will over compensate for the airways not within compression zones. Additionally, in all cases the value of the ratio used to determine the 30% most elliptical airways for paraffin embedding is always greater than the corresponding ratio for GMA. Thus more elliptical airways would be measured in paraffin sections.

In this study it has been possible to process GMA to give negligible changes from fixed to processed tissue. GMA does have its disadvantages. It is expensive and takes longer to process than paraffin. Its advantages outweigh these in that it demonstrates little or no artefact and gives qualitatively and quantitatively superior histological sections. Additionally, thinner sections can be taken which are more favourable for histomorphometry. These qualities made it a more appropriate embedding medium for a quantitative study such as this.

3.4. AWUV: REPRODUCIBILITY OF ITS MEASUREMENT

3.4.1. Introduction

The methodology and principles used to quantitate alveolar perimeter and then derive alveolar surface area *per* unit volume have already been described (sections 2.4.1.3 and 2.4.1.5). Third generation image analysers like the IBAS produce highly accurate quantitative data for each image analysed. This is a function of their high image resolution -in the case of the IBAS each image is made up of more than 250,000 individual pixels- and the morphometry techniques that they apply. In the case of perimeters image analysers like the IBAS use a process known as boundary chain encoding which is similar to manual digitisation in that the precise contours of object are defined as x,y coordinates. The close relationship between boundary chain encoding and digitisation means that the measurement error of the IBAS in measuring perimeters is very close to that already described eg by Fleege (1986 and 1987), Frolov and Maling and Williams. However, as AWUV is essentially a new measure of alveolar surface area, in that it is not measured by the proven technique of mean linear intercept, the reproducibility of its measurement had to be gauged.

To achieve this random areas from a number of lung tissue sections were located and measured. These were relocated and remeasured a few weeks later with no knowledge of the original result.

3.4.2. Material and Methods

3.4.2.1. Source of Material

Six sections were selected from material which had already been processed in GMA.

3.4.2.2. Selection of Fields

Eight random fields were selected from each of the six sections using an England Finder and alveolar perimeter per unit area measured. These measurements were repeated a few weeks later without knowledge of the original results.

3.4.2.3. Statistical Analysis

The difference between the first and the second measurements were gauged in more than one way. The difference between each field result was calculated thus:

$$\% \text{ Difference} = (2\text{nd}/1\text{st measurement} \times 100) - 100$$

thereby representing the difference as a signed percentage.

To calculate the average percentage difference between the first and second field measurements the absolute (ie unsigned) differences *per* field were summed and divided by the total number of fields assessed. Although this represents the average discrepancy, this figure does not indicate whether the second measurements were in general larger or smaller than the first. This was done by summing the signed differences for the individual fields. The equation below, represents the relationship between the first and second

measurements.

$$y_2 = y_1 + e$$

Where e is a random error it should, over a number of measurements, sum to zero. The sum of the signed differences should then sum to zero if this is the case. This was analysed statistically using the paired t-test.

Forty eight fields were analysed. In the absence of any bias the probability of obtaining a higher result on the second reading will equal the probability of obtaining a lower result is equal to 0.5. Hence, 24 fields should have a higher result on the second measurement. The actual value obtained was tested to see if any bias had indeed occured using the binomial test (Siegel), the formula of which is given below.

$$z = (x \pm 0.5) - nP \;/\; (nPQ)^{0.5}$$

Where; x is the number of fields on the second run with a higher value than that on the first, n is the number of observations, P is the hypothesised probability (0.5) of obtaining a higher measurement on the second run and Q is the probability (0.5) of obtaining a lower measurement on the second run. The term $(x \pm 0.5)$ corrects for continuity, with 0.5 being added if $x > nP$, but subtracted if $x < nP$.

Lastly, to attach a figure for the over all agreement between the two measurements, Pearson's correlation coefficient was calculated.

3.4.3. Results

The mean absolute difference between the two measurements was 2.01%, with individual differences ranging from almost 0% to 9%. This is shown in table 3.10 along with the mean differences for each of the six sections. The sum of the signed differences for the 48 fields was 1.03%. There was no significant difference between the two mean values (t=0.20, p=0.884) indicating that the errors involved were random and summed to zero over the 48 observations (Table 3.11).

Twenty six fields obtained a higher result on th second measurement. This was not significantly different from the hypothesised 24 (z=0.72, p=0.236).

There was a significant correlation between the two measurements (r=0.99, p<0.001).

Section	A	B	C	D	E	F
Mean Absolute Percent Difference	2.28	2.33	2.17	2.45	1.99	1.35

Over all mean absolute difference for the 48 fields= 2.01%
(Standard Error= 0.34% Range 0.1% to 8.7%)

Table 3.10: Mean absolute difference for the six sections and 48 fields measured (ie the sum of the unsigned differences between the first and second measurements).

Section	A	B	C	D	E	F
AWUV (mm^2/mm^3)						
1st Measurement	14.4	11.6	16.1	17.8	16.1	16.3
2nd Measurement	14.5	11.8	16.0	17.6	15.8	16.5
Difference	0.7%	1.9%	0.7%	1.1%	1.9%	1.4%

	1st Measurement	2nd Measurement	Difference
Grand Means	15.40	15.39	1.0%
Standard Error	0.514	0.510	

Testing differences between grand means: t=0.20, p=0.844.

Table 3.11: Differences between the means for the six sections and for the grand means (n=48).

3.4.4. Discussion

Results obtained demonstrate the IBAS measurements of alveolar surface area per unit volume to be very reproducible with an mean absolute error of 2.0%; ranging from almost 0% to around 9% for the individual fields. This close concordance of individual field values provides a highly significant correlation between the first and second measurements (r=0.99). Saetta *et al* (1985) have demonstrated that the mean linear intercept technique is equally accurate and reproducible for measuring alveolar surface area. Their correlation between measurements being r=0.97 with all second measurements being within 7% of the first measurements. There was no consistent bias, with the sum of the signed differences over the 48 fields being very low (+1.03%). This was reflected by the small and insignificant difference between the means.

Although there are no significant differences between the first and second measurements it is still pertinent to discuss possible sources of error.

There were two possible sources of error between the first and second measurements. The first relates to the location and relocation of the random England Finder fields. Once a field is located the England Finder is removed from the microscope stage and is replaced by the tissue section. This manoeuvre often causes a slight movement of the stage (these movements were observed by replacing the England Finder on the stage instead of the histological section). As the field had to be relocated for the second measurement there were two occasions when this could occur. This procedure should not provide a consistent bias but produce a random error which will sum to zero. The second possible source of error is in the interactive editing of images. Images are edited mostly to remove collections of macrophages or to fill the lumen of small vessels to exclude their inner aspect from airspace perimeter measurements. Errors incurred at this stage should be slight and again sum to zero. Analysis of the results upholds the hypothesis that both these errors sum to zero and do not affect the reproducibility of the AWUV measurements.

A digitiser tablet (eg the GIS) used to measure AWUV would share both of the above errors. The IBAS differs from such digitiser tablets in its speed and in that once an image has been edited and segmented the IBAS will always return the same value for that field. In contrast, with manual digitisation once the image has been located and the observer has identified the alveolar walls there is an additional error in the manual tracing of their contours.

CHAPTER 4

RESULTS

The format of this chapter is to present the results in the following order:

1. Summary Statistics

Summary statistics for all variables are presented. In a number of instances, where it is considered helpful or relevant, the distribution of variables is is also given.

2. Inter-Morphometry Correlations

Inter-morphometry correlations are presented before investigations into structure *vs* function analyses are attempted. The objective of this section is to look for anatomical inter-relationships, some of which may be cause-and-effect, while others are possibly coincidental. Bivariate and multivariate analyses are presented.

3. CT Scan Results

The aim of this section is to see whether CT scan assessments of lung density match assessments of emphysema. This involves comparisons with both the macroscopic and microscopic measurements, the latter being airspace wall surface area *per* unit volume.

4. Structure *vs* Function Analysis

This section looks for those morphometric variables which show significant correlations with clinical data. Latterly, multivariate analysis is employed to investigate which if any of these variables have an additive or independent effect on function.

5. Extrapolations to "Normal" Structure

On basis of the results presented in the previous four sections, attempts are made to identify a subgroup of cases which have little or no lung disease. From the relationships demonstrated by this subgroup extrapolations are made to postulate structural relationships which may be pertinent to the "normal" lung.

4.1. SUMMARY STATISTICS

With respect to the morphometric variables, forty four cases have data on the amount of macroscopic emphysema present in the mid-sagittal slice and on airspace surface area *per* unit volume. Thirty of these cases also have data on bronchiolar size, ellipticality, alveolar attachment number and mean inter-alveolar attachment distance. With respect to pulmonary function and CT scan, the availability of this data relates to the ability and/or willingness of patients to complete certain pulmonary function tests along with the logistics of putting patients through the desired range of tests in the allotted time (ie 24-48 hours prior to their operation). All data obtained are presented in the appendix and summary statistics on the background data for the cases are

given in table 4.1.

	Summary Statistics			
Variable	Mean	Range	S.D.	n
Age (yrs)	61	46-74	6.6	44
Height (M)	1.69	1.48-1.88	0.08	44
Weight (K)	66	45-94	11.6	41
(Sex		32 males and 12 females)		

Table 4.1: Background data for the study population. Abbreviations S.D.= Standard Deviation and n= number of cases.

4.1.1. Airspace Surface Area *per* Unit Volume (AWUV)

Distribution of AWUV for Individual Cases

In most cases AWUV is distributed normally (figures 4.1A to 4.1C) irrespective of the mean value. Where -in literally a handful of cases- this is not the case eg Figure 4.1D, the results are spread over a wider range and appear platykurtic. Cases exhibiting this type of distribution always have relatively high amounts of macroscopic emphysema, however, this is not to say that all cases with macroscopic emphysema have this type of distribution.

Bearing in mind the methodology employed to measure AWUV, some comments can be made on the AWUV values of the individual fields. With regard to the spread of data in cases with no acquired loss, the higher AWUV value most probably represent those fields consisting almost entirely of alveoli. Contrastingly, those fields with lower AWUV values probably correspond to fields selected around the vicinity of alveolar ducts. The

intervening values of the distribution will therefore represent a mixture of these two distinct respiratory areas.

Distribution of mean AWUV

AWUV was measured for all cases and mean AWUV ranged from 8.8 to 25.4 mm^2/mm^3 (range 16.6) with the mean value for the population being 18.1mm^2/mm^3. Summary statistics are given in table 4.2 and the distribution, as a histogram, is represented in Figure 4.2. In line with Central Limit Theorem (Sokal and Rohlf) although not all individual cases exhibit a normal distribution for AWUV, the mean values for the study group as a whole are normally distributed.

Distribution of LF5 AWUV

LF5 AWUV is the mean value of the lowest 5 AWUV fields measured for each case. LF5 AWUV values range from 1.9 to 21.3mm^2/mm^3 (range 19.4). This is a wider range than that obtained for mean AWUV (Table 4.2). The mean LF5 AWUV value for the population is 12.6mm^2/mm^3 and like mean AWUV is normally distributed.

RATIONAL BEHIND THE CALCULATION OF LF5

If all cases had presented a normal distribution for the individual AWUV fields then the relative rank of any LF5 AWUV value would closely approximate that of the mean AWUV value and accordingly mean AWUV could have been taken to represent most aspects of the distribution for each case. However, as noted above, some cases do not have a normally distributed AWUV and most

notably have a (wider) range of values from very low to very high. Where LF5 AWUV values are calculated for these cases their ranks are much lower than that of their respective means. Figures 4.1C and 4.1D are a case in point. Case 40 has a mean AWUV value 1.7 times greater than that of case 11, the latter providing the lowest mean AWUV value for the population. In contrast, the LF5 AWUV value of case 40 is exactly half that of case 11 and is the second lowest LF5 AWUV value obtained. The reason for this is clear when the two histograms are analysed. The results of case 40 are widely distributed with the 5 lowest values being well away from the mean whereas the AWUV values of case 11 although very low are still normally distributed with the lowest five fields being closer to the mean. That this occurs in a number of cases can be gauged by the strength of the correlation coefficient between mean and LF5 AWUV, ($r=0.83$, $n=44$, $p<0.001$) which although strong shows there is not a straight forward one-to-one mapping.

As a consequence of these observations it was felt that in many of the future analyses (eg in comparisons with CT measured lung density) a statistic which represented the least densely alveolated areas of the lung would be useful. Arbitrarily, the mean AWUV value of the five lowest fields was calculated.

Figure 4.1 (overleaf). Individual AWUV distributions for four cases showing that for most cases (figures 4.1A to 4.1C) AWUV is normally distributed irrespective of the magnitude of the mean AWUV value. In a handful of cases AWUV distributions appear platykurtic (eg Figure 4.1D). In this latter group LF5 AWUV values are relatively lower than the corresponding mean AWUV values.

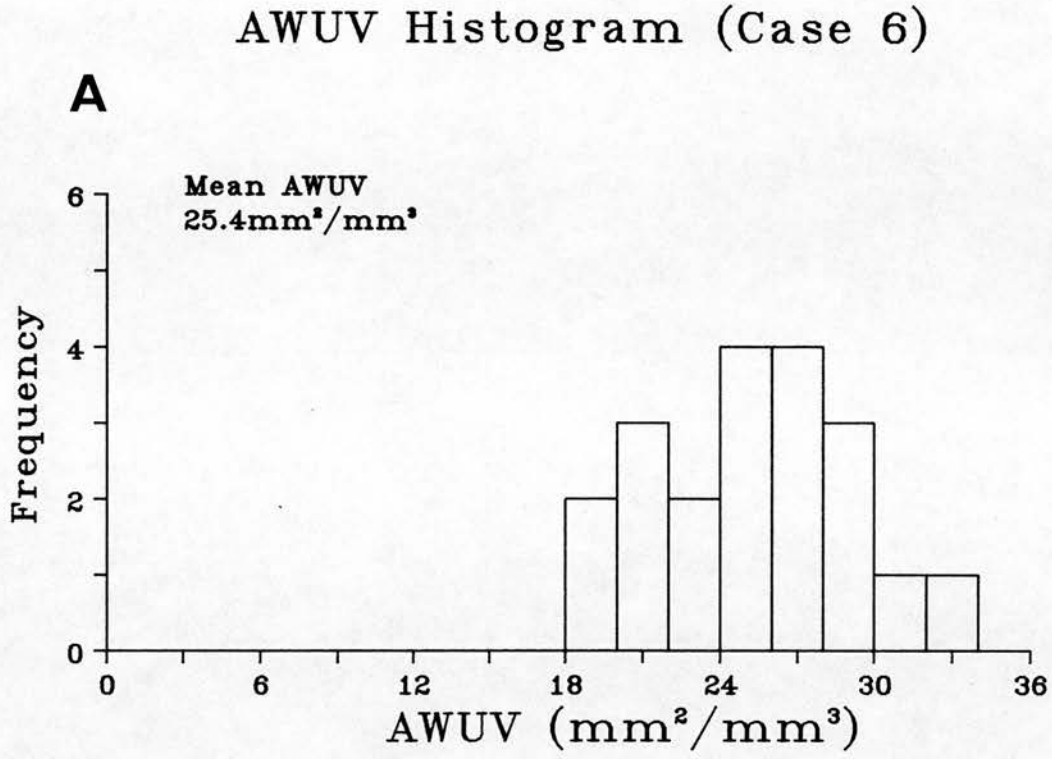
AWUV Histogram (Case 6)
A
Mean AWUV
25.4mm²/mm³
Frequency
0
2
4
6
0
6
12
18
24
30
36
AWUV (mm²/mm³)

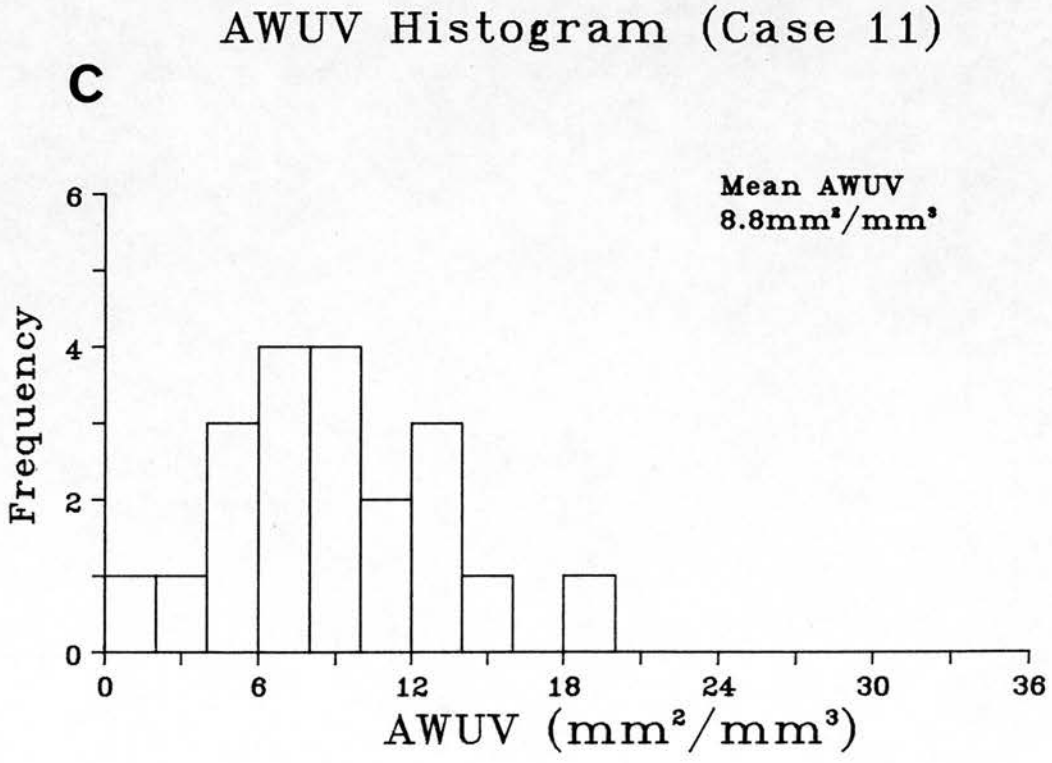
AWUV Histogram (Case 11)
C
Mean AWUV
8.8mm²/mm³
Frequency
0
2
4
6
0
6
12
18
24
30
36
AWUV (mm²/mm³)

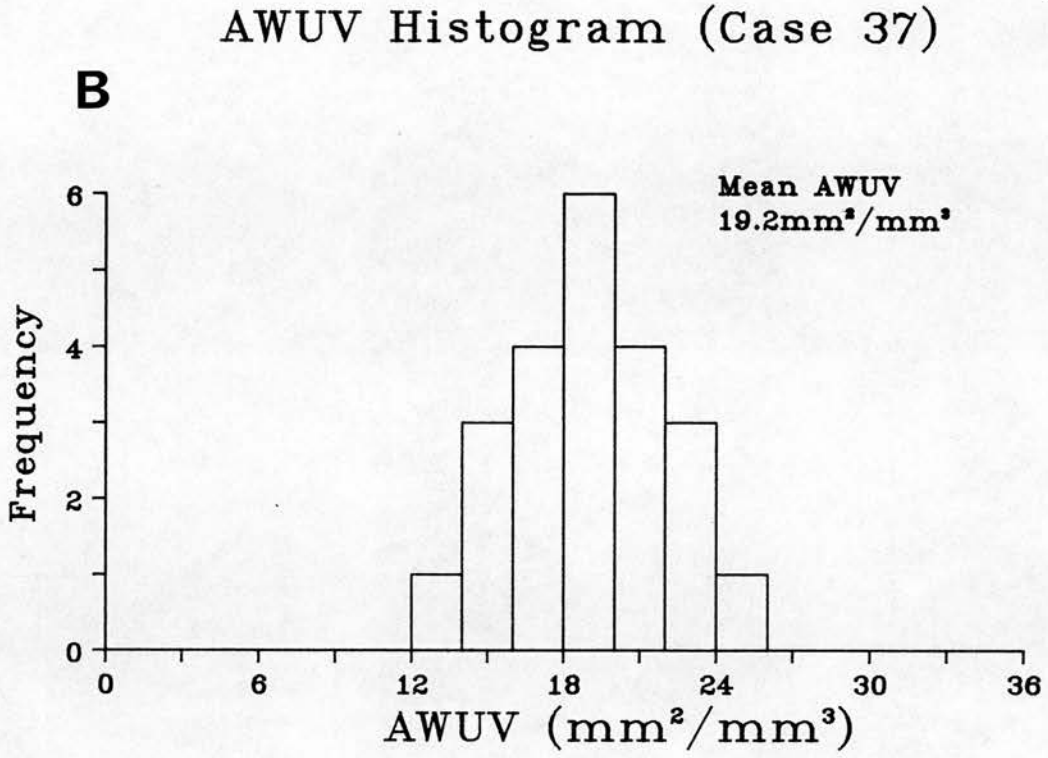
AWUV Histogram (Case 37)
B
Mean AWUV
19.2mm²/mm³
Frequency
0
2
4
6
0
6
12
18
24
30
36
AWUV (mm²/mm³)

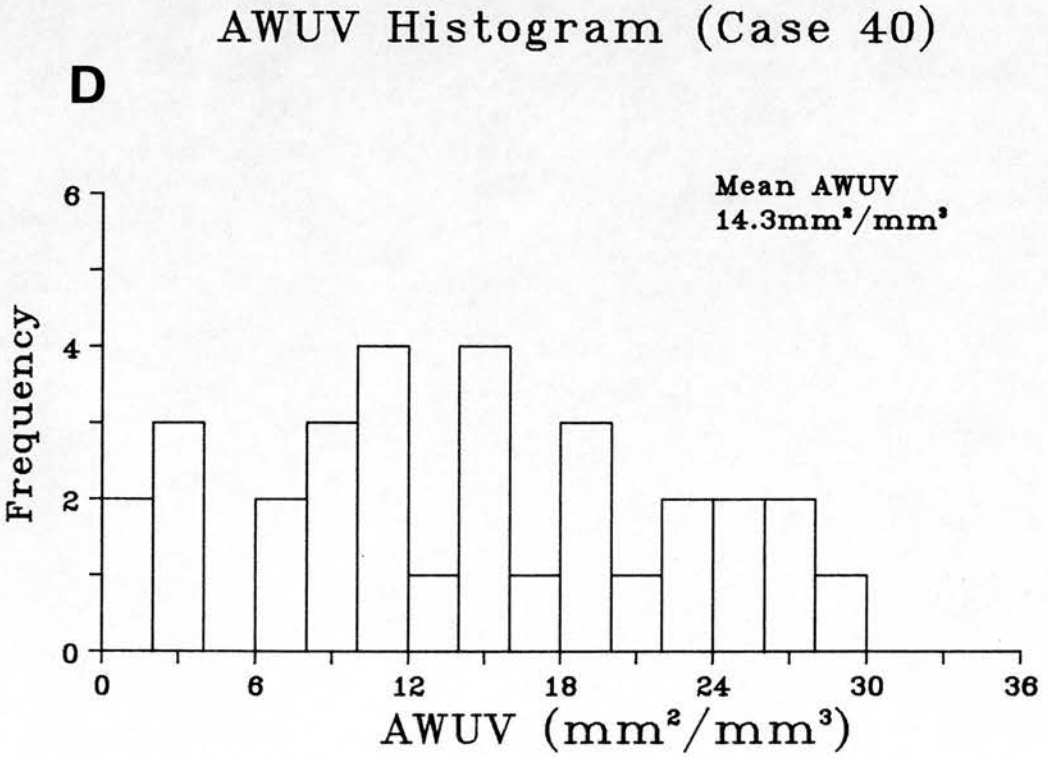
AWUV Histogram (Case 40)
D
Mean AWUV
14.3mm²/mm³
Frequency
0
2
4
6
0
6
12
18
24
30
36
AWUV (mm²/mm³)

Figure 4.2. Distribution of mean AWUV values for the study population. The over all mean value= 18.2mm^2/mm^3, S.D.= 3.3mm^2/mm^3 with n=44.

Figure 4.3. Distribution of mean luminal inter-alveolar attachment distance. This is normally distributed with a mean value= 174µm, S.D.= 26µm with n=30.

Distribution of Mean AWUV
(n=44)

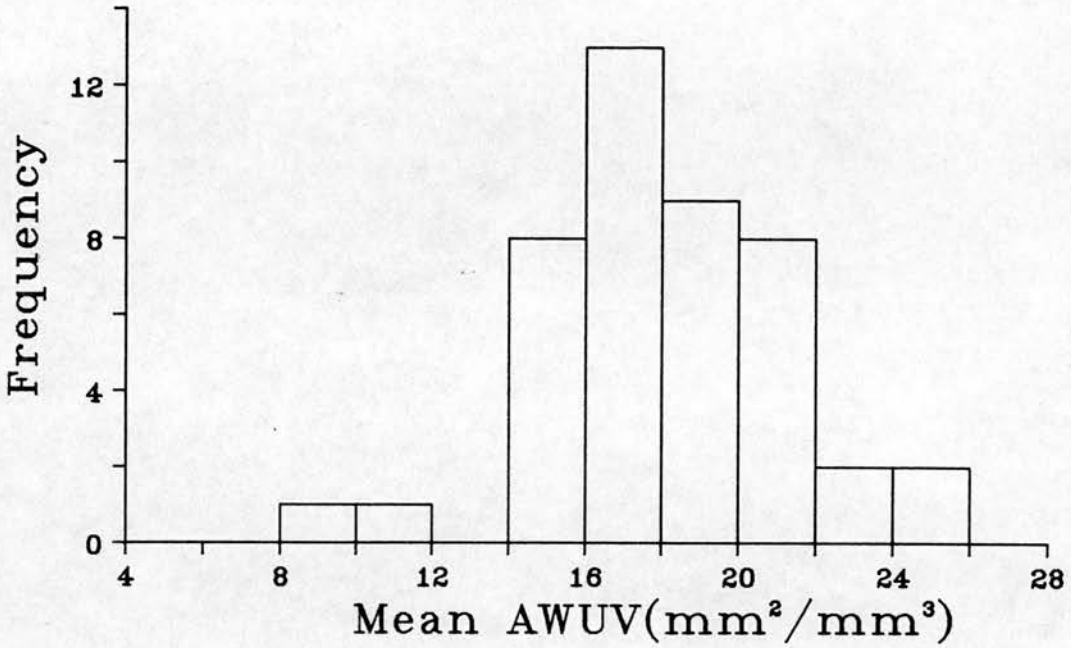

Distribution of Mean IAAD
(n=30)

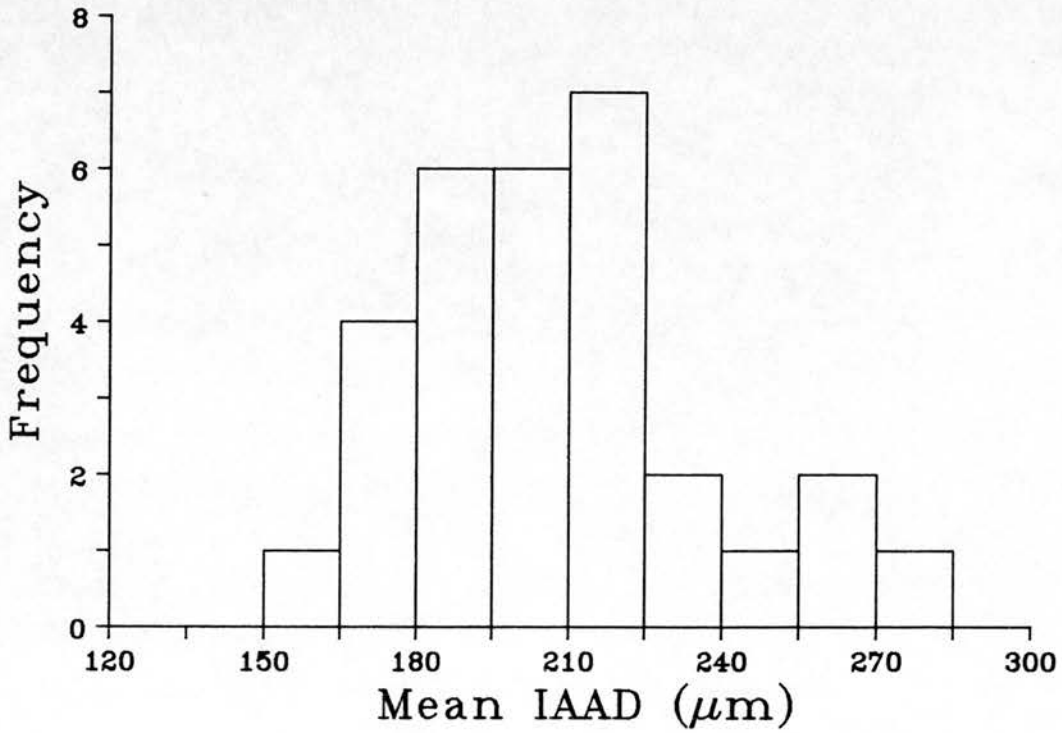

4.1.2. Peribronchiolar Alveolar Attachments

Mean Number *per* Airway

There is an average of 16.9 attachments *per* airway with individual mean values ranging from 11.9 to 22.3 (Table 4.2).

Mean Inter-Alveolar Attachment Distance

Only mean luminal inter-alveolar attachment distance is reported here, the reasons for this are given later. The mean value for the population is 174µm with values ranging from 133 to 244µm. The distribution is given in figure 4.3 and the summary statistics in Table 4.2.

Variable	Mean	Range	S.D.	n
AWUV				
Mean (mm^2/mm^3)	18.12	8.78-25.40	3.31	44
LF5 (mm^2/mm^3)	12.61	1.88-21.26	4.50	44
Peribronchiolar Attachments				
Mean Number per Airway	16.94	11.9-22.3	2.49	30
Mean IAAD (μm)	173.96	133-244	26.06	30
Bronchiolar Parameters				
Minimum Diameter (mm)	0.54	0.36-0.78	0.10	30
Measured Lumen Area (mm)	0.41	0.19-0.87	0.15	30
Theoretical Lumen Area (mm)	0.83	0.42 1.56	0.31	30
Epithelial Area (mm)	0.06	0.03-0.13	0.02	30
Wall Area (mm)	0.31	0.17-0.65	0.12	30
Ellipticality	1.52	1.28-1.96	0.17	30
Density(cm^{-2})	0.64	0.37-1.22	0.18	30
Macroscopic Emphysema				
Percentage Area	8	0-79	19.3	44

Table 4.2: Summary Statistics for Morphometric Variables. Abbreviations:S.D.= Standard Deviation, n= number of cases measured and Mean IAAD= Mean Inter-Alveolar Attachment Distance.

4.1.3. Bronchiolar Measurements

The measurements made on each bronchiole are represented schematically in figure 2.8 and the results obtained summarised in table 4.2.

Luminal Size

All measurements of luminal calibre (ie measured and theoretical lumen area and minimum diameter) are normally distributed. Minimum diameter varies from 0.36 to 0.78mm with an over all mean of 0.54mm. Measured cross sectional lumen area ranges from 0.18 to 0.87mm^2 and has a mean value of 0.41mm^2. The mean value for theoretical lumen area is 0.83mm^2 with individual

values ranging from 0.42 to 1.56mm^2.

IS THEORETICAL LUMEN AREA A USEFUL MEASUREMENT?

To assess which measurement is the best representation of bronchiolar size correlation coefficients for all three measurements of NRB size against epithelial and wall area where calculated (Table 4.3). This was done as one would, in general, expect lumen size to vary proportionately with the amount of epithelium and wall.

	Epithelial Area		Wall Area	
	r	p	r	p
Lumen Area	0.63	0.001	0.65	0.001
Minimum Diameter	0.50	0.003	0.53	0.001
Theoretical Lumen Area	0.73	0.001	0.84	0.001

Table 4.3: Correlation coefficients for the three measurements of lumen size against epithelial and wall areas.

Theoretical lumen area has the best correlations with epithelial and wall areas. Figure 4.4 demonstrates this to be a very close relationship for all cases. It is therefore reasonable to conclude that this parameter is the best representative of airway size. It is also evident that minimum diameter has the poorest correlations.

Figure 4.4. Bronchiolar epithelial area *vs* theoretical lumen area. Of the three measures of bronchiolar size theoretical lumen area has the best correlations with both epithelial and wall area. Correlation statistics; r=0.84, p=0.001 with n=30.

Figure 4.5. Histogram of bronchiolar ellipticality. Mean value= 1.52, S.D.= 0.17 with n=30. This parameter, obtained by calculating the ratio of maximum to minimum bronchiolar diameters, is normally distributed.

NRB Epithelial Area *vs*
Theoretical Lumen Area

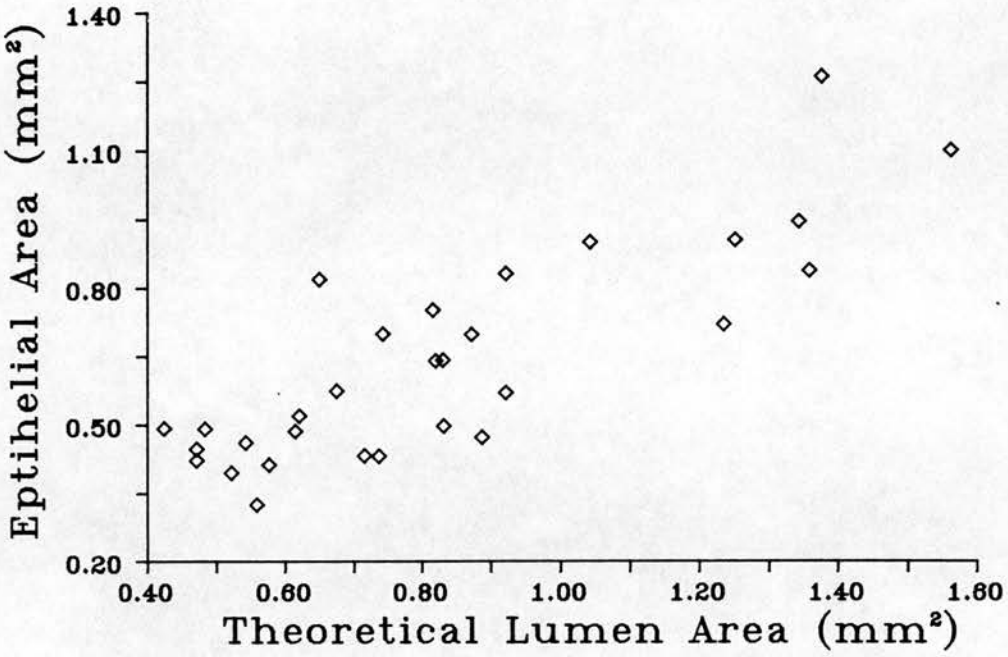

Distribution of
Bronchiolar Ellipticality (n=30)

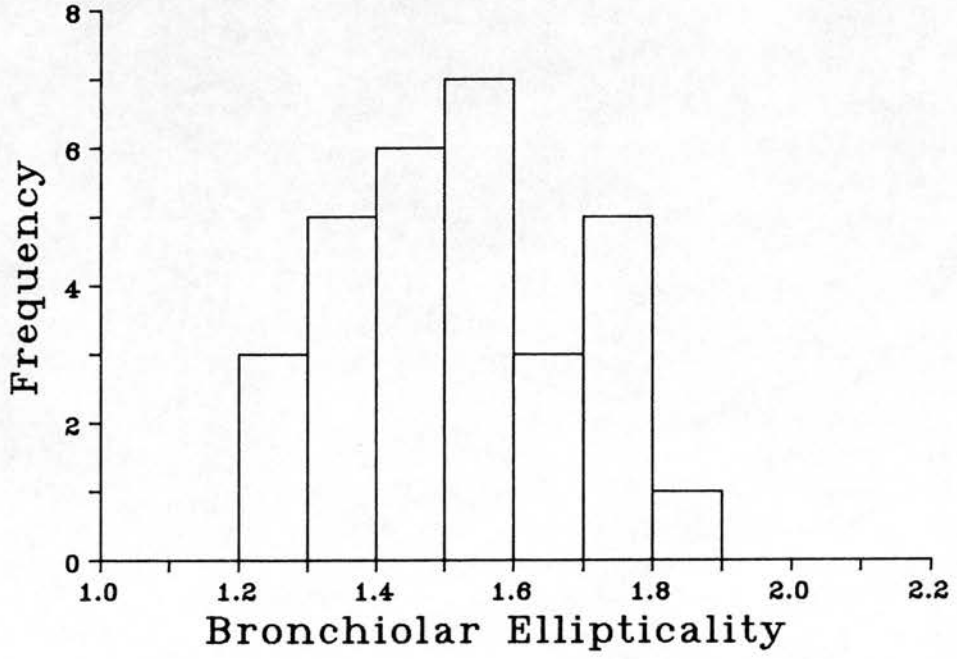

Bronchiolar Ellipticality

The ellipticality of bronchioles is represented by the ratio of the maximum diameter divided by the minimum diameter. This variable can therefore vary from one, where the two diameters are equal, to almost infinity where progressively larger values are obtained for progressively more elliptical airways.

The mean ratio obtained is 1.53 varying from 1.28 to 1.96 (table 4.2). Figure 4.5 is a histogram of the mean values for the thirty cases. It must be remembered that these are the mean ratios for the 70% most circular airways ie those thought to be more transversely as opposed to longitudinally or tangentially sectioned.

Bronchiolar Density

The average airway density is 0.64 bronchioles *per* cm^2 (Table 4.2). These figures are the density of airways accepted for the full range of measurements (ie those included by the 70th percentile ratio). Dividing these figures by 0.7 gives the density of bronchioles as defined by the criteria set out in section 2.4.2.3, which is 0.91 bronchioles per cm^2.

4.1.4. Macroscopic Emphysema

Percentage Area Of the Mid-Sagittal Slice

The proportion (as a percentage) of the mid-sagittal slice involved with

macroscopically identifiable emphysema was assessed for each case. The results obtained are summarised if Figure 4.6.

The ordinate of this histogram has two scales, the first starts at 0 and increases in increments of 1 up to the value of 10, thereafter the scale increases in increments of ten up to the value of 100. The majority of cases (21 out of 44) have less than 1% of their area involved with macroscopic emphysema.

Comparing the two halves of the histogram 37 cases have less than 10% while only 7 have more than 10% of their area involved with macroscopic emphysema. Cases with relatively large proportions of macroscopic emphysema were predominantly panacinar in type.

Summary statistics are given in Table 4.2, but it must be noted at this point that with the type of distribution obtained the mean and standard deviation are of little value except (if it were needed) to confirm that the results are not normally distributed.

A consequence of the distribution of macroscopic emphysema, *vis a vis* the application of appropriate correlation statistics, is that parametric statistics such as Pearson's correlation coefficient, which assume the data to be normally distributed, cannot properly be applied to ascertain the degree of covariance between macroscopic emphysema (by area) and other variables. The approach taken here has been to use Spearman's coefficient of rank correlation (r_s or rho), a non-parametric equivalent to Pearson's correlation coefficient. The appropriateness of this and other correlation tests used with this type of distribution is discussed later.

Figure 4.6. Distribution of macroscopic emphysema. This is measured as the percentage area of the midsagittal slice involved with macroscopic emphysema (ie airspaces larger than 1mm diameter). This parameter has a highly skewed distribution; mean value= 8%, S.D.=19.3% and n=44.

Figure 4.7. Mean AWUV *vs* the Percentage Area of Macroscopic Emphysema. There is little covariance between these two parameters. This is a result of the skewed distribution of macroscopic emphysema. This produces bivariate distributions which are inappropriate for correlation statistics.

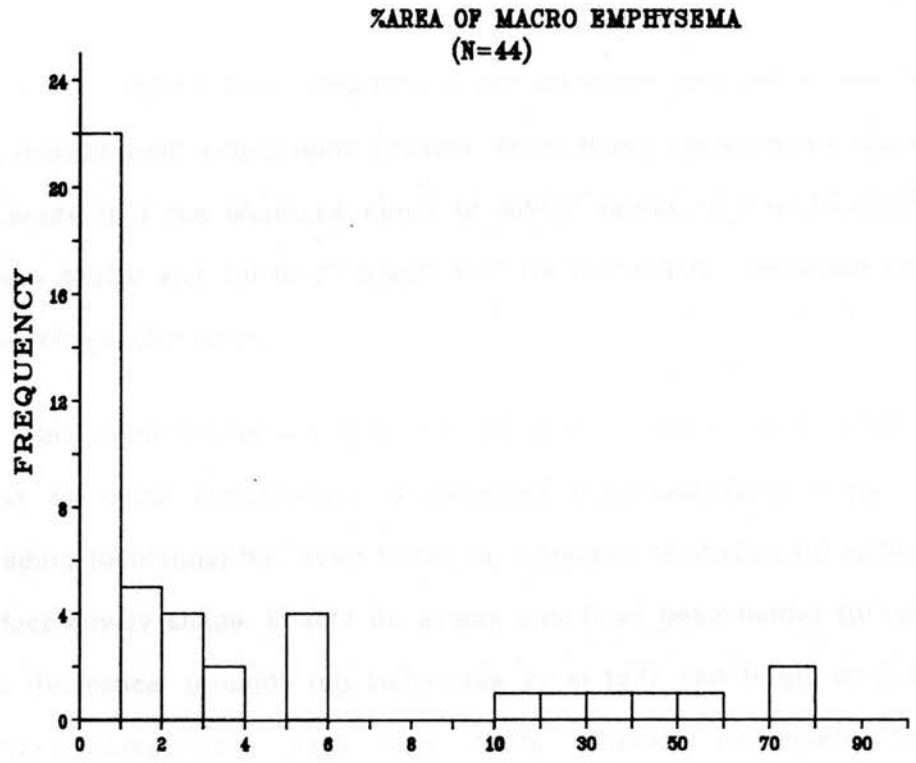

Mean AWUV *vs*
%Area of Macroscopic Emphysema

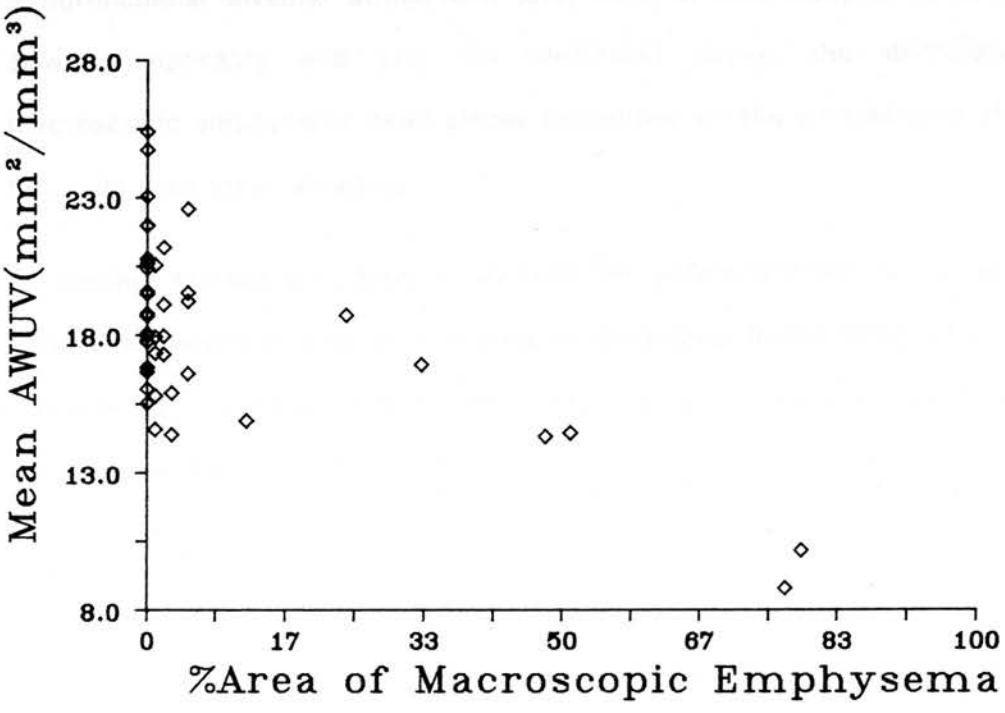

Lastly, it has been postulated elsewhere (Cosio *et al* 1980) that emphysema is associated with other pathological changes in the wall of bronchioles. Having measured epithelial and wall areas of bronchioles, it is possible to investigate whether any increase in these components coincides with decreases in AWUV and/or loss of peribronchiolar alveolar attachments.

4.2.2. AWUV and Other Variables

4.2.2.1. AWUV and Macroscopic Emphysema

Two measurements of over all alveolar loss have been made, one at the microscopic level (AWUV) and the other a measurement of the amount of macroscopic emphysema present in the mid-sagittal slice.

Mean AWUV, as a measure of airspace surface area, might be expected to correlate with the amount of macroscopic emphysema. The range of AWUV values at which macroscopic emphysema is present is very large (8.8 to 22.6mm^2/mm^3 for cases with 5% or more macroscopic emphysema) as is the range of AWUV for cases with no macroscopic emphysema at all (15.5 to 25.4mm^2/mm^3 -cf figure 4.7). Therefore, although cases with relatively large amounts of macroscopic emphysema have low AWUV values, in general there is little in the way of agreement between the two variables, and there is no cut off point at which low values of AWUV are clearly associated with the presence of macroscopic emphysema.

These observations suggest that any correlation coefficient obtained would rely heavily on those cases with significant amounts of macroscopic emphysema. To test this assumption Spearman's coefficient of rank correlation was calculated for all cases (n=44) and then for the subset of cases with less

than 12% macroscopic emphysema (n=37). Spearman's coefficient was calculated as the variables do not constitute a bivariate normal distribution (this was expected remembering the distribution of macroscopic emphysema). The correlation coefficients obtained are given in table 4.4. Significant correlations were obtained where all cases are included, but these diminish to insignificant levels for the smaller subset of cases that have less than 12% macroscopic emphysema. These findings therefore support the conclusion that for the study group as a whole there is little correlation between AWUV and macroscopic emphysema.

All Cases

	% Area of Macroscopic Emphysema	
	r	p
Mean AWUV	-0.47	0.001
LF5 AWUV	-0.56	<0.001

Cases with <12% Macroscopic Emphysema

	% Area of Macroscopic Emphysema	
	r	p
Mean AWUV	-0.22	0.094
LF5 AWUV	-0.24	0.075

Table 4.4: Correlation statistics for AWUV *vs* Macroscopic Emphysema firstly, for all cases and latterly for those cases with less than 12% Macroscopic Emphysema.

4.2.2.2. AWUV and NRB Measurements

AWUV and Measured Lumen Size

NRBs lacking cartilage in their walls have little inherent support to prevent collapse, but rely on radial alveoli to maintain their patency. Progressive alveolar loss may then be expected to bring about a depreciation in NRB size. Looking specifically at measured lumen size ie measured cross-sectional lumen area and minimum diameter, this does not correlate with either mean or LF5 AWUV, cf Table 4.5.

	Lumen Area		Minimum Diameter	
	r	p	r	p
Mean Awuv	-0.11	0.286	0.06	0.377
LF5 AWUV	-0.08	0.341	0.12	0.263

Table 4.5: Correlation coefficients for Mean and LF5 AWUV against measured cross-sectional lumen area and minimum diameter.

AWUV and Theoretical Lumen Area

As well as representing NRB size as measured cross-sectional lumen area and minimum diameter a theoretical cross-sectional lumen area has been calculated. This parameter represents a potential size achievable for an airway and is based upon the measured lumen circumference.

Visually (figure 4.8) there is, for all but three cases, a good degree of association between AWUV and theoretical lumen area. Correlation statistics

suggest that this association is weak with LF5 AWUV ($r=-0.36$, $n=30$, $p=0.024$) and non-significant with mean AWUV ($r=-0.22$, $p=0.126$).

AWUV *vs* Epithelial and Wall Areas

The correlation matrix for these variables is given in table 4.6. Before accepting these correlations at face value one must remember that AWUV and theoretical lumen area are similarly correlated and, as tabulated above, theoretical lumen area correlates strongly with both wall area ($r=0.84$) and epithelial area ($r=0.73$), indicating that increases in bronchiolar wall and epithelium simply reflect increases in lumen area.

To confirm that this is the case partial correlation coefficients were calculated for theoretical lumen area *vs* wall and epithelial area while controlling for AWUV. Doing this partial correlation coefficients of $r_p=0.72$ ($p<0.001$) for theoretical lumen area and wall area and $r_p=0.83$ ($p<0.001$) for theoretical lumen area and epithelial area were obtained. Contrastingly, where theoretical lumen area is held constant and partial correlation coefficients are calculated between AWUV *vs* wall and epithelial area, the results are non-significant. The respective partial correlations for mean AWUV are $r_p=-0.22$ ($p=0.127$) and $r_p=0.04$ ($p=0.424$), and for LF5 AWUV are $r_p=-0.08$ ($p=0.337$) and $r_p=0.06$ ($p=0.380$). This substantiates the finding that the bivariate correlations between AWUV and both wall and epithelium represent colinearity (cross-correlation) with the latter two variables simply reflecting increases in theoretical lumen area.

	Epithelial Area		Wall Area	
	r	p	r	p
Mean AWUV	-0.21	0.128	-0.30	0.051
LF5 AWUV	-0.31	0.049	-0.35	0.030

TABLE 4.6: Correlation coefficients for Mean and LF5 AWUV *vs* epithelial and wall area for all 30 cases.

4.2.2.3. AWUV and Bronchiolar Ellipticality

There is a definite, but variable linear relationship between AWUV and NRB ellipticality ($r=-0.51$, $n=30$, $p=0.002$). This relationship, being negative, indicates that as AWUV decreases airways are increasingly elliptical. The relationship between AWUV and NRB ellipticality improves when AWUV is represented by LF5 AWUV, figure 4.9 ($r=-0.69$, $p<0.001$).

Figure 4.8. Theoretical Lumen Area *vs* LF5 AWUV. Increases in theoretical lumen area are associated with decreases in AWUV. The influence of outliers returns relatively poor correlation statistics; $r=-0.36$, $p=0.024$ and $n=30$.

Figure 4.9. Bronchiolar Ellipticality *vs* LF5 AWUV. Increasing bronchiolar ellipticality covaries with increasing loss of AWUV; $r=-0.69$, $p<0.001$ and $n=30$.

Theoretical Lumen Area
vs LF5 AWUV

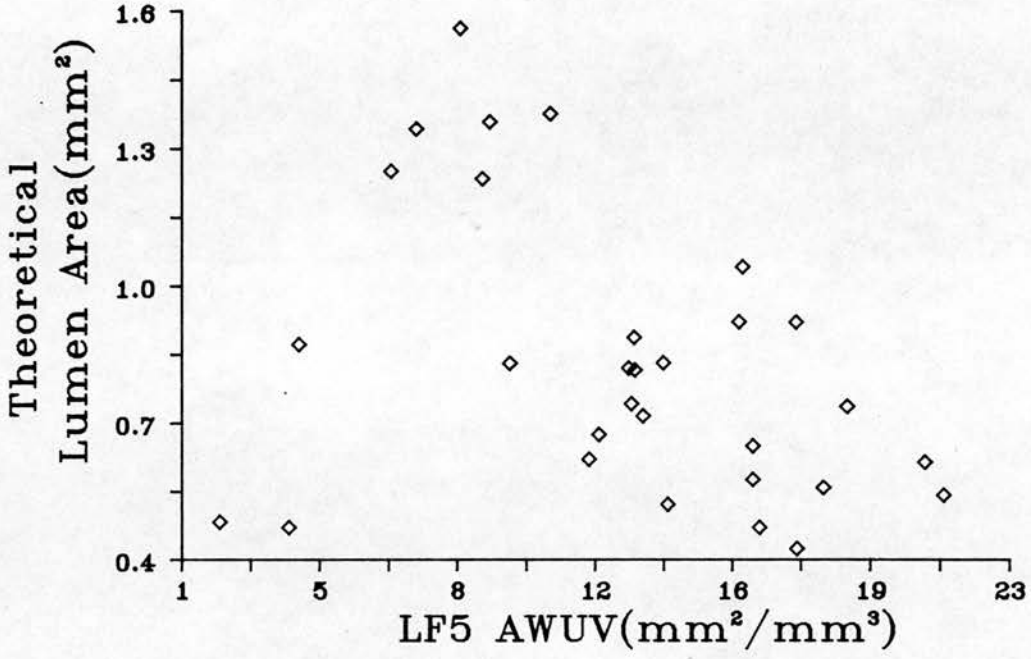

Bronchiolar Ellipticality
vs LF5 AWUV

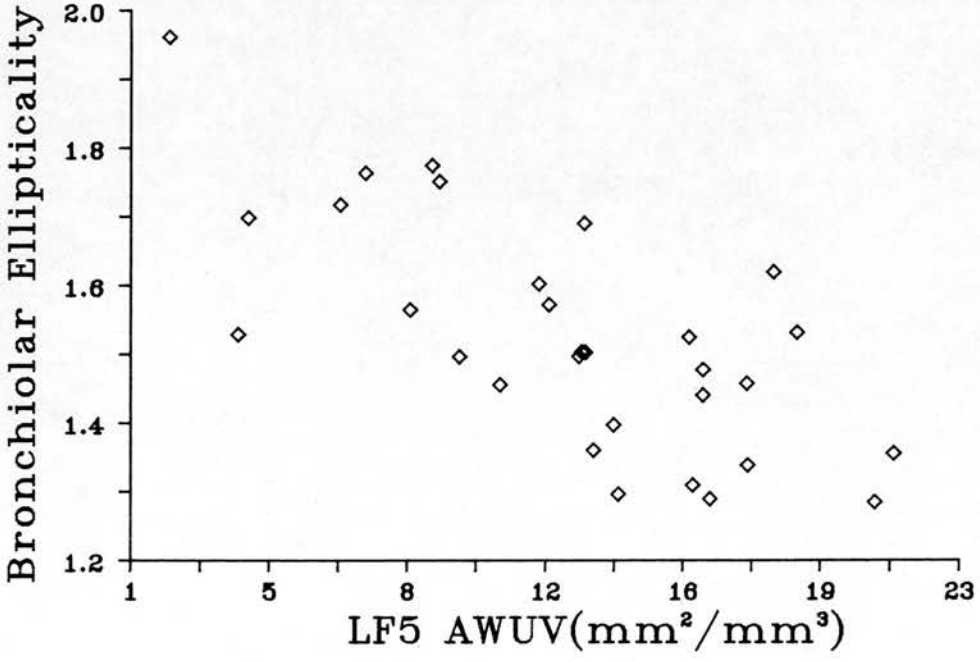

4.2.3. Alveolar Attachments and Other Variables

4.2.3.1. Alveolar Attachments and NRB Measurements

As expected, the mean number of attachments *per* airway correlates significantly with mean lumen area (r=0.57, n=30, p=0.001) and minimum diameter (r=0.54, p=0.001), simply reflecting the fact that larger bronchioles have more radial alveolar attachments.

This variability in the number of attachments relating to airway size has been normalised by dividing the measured bronchiolar circumferences (ie luminal, epithelial and mural) by the number of alveolar attachments. This gives a mean inter-alveolar attachment distance which is independent of airway size *per se* (neither the mean number of attachments nor mean inter-alveolar attachment distance correlate with total lung capacity or height), there being no evidence to suggest that alveolar size varies along the bronchial tree. Hence, mean inter-alveolar attachment distance results are concentrated on in the remainder of the results section.

Luminal, epithelial and mural mean inter-alveolar attachment distances were used in structure *vs* structure and structure *vs* function correlations. Almost without exception the most powerful and significant correlations were obtained using mean luminal inter-attachment distance. Mean wall inter-alveolar attachment distance demonstrated similar, but in general weaker correlations. For the sake of brevity and also probably clarity, correlation coefficients reported for radial alveolar attachments have been restricted to mean luminal inter-alveolar attachment distance.

Alveolar Attachments and Theoretical Lumen Area

The plot of theoretical lumen area and mean inter-alveolar attachment distance (figure 4.10) suggests there is an over all association between these two variables for the population as a whole with the exception of 2 outliers. The statistical influence of these two cases is such that the r value for the correlation coefficient is not significant ($r=0.25$, $n=30$, $p=0.093$).

Alveolar Attachments *vs* Wall and Epithelial Areas

There are no significant correlations between mean inter-alveolar attachment distance and either wall or epithelial area.

4.2.3.2. Alveolar Attachments and NRB Ellipticality

The evidence that small airways are mishapen in emphysema has been reviewed (section 1.5.5). Further to this significant correlations have been registered between AWUV and NRB ellipticality. The reason postulated for these relationships is that as bronchioles rely on radial alveolar attachments to maintain their integrity any alveolar loss may compromise this integrity. Having obtained significant correlations between AWUV and NRB ellipticality, one would expect airway ellipticality to likewise covary with measurements of peribronchiolar alveolar loss.

Bronchiolar ellipticality is dependent on and is strongly related to the mean inter-alveolar attachment distance ($r=0.62$, $p=0.001$). This association between ellipticality and mean inter-alveolar attachment distance is a fairly tight one (Figure 4.11) the trend being that as the mean inter-alveolar attachment

distance increases -presumably through loss of peribronchiolar alveoli- NRBs become progressively more elliptical. This correlation between mean inter-alveolar attachment distance and NRB ellipticality is stronger than that obtained for mean AWUV and NRB ellipticality, but similar to that obtained for LF5 AWUV and NRB ellipticality. It is also interesting to note that theoretical lumen area covaries with bronchiolar ellipticality with larger lumen areas being associated with more elliptical airways. The correlation coefficient is relatively low ($r=0.37$, $p=0.023$), however, where the one outlier, case 40, is excluded the correlation coefficient improves to $r=0.65$ ($p=0.001$).

4.2.3.3. AWUV and Alveolar Attachments

Having observed that both mean inter-alveolar attachment distance and AWUV correlate with airway ellipticality it would be reasonable to expect these two variables to correlate with one other. Indeed on the basis of the scatter plots of figures 4.9 and 4.11, one could conclude that peribronchiolar attachments and AWUV play a crucial role in maintaining the shape of bronchioles and that as AWUV decreases, through loss of alveolar walls, there is a corresponding loss of peribronchiolar attachments.

When correlated against mean inter-alveolar attachment distance both mean AWUV ($r=-0.32$, $p=0.043$) and LF5 AWUV ($p=-0.44$, $p=0.008$) provide weaker correlation coefficients than predicted above. It would appear from the plots (Figures 4.12 and 4.13) that while most points follow the general hypothesised relationship ie loss of AWUV covarying with loss of peribronchiolar attachments, there are a few notable exceptions.

Figure 4.10. Theoretical Lumen Area *vs* Mean Inter-Alveolar Attachment Distance. These two variables appear to covary for most cases with the exception of two outliers. The influence of these outliers is such that the correlation statistics are weak; r=0.25, p=0.093 and n=30.

Figure 4.11. Bronchiolar Ellipticality *vs* Mean Inter-Alveolar Attachment Distance. Loss of radial support offered by peribronchiolar alveolar attachments, reflected by an increase in mean inter-alveolar attachment distance, is associated with increasing bronchiolar ellipticality. Correlation statistics; r=0.62, p=0.001 and n=30.

Theoretical Lumen Area
vs Mean IAAD

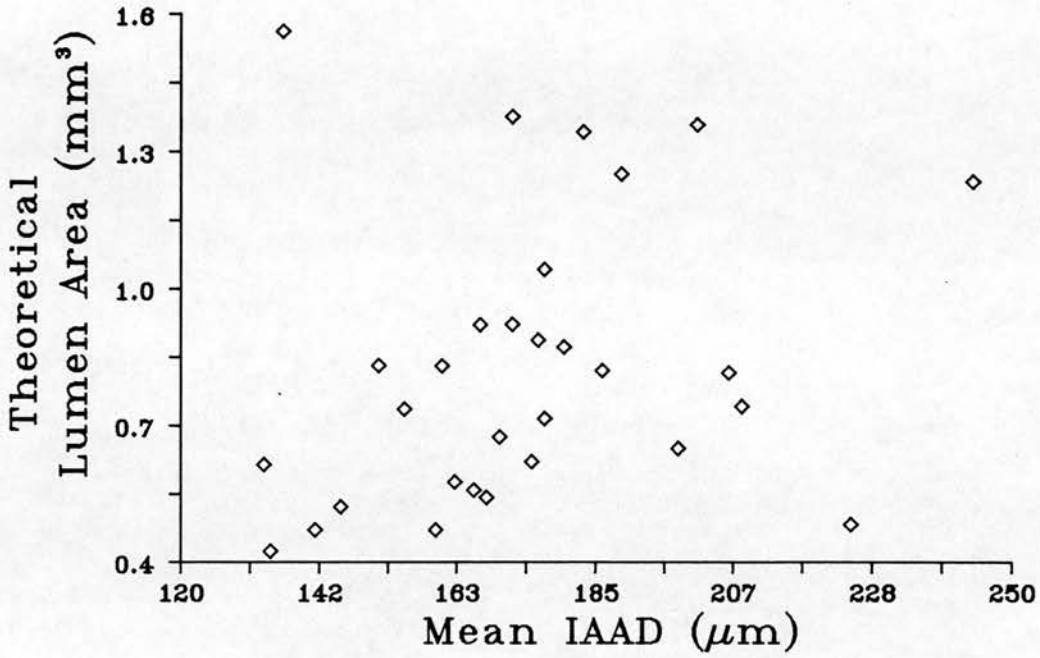

Bronchiolar Ellipticality
vs Mean IAAD

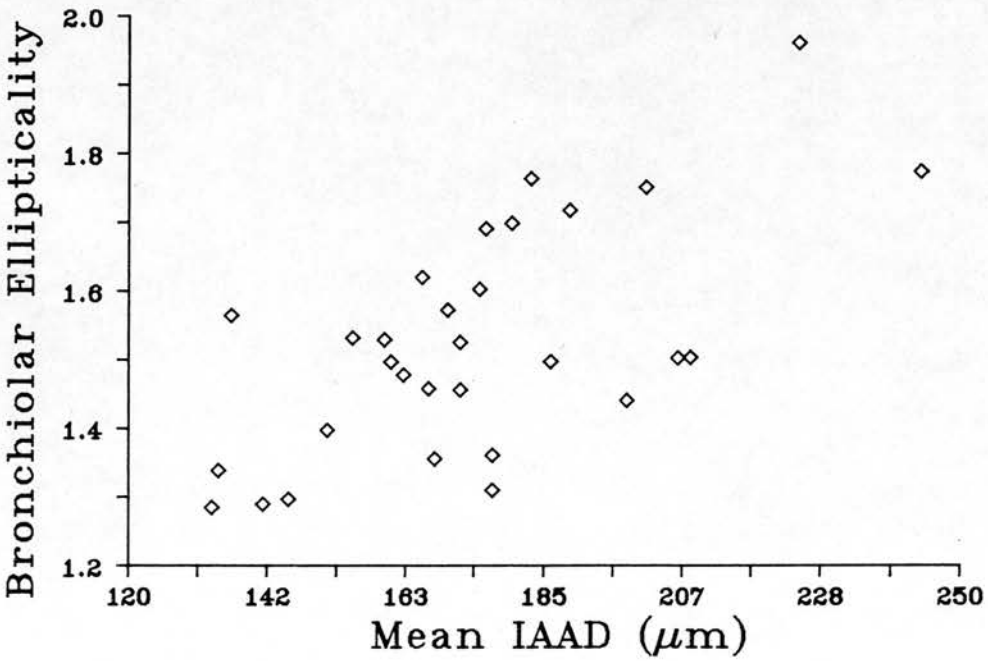

Figure 4.12. Mean Inter-Alveolar Attachment Distance *vs* Mean AWUV. For most cases peribronchiolar attachment and AWUV loss covaries. The association though is variable; r=-0.32, p=0.043 with n=30.

Figure 4.13. Mean Inter-Alveolar Attachment Distance *vs* LF5 AWUV. As with mean AWUV, mean inter-alveolar attachment distance has a variable but significant relationship with LF5 AWUV; r=-0.44, p=0.008 with n=30.

Mean IAAD *vs* Mean AWUV

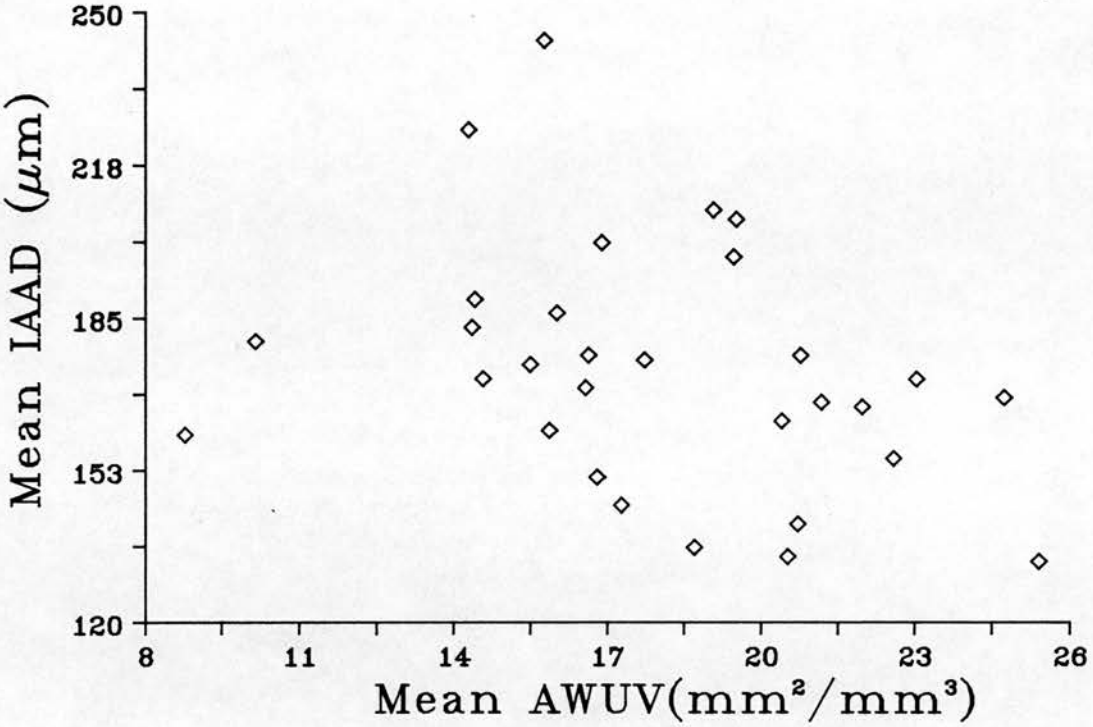

Mean IAAD *vs* LF5 AWUV

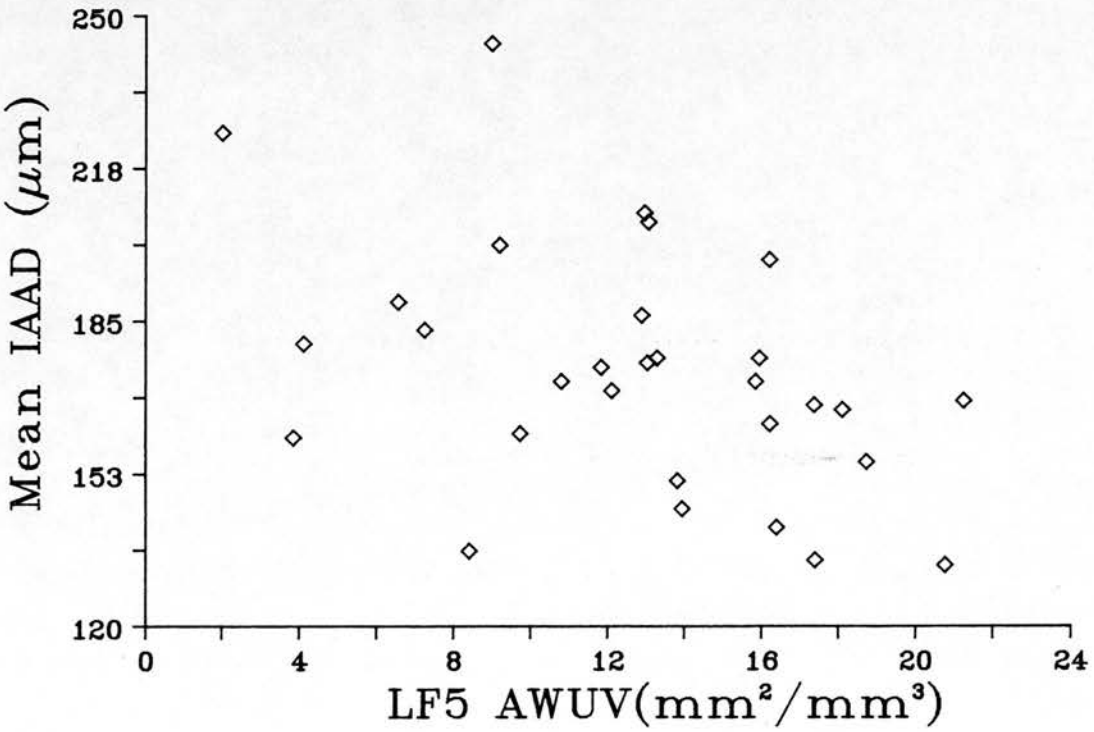

ASSIMILATION OF AWUV AND ATTACHMENT RESULTS

Two main points are evident when AWUV and mean inter-alveolar attachment distance are plotted against one other and against other variables.

1. Many of the bivariate distributions suggest that most cases exhibit a strong visual degree of association with a few cases being obvious outliers.

2. In general, AWUV and mean inter-alveolar attachment distance covary with each other and exhibit similar correlations with other morphometric variables.Multivariate analysis is used to further analyse these relationships.

The following text is a further analysis of these two observations.

1.AWUV AND ALVEOLAR ATTACHMENT OUTLIERS

Exploratory analysis of all bivariate plots was carried out as indicated in section 2.3 as recommended by Hartwigg and Dearing (1979).

Adopting this approach, it was noted that while most points (27 out of 30) exhibit a strong degree of association between AWUV and mean inter-alveolar attachment distance there are 3 notable outliers. These cases seem to indicate that the model proposed, ie that AWUV loss and alveolar attachment loss go hand in hand, may be too simplistic in its assumptions and that there may exist differing patterns of AWUV and peribronchiolar alveolar loss. Histological examination of the cases which lie off of the line of the others (cases 8, 11 and 17) -cf figures 4.14, 4.15 and 4.16, and the scatter plot of figure 4.17 where these cases are identified- provides evidence which suggests that this is indeed the case in that some cases, which have low AWUV values, have

relative retention of peribronchiolar alveolar attachments.

One can gauge the disparity of LF5 AWUV and mean inter-alveolar attachment distance values, in these three cases, by ranking the results from normal to abnormal for both variables. That is, the relative position of the results can be assessed by giving the lowest mean inter-alveolar attachment distance value a rank of 1 and the highest a rank of 30. With AWUV the highest value is given a rank of 1 and the lowest a rank of 30 as high values of AWUV represent normality. Doing this the disparity is (with mean luminal distance ranks given first) case 11; 8th and 29th, case 17; 3rd and 25th and case 8; 20th and 28th. On the face of it the disparity for case 8 might not seem that great, but it should be pointed out that there is a small group of cases with markedly low LF5 AWUV values, and while case 8 is amongst this group for LF5 AWUV, it is in the middle group for attachment loss. Mean AWUV shows a similar disparity in relative ranks when compared to mean inter-alveolar attachment distance.

Excluding this group of three cases with relative retention of attachments, the correlation coefficients for mean and LF5 AWUV respectively *vs* mean inter-alveolar attachment distance are $r=-0.46$ ($n=27$, $p=0.008$) and $r=-0.63$ ($p<0.001$). This is an improvement from $r=-0.32$ and $r=-0.44$ obtained for all 30 cases.

As both AWUV and attachment loss have been shown to affect airway ellipticality it is possible that the patterns of AWUV and attachment loss elucidated to above may show differential affects on this parameter. To test for this the correlation coefficients for mean and LF5 AWUV *vs* airway ellipticality have been reworked omitting those cases with retained attachments. The r values obtained are higher, $r=-0.55$ ($p=0.002$) for mean

AWUV and airway ellipticality and r=-0.77 ($p<0.001$) for LF5 AWUV and airway ellipticality -as opposed to the previous r values obtained for all 30 cases, ie r=-0.51 and r=-0.69, for mean and LF5 AWUV respectively. Figure 4.18, with the cases with retained attachment clearly marked, shows the stronger association which exists in the absence of cases with preferential retention of attachments. It is noticeable that the retention of attachments has assisted the airways in these three cases to maintain a more cylindrical profile and may be the reason that these cases do not fit the general trend for AWUV and airway ellipticality.

Likewise -by again removing the cases with low AWUV, but retained attachments- an improvement in the mean inter-alveolar attachment distance *vs* airway ellipticality correlation is evident (r=0.70, $p<0.001$), as opposed to the previous correlation coefficient of r=0.62.

These cases also affect the strength of the relationship between AWUV and theoretical lumen area. In figure 4.8 the two outliers at the bottom left hand side of the plot are cases with retention of attachments (cases 8 and 11). The third outlier is case 40 which is discussed immediately below. The other case with retention of attachments is not an outlier in this plot, but does lie at the periphery of the other points.

As well as the three cases with retention of attachments there is another occasional outlier. This is case 40 and as well as being an outlier in the plot of theoretical lumen area *vs* LF5 AWUV, it is an exception to the general relationship between theoretical lumen area *vs* airway ellipticality and also mean inter-alveolar attachment distance *vs* theoretical lumen area (cf figure 4.10 where case 40 is the outlier at the bottom right hand side). This case does not have retention of attachments (mean inter-alveolar attachment

distance= 225μm), but notably has a mean to LF5 AWUV ratio which, along with case 41, is far worse than all the other cases. (Case 40 mean:LF5 AWUV ratio= 0.14 whereas the range for all other cases, excluding case 41, is 0.4-0.89). In conjunction with this, this case has the most elliptical airways the second lowest LF5 value and a high proportion of macroscopic emphysema (48%) which is panacinar in type.

Figure 4.14 Two photomicrographs showing airways from two different cases (cases 6 and 11) at the same magnification (x100) showing similar inter-alveolar attachment distances.

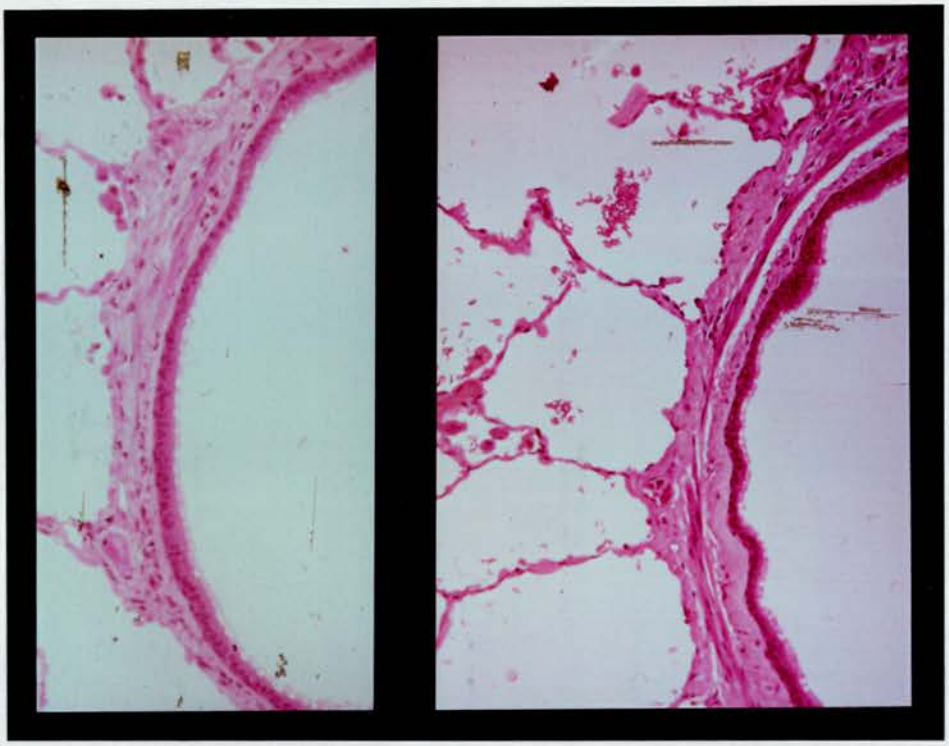

Figure 4.15 Lower magnification photomicrograph (x40) of the left hand side bronchiole of figure 4.14 showing normal alveolar architecture. This case (case 6) has the highest mean AWUV value of the study population ($25.4mm^2/mm^3$).

Figure 4.16 Lower magnification photomicrograph (x40) of right hand side bronchiole of figure 4.14 (case 11) showing considerable disruption of alveolar network away from the airway although there is retention of peribronchiolar alveoli. This case had the lowest mean AWUV value ($8.8mm^2/mm^3$) for the study group. It is noticeable that the circularity of the airway has been retained.

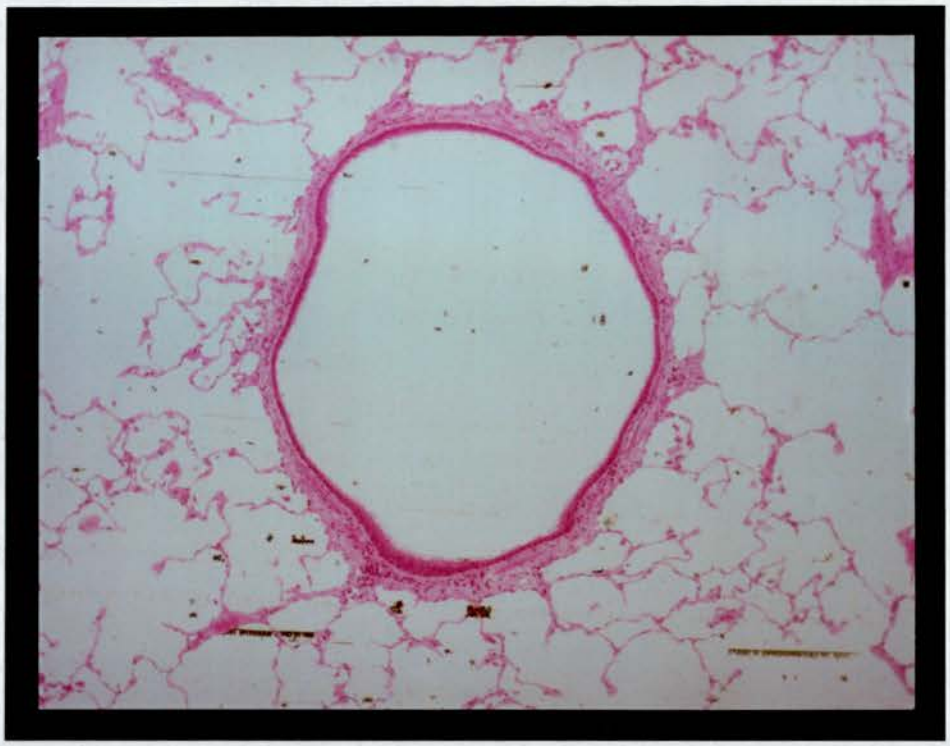

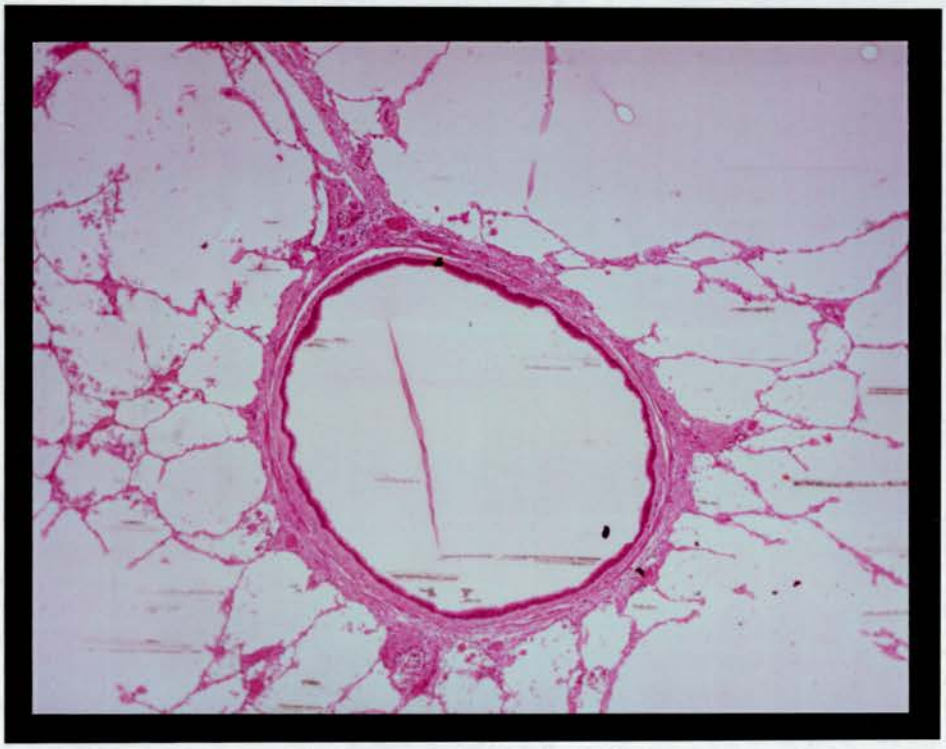

Figure 4.17. Mean Inter-Alveolar Attachment Distance *vs* LF5 AWUV. This figure is reproduced (cf figure 4.13) to highlight the influence of the three cases (filled symbols) with preferential retention of peribronchiolar attachments on correlation statistics. Recalculating the correlation statistics excluding these cases gives; $r=-0.63$, $p=<0.001$ with $n=27$.

Figure 4.18. Bronchiolar Ellipticality *vs* LF5 AWUV. This is a reproduction of figure 4.11 showing the influence of those cases with preferential retention of attachments; $r=-0.77$, $p<0.001$ and $n=27$ where the 3 cases with preferential retention are excluded.

Mean IAAD *vs* LF5 AWUV

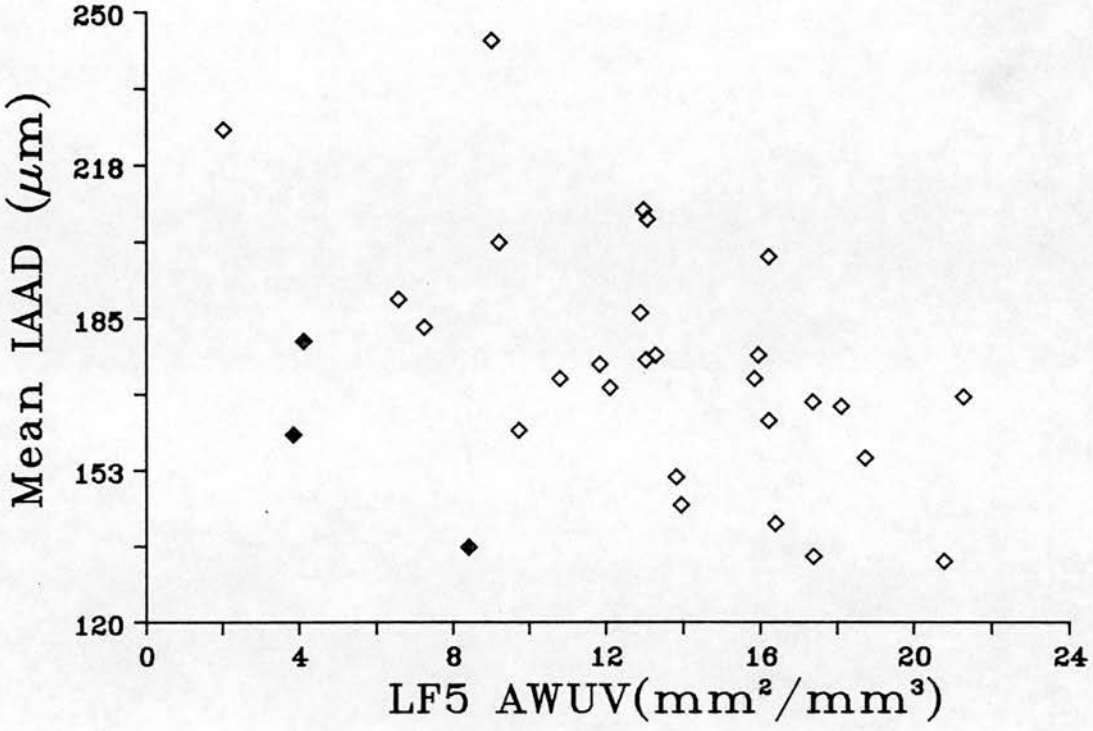

Bronchiolar Ellipticality *vs* LF5 AWUV

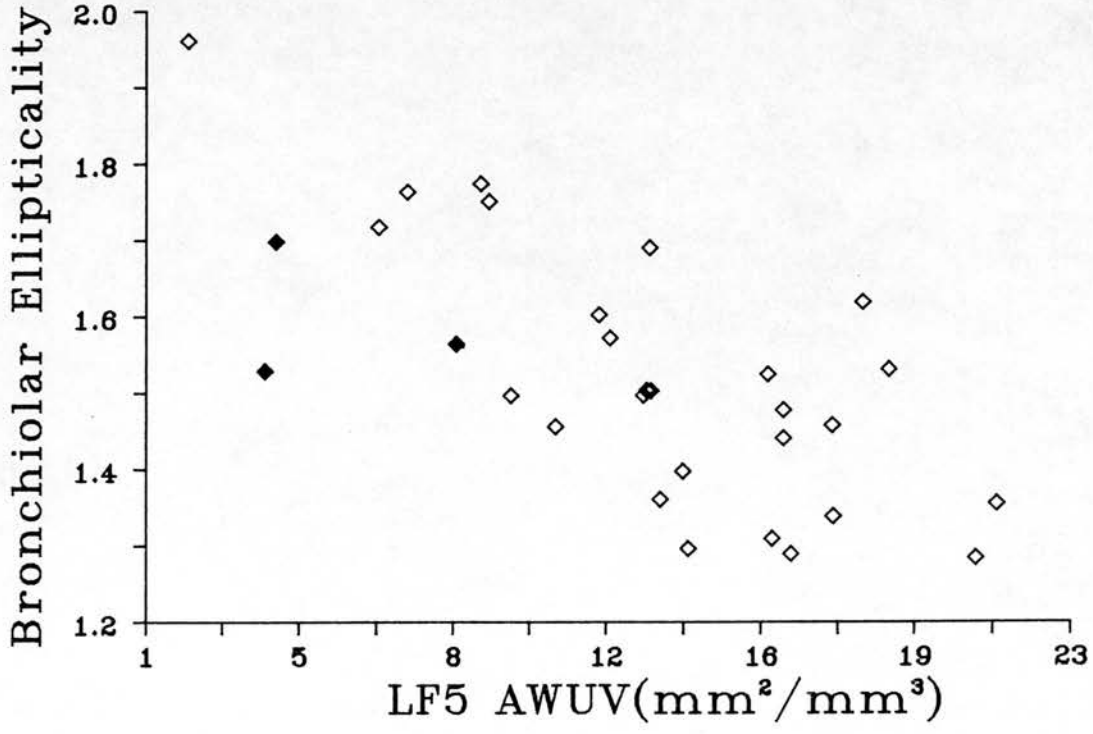

2.MULTIVARIATE ANALYSIS OF AWUV AND ALVEOLAR ATTACHMENTS

It has been established that AWUV and mean inter-alveolar attachment distance correlate with one another and with other variables, eg airway ellipticality. What one would like to establish is whether AWUV and mean inter-alveolar attachment distance have significant effects independent of one another and whether these effects are cumulative. Both of these can be tackled by using multiple regression techniques. Firstly, standardised partial regression coefficients (beta weights) are calculated to determine which of the morphometric variables have significant predictive value. It is worth restating that standardised partial regression coefficients are independent of the original units in which the variables were measured and predict the magnitude of change which will occur in the dependent variable given a one standard deviation change in the independent variables. Secondly, again using multiple regression techniques, the coefficient of multiple determination is ascertained to measure that proportion of the variation of the dependant variable which is accounted for by the independent (or causative) variables retained within the regression analysis.

Given that many workers have exhibited relationships between parenchymal loss and small airways deformity (cf section 1.5.5) a cause-and-effect relationship is proposed.

MULTIVARIATE ANALYSIS OF NRB ELLIPTICALITY[1]

[1]In an attempt to improve the clarity of the following analysis of variance tables mean inter-alveolar attachment distance is abbreviated, within these tables, to IAAD.

Mean AWUV and inter-alveolar attachment distance were input as potential independent variables in the multiple regression equation for airway ellipticality. Both are significant predictors, with the latter having the stronger predictive ability (table 4.7). Forty eight percent of the total variation in airway ellipticality is explained by these two variables.

LF5 AWUV has a stronger bivariate correlation with airway ellipticality than mean AWUV. Replacing mean AWUV in the regression with LF5 AWUV alters the relative importance of the predictive power (beta weights) of AWUV and mean inter-alveolar attachment distance and improves the coefficient of multiple determination to 0.62, ie 62% (table 4.8).

It was also noted that bronchiolar ellipticality itself covaries with theoretical lumen area. Although bronchiolar ellipticality is dependent on both mean AWUV and inter-alveolar attachment distance, where both of these are held constant (and the outlier case 40 is excluded) bronchiolar ellipticality and theoretical lumen area have a partial correlation coefficient of 0.42 ($p=0.014$). This indicates that bronchiolar ellipticality and theoretical lumen area covary independently of AWUV and mean inter-alveolar attachment distance.

Dependant Variable: NRB Ellipticality

ANOVA Table

	Degrees of Freedom	Sum of Squares	Mean Squares
Regression	2	0.422	0.211
Residual	27	0.392	0.015

F_{ratio}= 14.55 Significance of F_{ratio}= 0.0001

Regression Statistics

	Slope(B)	S.E.(B)	Beta Weights	t	p
Mean AWUV(X_1)	-0.014	0.006	-0.33	-2.373	0.025
Mean IAAD(X_2)	0.003	0.001	0.54	3.831	0.0007
(Constant=	1.18			5.367	0.0000)

Coefficient of Multiple Correlation (R^2)= 0.48

Hence:

$$\text{NRB Ellipticality} = 1.18 - 0.014(X_1) + 0.003(X_2)$$

Table 4.7: Multiple regression of NRB ellipticality with mean AWUV and mean inter-alveolar attachment distance (IAAD) as the independent variables.

Dependant Variable: NRB Ellipticality

ANOVA TABLE

	Degrees of Freedom	Sum of Squares	Mean Square
Regression	2	0.52	0.26
Residual	27	0.29	0.01

F_{ratio}= 24.44 Significance of F_{ratio}= 0.0000

Regression Statistics

	Slope(B)	S.E.(B)	Beta Weight	t	p
LF5 AWUV(X_1)	-0.018	0.004	-0.53	-4.140	0.0003
IAAD(X_2)	0.003	0.001	0.41	3.249	0.0031
(Constant=	1.290	0.175		7.356	0.0000)

Coefficient of Multiple Determination(R^2)= 0.62

Hence:

$$\text{NRB Ellipticality} = 1.29 - 0.018(X_1) + 0.003(X_2)$$

Table 4.8: Multiple regression of NRB ellpiticality with LF5 AWUV and mean inter-alveolar attachment distance (IAAD) as the independent variables.

4.3. CT Scan Correlations

4.3.1. Introduction to CT Scan Results

The aim of this section is to investigate whether lung density, as measured by CT scan, correlates with the measured proportion of macroscopic emphysema and/or microscopic lung density as measured by AWUV. The latter is a measure of lung density in that as the density of lung tissue decreases airspace surface area *per* unit volume will decrease in a similar fashion.

Figure 4.19 is a frequency distribution of the CT scan pixels of case 13. This case has normal function (FEV percent predicted= 75% and K_{co} percent predicted= 104%), a high mean and LF5 AWUV (24.7mm^2/mm^3 and 21.3mm^2/mm^3 respectively) and no macroscopic emphysema. The majority of the pixels in this distribution lie below -200 EMI units reflecting the over all low density of lung tissue. Within this distibution the relatively higher EMI pixel units represent lung tissue with relatively higher physical density ie those areas containing vessels or airways.

The CT scan frequency distribution of case 40 (figure 4.20) contrasts with that of case 13. This case has relatively poor function (FEV percent predicted= 53% and K_{co} percent predicted= 31%) low AWUV values (14.3 mm^2/mm^3 for mean AWUV and 2.0mm^2/mm^3 for LF5 AWUV) and has 48% macroscopic emphysema. In this latter figure the CT scan distribution has shifted to the left ie towards the EMI value representing air, indicating an over all reduction in the density of the lung.

These two cases represent extremes within the sample population. To investigate whether, in the population as a whole, decreases in CT scan

measured lung density correlate with decreases in AWUV and/or the amount of macroscopic emphysema the following statistics where calculated from the CT scans of each patient.

Modal EMI Number

The modal EMI value to represent the central location of CT scan frequency distributions.

5th percentile EMI number

As each pixel is an average of the mixture of air, tissue and blood present in each small reference volume, it was argued that that part of the distribution closer to the value for air would represent those areas of the lung with the lowest density. The EMI unit corresponding to the 5th percentile was calculated and taken to represent this area.

Range EMI Units (Mode to Lowest EMI unit)

Again, to represent the left hand side of each CT scan frequency distribution, the range from the lowest EMI unit to that of the mode was calculated.

4.3.2. Summary Statistics

The summary statistics for the measured CT parameters are given in table 4.9.

	Summary Statistics			
CT Scan Parameter (EMI Units)	Mean	Range	S.D.	n
5th Percentile	437	409-474	16.7	28
Median	412	380-450	17.8	28
Median to Lowest	25	12-59	11.2	28

Table 4.9: Summary statistics for the CT scan parameters. Abbreviations: S.D.= Standard Deviation and n= number of cases mesured. All data are expressed in EMI units.

4.3.3. CT Scan Correlations

4.3.3.1. Correlations with AWUV

The correlation coefficients obtained between CT scan and AWUV are presented in table 4.10. In CT terms the best correlations are obtained with the EMI number which defines the fifth percentile of the CT scan frequency distributions. With respect to AWUV the best correlations are obtained with LF5 AWUV ie the parameter -like the 5th percentile of the CT scan distributions- which represents the lowest areas of lung density. Over all the strongest correlation (figure 4.21) is between LF5 AWUV and the 5th percentile of the CT scan distributions ($r=-0.75$, $p<0.001$).

4.3.3.2. Correlations with Macroscopic Emphysema

In section 4.1.4 it was noted that the distribution of macroscopic emphysema was not normal, with half of the cases having less than one percent of their area involved with macroscopic emphysema. The nature of this distribution is reflected in the scatter plot of macroscopic emphysema *vs*

the EMI number defining the 5th percentile of the CT scan frequency distributions (figure 4.22).

From this plot it is clear that Pearson's correlation coefficient is inappropriate as the variables do not constitute a bivariate normal distribution. Furthermore, it can be observed that there is no over all relationship between macroscopic emphysema and the 5th percentile of the CT scans. Hence, any correlation coefficient (parametric or non-parametric) obtained from such a scatter plot would produce a coefficent, the strength of which, would be highly dependent on the few cases with marked amounts of macroscopic emphysema.

To support this contention Spearman's coefficient of rank correlation was calculated for macroscopic emphysema against the 5th percentile EMI unit (Table 4.11) for all cases and then re-calculated excluding those cases with 12% or more of their area occupied with macroscopic emphysema. In the latter analysis there is no correlation between CT scan and macroscopic emphysema.

To further prove that the AWUV *vs* CT scan plots exhibit linear relationships which include all cases, irrespective of the amount of macroscopic emphysema, the correlation coefficients presented in table 10 -calculated for all cases- are re-presented in table 4.11 with those cases with more than 12% macroscopic emphysema excluded. The correlation coefficients although reduced by a few points remain highly significant. The plot of LF5 AWUV *vs* the 5th percentile EMI value (figure 4.21) -where the cases with more than 12% macroscopic emphysema are marked- shows the realtionship to be linear for the whole population; there being no seperate relationship for those cases with marked macroscopic emphysema nor no point of inflection

where macroscopic emphysema is present.

From the results it is apparent that there is no association between macroscopic emphysema and lung density as measured by CT scan whereas there are strong and linear correlations between AWUV and CT scan parameters.

		CT Scan Parameters (EMI Units)		
		5th Percentile	Median	Median to Lowest
AWUV				
Mean	(r)	-0.63	-0.59	-0.13
	(p)	<0.001	0.001	0.475
LF5	(r)	-0.75	-0.57	-0.23
	(p)	<0.001	0.001	0.122

Table 4.10: Correlation coefficients for AWUV *vs* CT scan parameters (n=27).

All cases

		Macroscopic Emphysema	AWUV Mean	AWUV LF5
5th Percentile EMI Unit	(r)	0.48	0.63	0.75
	(p)	0.006	0.001	<0.001

Cases with <12% Macroscopic Emphysema

5th Percentile EMI Unit	(r)	0.08	-0.48	-0.55
	(p)	0.355	0.011	0.004

Table 4.11: Correlation coefficients for AWUV (Pearson's) and macroscopic emphysema (Spearmans's) *vs* the 5th percentile EMI unit for all cases and latterly for those cases with <12% macroscopic emphysema.

4.4. STRUCTURE *vs* FUNCTION RELATIONSHIPS

4.4.1. Introduction to Structure *vs* Function Analysis

Summary statistics for all pulmonary function data used in structure *vs* function analysis are presented in table 4.12 with the individual results for each case being given in the appendix.

	Summary Statistics			
Variable	Mean	Range	S.D.	n
Total Lung Capacity				
Absolute (L)	7.48	4.04-11.50	1.77	40
%Predicted	124	81-166	18.8	40
CO Transfer Factor				
Tco (mm/ml/kPa/min)	6.77	2.72-10.40	2.04	33
Kco (mm/ml/kPa/min/L)	1.27	0.41-1.88	0.38	32
FEV(1.0)				
Absolute (L)	2.25	1.35-3.75	0.63	44
%Predicted	82	47-123	20	44
SBNW Test				
Closing Volume (L)	0.91	0.19-1.96	0.42	30
CV/VC (%)	23	5-48	8.57	30
Slope of Phase III	3.27	0.38-6.40	1.63	27

Table 4.12: Summary statistics for pulmonary function variables. Abbreviations: S.D.= Standard Deviation, n= number of cases measured, SBNW Test= Single Breath Nitrogen Washout Test and CV/VC (%)= Closing Volume/Vital Capacity (%).

Figure 4.19: Top, presents the EMI pixel and AWUV distributions for case 14. This case has high mean and LF5 AWUV values (24.7mm^2/mm^3 and 21.3mm^2/mm^3, repectively), a correspondingly high CT asseessments of lung density (eg 5th percetile EMI value= 418) no macroscopic emphysema and normal lung function. Bottom is a transthoracic CT scan. Pixels values within the range -450 to -500 are highlighted to give a pictorial assessment of lung density. In this case very few pixels lie within this range.

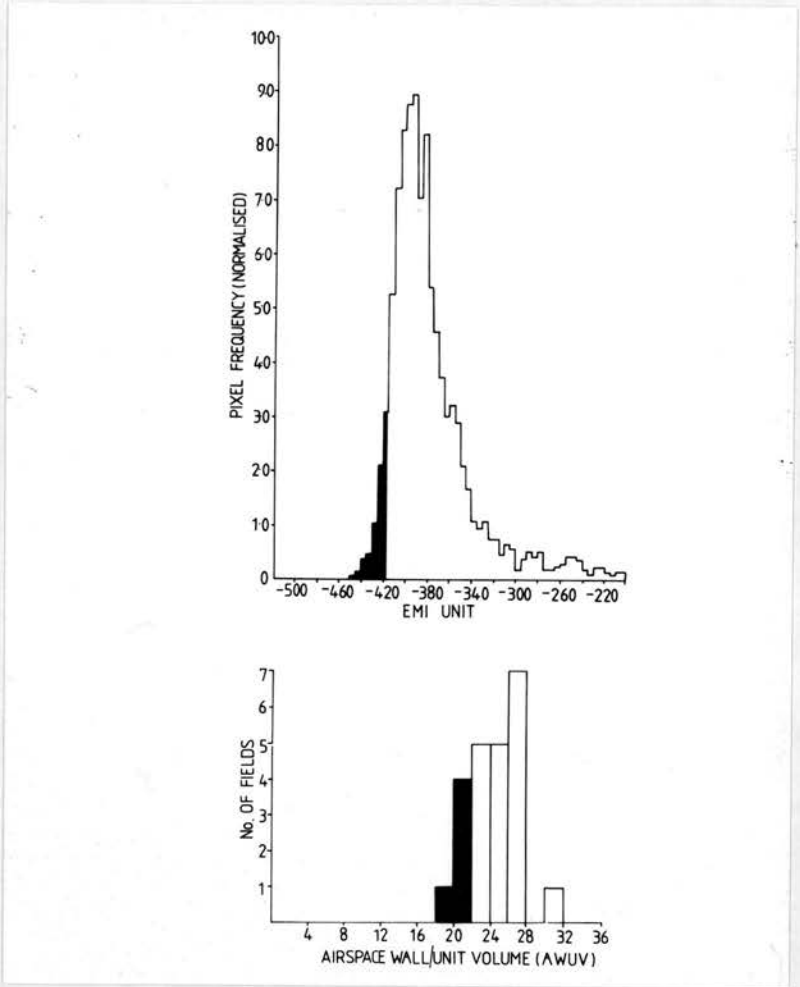
PIXEL FREQUENCY (NORMALISED)
100
90
80
70
60
50
40
30
20
10
0
-500 -460 -420 -380 -340 -300 -260 -220
EMI UNIT
No. OF FIELDS
7
6
5
4
3
2
1
4 8 12 16 20 24 28 32 36
AIRSPACE WALL/UNIT VOLUME (AWUV)

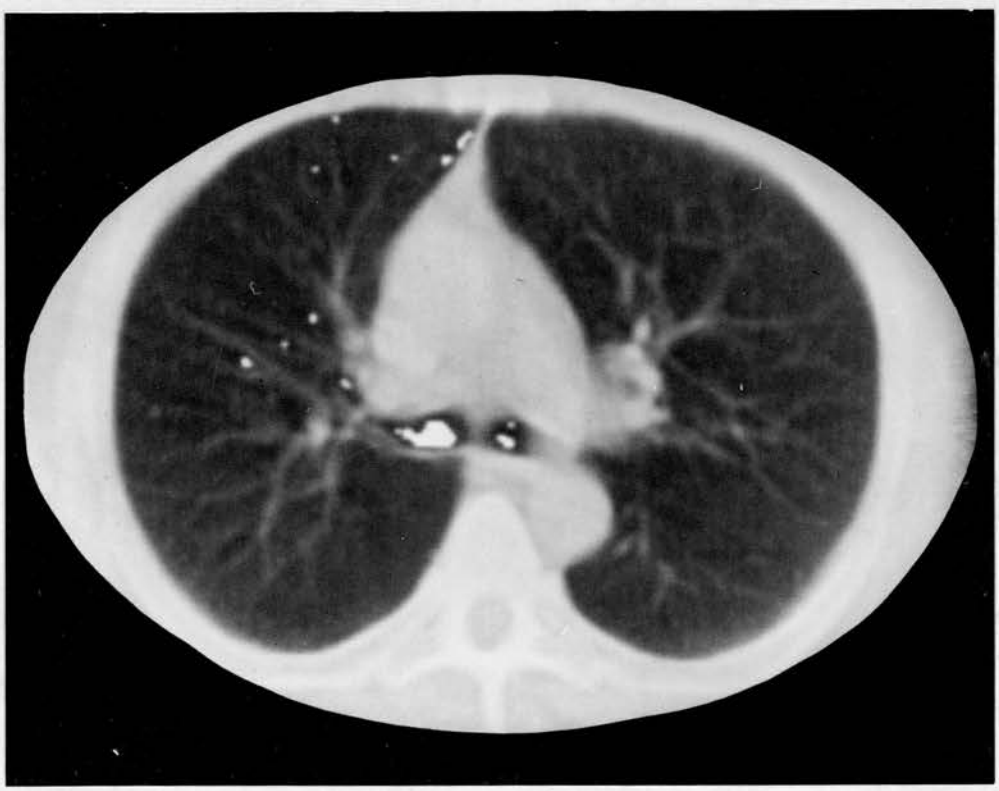

Figure 4.20: Top presents the EMI pixel and AWUV distribtuion for case 40. In contrast to the previous figure the EMI distribution has shifted to the left reflecting a decrease in lung density (5th percentile EMI value= 474). Mean and LF5 AWUV are correspondingly lower (14.3mm^2/mm^3 and 2.0mm^2/mm^3, respectively). This case has diminished function and 48% macroscopic emphysema. Bottom is the transthoracic CT scan for this case. In contrast to the previous case there are a large number of pixels lying within the -450 to -500 range.

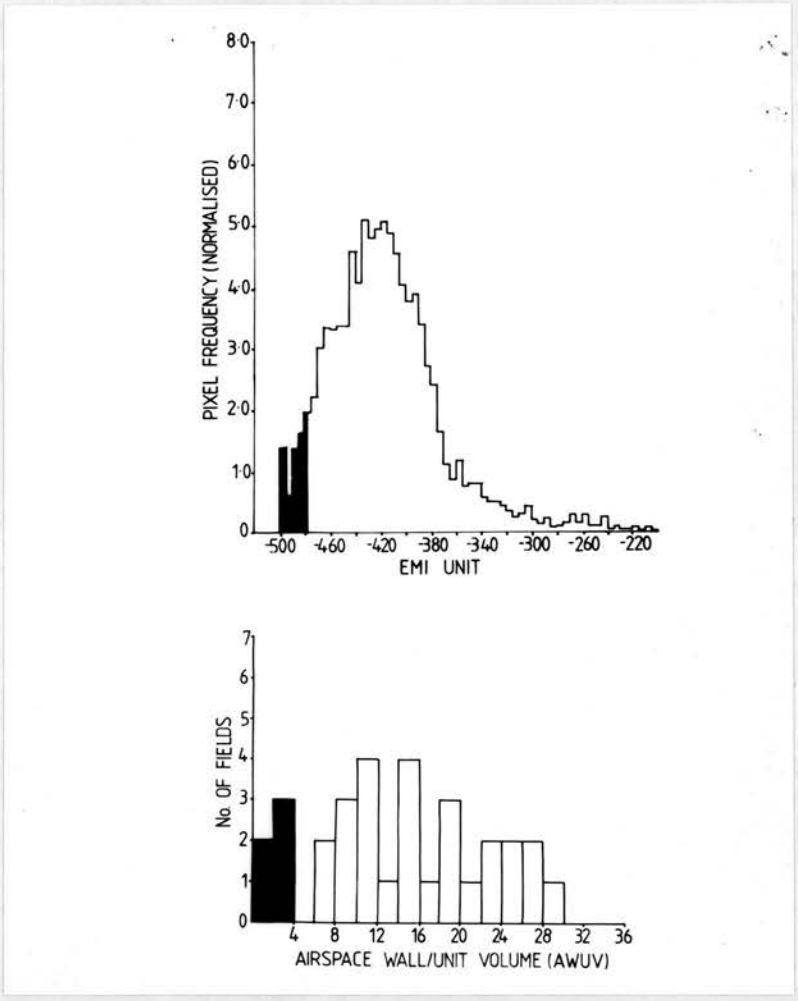
PIXEL FREQUENCY (NORMALISED)
8·0
7·0
6·0
5·0
4·0
3·0
2·0
1·0
0
-500 -460 -420 -380 -340 -300 -260 -220
EMI UNIT
No. OF FIELDS
7
6
5
4
3
2
1
0
4 8 12 16 20 24 28 32 36
AIRSPACE WALL/UNIT VOLUME (AWUV)

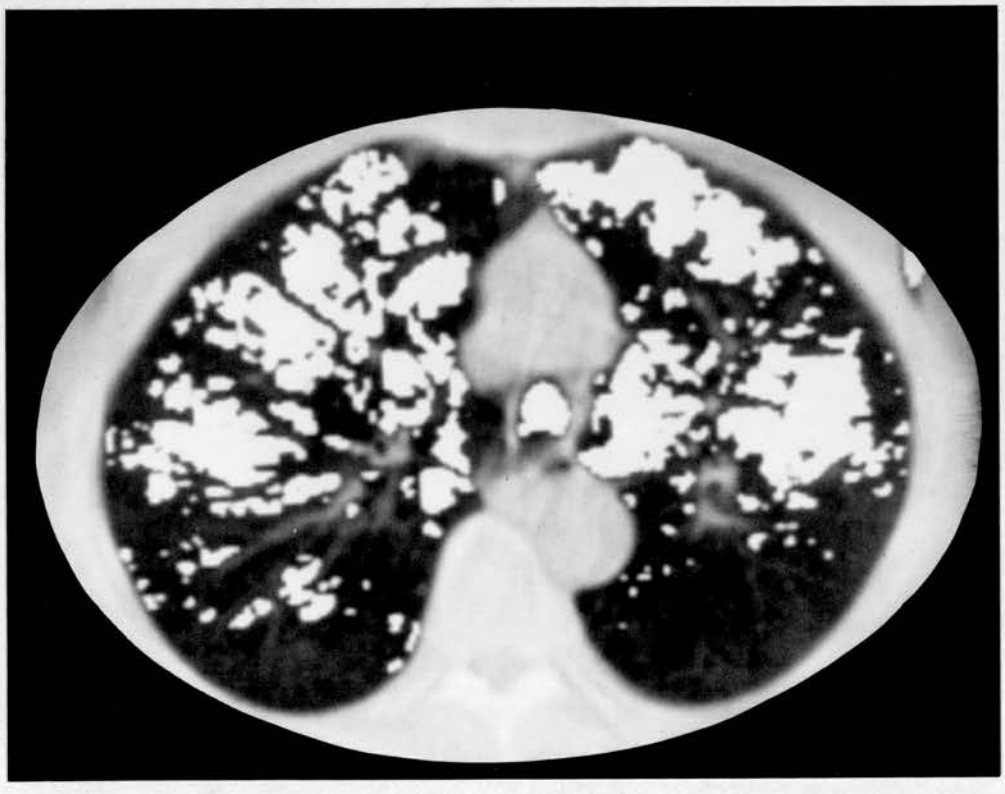

Figure 4.21. 5th percentile EMI value *vs* LF5 AWUV. These two parameteres exhibit a strong and linear relationship throughout the bivariate range ($r=-0.75$, $p<0.001$ with $n=28$).

Figure 4.22. 5th percentile EMI unit *vs* the Percentage Area of Macroscopic Emphysema. In contrast to the figure above there is little covariance and obviously no linear relationship between these two variables.

5th Percentile EMI Unit
vs LF5 AWUV

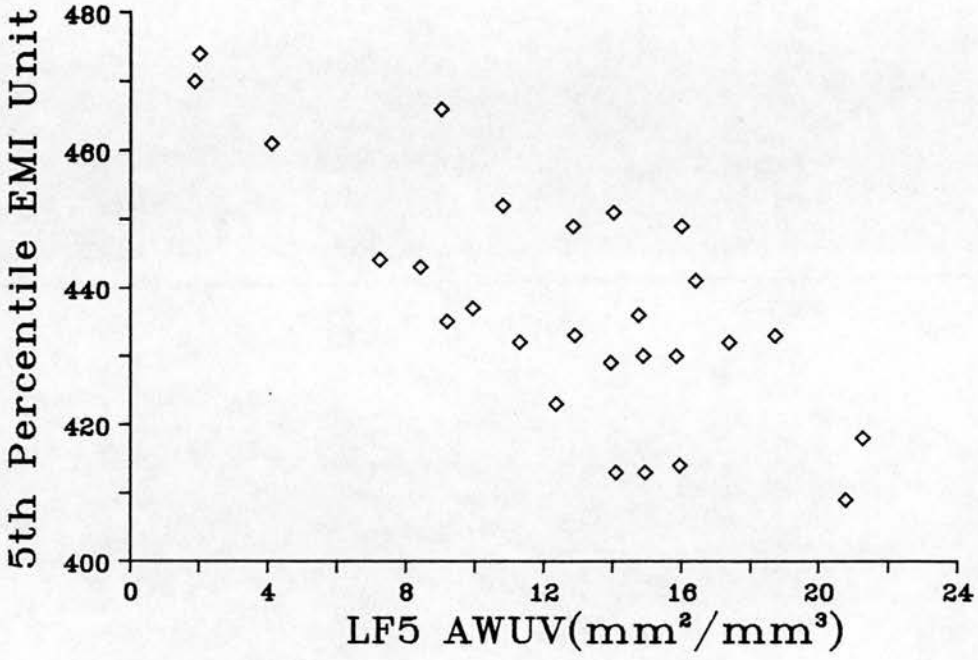

5th Percentile EMI Unit *vs*
%Area of Macroscopic Emphysema

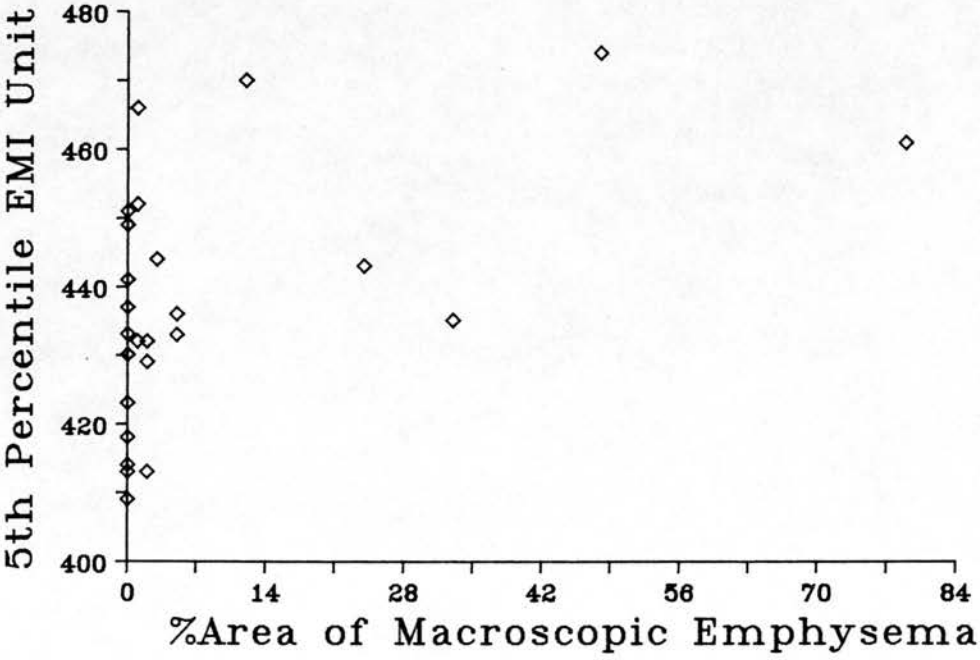

A degree of cross-correlation is evident within the morphometric variables. It is therefore likely that this will also occur in bivariate structure *vs* function correlations. Multivariate analysis is is applied to find out which morphometric variables are either the more deterministic. In the following structure *vs* function analysis standardised partial regression coefficients are calculated to identify the more important morphometric variables for each pulmonary function test. The coefficient of multiple determination is also presented with the multivariate analysis. Bivariate correlations and scattergrams are presented as it is still necessary to check the nature of these plots to see if there are any influential outliers which either make over all insignificant correlations appear significant or alternatively mask otherwise potentially important correlations (Hartwigg and Dearing 1979).

The following morphometric variables are used in bivariate structure *vs* function correlations (except for CO transfer factor analysis where AWUV data alone is used): AWUV, mean inter-alveolar attachment distance, NRB ellipticality and theoretical and measured lumen area. To simplify the presentation of data, correlation matrices are presented for each pulmonary function test itemising only those morphometric variables which exhibit significant bivariate structure *vs* function relationships.

4.4.2. Carbon Monoxide Transfer Factor[2]

The parameters which affect CO diffusing capacity are alveolar surface area and barriers to diffusion at the alveolar/capillary level eg alveolar interstitium

[2]Data for both T_{CO} and K_{CO} corrected for haemoglobin and/or carboxyhaemoglobin were available and used in structure/function correlations. Without exception the correlations obtained using this corrected data, although similar to uncorrected T_{CO} and K_{CO}, were always slightly weaker. Correlation coefficients quoted are for uncorrected T_{CO} and K_{CO}.

(Gibson 1984). Thus the only morphometric variable correlated against CO diffusing capacity, in this study, is AWUV.

CO transfer for the whole lung (T_{co}) is measured in absolute terms and is partially dependant on alveolar volume (V_A). K_{co} is independent of this, being a measure of CO uptake *per* unit lung volume. Disappointingly, only one of the 3 cases with preferential retention of attachments (case 17) completed the CO transfer test.

AWUV *vs* CO transfer correlations are given in table 4.13. The strongest correlation is obtained with LF5 AWUV. Figure 4.23 of K_{co} *vs* LF5 AWUV illustrates the strength of the relationship between these two variables. The correlation coefficients reflect the improvement gained when CO uptake is normalised to K_{co} and the lowest areas of lung density are represented as LF5 AWUV. In none of the plots of AWUV *vs* CO transfer was case 17 (ie preferential retention of attachments) an outlier.

The influence of **macroscopic emphysema** on CO transfer factor was initially tested by plotting the respective variables as scatter plots. That of macroscopic emphysema against K_{co} is presented as an example (figure 4.24) and is very similar to that obtained for macroscopic emphysema and T_{co}. The non-normal bivariate distribution obtained for these two variables is attributable to the non-normal distribution of macroscopic emphysema itself. The nature of this bivariate distribution renders Pearson's correlation coefficient inapplicable.

Analysing the scatter plot of macroscopic emphysema and K_{co} visually, it is clear that there is no over all association between these two variables. Cases with marked amounts of emphysema do have low K_{co} values, however, there is

a large range in K_{co} values for cases with little or no macroscopic emphysema.

Cotes (1975) indicates that T_{co} regresses with height, age and sex whereas K_{co} regresses with just age and sex. Multiple regression analysis was used to investigate whether these parameters helped to explain any additional variance in CO transfer over and above that explained by mean AWUV. With respect to T_{co} only sex (as a binary variable) remains within the regression equations along with either mean or LF5 AWUV (see tables 4.14 & 4.15). Sex and mean AWUV explain 41% of the variance in T_{co} -as opposed to 37% explained by AWUV alone. Sex and LF5 AWUV explain 58% -as opposed to 44% explained by LF5 AWUV alone. Neither age nor sex explain any additional variation in K_{co}.

		T_{co}	K_{co}
Mean AWUV	(r)	0.61	0.66
	(n)	34	33
	(p)	<0.001	<0.001
LF5 AWUV	(r)	0.73	0.84
	(n)	34	33
	(p)	<0.001	<0.001

Table 4.13: Significant bivariate correlations obtained for AWUV *vs* CO transfer factor analysis.

Figure 4.23. K_{co} *vs* LF5 AWUV. These two parameters have a highly significant and linear correlation ($r=0.84$, $p<0.001$ with $n=33$).

Figure 4.24. K_{co} *vs* the Percentage Area of Macroscopic Emphysema. Unlike the figure above there is very little and obviously no linear relationship between these two parameters.

K_{co} *vs* LF5 AWUV

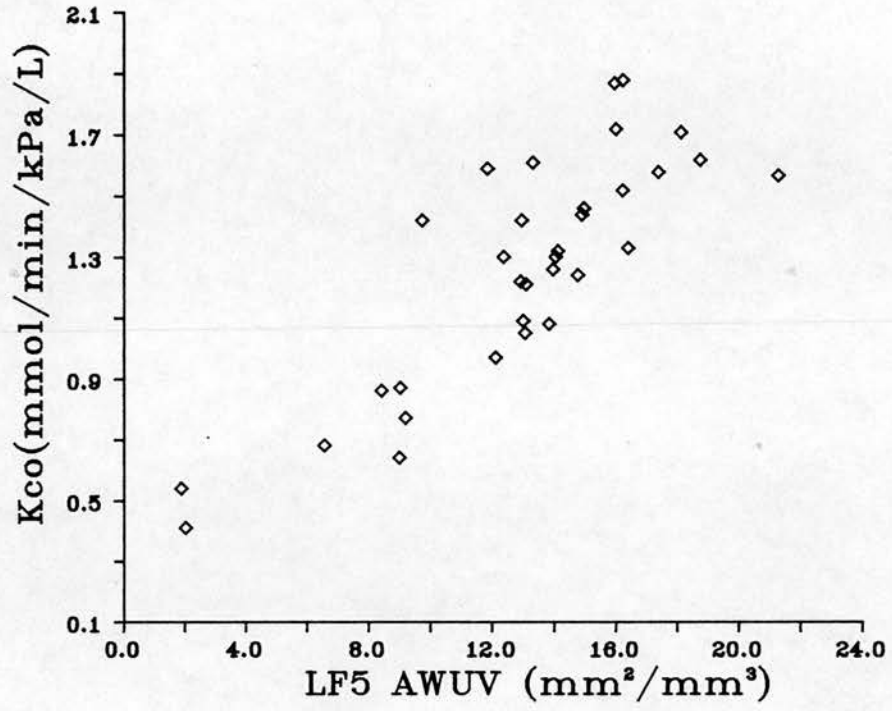

K_{co} *vs* %Area of
Macroscopic Emphysema

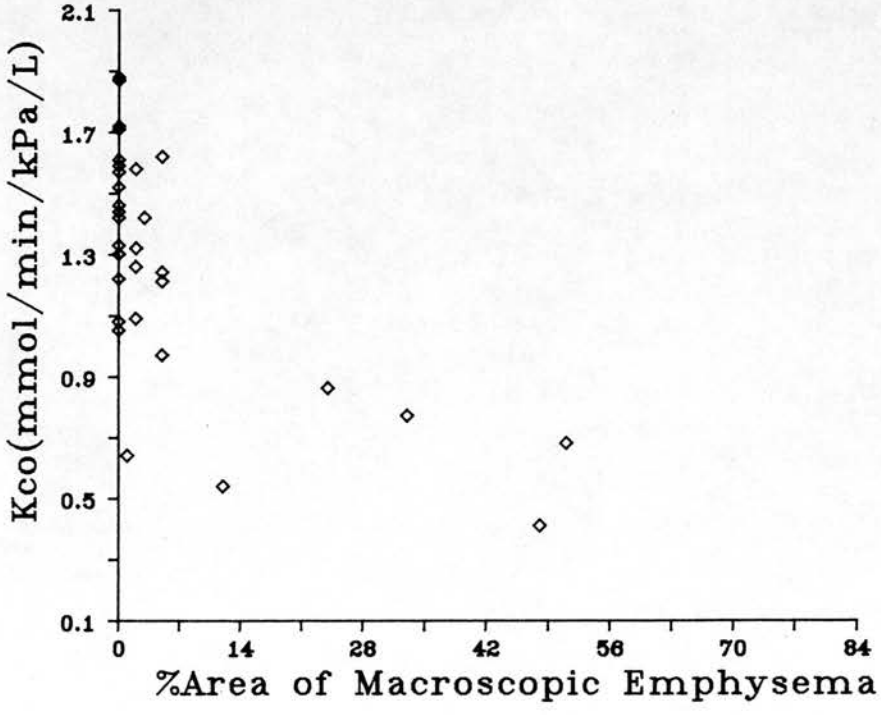

Dependant Variable: T_{co}

ANOVA TABLE

	Degrees of Freedom	Sum of Squares	Mean Square
Regression	2	64.27	32.13
Residual	31	80.00	2.58

F_{ratio}= 12.45 Significance of F_{ratio}= 0.0001

Regression Statistics

	Slope(B)	S.E.(B)	Beta Weight	t	p
Mean AWUV(X_1)	0.52	0.112	0.62	4.648	0.0001
SEX(X_2)	1.42	0.723	0.26	1.969	0.0579
(Constant=	-4.05	2.175		-1.863	0.0719)

Coefficient of Multiple Determination(R^2)= 0.41

Hence:

$$T_{co} = -4.05 + 0.52(X_1) + 1.42(X_2)$$

Table 4.14: Multiple regression of T_{co} with mean AWUV and SEX (as a binary variable) as the independent variables.

Dependant Variable: T_{co}

ANOVA TABLE

	Degrees of Freedom	Sum of Squares	Mean Square
Regression	2	87.54	43.77
Residual	31	56.73	1.83

F_{ratio}= 23.92 Significance of F_{ratio}= 0.0000

Regression Statistics

	Slope(B)	S.E.(B)	Beta Weight	t	p
LF5 AWUV(X_1)	0.37	0.056	0.74	6.572	0.0000
SEX(X_2)	1.49	0.609	0.28	2.446	0.0203
(Constant=	0.65	0.933		0.696	0.4919)

Coefficient of Multiple Determination(R^2)= 0.58

Hence:

$$T_{co} = 0.37(X_1) + 1.49(X_2)$$

Table 4.15: Multiple Regression of T_{co} with LF5 AWUV and SEX as independent variables.

4.4.3. Forced Expiratory Volume in One Second

Forced expiratory volume in one second ($FEV_{1.0}$), measured in absolute terms, varies with height, sex and age. To control for this variation, forced expiratory volume has also been expressed as percent predicted.

There are no significant correlations between $FEV_{1.0}$ (either in absolute terms or as percent predicted) and NRB measured lumen area or minimum diameter or theoretical lumen area.

The significant correlations between $FEV_{1.0}$ and the morphometric variables are given in Table 4.16. **Mean inter-alveolar attachment distance** has a weak correlation (figure 4.25) with $FEV_{1.0}$ absolute, but a highly significant correlation with FEV percent predicted ($r=-0.60$, $p<0.001$). **Airway ellipticality** correlates only with FEV percent predicted ($r=-0.35$ $p=0.028$). **AWUV** correlates with neither $FEV_{1.0}$ absolute nor percent predicted.

		$FEV_{1.0}$ Absolute	$FEV_{1.0}$ %Predicted
Mean IAAD	(r)	-0.32	-0.60
	(n)	30	30
	(p)	0.041	<0.001
Airway Ellip/y	(r)	NS	-0.35
	(n)		30
	(p)		0.028

Table 4.16: Significant morphometry *vs* $FEV_{1.0}$ correlations (IAAD= inter-alveolar attachment distance).

Multiple regression techniques were used to identify those variables which have significant predictive value for both $FEV_{1.0}$ absolute and percent

predicted. For $FEV_{1.0}$ absolute height, age and sex were entered into the initial regression equation along with the morphometric variables.

Only mean inter-alveolar attachment distance and sex remain within the regression equation as significant predictors for $FEV_{1.0}$ absolute -sex having the greater predictive value. These two variables account for 40% of the observed variation in measured $FEV_{1.0}$ (Table 4.17). In the multiple regression of $FEV_{1.0}$ percent predicted -where height, age and sex are integral to the calculation of predicted values- only mean inter-alveolar attachment distance has significant predictive value. This reflects the findings of the bivariate analysis.

In a parallel study measurements have been made on mean segmental bronchial diameter (by the present author). As $FEV_{1.0}$ is considered to relate to large airway calibre -at least in normal lungs (Osmanliev *et al* 1982)- this data was made available and incorporated into the multiple regression equation to test if segmental bronchial diameter provided any additional predictive value along with sex and mean inter-alveolar attachment distance.

Mean segmental bronchiolar diameter does increase the multiple coefficient of determination to R^2=0.47 and has itself significant predictive value in determining $FEV_{1.0}$ absolute (Table 4.18). Sex remains the best predictor with mean inter-alveolar attachment distance next.

Figure 4.25. Forced Expiratory Volume (expressed as percent predicted) *vs* Mean Inter-Alveolar Attachment Distance. This morphometric parameter has the highest correlation with FEV ($r=-0.60$, $p<0.001$ with $n=30$) indicating that airflow is impaired with loss of radial alveolar attachments.

FEV %Predicted *vs* IAAD

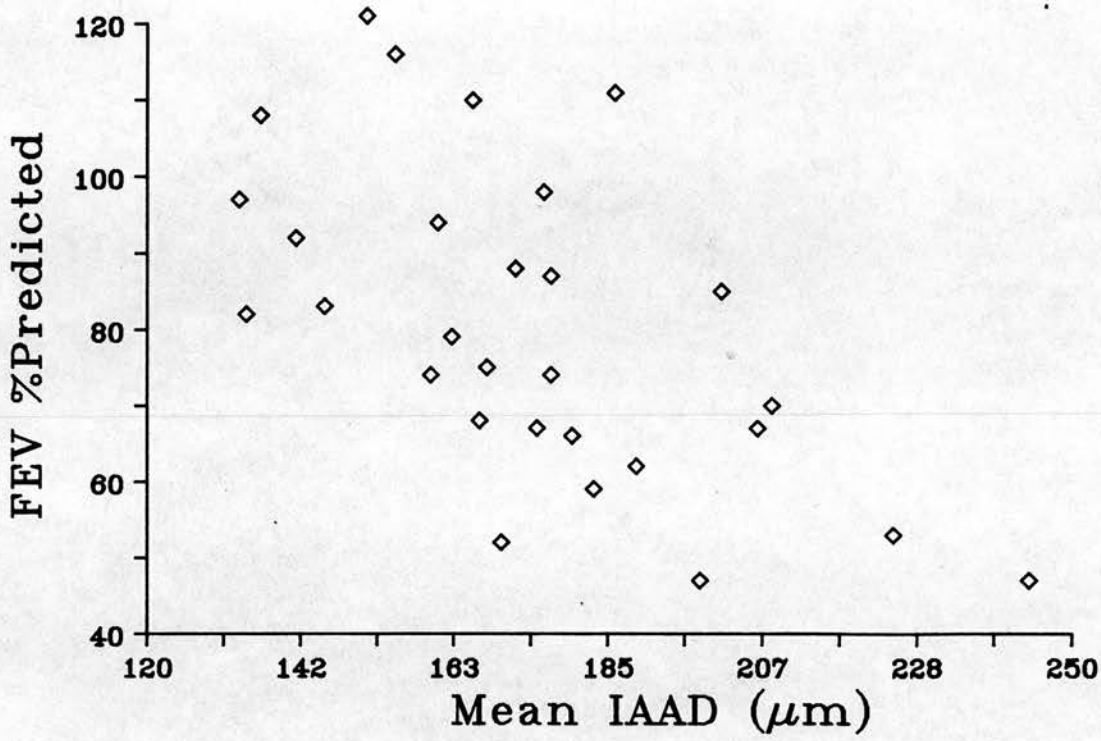

Dependant Variable: FEV Absolute

ANOVA TABLE

	Degrees of Freedom	Sum of Squares	Mean Square
Regression	2	6.19	3.09
Residual	27	7.82	0.29

F_{ratio}= 10.69 Significance of F_{ratio}= 0.0004

Regression Statistics

	Slope(B)	S.E.(B)	Beta Weight	t	p
SEX(X_1)	0.97	0.240	0.60	4.040	0.0004
IAAD(X_2)	-0.13	0.004	-0.48	-3.204	0.0035
(Constant=	3.75	0.674		5.566	0.0000)

Coefficient of Multiple Determination(R^2)= 0.40

Hence:

$$FEV_{1.0} = 3.75 + 0.97(X_1) - 0.13(X_2)$$

Table 4.17: Multiple regression of $FEV_{1.0}$ with sex and mean inter-alveolar attachment distance (IAAD) as independent variables.

Dependant Variable: FEV Absolute

ANOVA TABLE

	Degrees of Freedom	Sum of Squares	Mean Square
Regression	3	6.69	2.23
Residual	24	5.98	0.25

F_{ratio}= 8.96 Significance of F_{ratio}= 0.0004

Regression Statistics

	Slope(B)	S.E.(B)	Beta Weight	t	p
SEX(X_1)	0.85	0.226	0.55	3.723	0.0011
IAAD(X_2)	-0.13	0.004	-0.46	-3.206	0.0038
MSBD(X_3)	0.27	0.118	0.32	2.251	0.0338
(Constant=	2.72	0.776		3.512	0.0018)

Coefficient of Multiple Determination(R^2)= 0.47

Hence:

$$FEV_{1.0} = 2.72 + 0.85(X_1) - 0.13(X_2) + 0.27(X_3)$$

Table 4.18: Multiple regression of $FEV_{1.0}$ absolute with sex, mean inter-alveolar attachment distance (IAAD) and mean segmental bronchial diameter (MSBD) as independent variables.

4.4.4. Single Breath Nitrogen Washout Test

It has been shown that small airway support and shape are compromised in a number of cases through loss of peribronchiolar attachments and/or AWUV. The single breath nitrogen washout test was devised to estimate the lung volume at which small airways begin to close (closing volume). Like other subunits of lung volume this measurement is partly dependant on total lung volume itself. Closing volume can be normalised by expressing it as a percentage of vital capacity -CV/VC(%). A further parameter of the single breath nitrogen washout test is the over all inhomogeneity of small airway closure, this parameter being measured as the slope of phase III of the test. Two of the cases with retention of attachments (cases 8 and 11) completed the single breath nitrogen washout test whereas case 40 (a common outlier on other bivariate plots) did not. Significant correlations obtained with the parameters of the test are given in table 4.19.

Measured bronchiolar size does not correlate with closing volume, CV/CV% or the slope of phase III. However, **theoretical lumen area** does correlate with closing volume ($r=0.45$, $n=21$, $p=0.021$) and CV/VC(%) ($r=0.46$, $p=0.018$). There is though no significant relationship between the slope of phase III and theoretical lumen area ($r=0.13$, $n=19$, $p=0.301$).

The correlation obtained between **airway ellipticality** and CV is $r=-0.57$ ($n=21$, $p=0.004$) which improves to $r=-0.66$ ($p<0.001$) when closing volume is expressed as CV/VC(%). There is though, no significant correlation with the slope of phase III ($r=0.23$, $n=19$, $p=0.177$). **Mean inter-alveolar attachment** distance correlates with closing volume and CV/VC% ($r=0.38$, $p=0.045$) and ($r=0.58$, $p=0.003$), respectively and is the only morphometric variable to have a

significant relationship with the slope of phase III ($r=0.59$, $p=0.004$), the visual strength of which can be seen in figure 4.26.

Mean and LF5 AWUV have similar correlations with closing volume ($r=-0.44$, $p=0.006$) and ($r=-0.48$, $p=0.003$), respectively. These correlations do not improve when closing volume is represented as CV/VC% ($r=-0.40$, $p=0.011$) and ($r=-0.40$, $p=0.012$). AWUV does not correlate with the slope of phase III either as mean ($r=-0.13$, $p=0.266$) or LF5 AWUV ($r=-0.11$, $p=0.294$).

As mentioned above, two cases with retention of attachments completed the nitrogen washout tests. In none of the above structure *vs* function plots are these two cases outliers.

In summary, only measured lumen size does not correlate with closing volume and CV/CV(%). Of those variables which have significant correlations bronchiolar ellipticality has the strongest followed by mean inter-alveolar attachment distance. Contrastingly, only mean inter-alveolar attachment distance correlated significantly with the slope of phase III.

		Single Breadth Nitrogen Washout Test		
		Closing Volume	CV/VC%	Slope of Phase III
Mean AWUV	(r)	-0.44	-0.40	NS
	(n)	30	30	
	(p)	0.008	0.014	
LF5 AWUV	(r)	-0.48	-0.40	NS
	(n)	30	30	
	(p)	0.004	0.013	
Mean	(r)	0.38	0.59	0.59
IAAD	(n)	21	21	19
	(p)	0.004	0.003	0.004
Airway	(r)	0.57	0.66	NS
Ellip.	(n)	21	21	
	(p)	0.003	<0.001	
Theor.	(r)	0.44	0.46	NS
Lumen	(n)	21	21	
Area	(p)	0.021	0.018	

Table 4.19: Significant morphometry *vs* Single Breath Nitrogen Washout Test correlations.

Along with the morphometric variables height, age and sex were incorporated into the multiple regression analysis of closing volume. Only bronchiolar ellipticality is a significant predictor (Beta weight=0.54, t=3.02, p=0.007) explaining by itself 29% of the observed variation in closing volume.

For the multiple regression analysis of closing volume/vital capacity (%) only age was retained for the initial regression equation as CV/VC(%) does no regress with height or sex in normal lungs (Buist and Ross 1973). The final regression equation eliminated all variables except bronchiolar ellipticality and mean inter-alveolar attachment distance (table 4.20). Combined these two variables explain 46% of the measured variation in CV/VC(%). Replacing mean AWUV by LF5 AWUV in the regression analysis does not alter the final

regression equation or statistics.

Bivariate and multiple regression analysis of the slope of phase III both identify mean inter-alveolar attachment distance as the only significant morphometric variable. This has a Beta weight of 0.59 ($t=3.007$, $p=0.0079$) and explains 31% of the observed variation in the slope of phase III. The final regression equation (in conventional form) for the slope of phase III is thus:

$$\text{Slope of Phase III} = -3.47 + 0.038(\text{IAAD})$$

where IAAD is mean inter-alveolar attachment distance.

Figure 4.26. The Slope of Phase III *vs* Mean Inter-Alveolar Attachment Distance. This is the only parameter which correlates with this index of inhomogeneity of ventilation ($r=0.59$, $p=0.004$ with $n=19$).

Slope of Phase III
vs Mean IAAD

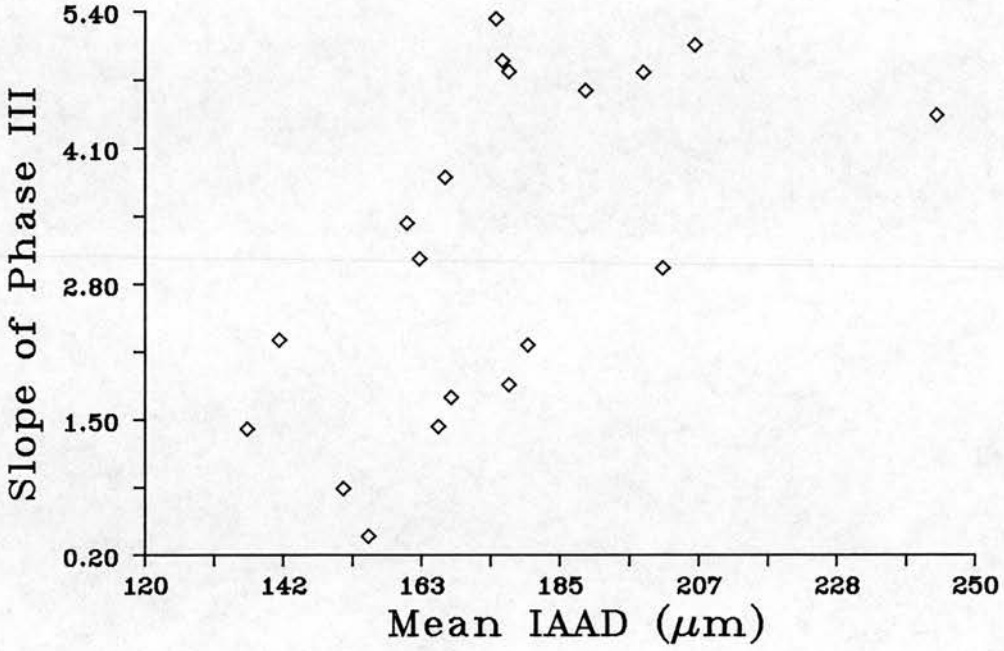

Dependant Variable: Closing Volume/Vital Capacity (%)

ANOVA TABLE

	Degrees of Freedom	Sum of Squares	Mean Square
Regression	2	850.45	425.22
Residual	18	796.08	44.23

F_{ratio}= 9.61 Significance of F_{ratio}= 0.0014

Regression Statistics

	Slope(B)	S.E.(B)	Beta Weight	t	p
IAAD(X_1)	0.13	0.072	0.33	1.762	0.0950
NRB Ellip.(X_2)	29.03	11.163	0.49	2.601	0.0181
(Constant=	-42.35	15.466		-2.738	0.0135)

Coefficient of Multiple Determination(R^2)= 0.46

Hence:

$$CV/VC(\%) = -42.35 + 0.13(X_1) + 29.03(X_2)$$

Table 4.20: Multiple regression of closing volume/vital capacity(%) with mean inter-alveolar attachment distance (IAAD) and bronchiolar ellipticality (NRB Ellip.) as the independent variables.

4.5. ASSESSING RELATIONSHIPS FOR "NORMAL" STRUCTURE

4.5.1. Introduction

The objective of this section is to propose structure/structure and structure/function models for "normal" lungs. These models are based upon a subgroup of cases with minimal or no disease. The results pertaining to this subgroup are compared with those of the complete sample and with the other subgroup thought to have some lung disease.

To achieve this exploratory analysis a subgroup of patients had to be extracted from the sample population. This was done based on the following results –which have been given above. Within the study group a spectrum of AWUV loss exists –a spectrum which when compared to lung density as measured by CT scan gives very highly significant correlations. The best structure/function relationships are obtained between AWUV and K_{co}. Therefore, in an attempt to identify those cases with little or no disease the study group was subdivided on the basis of their K_{co} results. Those cases with a K_{co} value within one standard deviation of that predicted were taken to have little disease, whilst those with K_{co} values worse than this were taken to have at least some disease. [3]

[3] K_{co} predicted values were taken from (Billiet *et al* [1963]) which were thought to be the most appropriate for this study group (Gould *et al*. However, these predicted values are based upon a heterogeneous group of both smokers and non-smokers and will therefore probably over estimate the number of "normal" cases. The threshold of 1 standard deviation should return a correct interpretation of patients in five out of six cases (Gibson 1984).

4.5.2. K_{co} Subdivisions

Thirty four of the 44 cases have K_{co} data. Of these 21 have K_{co} values within one standard deviation of that predicted, the other 13 have K_{co} values worse than this (values are tabulated in the appendix).

4.5.3. AWUV *vs* Body Size

Taking the sample population as a whole, mean AWUV has a significant correlation with total lung capacity. In contrast, there are no significant correlations between AWUV and height or body surface area[4].

Where this analysis is repeated for those cases with normal predicted values for K_{co}, there is no association between AWUV and total lung capacity, height or body surface area. Whereas, in the abnormal K_{co} group there is a significant correlation between mean AWUV and total lung capacity ($r=-0.57$, $n=13$, $p=0.021$), but none with either height or body surface area. Figures 4.27 and 4.28 are presented to illustrate theses findings and the correlation coefficients are summarised in table 4.21.

[4]Body surface area was calculated using the equation of Dubois and Dubois (1916)

All Cases

		TLC	Height	BSA
Mean AWUV	(r)	-0.34	-0.14	-0.12
	(n)	41	44	40
	(p)	0.015	0.185	0.235

K_{co} within 1SD of predicted

		TLC	Height	BSA
Mean AWUV	(r)	-0.06	-0.17	-0.06
	(n)	21	21	18
	(p)	0.389	0.228	0.407

K_{co} less than 1SD of predicted

		TLC	Height	BSA
Mean AWUV	(r)	-0.57	-0.28	-0.07
	(n)	13	13	12
	(p)	0.021	0.180	0.409

Table 4.21: Correlations between mean AWUV and indices of body size for: all cases, those cases with K_{co} within one standard deviation of predicted and those with K_{co} values worse than this. BSA is an abbreviation for body surface area and TLC for total lung capacity.

Figure 4.27. Total Lung Capacity *vs* Mean AWUV (for those cases with abnormal K_{co}. Where there is no correlation between TLC and mean AWUV for those cases with normal K_{co} there is a significant correlation for those with abnormal K_{co} ($r=-0.57$, $p=0.021$ with $n=13$).

Figure 4.28. Height *vs* Mean AWUV. As with body surface area and AWUV there is no relationship between height and AWUV.

Mean AWUV *vs* TLC Absolute

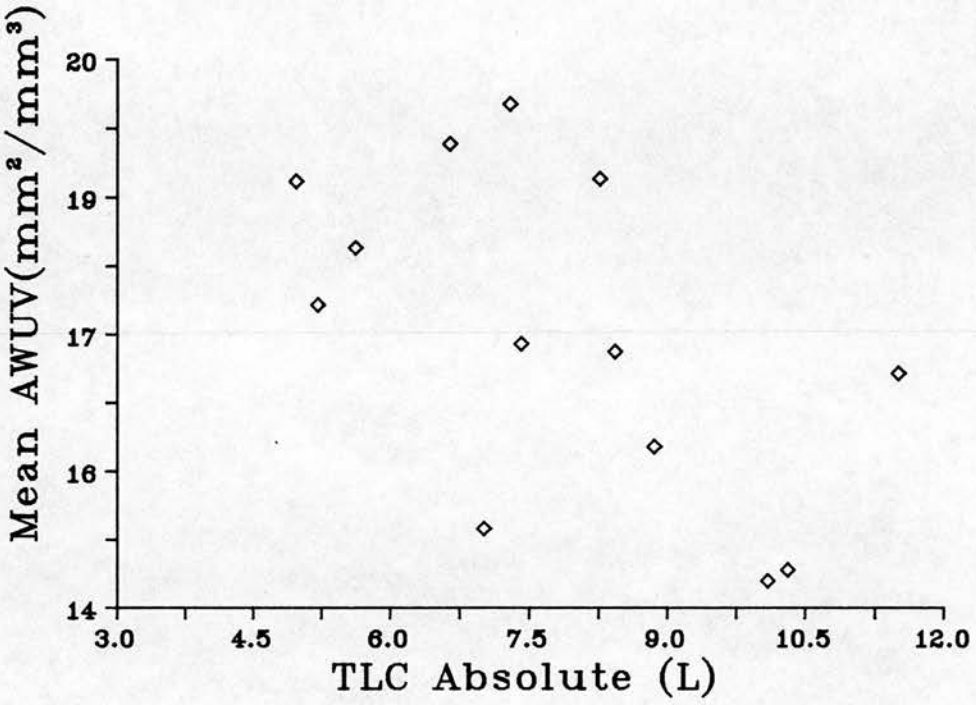

Mean AWUV *vs* Height

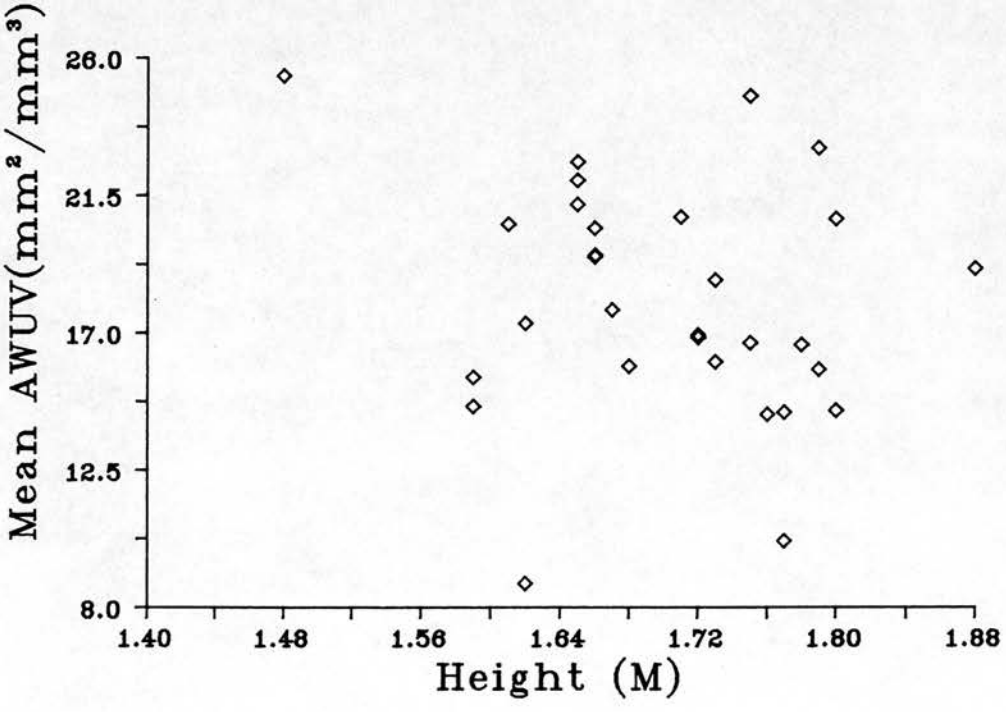

4.5.4. Airway Size and Body Size

Neither measured nor theoretical lumen area correlates with total lung capacity, height or body surface area either for the sample population as a whole, for those cases with normal K_{co} or those with abnormal K_{co}.

4.5.5. Airway Density and Body Size

In the above analysis cases were subdivided into two groups on the basis of their K_{co} results. As it is unlikely that airway density is affected, in this study group at least, airway density data was not subdivided on the basis of the K_{co} data.

Airway density (bronchioles *per* cm^2) is negatively related to body size, body surface area and total lung capacity for the sample population as a whole (the regression equations are given below). Inspection of the regression plots (see figure 4.29 of airway density *vs* height), suggests there are two distinct groups. The cases in the larger of these groups (n=23) have a lower airway density for a given height than those in the smaller group (n=5). Analysing these groups separately gives alternative regression equations (see below).

The regression equations for the whole group are;

1. Airway Density and Height:

$$y = 2.83 - 1.29(hgt) \quad [p<0.001]$$

2. Airway Density and Body Surface Area (BSA):

y= 1.52- 0.50(BSA) [p=0.007]

3. Airway Density and Total Lung Capacity:

y= 0.97- 0.04(TLC) [p=0.015]

For the larger group alone (n=23) the regression equations are;

1. Airway Density and Height:

y= 2.39- 1.06(hgt) [p<0.001]

2. Airway Density and Body Surface Area (BSA):

y= 1.20- 0.35(BSA) [p=0.003]

3. Airway Density and Total Lung Capacity:

y= 0.78- 0.03(TLC) [p=0.020]

and for the smaller group (n=5) the regression equations are;

1.Airway Density and Height:

y= 2.79- 1.09(hgt) [p=0.018]

2.Airway Density and Body Surface Area (BSA):

$y = 2.05 - 0.63(BSA)$ [p=0.038]

3. Airway Density and Total Lung Capacity:

$y = 1.32 - 0.05(TLC)$ [p=0.049]

It can be seen from figure 4.29 that the two regression equations for airway density *vs* height are very similar to one another. What is of interest is the relative difference in airway density when expressed *per* unit volume between these two groups. This can be assessed by first calculating the bronchiolar density (cm^{-2}) predicted by the two different regression equations for the extremes of the observed range in height ie *circa* 1.5 and 1.8 metres. Doing this the following values are obtained;

1. 0.8 and 0.48 bronchioles *per* cm^2 for 1.5 and 1.8 metres respectively, for the larger of the two groups, and
2. 1.16 and 0.83 bronchioles *per* cm^2 for the smaller group.

Weibel and Gomez (1962) provide a formula whereby total airway number (N) can be assessed;

ie $N = (Kn^{3/2})/(\beta Q^{0.5})$

K is a distribution related parameter which usually varies from 1.0 to 1.07 (Williams 1977) and which in most instances can be disregarded (Aherne and Dunnill), **β** is a shape factor relating to the average airway length:diameter ratio which should vary little between cases (cf the calculation of **β** in Weibel

and Gomez), **Q** is the volume proportion of bronchioles within the lung and **n** the number of bronchioles observed *per* unit area. Expressing **n** to the power 3/2 is essentially a factor correcting **n** from cm^2 to cm^3. There is insufficient data to calculate **N** for the study cases, but it is possible to assess the probable difference, as a proportion, between the two different groups. That is using the data calculated above (ie bronchioles *per* cm^2) for the two heights of 1.5 and 1.8m, knowing that K and **B** have little between-case effect and assuming for a given height Q varies little (or at least normally for the two groups) then $n^{3/2}$ is the deterministic factor. That is;

1. $(0.8 \text{ bronchioles } cm^{-2})^{3/2}=0.71$ and $(0.48 \text{ bronchioles } cm^{-2})^{3/2}=0.33$, whereas
2. $(1.16 \text{ bronchioles } cm^{-2})^{3/2}=1.54$ and $(0.83 \text{ bronchioles } cm^{-2})^{3/2}=0.76$.

These calculated values would be modified by **K**, **B** and **Q** into more appropriate bronchiolar density (*per* cm^3) results, however, the relative magnitude of difference would be maintained. Thus the cases in the smaller of the two groups are predicted to have around twice as many airways for a given height than those in the larger group.

This dichotomy in airway density is not repeated for airway size. The cases belonging to the smaller of the two groups being scattered throughout all of the airway size *vs* patient size plots.

It has been shown that decreases in AWUV are matched by increases in total lung capacity. Therefore, the regressions between airway density and total lung capacity may be influenced, by retaining in the regression equation, those cases with altered lung structure/function. If the cases with abnormal

K_{co} are removed (as above) then the regression analysis of airway density *vs* total lung capacity can be repeated using only those cases with normal K_{co}. However, by doing this there are only sufficient cases remaining in the larger group for meaningful statistical analysis, ie the subgroup of cases with relatively lower airway density. Repeating the regression equation for this group of cases gives:

Airway Density and Total Lung Capacity

$y = 0.91 - 0.04(TLC)$ [p=0.020]

Figure 4.29. Airway Density *vs* Height. Although there is a significant regression where all cases are used the plot suggests that two distinct groups may exist; with the smaller group of five cases (filled symbols) having an airway density (*per* cm^3) twice that of the larger group. Please refer to text for the regression equations.

Airway Density *vs* Height

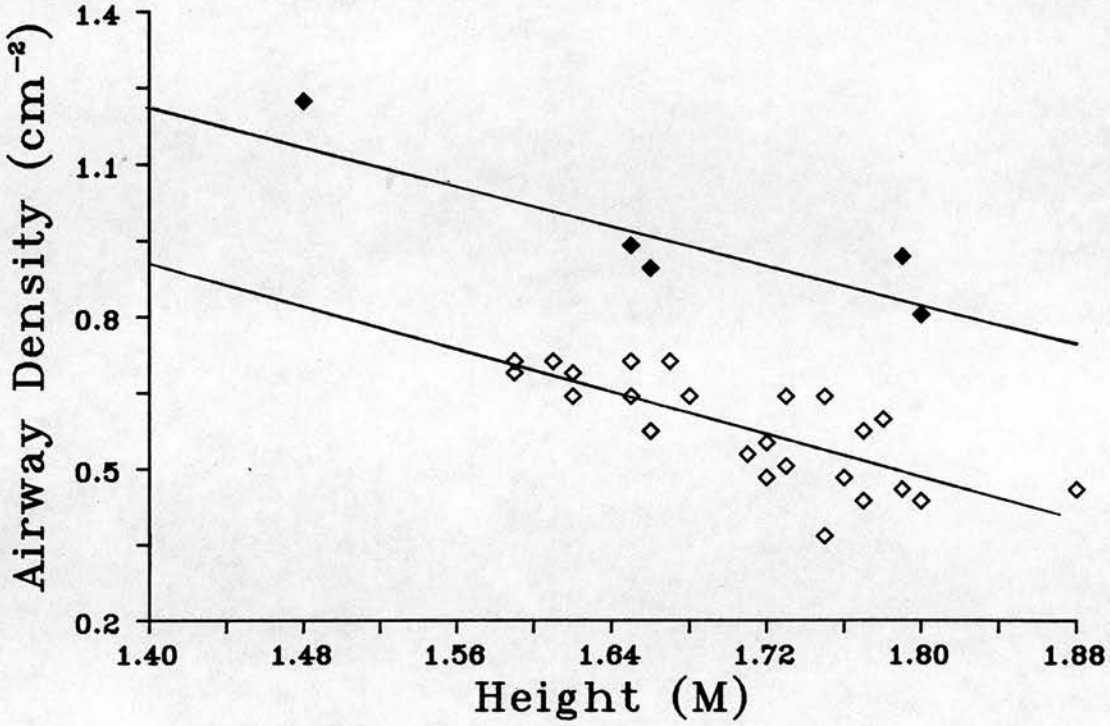

4.5.6. Other Parameters and Abnormal K_{co}

The following results are of interest and relate to the division of the study group on the basis of their K_{co} values. Minimum diameter is not significantly different in those cases with abnormal K_{co} from those cases with normal K_{co} however, theoretical lumen area is significantly higher in those cases with abnormal K_{co} (Table 4.22). Total lung capacity, expressed as percent predicted, is higher for those cases with abnormal K_{co} (Table 4.23), whereas mean AWUV is lower (Table 4.24).

	Minimum Diameter (mm)			
	Median	n	U	p
Kco<1SD	0.517	15		
Kco>1SD	0.548	9	66	NS

Ho: Accepted.

	Theoretical Lumen Area (mm^2)			
	Median	n	U	p
Kco<1SD	0.649	15		
Kco>1SD	0.830	9	34	.05

Ho: Rejected.

The null hypothesis for both tests is the same.

Ho: There is no difference in airway size between those cases with normal or abnormal K_{co}.

Hi: There is a difference.

Table 4.22: Tests to see whether either minimum diameter or theoretical lumen area differed between those cases with abnormal K_{co} as opposed to abnormal K_{co}. The Mann-Whitney U test was used.

	TLC % Predicted			
	Median	n	z	p
Kco<1SD	119	21		
Kco>1SD	131	13	1.66	.049

Ho: There is no difference in TLC percent predicted between cases with and without normal K_{co}.

Hi: Those cases with abnormal K_{co} have a larger TLC percent predicted (one tailed).

Ho: Rejected.

Table 4.23: Tabulated test to determine whether TLC percent predicted is greater in those cases with abnormal K_{co}. The Mann-Whitney U test was used with U being converted to a z value.

	AWUV (mm^2/mm^3)			
	Median	n	z	p
Kco<1SD	19.2	21		
Kco>1SD	16.9	13	2.55	.005

Ho: There is no difference in mean AWUV between cases with and without normal K_{co}.

Hi: AWUV is larger in those cases with normal k_{co} (one tailed).

Ho: Rejected.

Table 4.24: Tabulated test to determine whether mean AWUV is greater in those cases with normal K_{co}. The Mann-Whitney U test was used with U being converted to z.

CHAPTER 5

DISCUSSION

5.1. COMPARISONS WITH OTHER STUDIES

5.1.1. Introduction

This is a study of structure *vs* structure and structure *vs* function in a group of surgical cases who completed a battery of pre-operative pulmonary function tests. The initial part of this discussion compares the morphometric results obtained in this study with those reported by other comparable studies. Differences in methodologies are noted and, where possible, data manipulations are carried out to facilitate a wider range of comparisons. Inter-morphometry comparisons are discussed, highlighting those variables which have the greatest effect on other morphometric variables. This analysis is followed by an examination of CT scan *vs* AWUV (a microscopic assessment of alveolar loss) and an assessment of macroscopic emphysema. Structure *vs* function relationships are then discussed. Again, those variables which have the best relationship with function are identified and possible cause-and-effect models proposed.

5.1.2. Comparable Studies

Comparisons between surgical and autopsy based studies are difficult as these can differ with respect to the overall severity of disease, the presence of end-stage disease and/or terminal infections.

Patients must have a good chance of surviving the surgical process and

have a reasonable lifestyle thereafter for surgery to be a feasible option. This means that their remaining lung tissue must be relatively free of disease. Thus, in surgical series there is a procedure that selects cases with milder lung disease than that found in non-sudden death autopsy based studies. For example, in comparison with the present group of cases, which have predominantly mild lung disease and FEV percent predicted ranging from 47-123%, the autopsy group of Nagai *et al* (1985a) had moderate to severe lung disease with FEV percent predicted values which range from 11 to 57%.

A potential complicating factor for structure *vs* function analysis in autopsy series is that the observed morphology may not relate to pulmonary function measured some time prior to the patients death. This is because of changes associated with end-stage disease and/or terminal infections (Niewoehner and Kleinerman 1974) eg purulent bronchitis, luminal obliteration, local abcess formation and dilatation of bronchioles (Thurlbeck 1976). Such complicating factors are unlikely to be present in surgical cases.

For the reasons given above, where possible, data comparisons are made between this and other surgical series.

5.1.2.1. Macroscopic Emphysema

In this study the severity of macroscopic emphysema, present in the mid-sagittal slice, was measured directly. A comparison of the amount and distribution of macroscopic emphysema in this and other series is difficult for two main reasons. Firstly, few surgical series have assessed the severity of macroscopic emphysema and secondly, the assessment of macroscopic emphysema is non-standardised and often made on a semi-quantitative basis.

Comparable studies are (Bergin *et al* (1986), Cosio *et al* (1977), Pare *et al* (1982) and Berend *et al* (1979b)). These series are not only similar in their use of surgical material, but in the following aspects: the mean age of the study groups, the ratio of males to females studied (excluding the study of Berend, where notably fewer females are included) and in the over all pulmonary function of the groups.

A range of methods have been employed to measure macroscopic emphysema. Some studies have used the picture grading method of Thurlbeck (Cosio *et al* 1977) or a modification of this technique (Pare *et al* 1982 and Bergin *et al* 1986) whereas Berend *et al* (1979b) used both picture grading and point counting and also measured alveolar surface area by the mean linear intercept method.

As picture grading utilises scores that are "arbitrary intuitive milestones in the spectrum of severity of various types of emphysema" (Thurlbeck *et al* 1969) -cf section 1.5.3.3- it is not possible to compare, directly, picture grading results with absolute measures of emphysema. An example of the disparity between these two methods is evident from the results tabulated by Berend *et al* (1979b). These workers provide data on picture grading scores alongside the corresponding absolute measurements of macroscopic emphysema -measured by Dunnill's point count method and represented as a percentage of the total area of the midsagittal lung slice. The following examples have been taken from their table; case 1 has 0% macroscopic emphysema but a corresponding picture grade of 15, case 2 has 3% and a picture grade of 20 and case 6 has 19% with a grade of 50. Apparently higher grades (as opposed to absolute values) are obtained for cases with little or no macroscopic emphysema as, in the picture grading system, mild emphysema is

given an arbitrary score of 20 and moderate emphysema a score of 50. The arbitrary scale used in picture grading means that there is no conversion factor that will reliably translate these scores into absolute measures. These examples highlight the difficulty in making inter-series comparisons where relative and absolute measures are concerned.

comparisons, a grade of up to 5 is estimated to be equivalent to an absolute score of less than 1% emphysema. Using this estimate; 59% of Bergin's cases have a score of 5 or less, 50% of Cosio's, 56% of Pare's and 50% of Berend's. This compares to 56% of cases in this study which have less than 1% of their area involved by macroscopic emphysema. Therefore these studies have a similar incidence of macroscopic emphysema, the distribution of which is profoundly non-normal; being similar to that of a Poisson distribution. The distribution of emphysema presented by Bergin *et al* is highly similar in profile to that of this study, even though their data is in the form of picture scores.

5.1.2.2. AWUV

The technique presented in this study to quantitate airspace wall surface area *per* unit volume is a new one. AWUV data can be compared with other measurements of alveolar surface area data obtained by other studies -most of whom use the mean linear intercept technique. Before doing this methodological differences between the measurement of Lm and AWUV are noted.

One major difference between mean linear intercept and the image-analysis based technique used in this study is that, with the latter, highly accurate results can be obtained for each individual field. This quality

has been noted previously by, amongst others, Aherne and Dunnill -cf section 1.5.2. This allows both the distribution within a case, and distribution statistics other than the mean, to be analysed. This has proven to be very useful in this study, with the mean of the lowest five AWUV fields (LF5 AWUV) providing additional and valuable information over and above that provided by the mean AWUV value. Analysing individual AWUV distributions also revealed there to be an even distribution of AWUV loss in most cases.

Having noted this difference, mean linear intercept and AWUV are closely linked in that one can convert Lm data into comparable AWUV terms of airspace surface area per unit volume ie mm2/mm3. This is apparent from the formula used to convert Lm into alveolar surface area for a given lung volume (V).

ie Surface Area = 4 x V / Lm

For AWUV the volume (V) is $1mm^3$. Thus Lm data converted into equivalent AWUV units is:

AWUV Surface Area(mm^2) = 4 x 1mm3 / Lm(mm)

Lm data provided by other authors can therefore be expressed in the same units as AWUV and be compared with the results obtained in this study.

Before making these comparisons methodological differences between Lm and AWUV measurements are noted. The main difference between this and other studies is in the criteria applied to define whether a selected histological field is appropriate for measurement. Studies using the standard Lm technique

reject fields if they contain bronchi or vessels "of such a size that it had been excluded previously as 'non-parenchyma'" (Thurlbeck 1967b). Where 'non-parenchyma' is any non-alveolated structure larger than 1mm in diameter. The remaining smaller airways and vessels -termed "coarse parenchyma" by Weibel (1984)- are included in the calculation of Lm. Contrastingly in this study all fields containing coarse parenchyma (eg smaller non-respiratory and respiratory bronchioles) are excluded from the analysis. AWUV data is thus representative of the alveolated portion of the lung.

The net effect of these differences is that AWUV values reported in this study should be greater than those reported by studies using the Lm technique. A comparison between the two techniques suggested that approximately 1 in 10 fields accepted for the measurement of Lm was not appropriate for the measurement of AWUV. This will vary from case to case with, in general, the number of rejected fields being more in those cases with a greater bronchiolar density (cf section 5.5.3).

From the comparable surgical series listed above only Berend *et al* (1979b) measured Lm, the others (Bergin *et al* 1986, Cosio *et al* 1977 and Pare *et al* 1982) assessed emphysema only on a macroscopic basis. Berend *et al* report Lm-derived AWUV to vary from 8.9 to 20.0mm2/mm3. These values are highly comparable to those reported here. Unfortunately, Berend *et al* do not indicate the criteria used to accept or reject histological fields, but it is likely that they used the standard Lm procedure.

Damiano *et al* (1986), studying the immunolocalisation of elastase in emphysematous lungs, measured Lm in eight surgical cases. Their equivalent AWUV values range from 8.9 to 18.2mm2/mm3. Although they do not specifically state it, it is likely that these authors excluded only those fields

with "larger bronchioles or major blood vessels" as this was the procedure carried out in their microscopic picture grading of emphysema. Their AWUV values should likewise be less than those of this study.

Saetta *et al* (1985), using a mixture of sudden-death (non-smokers) and surgical cases (smokers) obtained Lm-derived AWUV values of 7.4 to 18.6mm2/mm3. Again, fields with coarse parenchyma were included in the calculation of Lm.

In summary, Lm-derived values of AWUV gleaned from studies directly comparable to this study, have results which are similar. The tendency for the AWUV values in this study to be higher can be accounted for by the differences in criteria used to define which histological fields are acceptable for measurement of Lm or AWUV. The difference is that coarse parenchyma ie non-alveolated structures with an internal diameter less than 1mm, are included in the calculation of Lm, whereas such fields are excluded in the calculation of AWUV.

All the above studies used lung tissue embedded in paraffin when assessing Lm. This has known artefacts which render the data softer (cf section 3.3).

5.1.2.3. Non-Respiratory Bronchiolar Size

Before comparisons with other studies are made, methodological differences between this and other studies have to be discussed. These include differences in embedding, sampling and the parameters measured.

Both tissue embedding and sampling affect measured airway size. Lung tissue embedded in paraffin is susceptible to variable shrinkage and

compression artefact (section 3.3). Compression is zonal and affects only one plane of the section. The changes caused by these factors cannot therefore be corrected by the calculation of simple linear shrinkage factors. Glycol methacrylate does not suffer from these artefacts and as such was used as the embedding medium throughout this study.

Important sampling differences concern the initial macroscopic or stage 1 sampling of tissue blocks from the lung and latterly the microscopic or stage 2 selection of airways from processed tissue. The latter is discussed first.

In this study all membranous bronchioles lacking mucous glands and cartilage in their walls were accepted for measurement. This contrasts with the selection of other studies -of which Matsuba and Thurlbeck (1971 and 1972) are standard references- where the sampling of bronchioles is limited to those that have an internal diameter of 2mm or less -ie "small airways". This sampling procedure is a consequence of the work of Hogg *et al* (1968) who found small airways to be the major site of increased resistance to airflow in patients with airway obstruction in chronic obstructive lung disease. As a result of these findings, many studies have limited their selection of bronchioles to those with an internal diameter of 2mm or less. This 2mm criterion is an "arbitrary definition" (Matsuba and Thurlbeck 1971) of small airways which also relates to the calculation of Reynold's number (Hogg 1982). This predicts that laminar flow exists in airways with an internal diameter of 2mm or less.

Arguing against this as a valid sampling procedure, if tissue embedding and/or disease affects airway size -especially in an undefined manner- then it is inappropriate to use airway size itself as a selection criterion. Thus all membranous bronchioles were initially selected for quantitation in this study.

However, criteria were developed to exclude those which were cut at extreme angles.

A potential advantage accrues from selecting all non-respiratory bronchioles, as opposed to only small airways. One of the objectives of this study was to investigate whether bronchiolar size relates to stature (lung volume, body surface area and height). For this analysis to be valid it was imperative that the airway selection procedure did not contain any potential systematic bias.

The data of Weibel (1963), Horsfield and Cummings (1968) and Hansen and Ampaya (1975) suggests that airway calibres are linked throughout the bronchiolar tree while other workers have found large airway size and body size to be related (cf section 1.2.1.1). If bronchiolar size is related to body stature/lung volume -a point that Matsuba and Thurlbeck (1971) could not disprove- selecting only small airways will contain a systematic bias against larger individuals and males in general -males having larger lung volumes than females of the same height (Gibson 1984). Given the markedly skewed distribution of bronchiolar size (Salmon *et al* 1982) -and also the distributions plotted by Matsuba and Thurlbeck 1971, 1972 and 1973- a selection procedure that specifically excludes the upper values can have a significant effect on individual mean values obtained for each case. Selecting all non-respiratory bronchioles does not contain this systematic bias.

That the two selection techniques produce different results can be ascertained from the data provided by Sasaki *et al* (1986). These workers measured the internal diameter of all bronchioles and then small airways in the same 16 autopsy cases. From their tabulated data, mean bronchiolar diameter is 0.714mm whereas mean small airway diameter is 0.625mm, or

87.5% that of mean bronchiolar diameter. These two measurements are significantly different as judged by the paired t-test (t=3.08, p=0.008). These calculations have been made by the present author from the data tabulated by Sasaki *et al*

With respect to macroscopic stage 1 sampling, the region of the lung from which tissue is sampled is important as bronchiolar calibre decreases, whereas bronchiolar density increases towards the periphery of the lung. Distally, there will be a larger proportion of small airways.

In this study tissue blocks were sampled from the lateral two sub-pleural slices. This is similar to the procedure proposed by Matsuba and Thurlbeck (1971 and 1972) -where tissue blocks are sampled from the lateral slices- and adhered to by other studies (Nagai *et al* 1985a). A similar sampling regime was employed by Wright *et al* (1983) sampling from the medial and lateral slices. Other sampling regimes include random sampling from all slices (Niewoehner and Kleinerman 1974) or from all slices except the mid-sagittal slice (Berend *et al* 1979b, Hale *et al* 1984 and Cosio *et al* 1980). However, some studies fail to document their tissue sampling procedure; Pare *et al* 1985, Niewoehner and Kleinerman 1974 and Salmon *et al* 1982).

Some of the variability in bronchiolar/small airway morphometry data may relate to differences in macroscopic sampling procedure. The precise amount, however, is impossible to quantitate.

Much interest has centred on peripheral airway size since the work of Hogg *et al* (1968). In this study three measurements of bronchiolar size have been made. One of these, theoretical lumen area, is unique to this study. Data on measured lumen area within the literature is scarce as the majority of

morphometric studies have measured airway size as minimum diameter. Below, it is argued that minimum diameter is not the best measurement of airway size and theoretical lumen area is proposed as an alternative and more representative measurement.

Correlations carried out to test which measure of airway size has the best correlations with epithelial and wall area revealed theoretical lumen area to be the best correlate and minimum diameter the poorest.

Minimum diameter is measured on the assumption that airways are cylindrical. Where cylinders are cut at a variety of angles the minimum diameter (largest diameter in the shortest plane) is representative of the cross-sectional diameter of the cylinder. Nagai *et al* (1985a), Anderson and Foraker (1968) and Linhartova *et al* (1971, 1973, 1974 and 1982) and the data of this study (see below) all show that airway shape is altered with loss of alveolar walls. Minimum diameter will thus underestimate airway size in cases with loss of alveolar walls and elliptical airways. This is clearly shown by some of the three-dimensional reconstructions of Linhartova *et al* (1974).

The usefulness of a measurement of airway size can be judged by its ability to reflect changes associated with lung disease. A number of morphometric studies have been unable to demonstrate differences in mean small airway diameter between cases with and without macroscopic emphysema (Petty *et al* 1986, Hale *et al* 1984 and Matsuba and Thurlbeck 1972) or between smokers and non-smokers (Cosio *et al* 1980). It has already been noted that minimum diameter will underestimate airway size in diseased cases as the airways will be elliptical. Where little or no significant difference has been found between diseased and non-diseased, or smoking and non-smoking, groups the possibility arises that the the diseased and smoking

individuals have, on average, larger airways.

This hypothesis is supported by data obtained in this study. Neither AWUV nor mean inter-alveolar attachment distance correlate with measured lumen area or minimum diameter, but both correlate with theoretical lumen area. The relationships with theoretical lumen area indicate that lumen area increases with progressive loss of alveolar walls. Additionally, although there is no significant difference in minimum diameter between cases with and without normal K_{co} values there is a significant difference in theoretical lumen area; the cases with abnormal K_{co} having a larger mean theoretical lumen area.

Although some studies have failed to find differences in peripheral airway size Nagai *et al* (1985a) found individuals with moderate to severe chronic airflow obstruction to have, on average, smaller peripheral airways than their control group. This data suggests that in early emphysema peripheral airway size, or at least the maximum size obtainable, increases.

Representing airway size as theoretical lumen area has another advantage. The main differences between autopsy and surgical material have been discussed above. There is an additional complicating factor where peripheral airway size is concerned. This relates to the presence of muscle tone in surgical material, and the effect has been quantitated by Berend *et al* (1981). Measuring the minimum diameter of small airways in autopsy and surgical material, they found the size of the latter to be considerably smaller (0.52mm as opposed to 0.83mm). This led them to conclude that "bronchiolar diameters in lungs or lobes obtained by different means may not be directly compared". This finding severely limits the number of inter-study comparisons that can be made.

Of the previously identified comparable surgical based studies only Berend *et al* (1979b) measure small airway diameter -which for their cases is 0.43mm. The mean bronchiolar diameter for this study is 0.54mm. Using Sasaki's finding -that mean small airway diameter is 87.5% of mean bronchiolar diameter in the same cases- the mean bronchiolar diameter found in this study can be converted to mean small airway diameter. Doing this gives a mean small airway diameter of 0.47mm. This compares well to the 0.43mm found by Berend and coworkers. [This correction is not exact as Sasaki *et al* appear to have sampled bronchioles throughout the lung. This should give a smaller proportion of airways less than 2mm internal diameter and, in general, larger bronchioles than obtained here].

Theoretical lumen area was designed to represent airways in the absence of muscle tone and at their maximum potential size. That this is a valid assumption is supported by the work of James *et al* (1987). These workers devised a study to determine which bronchiolar parameters were the most constant at various volumes, 25% to 100% TLC -using guinea pig lungs- and between fresh and pharmacokinetically relaxed states, using resected human tissue. Their conclusion was that "in quantitative histological studies of lung Ci (the internal circumference of the lumen defined by the epithelium) should be used to match airway size because it remains constant throughout a wide range of airway narrowing". Representing airway size in the absence of muscle tone provides some comparability between surgical and autopsy material. Before comparisons can be made theoretical minimum diameter must be ascertained, ie

$$\text{Theoretical Lumen Diameter} = 2 \times (TLA/\pi)^{0.5}$$

where TLA is theoretical lumen area.

Calculating this for each case gives an average theoretical bronchiolar diameter of 0.89mm for the study population. Using the correction factor calculated from Sasaki's data this equates to an average small airway diameter of circa 0.78mm.

Before comparing these values with those obtained by autopsy-based series one last factor has to be taken into consideration. In autopsy material, due to the denudation of epithelium (Nagai *et al* 1985a), airway diameter is measured from the basement membrane whereas the quality of the material in this (and other surgical series) is such that the diameter can be measured from the epithelium. If one assumes the height of the epithelium to be circa 20µm the corresponding mean bronchiolar diameter for this study is *circa* 0.93mm and *circa* 0.82mm for mean small airway diameter.

The following mean small airway diameters are taken from the most comparable autopsy based studies; 0.65mm for cases without macroscopic emphysema (Petty *et al* 1986), 0.67mm again for cases without macroscopic emphysema (Petty *et al* 1981), 0.83mm from sudden death cases of non-pulmonary origin (Niewoehner and Kleinerman 1974), and 0.76mm for non-emphysematous lungs (Matsuba and Thurlbeck 1971).

Accepting the criticism of minimum diameter as an accurate representation of airway size, the mean theoretical minimum diameter value obtained in this study is comparable with those reported by the above autopsy based studies. This suggests that the technique of smoothing the lumen circumference may be a useful one that allows some comparisons to be made between surgical and autopsy based studies.

If theoretical lumen area does remove the effect of muscle tone then expressing measured lumen area as a proportion of theoretical lumen area may give an index of airway reversibility. Unfortunately, insufficient data was available to complete this analysis for this study.

5.1.2.4. Airway Density

Measurements of airway density are important as airway density is proportional to the number of terminal bronchioles and thus acinar units. This in turn gives a relative indication of acinar size. Before reviewing data in the literature factors which affect this measurement are noted. These factors include body size, sampling procedure and pathological changes.

Where individuals have the same total number of airways smaller individuals and females in general will have higher airway densities. Studies with dissimilar study populations, with respect to stature and sex or who have used study groups containing only or predominantly one sex, will therefore produce "softer" airway density data. With regard to sampling procedure, as airway size decreases but density increases towards the periphery of the lung, macroscopic sampling procedures will influence airway density. In particular, studies that sample from the lateral sagittal slices should obtain a proportionately greater number of small airways (ie those less than 2mm internal diameter). Additionally, pathological changes can affect observed airway density values. For example, scarring can make categorical recognition of airways difficult and thus produce reduced airway density results. These factors individually, or in combination, will account for some of the reported variation in airway density figures.

A review of data on this subject was carried out by Matsuba and Thurlbeck

(1971). This review includes the work of Bergin *et al* (1969) and Anderson and Foraker (1962). The mean airway density results reported by Matsuba and Thurlbeck (including these two other studies) range from 0.77 to 0.81 small airways *per* cm^2.

Since then a number of other workers have also measured small airway density and the range of results found has increased. Results, expressed as the number of small airways per cm^2, and the type of study population used are summarised below. 0.65 for sudden-death cases (Berend *et al* 1981), 0.86 again for sudden-death cases (Niewoehner and Kleinerman 1974), 1.01 in autopsy cases with moderate to severe emphysema (Nagai *et al* 1985a), 1.19 for autopsy cases with no emphysema and 0.89 for autopsy cases with emphysema (Petty *et al* 1981) and 0.86 for smokers and 0.84 for non-smokers in sudden-death cases (Cosio *et al* 1980). Bronchiolar density in this study is 0.91 per cm^2. Matsuba and Thurlbeck (1971) estimate that around 6% of bronchioles are excluded by the small airway definition. This being so the equivalent small airway density for this study will be *circa* 0.86 per cm^2. This figure is around the middle of the range reported by the above authors.

5.2. INTER-MORPHOMETRY RELATIONSHIPS

5.2.1. AWUV and Macroscopic Emphysema

In the results section it was argued that any statistical relationship calculated for the bivariate plot of AWUV *vs* macroscopic emphysema -even though it be a non-parametric test of association- would be dependent on the handful of cases with more than 12% macroscopic emphysema. This was demonstrated to be the case by calculating two sets of correlation coefficients: one for the whole sample population and the other excluding those cases with more than 12% macroscopic emphysema. This first group of correlation coefficients suggested that there was a good association between the two variables, a statistic at variance with the visual bivariate plot of the parameters. The second set of correlation coefficients reported no significant covariance. This latter set is more in agreement with the plot of the variables.

This influence of outliers, or lack of "resistance" to outliers in correlation statistics, is discussed by Hartwigg and Dearing (1979). These authors demonstrate that even the Tukey Line (a correlation statistic specifically designed to be resistant to outliers) is still affected by patent outliers. These authors demonstrate the usefulness of exploratory and visual analysis of data preceding the application of possibly non-appropriate statistical tests.

In summary, bivariate plots involving data on macroscopic emphysema are inappropriate for correlation statistics. However, inferences can be made from the visual scatter of data. From the bivariate plot with AWUV it is clear that there is in general a very poor and non-linear relationship between these two variables. However, it can be observed that cases with a relatively large

amount of macroscopic emphysema have low AWUV values, but cases with little or no macroscopic emphysema can have equally low values of AWUV.

Does the Range of AWUV reflect airspace loss?

It is the contention of this thesis that the threefold range of AWUV values and histological appearance of cases (cf the last part of figure 2.7 and also figures 4.15 and 4.16) reflects a spectrum of alveolar wall loss. It is possible, using models of alveolar structure, to re-express AWUV data to lend support to this hypothesis. It is accepted that the models used may not rigorously represent airspace shape, but it is considered that these models help to put the range of AWUV values into perspective.

Weibel (1963) in his intricate and detailed study of five human lungs provides six models of alveolar shape which facilitate the conversion of surface areas into diameters of equivalent spheres. The most appropriate model is probably Model F, which represents alveolar shape as a sphere, as it is unlikely that airspaces in emphysema will adhere to any of the more detailed models. The model is not a complete sphere, but one with a portion (estimated to be one fifth) missing to represent the area of an alveolus that communicates with the supplying alveolar duct or sac.

Using this model it can be shown that the normally accepted threshold for the identification of macroscopic emphysema ie airspace size larger than *circa* 1mm in diameter, has an mean AWUV value of $6.0mm^2/mm^3$. That is;

$$\text{Surface Area (SA)} = 5/6\ (4\pi r^2)$$

$$= 2.62mm^2$$

and

Volume (V)= 5/6 ($4/3\pi r^3$)

= $0.44mm^3$

Therefore,

SA/V= $6.0mm^2/mm^3$

Thus, where average airspace size throughout a lung is 1mm -corresponding to 100% macroscopic emphysema- the approximate AWUV value is $6.0mm^2/mm3$. The lowest mean AWUV value ($8.8mm^2/mm^3$), is very close to this figure and is associated with 78% macroscopic emphysema in the mid-sagittal slice. This value, though, is part of a continuum of AWUV results which are normally distributed. Therefore, this continuum represents varying amounts of alveolar wall loss.

Additional data transformations are possible to substantiate further this statement. The individuals in Weibel's study were all autopsy cases having died of non-respiratory illnesses. Weibel calculates the average alveolar diameter for these cases to be 0.250mm; assuming the 5/6ths spheric model. Recalculating this figure as surface area per unit volume (ie AWUV) gives a value of $24.0mm^2/mm^3$. This value of AWUV is derived solely from alveoli and in reality would be slightly less when one includes alveolar ducts and sacs as these have a lower surface area *per* unit volume. Accepting this, the figure is in good agreement with mean AWUV values obtained, in this study, for cases with normal alveolar architecture (cf the last part of figure 2.17 showing case

13 and case figure 4.15 showing case 6).

From AWUV data it is possible to calculate corresponding radii and volumes of equivalent spheres assuming Weibel's 5/6ths s spheric model. To do this the relationship between spheric surface area and volume is utilised:

$$SA/V = (4\pi r^2)/(4/3\pi r^3)$$

$$= 3/r$$

AWUV, being surface area *per* unit volume can be assimilated into this formula to first calculate the radius:

ie where $SA/V = 3/r$

$$r = 3xV/SA$$

Therefore for AWUV;

$$r = 3 \times 1mm^3/\text{Alveolar Surface Area } (mm^2)$$

The volume is then:

$$\text{Volume of 5/6ths sphere} = 5/6\ (4/3\pi r^3)$$

$$= 10/9\ \pi r^3$$

Calculating these for the highest and lowest mean AWUV values gives the following values for airspace radius and volume:

$AWUV = 25.4mm^2/mm^3$

$Radius = 3 \times 1mm^3/25.4mm^2$

$= 0.118mm$ (diameter= 0.236mm)

$Volume = 10/9 \times \pi r^3$

$= 5.73mm^3 \times 10^{-3}$

and

$AWUV = 8.8mm^2/mm^3$

$Radius = 3 \times 1mm^3/8.8mm^2$

$= 0.341mm$ (diameter= 0.682)

$Volume = 10/9 \times \pi r^3$

$= 1.38mm^3 \times 10^{-1}$

As with AWUV, there is a threefold range in airspace radius, but a twenty fold range in volume.

These analyses support the contention that the AWUV results represent a

continuum of alveolar wall loss from that of notable loss, 8.8mm^2/mm^3 (which had an associated figure of 78% macroscopic emphysema) to that associated with little or no loss at all and that macroscopic measurements possibly refer to only one end of the spectrum of emphysema.

This approach to, and conclusions drawn from, the AWUV data differs from the approach of other studies (eg Thurlbeck 1967b and 1967c). These set out to establish baseline data on Lm (which is directly related to AWUV) for cases with no macroscopic emphysema. Their assumption was that the absence of macroscopi c emphysema indicated that there had been no destruction of alveolar walls. Although increase in airspace size is one of the defining features of emphysema, no one has yet defined normality (the 1mm threshold being arbitrarily chosen). The diagnosis of emphysema at its earlier stages is therefore still undefined. As the 1mm threshold has a potential 75% loss of surface area (ie 6.0 as opposed to 24.0mm^2/mm^3) it is conceivable that loss prior to this can have considerable implications for function. Indeed the clinical correlations with AWUV support this hypothesis. Baseline data on Lm for cases with no macroscopic emphysema does not therefore represent a condition of no alveolar wall destruction. Additionally, AWUV and macroscopic emphysema do not show a linear relationship, and as such macroscopic assessment of emphysema may be too crude a measure to reflect accurately loss of surface area.

This is in part backed up by the findings of Damiano *et al* (1986). Using surgical material and a histological (ie microscopic based) grading system to assess parenchymal loss they obtained a much better association between this type of picture grading and mean linear intercept, there being only one case of overlap between the three grades employed. Converting Damiano's Lm to

AWUV values gives a similar range to that found here (ie 8.7 to 18.2 mm^2/mm^3).

Few studies have assessed emphysema both macroscopically and microscopically. One comparable study, in its use of surgical material, is that of Berend *et al* (1979b). This group measured parenchymal loss as Lm and macroscopically by point counting. Converting Lm to AWUV their over all range of AWUV values is similar to that given here (and Damiano's) being 8.9 to 20mm^2/mm^3. Their results also exhibit a disparity between macroscopic and microscopic assessments, those cases with 0% macroscopic emphysema ranging from 11.8 to 20mm^2/mm^3 with those with 5% ranging from 8.9 to 16.7mm^2/mm^3. It is probably worth restating, for comparative purposes, that the AWUV range (in this study) for cases with no macroscopic emphysema is 15.5 to 25.4mm^2/mm^3 and for those cases with 5% or more macroscopic emphysema is 8.8 to 22.6mm^2/mm^3.

The following study (Salmon *et al* 1982), is interesting as the authors themselves convert their Lm data into Alveolar Surface to Volume Ratio (ASVR), another acronym for AWUV and likewise expressed as mm^2/mm^3. These authors report ASVR (AWUV) values ranging from 13.6 to 21.0mm^2/mm^3 for cases with no macroscopic emphysema. This study differs from ours in their use of sudden-death autopsy material.

Bringing these observations together it can be said that:

AWUV and Lm demonstrate poor relationships with both the presence and amount of macroscopic emphysema.

The 1mm threshold, although giving a standard whereby macroscopic emphysema can be recognised and its amount and distribution measured, does not accurately represent "early" loss.

Microscopic loss (which can be measured as Lm or AWUV) can be considerable before reaching the 1mm threshold and has (as discussed later) significant structural and functional correlations.

The two major types of macroscopic emphysema are centriacinar and panacinar. More analysis of the patterns of alveolar loss are required before it is possible to say how these two types of macroscopic emphysema relate to microscopic loss. Given that visible centriacinar lesions account for relatively little absolute alveolar wall loss (Dunnill 1964) they themselves cannot account for the observed range in AWUV values. Indeed those cases with marked AWUV loss have predominantly panacinar emphysema.

5.2.2. AWUV and Alveolar Attachments

AWUV and mean luminal inter-alveolar attachment distance are the two most important morphometric variables. When planning this study it was originally thought that these two measurements would in all likelihood parallel one another and that measurement of mean inter-alveolar attachment distance may provide a simple and quick way of estimating AWUV loss. Although there is a general trend for AWUV and mean inter-alveolar attachment values to covary the association is variable and there are definite exceptions to this observation.

These exceptions were identified by ranking cases on their relative mean inter-alveolar attachment distance and AWUV values and then comparing the ranks obtained. However, it is of equal importance that a histological review of the airways of these cases clearly demonstrated patterns of retention around the periphery of bronchioles, whereas adjacent areas showed definite

parenchymal loss of a more extensive nature. Photomicrographs of this have been presented (figures 4.14, 4.15 and 4.16), but it is worth noting that this preferential retention of alveolar attachments is not limited to bronchioles but is apparent around other structures eg septae and blood vessels, as well.

Reasons for these patterns of alveolar loss are not easily defined. Cosio *et al* (1980) hypothesised that inflammation of small airways may precede and cause loss of peribronchiolar attachments in the immediate vicinity of the inflammation. If this were so, differences in the bronchiolar inflammatory response of patients to irritants such as cigarette smoke may account for these observations. Wright *et al* (1984) and Berend (1981) found no association between small airway inflammation and the presence of macroscopic emphysema. Inflammation and scarring might be expected to increase the bulk of bronchiolar walls. If Cosio's hypothesis is correct, increases in bronchiolar wall should relate to increased inter-alveolar attachment distance. In this study there is no correlation between airway wall area and mean inter-alveolar attachment distance. This suggests that bronchiolar inflammation is not linked with loss of peribronchiolar alveoli.

With respect to over all alveolar loss, Nagai *et al* (1985a and 1985b) found no association between airway inflammation and Lm. Likewise, in this study there are no independent correlations between loss of AWUV and increases in either wall or epithelial area. There is then no evidence from this study which supports the hypothesis that airway inflammation and loss of either peribronchiolar alveoli or AWUV are causally linked.

A further hypothesis that may explain the differential loss of AWUV and peribronchiolar attachments relates to the enzyme inhibitor hypothesis. Work (Janoff 1983) has shown there to be a bronchial mucous protease inhibitor.

Individual variations in the production and/or activity of this anti-protease may play a part in limiting proteolytic peri- and/or bronchiolar damage. Lastly, recent work (Damiano *et al* 1987) has suggested that mast cells secrete a powerful proteolytic enzyme. This being so, smoking induced proliferation of mast cells (Lumsden *et al*) in conjunction with the production of this enzyme in relation to the balance of possible anti-proteases could be important factors. Though whether processes taking place in inner aspects of airways can affect structures within alveolar walls remains to be proven.

5.2.2.1. Correlations with Bronchiolar Calibre

Hogg *et al*, using retrograde catheters, registered increases in airflow resistance in peripheral airways in individuals with chronic obstructive airflow disease. The most common interpretation of this finding attributes this to a reduction in peripheral airway calibre. Although data on airway resistance was not available, data from this study suggests that this is not the case. Indeed most results indicate that airway size may increase with progressive alveolar loss.

Section 5.1.2.3 discussed whether minimum diameter was a good representation of airway size -this being the measurement made by most studies. In this section theoretical lumen area was proposed as a more appropriate measurement. Some of the results used in section 5.1.2.3. are also appropriate to the following discussion.

Minimum diameter was shown to be an insensitive measurement in identifying differences between smokers and non-smokers and cases with and without macroscopic emphysema (cf section 5.1.2.3). Minimum diameter does not correlate with alveolar wall loss whether represented by AWUV or mean

inter-alveolar attachment distance.

Contrastingly, theoretical lumen area is larger in cases with abnormal K_{co} and also regresses with both AWUV and mean inter-alveolar attachment distance -increasing with progressive alveolar loss. These latter results suggest that theoretical lumen area increases as a result of alveolar wall destruction.

This suggestion may appear to contradict the work of Hogg *et al* However, there are arguments that could explain why theoretical lumen area will increase where there is loss of peribronchiolar alveoli and AWUV.

During the respiratory cycle bronchiolar calibre constantly alters, being at its maximum after a complete inspiration. During the expiratory phase the situation can be envisaged where bronchioli within a lung with reduced peribronchiolar alveoli and AWUV -and hence lacking immediate and adjacent support offered by these (cf Ranga and Kleinerman on the dynamic force acting on bronchioles)- decrease in size more rapidly than bronchioles within a lung with no alveolar loss. This hypothesis is supported by the bivariate correlations that both AWUV and mean inter-alveolar attachment distance demonstrate with both closing volume and CV/VC(%), indicating that in the full respiratory manoeuvre required by the single breath nitrogen test there is premature closure of bronchioles. Such premature closure is usually attributed to reduced parenchymal support.

Having reached a smaller size at expiration airways in diseased lungs will require a greater force to both reopen any bronchioles that may have collapsed and to re-establish a "normal" airway calibre for those that have a diminished size. In addition, airways which have larger theoretical lumen areas

are more elliptical (r=0.55) -case 40 excluded. Where two airways have the same cross-sectional lumen area, but differ in configuration, the more elliptical airway will have a greater resistance to airflow as it has a greater surface area to volume ratio. For airflow to be equal in these two airways the elliptical airway has to have a greater cross-sectional lumen area.

Therefore, where airway shape is compromised (and it has been shown that 62% of the variation in airway shape is accounted for by a combination of AWUV and mean inter-alveolar attachment distance) a relatively larger lumen area is required to maintain normal levels of airflow.

It may then be expected that larger theoretical lumen areas may be associated with increases in certain lung volumes (eg TLC and closing volume), in that larger lung volumes may be required to fully open airways with diminished parenchymal support while, on the other hand, airways lacking radial support will close premature causing an increase in closing volume. Theoretical lumen area correlates significantly with both closing volume and CV/VC(%). Where the subgroup of cases with abnormal K_{co} have a significantly higher theoretical lumen area they also have a significantly higher TLC percent predicted. AWUV is significantly lower in this subgroup.

Thus, during different phases of the respiratory cycle it can be envisaged that airway size, in cases with alveolar loss, is smaller at expiration and larger at inspiration than those with no alveolar loss. This does not contradict the work of Hogg *et al* (1968), but places the emphasis on bronchiolar support as this affects both airway size and ellipticality.

There is a mechanistic argument which supports the hypothesis that airways in lungs with alveolar loss are smaller at expiration and larger at

inspiration than those in normal lungs. Newton's second law demonstrates that, where an applied force is divided into a number of channels, the force exerted along each channel is proportional to the force applied and the number of channels. When the inspirational force applied is similar and when there is a reduction in the alveolar network (AWUV) and peribronchiolar alveoli, the force along each airspace wall will be increased. Thus the force applied to bronchioles along each radial attachment, and likewise along each airspace wall, will be greater in those cases with alveolar loss, perhaps explaining the observed increase in theoretical lumen area.

This argument most probably applies only to cases with relatively mild lung disease, because where large emphysematous spaces develop there will be an uneven disappation of forces throughout the lung. There may then be regions within a lung where airways, having collapsed on expiration, may not obtain sufficient force to reopen, whereas other airways with uneven distribution of attachments and surrounding parenchyma will have unbalanced forces holding them open during inspiration. Such mishapen and tortuous airways have been shown to exist in macroscopically emphysematous lungs in both 2 and 3 dimensions by Linhartova *et al* (1971), who also demonstrate that this phenomenon exists along the pathway of individual airways in severe emphysema.

It is noticeable in the AWUV *vs* theoretical lumen area plots that there are three cases that do not adhere to the general relationship. These three cases correspond to the previously identified group of cases which have preferential retention of attachments. This phenomenon has modified the effect of their AWUV loss in retaining a relatively smaller theoretical lumen area than other cases with similar AWUV values.

5.2.2.2. Correlations with Airway Ellipticality

Airway ellipticality, as determined by the ratio of the airway diameters, is highly correlated with both AWUV and mean inter-alveolar attachment distance. This again is in agreement with the findings of Linhartova *et al* (1971), who found airway shape to be related to loss of radial attachments, and Nagai *et al* (1985a) who found it to relate to mean linear intercept.

The correlation obtained by Nagai ($r=-0.45$), between Lm and their index of airway deformity, is directly comparable with that found in this study, as their index of airway deformity, like airway ellipticality, is based upon the ratio of the airway diameters. Mean AWUV has a similar correlation with airway ellipticality ($r=-0.51$).

LF5 AWUV displays a stronger correlation with airway ellipticality ($r=-0.71$) than mean AWUV. Focal areas with decreased AWUV may cause decreased airway stability, thus accounting for this observation. Those cases with a relatively lower LF5 than mean AWUV value have in general more elliptical airways.

The factor identified by Linhartova *et al* (1971) is that immediately peribronchiolar alveoli play an important role in maintaining the patency of bronchioles. This finding is borne out by the correlation between mean inter-alveolar attachment distance and airway ellipticality ($r=0.65$). Therefore, where attachments have progressively larger areas of airway to support these airways become progressively elliptical.

Again, it was noted in the results section that not all the cases followed the same general relationship between AWUV and airway ellipticality. The

cases deviating from this relationship being those that histologically demonstrated preferential retention of peribronchiolar alveoli. From the plot of AWUV *vs* airway ellipticality it is apparent that these cases have more circular airways than other cases with equivalent AWUV values. Thus the retention of peribronchiolar attachments has assisted these airways in maintaining their patency. Likewise in the mean inter-alveolar attachment distance *vs* airway ellipticality plot it can be observed that those cases which have relatively greater AWUV loss lie at the periphery of the relationship, indicating that their relatively greater loss of AWUV has had some effect on airway patency even though there has been a retention of attachments.

It was of interest to assess the relationship between airway ellipticality and both AWUV and mean inter-alveolar attachment distance in the absence of those cases with preferential retention of radial attachments. The correlations with AWUV both improved -r=-0.55 for mean AWUV and r=-0.77 for LF5 AWUV-, similarly the correlation with mean inter-alveolar attachment distance also improved (r=0.70).

Evidence has been presented by previous workers (section 1.5.3.4) showing that airway shape is related to both peribronchiolar attachment loss and loss of adjacent parenchyma. It is thus appropriate to assume a cause-and-effect model and use multiple regression techniques to investigate the relative importance of AWUV and mean inter-alveolar attachment distance in predicting airway ellipticality.

Where mean AWUV is used, both this and mean inter-alveolar attachment distance have significant predictive ability (β weights), with the latter being the more powerful. The combined influence of these two variables accounts for 48% of the observed variation in airway ellipticality.

LF5 AWUV has a stronger bivariate correlation with airway ellipticality than mean AWUV. Similarly, LF5 AWUV has a stronger predictive value than mean AWUV when placed in the regression equation with mean inter-alveolar attachment distance. This better predictive value is also reflected in the higher coefficient of multiple determination obtained with LF5 AWUV and mean inter-alveolar attachment distance -these two variables in combination accounting for 62% of the over all variation in airway ellipticality.

From these analyses it can be concluded that airway ellipticality is highly dependent on the combined influence of the immediate support offered by peribronchiolar alveoli and the over all alveolar network (AWUV), and that where there is preferential retention of the former, against a background of more severe AWUV loss, bronchioles are assisted in retaining a more spherical (and hence cylindrical) configuration.

5.3. CT SCAN CORRELATIONS

The objective of this section was to test for correlations between CT scan derived measurements of lung density and measurements of lung alveolar loss. Two measurements of over all lung alveolar loss were made: the percentage of the mid-sagittal slice involved with macroscopic emphysema and airspace surface area *per* unit lung volume. These measurements were compared with three CT scan measurements of lung density. These CT scan measures are extracted from the EMI distribution of pixel values and are; the modal EMI number, the EMI pixel range from the lowest value to the modal value and lastly, the value which defines the 5th percentile of the EMI distribution.

5.3.1. Correlations with AWUV

With respect to the significant bivariate plots of CT *vs* AWUV, it is apparent that these relationships are linear throughout the complete bivariate range. Notably, there is no alteration in the relationships where cases with macroscopic emphysema are present. The strongest correlations obtained are between AWUV and the EMI value defining the 5th percentile of the distributions. Over all the best correlation is between LF5 AWUV and the 5th percentile value ($r=-0.75$), ie those areas of least density represented by both techniques.

That is, AWUV represents airspace wall surface area *per* unit volume. Decreases in surface area *per* unit volume, as evidenced in this study, can be brought only about by increases in airspace size. These in turn can only result from a loss of airspace walls that is equivalent to a decrease in the density of

lung parenchyma. LF5 AWUV represents those areas within the lung that have the lowest surface area *per* unit volume and hence the lowest density. These areas should correspond to the leftmost tail (ie lowest values) of the EMI pixel distribution. Were LF5 AWUV proportional to mean AWUV in all cases, then the correlations obtained between both mean and LF5 AWUV and other variables would be highly similar. However, it has already been noted that although AWUV has the same (normal) distribution for most cases, there are a subset of cases where LF5 AWUV values are more disparate from their respective mean values. These values have relatively lower positions in the bivariate plot of LF5 AWUV (as opposed to mean AWUV) *vs* the 5th percentile EMI value. This alteration in relative position increases the strength of the correlation.

Thus, both LF5 AWUV and 5th percentile EMI values produce similar results in identifying areas with the least density of airspace walls.

Relative to the 5th percentile EMI value, modal EMI value returns poorer correlations with both mean and LF5 AWUV. Modal EMI has disadvantages in that, by definition, it represents the central location of each EMI pixel distribution. It therefore represents all structures within the scanned lung slice and is less sensitive (than the 5th percentile EMI value) to changes in the leftmost tail; changes that represent a decrease in density of the alveolated portion of the lung. This reduced sensitivity to loss of airspace walls is reflected by the similar correlations modal EMI number has with both mean and LF5 AWUV.

The only insignificant CT parameter is the value defining the EMI pixel range from the lowest to the modal EMI value. Two factors may account for this;

1. As noted above, modal EMI number in representing central location, is less sensitive to changes in the tail of the EMI distribution.

2. The lowest EMI value may be represented by a single pixel value. This value may in a number of cases be unrepresentative.

Summarising, in relation to CT scanning, when one concentrates on the EMI values that correspond to the least dense areas of the lung and when there is a reliable representation of this part of the CT scan distribution, one can obtain an assessment of lung density which corresponds with alveolar loss as measured by AWUV.

As an *addendum* is should be stated that when a group of cases with more progressive emphysema than those of this study are analysed, a larger threshold than the 5th percentile will have to be employed, as this figure in a number of such cases may be rated as -500 EMI units due to the extent of alveolar loss. This would impair the ability of the CT scanning method to accurately quantitate loss above a certain threshold.

5.3.2. CT and Macroscopic Emphysema

CT scanning parameters and macroscopic emphysema have little or no covariance with one another. This is clearly demonstrated by the CT scan *vs* macroscopic emphysema plots. Cases with larger amounts of macroscopic emphysema tend to have low EMI values. These can provide significant differences in mean lung density figures between groups with and without macroscopic emphysema -cf Hayhurst *et al* and Rosenblum *et al*. But, there is no linear relationships between CT scan values and the amount of macroscopic emphysema present. This contrasts sharply with the CT scan *vs*

AWUV plots which are linear throughout their complete bivariate range. Neither is there a threshold value at which macroscopic emphysema is apparent.

Significant correlation values for CT scan *vs* macroscopic emphysema can be generated. These are inappropriate to the bivariate plot of the variables relying as they do on a handful of cases with more than 12% macroscopic emphysema. (This influence –or lack of resistance– to outliers by correlation statistics has already been discussed). As shown in the results section, where these few cases are omitted from the calculation of the correlation coefficients the covariance drops to insignificant levels. This again contrasts with the CT scan *vs* AWUV plots, where, if the same cases are omitted from the calculations, the CT scan *vs* AWUV correlation coefficients remain highly significant. This again, supports the observation made earlier that the CT scan *vs* AWUV plots have relationships that are linear throughout their bivariate range and likewise supports the hypothesis that the observed range of AWUV represents a continuum of airspace loss, a spectrum of loss independent of the presence and amount of macroscopic emphysema.

Conversely, the absence of linear relationships between macroscopic emphysema and CT measurements of lung density indicates that the amount and presence of macroscopic emphysema does not accurately reflect the underlying loss of alveolar walls within a lung.

There is at present insufficient information to present definitive hypotheses that can account for the disparity between what is essentially a microscopic evaluation of emphysema and the amount of macroscopic emphysema. Having noted that there are different patterns in the microscopic loss of airspace walls –ie as evidenced by the cases with different AWUV distributions and also cases that have preferential retention of peribronchiolar attachments– there

may be no single unifying explanation.

5.3.3. Comparisons with other studies

Radiological diagnosis of macroscopic emphysema is very often inaccurate (Thurlbeck 1976 and Thurlbeck *et al* 1970b) even when the extent of emphysema is severe (Thurlbeck and Simon 1978). This study agrees with these findings -when the issue of macroscopic emphysema is concerned- accepting that the predominantly mild emphysema of this study group would be especially difficult to diagnose. The significant correlations between CT scan and AWUV are thus all the more important, especially when one considers the linearity of the scatter plots.

Other workers (Pare *et al* 1982) have found **k** (the exponential factor of pressure volume curves) to be a good predictor of macroscopic emphysema. However, their correlation coefficient is not particularly strong ($r=-0.35$) and the mean percent predicted values of **K** for cases with no and mild macroscopic emphysema are not significantly different. Their relationship though, is with macroscopic emphysema. The evidence of this study indicates that this is not a reliable measure of over all alveolar loss.

Bergin *et al* (1986) by subjectively grading CT scans and relating the results to grades of macroscopic emphysema, concluded that CT scanning can have an important adjunct role in the diagnosis of emphysema. The technique developed in this study uses objective measurements for CT scanning. Such objective criteria usually have greater reproducibility associated with them. This in conjunction with the strong linear correlations obtained, improve the potential role of CT scanning in the diagnosis of emphysema.

In conclusion, CT scanning and measurements of AWUV, handled in an appropriate manner, can produce strong linear correlations that relate independent measurements of lung density to measured loss of airspace walls. These correlations indicate that it is possible to identify and assess early stage alveolar loss within lungs.

5.4. STRUCTURE *VS* FUNCTION ANALYSIS

5.4.1. Analysis of CO diffusing Capacity

Both the total diffusing capacity of the lung (T_{co}) and the rate of uptake per unit lung volume (K_{co}) have very highly significant correlations with AWUV. For most of the discussion of CO diffusion it will be more appropriate to concentrate on the analysis of K_{co} data for the following reasons;

- Both K_{co} and AWUV are expressed *per* unit lung volume. - T_{co} is influenced by maldistribution of ventilation whereas K_{co} is not (Gibson 1984).
- T_{co} is related to alveolar volume (V-[A]) and regresses with patient height.

K_{co}, the diffusing capacity *per* unit volume is strongly associated with the alveolar surface area *per* unit volume available for gas exchange. Alveolar surface area is not the only factor that determines the diffusing capacity of the lung. Having reached the proximal side of alveolar walls, CO molecules must traverse the alveolar epithelium, interstitium, endothelium, blood plasma, red cell membrane and red cell interior before combining chemically with haemoglobin (Gibson). All of these represent barriers to diffusion and all will have their own diffusion coefficients (Weibel 1984). No measure of these parameters has been made in this study and hence their influence on diffusion cannot be commented on, except to say that the high bivariate correlation between K_{co} and LF5 AWUV -which has an associated coefficient of determination of 0.71 (or 71%)- suggest that either AWUV is the major determinant or that these parameters covary with AWUV. Qualitatively, there

appeared to be no evidence of large scale thickening of alveolar walls in the patients of this study group.

The finding that AWUV is the major dependent is in agreement with Gibson (1984), who states that "the probable cause of low K_{co} is a reduction of alveolar surface area because of the breakdown of alveolar walls into larger airspaces".

One advantage that single breath CO assessment of lung diffusion capacity has is that it is limited by diffusion rather than perfusion. This relates to the high affinity that haemoglobin has for CO, plus the low concentration of CO required to test the diffusion capacity of the lung. Thus haemoglobin is not saturated and there is no requirement for replenishment of blood cells. This means that the rate of blood flow has little effect on the diffusing capacity of the lungs (Gibson).

The stronger correlation that K_{co} has with LF5 AWUV is related to the relatively slow process of gaseous diffusion -this being the slowest phase of gas transport within the lungs. As discussed previously, LF5 AWUV represents those areas within the lungs with minimal airspace surface area and therefore represents those cases that have relatively larger airspaces. With the rate of CO uptake being dependent on time any increase in distance that gas diffusion has to work over will lead to a dimunition in the uptake of CO.

Few studies have correlated microscopic assessments of lung alveolar loss with CO diffusing capacity. One study that has is that of Thurlbeck *et al* (1970b). Using equations previously derived (Thurlbeck 1967b) these authors obtained a high correlation between an index of relative alveolar surface area loss (ie percent predicted alveolar surface area standardised to a five litre

lung) with percent predicted CO diffusion capacity. The relationship between these two variables -like that reported for CO *vs* AWUV plots by this study- although containing a degree of scatter, is linear throughout the complete bivariate range. This relationship has not been taken further by the original authors.

This contrasts with comparisons between macroscopic emphysema and diffusion capacity (eg Berend *et al* 1979a, Thurlbeck *et al* 1970b and Pare *et al* 1982). The bivariate plots of macroscopic emphysema *vs* CO uptake obtained by these authors (see Gould *et al* 1987 and Greaves and Colebatch 1986 for the plots of Thurlbeck *et al* and Pare *et al*) are very similar to that obtained in this study. Significant correlations coefficients can be calculated from the data, but the lack of linearity and the obviously high amount of unexplained variation within the plots reveals there to be a poor association between macroscopic assessments of emphysema and CO uptake.

AWUV and sex are the only two important variables in the multiple regression analysis of T_{co}; increasing the coefficient of determination to 58% where LF5 AWUV and sex are the independent variables. Sex as a significant factor may account for many differences, some of which may be related to stature (Gibson). It is therefore difficult to positively identify the precise variation accounted for by this parameter. This is still less than the variance explained by LF5 AWUV alone (R^2=0.71) with respect to K_{co}. That sex is not an important parameter in the multiple regression analysis of K_{co} is understandable in that differences between the sexes are less pronounced for K_{co} than T_{co} (Gibson).

In summary, AWUV accounts for a high proportion of the observed variation in CO uptake (as K_{co}). Measuring AWUV and CO uptake in similar

units increases the explained variation. Contrastingly, macroscopic emphysema, whether measured in relative or absolute amounts, has poor functional correlations with the diffusion capacity of the lungs.

5.4.2. Analysis of $FEV_{1.0}$

Bivariate analysis indicates that -among the morphometric variables- $FEV_{1.0}$ absolute only correlates with mean inter-alveolar attachment distance. This is a relatively weak correlation ($r=-0.35$) that improves to $r=-0.60$ when $FEV_{1.0}$ is expressed as percent predicted. This improvement is due to some of the variation in stature being taken into account. The only other significant (but weak) correlation with $FEV_{1.0}$, as percent predicted, is with bronchiolar shape.

For the multiple regression analysis of $FEV_{1.0}$ data on segmental bronchial calibre was made available. As a result of the significant contribution made by this data, the following discussion pertains to the regression equation obtained with its use.

The significant variables that predict $FEV_{1.0}$ absolute are sex, mean inter-alveolar attachment distance and mean segmental bronchial diameter -in that order. Only mean inter-alveolar attachment distance is a significant predictor of $FEV_{1.0}$ percent predicted (Beta weight=-0.60, $t=-4.01$, $p=0.004$), with multiple regression adding little information above that obtained from the bivariate analyses. The final regression equation for $FEV_{1.0}$ percent predicted being:

$$FEV_{1.0}\%predicted = 163.015 - 0.60(IAAD)$$

where IAAD is mean-inter alveolar attachment distance.

Sex as the best predictor for $FEV_{1.0}$ absolute may reflect differences in stature as females have significantly smaller lung volumes than males of comparable sizes (Gibson). Relative muscularity may be important. Differences in muscularity between the sexes may also be pertinent. After sex mean inter-alveolar attachment distance -which pertains only to bronchioles- has greater predictive strength than mean segmental diameter. The findings of this study are therefore in agreement with that of Hogg *et al* (1968), Zamel *et al* (1976) and Silvers *et al* (1972) who all found peripheral airways to be the major site of increased resistance to airflow in chronic obstructive lung disease. This is in contrast to normal lungs where the main site of resistance to airflow resides with the central airways (Macklem and Mead 1967) where $FEV_{1.0}$ correlates highly with bronchial calibre (Osmanliev *et al* 1982).

As discussed previously, mean inter-alveolar attachment distance reflects the relative radial support offered to bronchioles by the peribronchiolar alveoli. Hughes *et al* (1974) opined that "parenchyma confers a stiffness upon intrapulmonary airways during expiratory flow by virtue of tissue attachments". Where there is a loss of radial support bronchiolar patency is compromised. Airways that suffer a loss of radial support will have accelerated decrease of bronchiolar size on expiration ultimately leading to premature collapse of bronchioles. In addition to the multiple and bivariate analysis of $FEV_{1.0}$ the correlations between mean inter-alveolar attachment distance and bronchiolar ellipticality, CV/VC(%) and the slope of phase three (in conjunction with the aforementioned studies) support this hypothesis.

5.4.3. Analysis of the Single Breath Nitrogen Test

The bivariate analysis of closing volume and CV/VC(%) reveals that AWUV,

theoretical lumen area, mean inter-alveolar attachment distance and bronchiolar ellipticality all have significant correlations. As these variables are to some extent colinear it is not surprising that where one or more are highly associated with a given functional variable, others also return significant correlations. It is noticeable that only two (mean inter-alveolar attachment distance and bronchiolar ellipticality) have notably stronger correlations with CV/VC(%) -which has less inherent variation than closing volume itself. It is perhaps predictable that variables that exhibit this pattern are functionally related with closing volume as opposed to being colinear with other morphometric variables. The multiple regression analysis of closing volume supports this hypothesis.

Little additional information was obtained from multiple regression of closing volume, only bronchiolar ellipticality was identified as a significant predictor. More information was obtained from the multiple regression analysis of CV/VC(%). The standardisation of closing volume as a ratio of vital capacity renders closing volume independent of both height and sex, regressing only with age (Buist and Ross 1973).

Bronchiolar ellipticality and mean inter-alveolar attachment distance are significant predictors of CV/VC(%) and account for 46% of its variation. Closing volume -which corresponds to phase IV of the single breath nitrogen test- is attributable to the closure of small airways (Netter *et al* 1979). Multiple regression analysis indicates that where airways are elliptical and lack radial support they will close earlier or prematurely.

That mean inter-alveolar attachment is a significant predictor is in agreement with the belief that bronchiolar integrity is dependent on the support offered by the surrounding alveolar walls. In addition, it is arguable

that opposing sides of more elliptical airways are more likely to touch than in spherical airways. This is perhaps too simplistic an interpretation of bronchiolar ellipticality as a significant predictor of CV/VC(%). Bronchiolar ellipticality is itself determined by other parameters and may vary continuously throughout the respiratory cycle.

Mean inter-alveolar attachment distance and AWUV have already been identified as significant determinants of bronchiolar ellipticality. Others may be the elastin and/or the collagen content of alveolar walls. Thurlbeck (1983) has suggested that there is a loss of elastin prior to destruction of alveolar walls, while Damiano *et al* (1986) report a correlation between Lm and the amount of neutrophil derived elastase in contact with interstitial elastin. Additionally, elastin repair may be impeded in smokers (Osman *et al* 1982 and Laurent *et al* 1983). Hence, AWUV and mean inter-alveolar attachment distance may reflect the quantity of alveolar support to bronchioles, but not necessarily the quality. Bronchiolar ellipticality as a significant variable may then represent the influence of other parameters, the effects of which are related to premature closure of airways.

In the light of the regression equations derived by Buist and Ross (1973a) -where CV/VC(%) regresses with age- it is perhaps surprising that this parameter was not identified as a significant predictor in this study. Two reasons may account for this. Firstly, the cases analysed in this study comprise a restricted age range and secondly, Buist and Ross used only non-smoking individuals. As smoking correlates with the frequency of abnormalities in closing volume tests (Buist and Ross 1973b) the smoking habits of individuals in this study may have obscured any relationship with age.

Mean inter-alveolar attachment distance is the only morphological variable against which the slope of phase III regresses. The slope of phase III is a sensitive measure of evenness of ventilation (Gibson). Therefore, as well as determining the lung volume at which bronchioles close (along with bronchiolar ellipticality), loss of immediate peribronchiolar support -as represented by increasing mean inter-alveolar attachment distance- is also a significant factor in determining homogeneity of ventilation.

5.5. RELATIONSHIPS FOR NORMAL STRUCTURE

5.5.1. AWUV: Relationships with Stature and TLC

This study contends that the observed range of AWUV values represents a spectrum of alveolar loss. Subdividing the cases on the basis of their K_{co} data reveals that increases in total lung capacity (TLC) correlate with decreases in AWUV for those cases with abnormal K_{co}. In contrast, AWUV is not related to TLC in the normal K_{co} subgroup and is not related to either height or body surface area for both K_{co} subgroups and for the study group as a whole.

The latter finding indicates that AWUV *per se* is nor related to body stature or lung volume. This finding is supported by the findings of other workers. Thurlbeck (1967b) found Lm to be independent of body size in non-emphysematous lungs. This suggested that alveolar size was likewise independent of stature. Angus and Thurlbeck (1972) in a follow-up study confirmed this hypothesis finding total alveolar number to be related to height. The hypothesis put forward by Hansen *et al* (1975b) is that alveolar multiplication is a space filling phenomenon. Larger lungs having a greater volume to fill will therefore have more alveoli. Thus the opinion that alveolar number is constant at around 300 millions -and that increases in alveolar surface area are brought about by increases in alveolar size as opposed to alveolar number (Weibel 1963 and Dunnill 1962a)- is altered (Dunnill 1982a). Current opinion is that individuals of larger stature have larger acinar units with more, but not necessarily larger, alveoli.

As the mean size of peripheral airspaces determine alveolar surface area to volume ratio (AWUV) the relationship between AWUV and TLC -observed for

the individuals with abnormal K_{co} transfer values- is an acquired one with decreases in AWUV being associated with increases in TLC. This result has added importance as it has been observed in cases with relatively early stage lung disease. This statement is in agreement with the editorial comments of Greaves and Colebatch (1986) who consider that early parenchymal loss may be detected by an "asymptomatic rise in lung distensibility". This opinion arises from their review of a number of studies (where in some cases additional data analysis is performed) and is based upon the findings that decreases in elastic recoil pressure correlate better with lung function tests than the presence or severity of (macroscopic) emphysema and also corresponded to increases in lung distensibility (TLC and FRC).

5.5.2. Airway Size and Body Size

No measures of bronchiolar size correlates with lung volume, body height or body surface area. This is in agreement with the findings of Matsuba and Thurlbeck (1972), accepting that their conclusions relate to small airways. It may appear to contradict the findings of Weibel (1963) and Horsfield and Cummings (1968) who present equations that link airway sizes throughout the tracheobronchial tree. However, these equations are based upon meticulous studies of a very few cases. Therefore, although these equations describe the relationship between sizes throughout the lung they may not pertain to the population as a whole, but vary from individual to individual.

5.5.3. Airway Density and Body Size

The plots of airway density against the two measures of stature and lung volume suggest there are two distinct groups within the sample. The smaller

of these groups having an airway density twice that of the larger group.

Analysing the data for all cases produces significant regressions for TLC, height and body surface area. Without exception all these equations improve when the sample is divided into two subgroups. The equation obtained between airway density and height, for all cases, is very similar to that obtained by Matsuba and Thurlbeck (1972). These two equations are:

Airway Density= 2.83 - 1.3(hgt)

(present study)

Airway Density= 3.24 - 1.5(hgt)

(Matsuba and Thurlbeck)

Where height is in metres.

The suggestion is made in this thesis that there may be a dichotomy within the population with respect to airway density and acinar size. Matsuba and Thurlbeck do not make this suggestion, but if one views their plot it is possible that two of their eighteen cases lie off the rather tight line of the others (the corresponding figure for this study is 5 out of 28). This may be due to natural variation, but these point do lie off the line in a manner similar to that of the smaller subgroup identified in this study. The observation that the smaller subgroup has a relative airway density twice that of the larger group suggests that the individuals of this group have an extra generation of airways. That this doubles airway density is in line with symmetrical dichotomy which occurs on division of peripheral airways and suggests that there may be variations in the development of airways in the lung. The source of this variation may be genetic, related to diet, disease or some other factor or

factors.

5.6. SUMMARY OF FINDINGS

- Paraffin embedding causes variable shrinkage and compression. This affects airway size and shape and cannot be controlled for adequately by linear shrinkage factors.

- Glycol methacrylate has negligible processing artefact.

- The construction of airway ellipticality cumulative frequency distributions allows the most elliptical airways (30%) to be reliably excluded on an objective basis.

- England Finder graticules provide a quick and inexpensive method for randomly sampling alveolated areas of the lung.

- The IBAS 2 image analyser provides a quick, accurate and reproducible interactive method for measuring airspace surface area *per* unit volume. This technique also allows individual distributions to be analysed.

- Differences between surgical and autopsy based studies limit the number of possible inter-series comparisons.

- Allowing for differences in quantitation, the incidence of macroscopic emphysema witnessed in this study is comparable to that of other surgical series.

- AWUV data of this study are similar to Lm-derived AWUV data of other comparable studies.

- Bronchiolar size and density results obtained in this study lie within the ranges previously reported in the literature.

- Selecting all bronchioles as opposed to small airways ie bronchioles smaller than 2mm internal diameter, is a better sampling strategy as airway size is affected by both disease and tissue processing. These will influence the accurate sampling of only small airways.

- Minimum diameter is not an accurate representation of airway size. Theoretical lumen area is a better representation of airway size.

- Theoretical lumen area varies with loss of alveolar walls and is greater in the group of patients with abnormal gas diffusion. Neither of these are true for minimum diameter.

- Theoretical lumen area circumvents the problem of airway tone in surgical specimens allowing some comparisons to be made between autopsy and surgical studies.

- Microscopic emphysema (AWUV) has a poor relationship with macroscopic emphysema. (The AWUV range found for cases with no macroscopic emphysema is similar to that found by other studies.

- Macroscopic emphysema is an insensitive recognition of loss of airspace surface area -75% loss being required for reliable macroscopic identification. The range of AWUV values representing a spectrum of alveolar wall loss.

- Different patterns of microscopic emphysema exist. The one observed in this study involves preferential retention of radial alveolar attachments. Other patterns may exist.

- Neither loss of radial attachments nor AWUV are independently related to increases in bronchiolar wall or epithelium.

- AWUV is not related to body stature.

- Bronchiolar size is not related to body stature.

- Decreases in AWUV are associated with mild increases in total lung capacity.

- Loss of AWUV and bronchiolar ellipticality both affect bronchiolar ellipticality.

- Preferential retention of attachment affects modifies the affect of more severe AWUV loss helping airways to retain their ellipticality.

- CT scan assessment of lung density has strong linear relationships with AWUV, but none with macroscopic emphysema. This suggests that the range of AWUV loss has a measurable effect on lung density and reinforces the finding that macroscopic emphysema is an insensitive measure of at least early microscopic loss.

- Early emphysema may be identified in life by CT scanning.

- AWUV has strong linear relationships with the diffusion capacity of the lung. 71% of the variation in diffusion capacity can be explained by AWUV.

- Approximately, 50% of the variation in $FEV_{1.0}$ is accounted for by three variables. Of the bronchiolar variables only mean inter-alveolar attachment distance is a significant predictor of $FEV_{1.0}$. Other predictors are sex and mean segmental bronchiolar size.

- 46% of the variation in closing volume/vital capacity (%) is explained by bronchiolar shape and mean inter-alveolar attachment distance.

- Only mean inter-alveolar attachment distance correlates with alterations in the slope of phase III of the single breath nitrogen test. (This reflecting inhomogeneity of ventilation).

- There may exist a dichotomy within the population with respect to airway density and thus acinar size, with a subgroup of individuals having twice as many acinar units.

REFERENCES

Aherne WA, Dunnill MS. (1982) Morphometry. Arnold, London.

American Thoracic Society. (1959) Report of Committee on preparation of human lungs for macroscopic and microscopic emphysema. Am Rev Respir Dis 80: Suppl 114-117.

American Thoracic Society. (1962) Chronic bronchitis, asthma and pulmonary emphysema. Am Rev Respir Dis 85: 762-768.

Anderson WF, Anderson AE, Hernandez JA, Foraker AG. (1964) Topography of aging and emphysematous lungs. Am Rev Respir Dis 90: 411-423.

Anderson AE and Foraker AG. (1968) Relative dimensions of bronchioles and parenchymal spaces in lungs from normal subjects and emphysematous patients. Am J Med 32: 218-226.

Angus GE, Thurlbeck WM. (1972) Number of alveoli in human lung. J Appl Physiol 32: 483-485.

Baker JR. (1966) Cytological technique. 5th Ed Methuen London.

Berend N. (1981) Lobar distribution of bronchiolar inflammation in emphysema. Am Rev Respir Dis 124: 218-220.

Berend N, Woolcock AJ, Martin GE. (1979a) Correlation between the function and structure of the lung in smokers. Am Rev Respir Dis 119: 695-705.

Berend N, Woolcock AJ, Martin GE. (1979b) Relationship between bronchial and arterial diameter in normal lungs. Thorax 34: 354-358.

Berend N, Wright JL, Thurlbeck WM, Martin GE, Woolcock JA. (1981) Small airways disease: Reproducibility of measurements and correlation with lung function. Chest 79: 263-268.

Bergin C, Muller N, Nichols DM, Lillington G, Hogg JC, Mullen B, Grymaloski MR, Osborne S and Pare PD. (1986) The diagnosis of emphysema. Am Rev Respir Dis 133: 541-546.

Bignon J, Andre-Bougaran J and Brouet G. (1970) Parenchymal, bronchiolar and bronchial measurements in centribulobular emphysema. Thorax 25: 556-567.

Bignon J, Khoury F, Andre J, Brouet G. (1969) Morphometric study in chronic obstructive broncho-pulmonary disease. Am Rev Respir Dis 99: 669-695.

Billiet L, Baiser W, Naedts JP. (1963) Effect de la taille, du sexe et de l'age sur le capacite de diffusion pulmonaire de l'adult normal. J Physiol 55: 199-200.

Boyden EA. (1949) A synthesis of the prevailing patterns of the bronchopulmonary segments in the light of their variations. Dis Chest 15: 657-668.

Boyden EA, Hartmann J. (1946) An analysis of variation in the bronchopulmonary segments of the left upper lobes of fifty lungs. Am J Anat 79: 321-360.

Boyden EA and Scannell JG. (1948) An analysis of variations in the bronchovascular pattern of the right upper lobe of fifty lungs. Am J

Anat 82: 27-72.

Brewer DB. (1968) The form and nomenclature of the air-spaces of the human lung. In: Form and Function in the Human Lung. G Cumming, LB Hunt (eds). E & S Livingstone Ltd., Edinburgh and London.

Bucher U, Reid L. (1961) Development of the intrasegmental bronchial tree: The pattern of branching and development of cartilage at various stages of intra-uterine life. Thorax 16: 207-218.

Buist AS and Ross BB. (1973a) Predicted values for closing volumes using a modified single breath nitrogen test. Am Rev Respir Dis 107: 744-752.

Buist AS and Ross BB. (1973b) Quantitative analysis of the alveolar plateau in the diagnosis of early airway obstruction. Am Rev Respir Dis 108: 1078-1087.

Burrows B. (1981) An overview of obstructive lung diseases. In: Medical Clinics of North America 65 (3). Saunders, Philadephia.

Campbell EJ, White, RR, Senior RM and Rodriguez RJ. (1979) Receptor-mediated binding and internalisation of leukocyte elastase by alveolar macrophage *in vitro*. J Clin Invest 64: 824-833.

Campbell H and Tambeieff SA. (1952) Calculation of internal surface area. Nature 170: 117.

Campbell IA. (1983) Smoking. In: Recent Advances in Respiratory Medicine. Eds Flenley DC and Petty TL. Churchill Livingston,

Edinburgh.

Carlile A, Edwards C. (1983) Structural variation in the named bronchi of the left lung. A morphometric study. Brit J Dis Chest 77: 344-348.

Carp H, Miller F, Hoidal JR and Janoff A. (1982) Potential mechanism of emphysema: - proteinase inhibitor recovered from lungs of cigarette smokers contains oxidased methionine and has decreased elastase inhibitory capacity. Proc Natl Acad Sci 79: 2041-2045.

Carson FL, Martin JH and Lynn JA. (1973) Formalin fixation for electron microscopy. A re-evaluation. Am J Clin Path 59: 365-373.

Chalkley BW. (1943) Method for the quantitative morphologic analysis of tissue. J Natl Canc Inst 4: 47-53.

Churg A, Wright JL, Wiggs B, Pare PD, Lazar N. (1985) Small airways disease and mineral dust exposure. Am Rev Respir Dis 131: 139-143.

Ciba Guest Symposium. (1959) Terminology, definitions and classification of chronic pulmonary emphysema. Thorax 14: 286-299.

Cosio MG, Ghezzo H, Hogg JC, Corbin R, Loveland M, Dosman J, Mackleman PT. (1977) The relations between structural changes in small airways and pulmonary function tests. N Eng J Med 298: 1277-1281.

Cosio MG, Hale KA and Niewoehner DE. (1980) Morphological and

morphometric effects of prolonged cigarette smoking on the small airways. Am Rev Respir Dis 122: 265-271.

Cotes JE. (1975) Lung function: Assessment and applications in medicine. 3rd Edition. Blackwell Scientific Publications, Oxford, London, Edinburgh.

Cotes JF and Hall AM. (1970) The transfer factor for the lung, normal values in adults (1970) In: Normal values for respiratory function in man. ed Arcangelli P, Torino, Panminerva Medica pp 327-343.

Cromie JB. (1961) Correlation of anatomic pulmonary emphysema and right ventricular hypertrophy. Am Rev Respir Dis 84: 657-662.

Dalquen P, Oberholzer M. (1983) Correlations between functional and morphometrical parameters in chronic obstructive lung disease. In: Pulmonary Diseases. Muller KM (ed). Springer-Verlag, Berlin, Neidelberg, New York, Tokyo.

Damiano VV, Schulman E, Kucich U and Weinbaum G. (1987) Elastase in mast cells. Am Rev Respir Dis 135: A290.

Damiano VV, Tsang A, Kucich U, Abrams WR, Rosenbloom J, Kimbel P, Fallchnejad M and Weinbaum G. (1986) Immunolocalisation of elastase in human emphysematous lungs. J Clin INvest 78: 482-493.

Dayman H. Mechanics of airflow in health and emphysema. (1951) J Clin Invest 30: 1175-1190.

Delesse A. (1970) Procede mechanique pour determines la composition des roches. CR Acad Sci (Paris) 25: 544.

Deppiere A, Bignon J, Lebeau A, Brouet G. (1972) Quantitative study of parenchymal and small conductive airways in chronic nonspecific lung disease. Chest 62: 699-708.

Disbrey BD and Rack JH. (1970) Histological laboratory methods. E & S Livingstone, Edinburgh and London.

Drury RAB and Wallington EA (1967) Carleton's histological technique. 4th ed, Oxford University Press, London.

Dubois D and Dubois EF. (1916) Clinical calorimetry. X A formula to estimate the approximate body surface area if height and weight be known. Arch Intern Med 17: 863-871.

Duguid JB, Lambert MW. (1964) The pathogenesis of coal miner's pneumoconiosis. J Path Bact 88: 389-403.

Duguid JB, Young A, Cauna D, Lambert MW. (1964) The internal surface area of the lung in emphysema. J Path Bact 88: 405-421.

Dunnill MS. (1962a) Postnatal growth of the lung. Thorax 17: 329-333.

Dunnill MS. (1962b) Quantitative methods in the study of pulmonary pathology. Thorax 17: 320-326.

Dunnill MS. (1964) Evaluation of a simple method of sampling the lung for quantitative histological analysis. Thorax 19: 443-448.

Dunnill MS. (1982a) The problem of lung growth (Editorial). Thorax 37: 561-563.

Dunnill MS. (1982b) Emphysema. In: Pulmonary Pathology, Churchill Livingston, Edinburgh.

Dunnill MS, Massarella GR, Anderson JA. (1969) A comparison of the quantitative anatomy of the bronchi in normal subjects in status asthmaticus, in chronic bronchitis and in emphysema. Thorax 24: 176-179.

Fernie JM. (1985) Morphometry of muscular pulmonary arteries with special reference to the effects of age and smoking. PhD Thesis, University of Edinburgh.

Ferris BG, Anderson DO and Zickmantel R. (1965) Prediction values for screening tests of pulmonary function. Am Rev Respir Dis 91: 252-261.

Fleege JC, Baak JPA and Smeulders AWM. (1986) Reproducibility of morphometric assessment with a graphic tablet. Analysing system parameters. Fourth International Symposium on Morphometry in Morphological Diagnosis, London.

Fleege JC, Baak JPA, Smeulders AWM. (1987) Reproducibility of morphometric assessment with a graphic tablet. I. Analysing measurement system parameters. (in press)

Flenley DC and Warren PM. (1980) Chronic bronchitis and emphysema, Blue bloaters and pink puffers. In: Recent Advances in Respiratory Medicine 2. ed Flenley DC, Churchill Livingston, Edinburgh

Fletcher C, Peto R, Tinker C and Speizer FE. (1976) The natural history of chronic bronchitis and emphysema. Oxford University

Press, Oxford.

Fraser RG. (1961) Measurement of the calibre of human bronchi in three phases of respiration by cinebronchography. J Canad Assoc Radiol 12: 102-112.

Frolov YS, Maling DH. (1969) The accuracy of area measurement by point counting techniques. Cart J 6: 21-35.

Fulmer JD, Roberts WC, Von Gal ER and Crystal RG. (1977) Small airways in idiopathic fibrosis. J Clin Invest 60: 595-610.

Gibson GJ. (1984) Clinical tests of respiratory function. MacMillan Press, London.

Gladman T, Woodhead JH. (1960) The accuracy of point counting in metallographic investigations. J Iron Steel Inst (February 1960): 189-193.

Glagolev AA. (1933) On the geometrical methods of quantitative mineralogic analysis of rocks. Transactions of the Institute of Economic Mineralogy and Metallurgy, Moscow pp59.

Glagolev AA. (1934) Quantitative analysis with the microscope by the "Point Method". Engineering and Mining Journal 135: 399.

Goodard PR, Micholson EM, Watt I. (1982) Computed tomography in pulmonary emphysema. Clin Radiol 33: 379-387.

Gough J. (1952) Discussion on the diagnosis of pulmonary emphysema. Proc Roy Soc Med 45: 576-577.

Gough J, Wentworth JE. (1949) Use of thin sections of entire organs in morbid anatomic studies. J Roy Micros Soc 69: 231-235.

Gould GA, MacNee WM, McLean A, Warren PM, Redpath A, Best JJK, Lamb D, Flenley DC. (1987) CT measurements of lung density in life can quantitate distal air space enlargement - an essential defining feature of human emphysema. Am Rev Respir Dis (in press).

Greaves IA, Colebatch HJH. (1986) Observations on the pathogenesis of chronic airflow obstruction in smokers: implications for the detection of 'early' lung disease. Thorax 41: 81-87.

Green M, Mead J, Turner JM. (1974) Variability of maximum expiratory flow volume curves. J Appl Physiol 37: 67-74.

Gross P, Pfitzer EA, Tolker E, Babyak M, Kaschak M. (1965) Experimental emphysema: its production with papain in normal and silicotic rats. Arch Environ Health 11: 50-58.

Grumby G, Soderholm B. (1963) Spirometric studies in normal subjects. III. Static lung volumes and maximum voluntary ventilation in adults with a note on physical fitness. Acta Med Scand 173: 199-206.

Hahn HL, Graf PD, Nadel JA. (1976) Effect of vagal tone on airway diameters and on lung volume in anaesthetised dogs. J Appl Phys 41(4): 581-589.

Hale FC, Olsen CR, Mickey MR. (1968) Measurement of bronchial wall components. Am Rev Respir Dis 98: 978-987.

Hally D. (1964) A counting method for measuring the volumes of

tissue components in microscopical sections. Quart J Micro Sci 105: 503-517.

Hanna GM, Daniels CL, Berand N. (1985) The relationship between lung size and airway size. Br J Dis Chest 79: 183-188.

Hansen JE, Ampaya AP, Bryant GH, Nairn JJ. (1975) Branching pattern of airways and air spaces of a single human terminal bronchiole. J Appl Physiol 38: 983-989.

Hansen JE, Ampaya EP. (1975) Human air space shapes, sizes, areas and volumes. J Appl Physiol 38: 990-995.

Hartwig F, Dearing BE. (1970) Explanatory data analysis. In: Series Quantitative applications in the Social Sciences. Sage Publications, Beverley Hills, USA.

Hasleton PS. (1972) The internal surface area of the adult human lung. J Anat 112: 391-400.

Hayhurst MD, MacNee WM, Wright D, McLean A, Lamb D, Flenley DC. (1984). The diagnosis of pulmonary emphysema by CT scanning. Lancet ii: 320-322.

Hayward J, Reid L. (1952) Observations on the anatomy of the intrasegmental bronchial tree. Thorax 7: 89-97.

Heard BE. (1958) A pathological study of emphysema of the lungs with chronic bronchitis. Thorax 13: 136-149.

Heard BE. (1960) Pathology of pulmonary emphysema. Am Rev Respir Dis 82: 792-799.

Heard BE. (1969) The pathology of chronic bronchitis and emphysema. J & A Churchill Ltd, London.

Henning A. (1959) A critical survey of volume and surface measurement in microscopy. Zeiss Werkzeitschriff, no. 30, Carl Zeiss, Germany.

Heppleston AG, Leopold JG. (1961) Chronic pulmonary emphysema. Am J Med 31: 279-291.

Hogg JC. (1982) The respiratory airways. In: Pulmonary Medicine (2nd ed) eds Guenter AC and Welch MH.

Hogg JC, Macklem PT, Thurlbeck WM. (1968) Site and nature of airway obstruction in chronic obstructive lung disease. N Eng J Med 278: 1355-1360.

Horsfield K. (1974) The relation between structure and function in the airways of the lung. Brit J Dis Chest 68: 145-160.

Horsfield K. (1978) Quantitative morphology and structure: Functional correlations in the lung. In: The Lung. Int Acad Pathol Monograph 19, eds Thurlbeck WM, Abell MR, Williams and Wilkins, Baltimore, USA.

Horsfield K. (1981) Smoking and the lung. In: Scientific Foundations of Respiratory Medicine, eds Scadding JG and Cumming G. London, Heinemann Medical.

Horsfield K, Cumming G. (1968) Morphology of the bronchial tree in man. J Appl Physiol 24: 373-383.

Hughes JMB, Hoppin FG, Mead J. (1971) Effect of lung inflation on bronchial length and diameter in excised lungs. J Appl Phys 32(1):25-35.

Hughes JMB, Jones HA, Wilson AG, Grant BJB, Pride NB. (1974) Stability of intrapulmonary bronchial dimensions during expiratory flow in excised lungs. J Appl Physiol 37: 684-694.

Idell S, Cohen AB. (1983) The protease-inhibitor hypothesis of emphysema. In: Recent Advances in Respiratory Medicine, eds. Flenley DC and Petty TL, Churchill Livingston, Edinburgh.

James AL, Moreno RH, Hogg JC and Pare PD. (1987) Morphometric comparison and calculation of muscle shortening in relaxed and contracted airways. Am Rev Prespir Dis 135(4):A270.

Janoff A. (1983) Biochemical links between cigarette smoking and pulmonary emphysem. J Appl Physiol 55: 285-293.

Janoff A. (1985) Elastases and emphysema. Am Rev Respir Dis 132: 417-433.

Janoff A, Carp H. (1977) Possible mechanism of emphysema in cigarette smokers: Cigarette smoke condensed supresses proteinase inhibitors in vitro. Am Rev Respir Dis 116: 65-72.

Jesseph JE, Meredino KA. (1957) The dimensional interrelationships of the major components of the human tracheobronchial tree. Surg Gynecol Obstet 105: 210-214.

Jones RS, Meade F. (1961) A theoretical and experimental analysis of anomalies in the estimation of pulmonary diffusion capacity by the single breath method. Quart J Exp Physiol 46: 131-143.

Karlinsky JB, Snider GC. (1978) Animal models of emphysema. Am Rev Respir Dis 117: 1109-1134.

Knudson RJ, Slabin RC, Lebowitz MD, Burrows B. (1976) The maximum expiratory flow volume curve. Normal standards, variability and effects of age. Am Rev Respir Dis 113: 587-600.

Kory RC, Callahan R, Boren HG, Syner JC. (1961) The veterans administration - Army cooperative study of pulmonary function. I. Clinical Spirometry in normal man. Am J Med 1961: 243-258.

Kunze M. (1983) Smoking trends in Europe. Eur J Respir Dis 64 Suppl 126: 103-106.

Langston C, Waszkiewicz E, Thurlbeck WM. (1979) A simple method for the representative sampling of lungs of diverse size. Thorax 34: 527-530.

Laurell CB, Eriksson S. (1963) The electrophoretic A-1-globulin pattern of serum in alpha-1-antitrysin deficiency. Scand J Clin Lab Invest 15: 131-140.

Laurent P, Janoff A, Herbert MK. (1983) Cigarette smoke blocks cross-linking of elastin in vitro. Am Rev Respir Dis 127: 189-192.

Lefcoe N, Ashley MJ, Poderson LL, Keays JJ. (1983) The health risks of passive smoking - the growing case of control measures in

enclosed environments. Chest 84: 90-95.

Leopold JG, Gough J. (1957) The centrilobuloar form of hypertrophic emphysema and its relation to chronic bronchitis. Thorax 12: 219-235.

Linhartova A, Anderson AE. (1983) Small airways in severe PLE: Mural thickening and premature close. Am Rev Respir Dis 127: 42-45.

Linhartova A, Anderson AE, Foraker AG. (1971) Radial traction and bronchiolar obstruction in pulmonary emphysema. Arch Pathol 92: 384-391.

Linhartova A, Anderson AE, Foraker AG. (1973) Nonrespiratory bronchiolar deformities. Arch Pathol 95: 45-48.

Linhartova A, Anderson AE, Foraker AG. (1974) Topology of nonrespiratory bronchioles of normal and emphysematous lungs. Hum Pathol 5: 729-735.

Linhartova A, Anderson AE, Foraker AG. (1977) Further observations on luminal deformity and stenosis of nonrespiratory bronchioles in pulmonary emphysema. Thorax 32: 53-59.

Linhartova A, Anderson AE, Foraker AG. (1982) Affixment arrangements of peribronchiolar alveoli in normal and emphysematous lungs. Arch Pathol Lab Med 106: 499-502.

Loeb LA, Ernster VL, Warner KE, Abbotts J, Laszio J. (1984) Smoking and lung cancer: an overview. Cancer Res 44: 5940-5958.

Joyce Loebl, J. (1985) Image Analysis: Principles and Practice.

Joyce Loebl, Gateshead, England.

Lucey EC. (1983) Experimental emphysema. In: Clinics in Chest Medicine, ed Snider GL, WB Saunders Co, Philadelphia.

Lumsden AB, McLean A, Lamb D. (1984) Goblet and Clara cells of human distal airways: Evidence for smoking induced changes in their numbers. Thorax 39: 844-849.

Macklem PT, Mead J. (1967) Resistance of central and peripheral airways measured by a retrograde cathetor. J Appl Physiol 22: 395-401.

Matsuba K, Thurlbeck WM. (1971) The number and dimensions of small airways in nonemphysematous lungs. Am Rev Respir Dis 104: 516-528.

Matsuba K, Thurlbeck WM. (1972) The number and dimensions of small airways in emphysematous lungs. Am J Pathol 67: 265-276.

Matsuba K, Thurlbeck WM. (1973) Disease of the small airways in chronic bronchitis. Am Rev Respir Dis 107: 552-558.

Mead J. (1980) Dysanapsis in normal lungs assessed by the relationship between maximal flow, static record and vital capacity. Am Rev Respir Dis 121: 339-342.

Mitchell RS, Stanford RE, Johnson JM, Silvers GW, Dart G, George MS. (1976) The morphologic features of the bronchi, bronchioles, and alveoli in chronic airway obstruction. A clinicopathological study. Am Rev Respir Dise 114: 137-145.

Nagai A, West WM, Paul JL, Thurbeck WM. (1985a) The National

Institute of Health Positive Pressure Breath Trial: Pathology Studies. I. Interrelationships between morphologic lesions. Am Rev Respir Dis 132: 937-945.

Nagai A, West WM, Thurlbeck WM. (1985a) The National Institutes of Health Intermittent Positive-Pressure Breathing Trial: Pathology Studies. II. Correlations between morphologic findings, clinical findings and evidence of expiratory air-flow obstruction. Am Rev Respir Dis 132: 946-953.

Netter FH, Altose MD, Cherniack NS, Lahiri S, Heinemann HO. (1979) Respiratory System: Physiology. In: The Ciba Collection of Medical Illustrations, Ciba, New Jersey, USA.

Niewoehner DE, Kleinerman J. (1974) Morphologic basis of pulmonary resistance in the human lung and effects of aging. J Appl Physiol 36: 412.

Niewoehner DE, Kleinerman J, Rice DB. (1974) Pathologic changes in the peripheral airways of young cigarette smokers. New Eng J Med 291: 755-758.

Ogilvie CM, Forster RE, Blakemore WS, Morton JW. (1957) A standardised breath holding technique for the clinical measurement of the diffusing capacity of the lung for carbon monoxide.

Oosthuyzen EJ. (1980) An elementary introduction to image analysis - A new field of interest at the National Institute of Metallurgy. Reprint No 2058, National Institute of Metallurgy, Randburg, South Africa.

Osman M, Canter J, Roffman S, Turino GM, Mandl I. (1982) Tobacco smoke exposure retards elastin repair in experimental emphysema. Am Rev Respir Dis 125(2): 213.

Osmanliev D, Bowley N, Hunter DM, Pride NB. (1982) Relation between tracheal size and FEV1.0 in young men. Am Rev Respir Dis 126: 179-182.

Pare PD, Brooks, LA, Bates J, Lawson LM, Nelems JMB, Wright JL, Hogg JC. (1982) Experimental analysis of the lung pressure-volume curve as a predictor of pulmonary emphysema. Am Rev Respir Dis 126:54-61.

Pare PD, Brooks A, Coppin A, Wright JL, Kennedy S, Dahlby R, Mink S, Hogg JC. (1985) Density dependance of maximal expiratory flow and its correlation with small airway disease in smokers. Am Rev Respir Dis 131: 521-526.

Parker H, Horsfield K, Cumming G. (1971) Morphology of distal airways in the human lung. J Appl Physiol 31: 386-391.

Peach H, Shah D, Morris RW. (1986) Validity of smokers information about present and past cigarette brands - implications for studies of the effects of falling tar yields of cigarettes on health. Thorax 41: 203-207.

Peto R, Speizer FE, Moore CF, Fletcher CM, Tinker CM, Higgins ITT, Gray RG, Richards SM, Gilliland J, Norman-Smith B. (1983) The relevance in adults of airflow obstruction, but not of mucous hypersecretion to mortality from chronic lung disease. Am Rev Respir Dis 128: 491-500.

Petty TL, Silvers WG, Stanford RE. (1981) Functional correlations with mild and moderate emphysema in excised human lungs. Am Rev Respir Dis 124: 700-704.

Petty TL, Silvers, WG, Stanford PE. (1982) Small airway dimension and size distribution in human lungs with an increased closing capacity. Am Rev Respir Dis 125: 535-539.

Petty TL, Silvers GW, Stanford RE. (1984) Small airways disease is associated with elastic recoil changes in excised human lungs. Am Rev Respir Dis 130: 42-45.

Petty TL, Silvers WG, Stanford RE. (1986) Radial traction and small airways disease in excised human lungs. Am Rev Respir Dis 133: 132-135.

Pride NB. (1983) Which smokers develop airflow obstruction? Eur J Respir Dis Suppl 126 64: 79-83.

Ranga V, Kleinerman J. (1978) Structure and function of small airways in health and disease. Arch Pathol Lab Med 102: 609-617.

Rimpela AH, Rimpela MK. (1985) Increased risk of respiratory symptoms in young smokers of low tar cigaretts. Br Med J 290:1461-1463.

Rosenbleum JL, Mauceri RA,Wellenstein DE, Bassans DA, Cohen WN, Heitzman ER. (1978) Computed tomography of the lung. Radiology 129:521-524.

Rosenbleum JL, Mauceri RA, Wellenstein DE, Thomas FD, Bassans A,

Raasch BN, Chamberlain CC, Hertzman ER. (1980) Density pattersn in normal lung as determined by computed tomography. Radiology 137: 409-416.

Rosiwall (1898) A simple surface measurement to determine the quantitative content of the mineral constituents of a strong aggregate. Verhandlungen der KK Gedogischen Reichsanstalt Wien 5-6, 143.

Royal College of Physicians. (1971) Smoking and health now. A Report of the Royal College of Physicians. Pitman Medical and Scientific, London.

Royal College of Physicians. (1977) Smoking or health. The Third Report from the Royal College of Physicians of London. Pitman medical and Scientific, London.

Royal College of Physicians. (1983) Health or smoking. Follow-up Report of the Royal College of Physicians. Churchill Livingstone, Edinburgh.

Russel MAH. (1983) Smoking, nicotine addition and lung disease. Eur J Respir Dis, Suppl 126 64: 85-89.

Ryder RC, Thurlbeck WM, Gough J. (1969) A study of interobserver variation in the assessment of the amount of pulmonary emphysema in paper mounted whole lung sections. Am Rev Respir Dis 99: 354-364.

Saetta M, Skinner RJ, Angus E, Kim WD, Wang N, King M, Ghezzo H, Cosio MG. (1985) Destructive index: a measurement of lung

parenchyma destruction in smokers. Am Rev Respir Dis 131: 764-769.

Salmon RB, Saidel GM, Inkley S, Niewoehner DE. (1982) Relationship of ventilation inhomogeneity to morphologic variables in excised human lungs. Am Rev Respir Dis 126: 686-690.

Sasaki H, Okayana H, Aikawa T, Shimura S, Sezkawa K, Yanai M, Jakishima J. (1986) Central and peripheral airways as determinants of ventilatory function in patients with chronic bronchitis, emphysema and bronchial asthma. Am Rev Respir Dis 1341 1182-1189.

Schreider JP, Raabe OG. (1981) Structure of the human resiratory acinus. Am J Anat 162: 221-232.

Schroeder LD, Sjoquist DL, Stephen PE. (1986) Understanding regression, analysis. In: Quantitiative applications in the social sciences. Sage Publications Ltd, Beverly Hills, USA.

Siegel S. (1956) Non-parametric statistics for the behavioural sciences. McGraw-Hill, Kogakusha, Tokyo, Japan.

Silvers WG, Maisel JC, Petty TL, Mitchell RS, Filley GF. (1972) Central airway resistance in excised emphysematous lungs. Chest 61: 603-612.

Sims, B. (1974) A simple method of preparing 1-2um sections of large tissue blocks using glycol methacrylate. J Microscopy 101:223-227.

Snider GL. (1983) A perspective on emphysema. In: Clinics in Chest Medicine: Emphysema. WB Saunders, Philadelphia.

Sobonya RE, Burrows B. (1983) The epidemiology of emphysema. Clinics in Chest Medicine: Emphysema. WB Saunders, Philadelphia.

Sokal RR, Rohlf FJ. (1980) Biometry: the principles and practice of statistics in biological research. (1980) (2nd ed) WH Freeman & Co, San Francisco.

Spencer H. (1985) Pathology of the lung. 4th Edition. Pergammon Press, Exeter.

SPSS Inc. (1983) User's Guide SPSS. McGraw-Hill Book Co, New York.

Steinfeld JL. (1984) Smoking and health. West J Med 141: 878-883.

Stone PJ. (1983) The elastase-antielastase hypothesis of the pathogenesis of emphysema. In: Clinics in Chest Medicine: Emphysema. WB Saunders Co, Philadelphia.

Storey WF, Staub NC. (1962) Ventilation of terminal air units. J Appl Physiol 17: 391-397.

Sutinen S, Koistinen J, Paakbo P. (1985) A necropsy study of Pi phenotypes, emphysema and smoking. Acta Path Microbiol Immunol Scand 93: 183-188.

Tager IB, Munoz, A, Rosner B, Weiss, S, Caray V, Speizer FE. (1985) Effect of cigarette smoking on the pulmonary function of children and adolescents. Am Rev Respir Dis 131: 752-759.

Thurlbeck WM. (1962) The incidence of pulmonary emphysema. Am Rev Respir Dis 87: 206-215.

Thurlbeck WM. (1967a) Measurement of pulmonary emphysema. Am Rev Respir Dis 95: 752-764.

Thurlbeck WM. (1967b) The internal surface area of nonemphysematous lungs. Am Rev Respir Dis 95: 765-773.

Thurlbeck WM. (1967c) Internal surface area and other measurements in emphysema. Thorax 22: 483-496.

Thurlbeck WM. (1976) Chronic airflow obstruction in lung disease. In: Major problems in Pathology, Series No 5. Bennington JL (ed). WB Saunders & Co, Philadelphia.

Thurlbeck WM. (1983) Overview of the pathology of pulmonary emphysema in the human. In: Clinics in Chest Medicine: Emphysema. WB Saunders & Co, Philadelphia.

Thurlbeck WM, Dunnill MS, Hartung W, Heard B, Heppleston GA, Ryder RC. (1970a) A comparison of three methods of measuring emphysema. Hum Pathol 1: 215.

Thurlbeck WM, Haines JR. (1975) Bronchial dimensions and stature. Am Rev Respir Dis 112: 142-145.

Thurlbeck WM, Henderson JA, Fraser RG,, Bates DV. (1970b) Chronic obstructive lung disease. Medicine 49: 81-145.

Thurlbeck WM, Horowitz I, Siemiatycki J, Dunnill MS, Maisel JC, Pratt P, Ryder R. (1969) Intra- and inter-observer variations in the assessment of emphysema. Arch Environ Health 18: 646-659.

Thurlbeck WM, Ryder RC, Sternby N. (1974) A comparative study of

the severity of emphysema in necropsy populations in three different countries. Am Rev Respir Dis 109: 239-248.

Thurlbeck WM, Simon G. (1978) Radiographic appearance of the chest in emphysema. Am J Roentgenol 13: 429-440.

Tomkeieff SI. (1945) Linear intercepts, areas and volumes. Nature 155: 24.

Van Reek J. (1984) Smoking behaviour in the Netherlands and the United Kingdom 1958-1982. Rev Epidem et Sante Publ 32: 383-390.

Von Hayek H. (1960) The human lung. Hafner Publishing Co Inc, New York.

Walker JR, Keiffer JE. (1966) Ciliostatic compoents in the gas phase of cigarette smoke. Science 153: 1248-1250.

Wegener OH, Koeppe P, Oeser H. (1978) Measurement of lung density by computed tomography. J Comp Assist Tomog 2: 263-273.

Weibel ER. (1963) Morphometry of the human lung. Springer Verlag, Berlin.

Weibel ER. (1984) Morphometric and sterological methods in respiratory physiology including fixation techniques. In: Techniques in the Life Sciences. Physiology - Volume P4/1, Techniques in Respiratory Physiology - Part I. Otis AB (ed). pp401/1 - p401/35.

Weibel ER, Gomez MD. (1962) A principle for counting tissue structures on random sections. J Appl Physiol 17: 343-348.

Weibel ER, Kistler GS, Scherle WF. (1966) Practical sterological methods for morphometric cytology. J Cell Biol 30: 23-38.

Weibel ER, Vidone RA. (1961) Fixation of the lung by formalin steam in a controlled state of air inflation. Am Rev Resp Dis 84: 856-861.

Williams MA. (1977) Quantitative methods in biology. In: Practical Methods in Electron Microscopy. Glauert AM (ed). North Holland, Amsterdam, New York, Oxford.

Wilson HG. (1922) Terminals of human bronchiole. Amer J Anat 30: 267-287.

Wright BM, Slavin G, Kreel L, Callan K, Sandin B. (1974) Postmortem inflation and fixation of human lungs: a technique for pathological and radiological correlations. Thorax 29: 189-194.

Wright JL, Cosio M, Wiggs B, Hogg JC. (1985) A morphologic grading system for membranous and respiratory bronchioles. Arch Pathol Lab Med 109: 163-165.

Wright JL, Lawson LM, Pare PD, Biggs BJ, Kennedy S, Hogg JC. (1983) Morphology of peripheral airways in current smokers and ex-smokers. Am Rev Respir Dis 127: 454-477.

Wright JL, Wiggs BJ, Hogg JC. (1984) Airway disease in upper and lower lobes in lungs of patients with or without emphysema. Thorax 39: 282-285.

Zamel N, Hogg J, Gelb AF. (1976) Mechanisms of maximal expiratory

flow limitation in clinically unsuspected emphysema and obstruction of the peripheral airways. Am Rev Respir Dis 113: 337-345.

APPENDIX

A. Background data (age, sex etc)

B. Bronchiolar and bronchial data

C. Bronchiolar attachments, shape and density

D. AWUV data

E. CT scan data

F. CO transfer factor data

G. FEV and TLC data

H. Single breath nitrogen washout data

I. A proof for the APUA to AWUV transformation

J. Rational for theoretical lumen area equation

APPENDIX A: Background data on study population

CASE NO	AGE (yrs)	SEX	HEIGHT (metres)	WEIGHT (kilos)	BODY SURFACE AREA (m^2)	SPECIMEN
1	61	M	1.72	60.1	1.71	R upper lobe
2	56	M	1.73	74.5	1.88	R middle lobe
3	63	M	1.62	60.5	1.54	R upper lobe
4	63	M	1.77	61.0	1.76	R upper lobe
5	64	M	1.80	71.0	1.90	R lower lobe
6	51	F	1.48	47.5	1.39	L lower lobe
7	54	M	1.88	70.5	1.95	R lung
8	63	M	1.77	65.4	1.81	R upper lobe
9	62	F	1.59	49.1	1.48	L lower lobe
10	56	M	1.79	63.3	1.80	R upper lobe
11	53	F	1.62	51.0	1.53	R upper lobe
12	51	M	1.65	63.5	1.70	R lower lobe
13	53	M	1.75	82.9	1.99	R lower lobe
14	56	F	1.61	49.0	1.50	R lower lobe
15	56	M	1.68	66.1	1.75	L upper lobe
16	69	F	1.65	-	-	R upper lobe
17	58	M	1.73	61.9	1.74	R lower lobe
18	61	M	1.72	64.8	1.77	L upper lobe
19	62	M	1.80	59.4	1.76	L upper lobe
20	71	M	1.79	72.0	1.90	R upper lobe
21	63	M	1.78	88.8	2.07	L lower lobe
22	59	M	1.66	78.6	1.87	R lower lobe
23	57	M	1.65	60.4	1.66	L upper lobe
24	68	M	1,66	82.1	1.90	R lower lobe
25	66	M	1.71	93.6	2.05	L upper lobe
26	56	F	1.59	62.1	1.64	R upper lobe
27	70	M	1.67	59.0	1.66	R upper lobe
28	59	F	1.66	67.8	1.75	R upper lobe
29	65	M	1.76	81.4	1.98	R lung
30	48	M	1.71	71.6	1.83	L upper lobe
31	66	M	1.67	70.5	1.79	R upper lobe
32	46	F	1.53	45.1	1.39	R middle lobe
33	64	M	1.75	78.0	1.94	L upper lobe
34	54	F	1.57	57.5	1.57	L upper lobe
35	59	M	1.70	-	-	L upper lobe
36	63	M	1.68	83.5	1.93	L lower lobe
37	58	M	1.70	-	-	R upper lobe
38	59	F	1.62	68.5	1.73	R lung
39	74	M	1.76	75.2	1.91	L upper lobe
40	66	M	1.76	59.4	1.73	L upper lobe
41	69	M	1.70	55.1	1.63	R upper lobe
42	65	F	1.67	57.0	1.64	L lower lobe
43	71	F	1.70	53.0	1.61	R upper lobe
44	59	F	1.45	-	-	L lower lobe

APPENDIX B: Bronchus and bronchial morphometry data

CASE NO	MINIMUM DIAMETER (mm)	MEASURED LUMEN AREA (mm^2)	THEORETICAL LUMEN AREA (mm^2)	EPITHELIAL AREA (mm^2)	WALL AREA (mm^2)	SEGMENTED BRONCHUS AREA (mm^2)
1	.610	.473	1.358	.084	.403	14.80
2	.574	.429	.819	.064	.298	13.34
3	.572	.370	.521	.039	.211	9.71
4	.526	.525	1.343	.095	.612	17.53
5	.486	.266	.471	.045	.306	24.98
6	.653	.522	.614	.049	.165	12.14
7	.530	.340	.742	.070	.399	18.66
8	.552	.426	.872	.070	.250	14.19
9	.781	.875	1.376	.126	.655	17.38
10	.566	.422	.921	.057	.186	-
11	.457	.282	.471	.042	.251	7.50
12	.460	.273	.921	.083	.364	10.77
13	.525	.337	.542	.046	.185	20.98
14	.496	.262	.424	.049	.183	16.27
15	.480	.386	.831	.050	.295	14.68
16	.447	.264	.736	.043	.217	18.96
17	.600	.470	1.562	.110	.499	10.33
18	.561	.437	.830	.064	.236	14.28
19	.548	.528	1.251	.090	.367	20.33
20	.562	.542	1.234	.072	.286	10.06
21	.420	.221	.674	.057	.266	15.71
22	.585	.439	.649	.082	.291	7.70
23	.411	.215	.558	.032	.200	34.69
24	.517	.429	.576	.041	.196	9.36
25	.749	.729	1.042	.090	.501	27.02
26	.433	.238	.620	.052	.309	11.79
27	.496	.389	.887	.047	.200	20.44
28	.523	.354	.815	.075	.258	27.12
29	-	-	-	-	-	-
30	-	-	-	-	-	-
31	-	-	-	-	-	-
32	-	-	-	-	-	-
33	.724	.595	.715	.043	.352	21.25
34	-	-	-	-	-	-
35	-	-	-	-	-	-
36	-	-	-	-	-	-
37	-	-	-	-	-	-
38	-	-	-	-	-	-
39	-	-	-	-	-	-
40	.355	.185	.483	.049	.251	-
41	-	-	-	-	-	-
42	-	-	-	-	-	-
43	-	-	-	-	-	-
44	-	-	-	-	-	-

APPENDIX C: Peribronchiolar alveolar attachment and bronchiolar ellipticality and density data ·

THESNO	Attachments per airway	IAAD (um)	Ellipticality	Density (cm^{-2})
1	22.3	0.201	1.750	0.482
2	14.6	0.186	1.496	0.643
3	16.5	0.145	1.296	0.643
4	20.3	0.183	1.763	0.574
5	16.7	0.141	1.289	0.436
6	18.2	0.133	1.284	1.224
7	15.1	0.208	1.503	0.459
8	17.8	0.180	1.698	0.436
9	20.8	0.172	1.455	0.689
10	19.6	0.172	1.524	0.459
11	16.8	0.160	1.528	0.689
12	15.5	0.167	1.457	0.941
13	18.1	0.168	1.355	0.643
14	17.1	0.134	1.338	0.712
15	17.4	0.161	1.496	0.643
16	14.0	0.155	1.531	0.643
17	20.0	0.136	1.564	0.505
18	18.3	0.151	1.397	0.551
19	18.0	0.189	1.717	0.804
20	14.9	0.244	1.774	0.919
21	14.5	0.170	1.571	0.597
22	12.2	0.198	1.440	0.574
23	16.0	0.166	1.619	0.712
24	19.4	0.163	1.477	0.896
25	19.4	0.177	1.309	0.528
26	16.0	0.175	1.602	0.712
27	15.3	0.176	1.690	0.712
28	14.2	0.205	1.502	0.574
29	-	-	-	-
30	-	-	-	-
31	-	-	-	-
32	-	-	-	-
33	17.4	0.177	1.360	0.367
34	-	-	-	-
35	-	-	-	-
36	-	-	-	-
37	-	-	-	-
38	-	-	-	-
39	-	-	-	-
40	11.9	0.225	1.961	0.482
41	-	-	-	-
42	-	-	-	-
43	-	-	-	-
44	-	-	-	-

APPENDIX D: Mean and LF5 AWUV Data

THESNO	MEAN AWUV (mm^2/mm^3)	LFS AWUV (mm^2/mm^3)
1	16.891	9.192
2	16.012	12.890
3	17.273	13.939
4	14.360	7.230
5	20.718	16.385
6	25.402	20.769
7	19.083	12.968
8	10.153	4.110
9	14.569	10.794
10	23.039	15.838
11	8.779	3.846
12	21.183	17.370
13	24.738	21.261
14	20.521	17.395
15	15.872	9.727
16	22.578	18.718
17	18.701	8.412
18	16.606	13.817
19	14.416	6.554
20	15.770	8.996
21	16.578	12.098
22	19.472	16.206
23	21.970	18.100
24	20.403	16.208
25	20.772	15.933
26	15.498	11.829
27	17.728	13.042
28	19.519	13.069
29	20.590	9.832
30	16.782	12.839
31	17.943	14.094
32	17.944	12.919
33	16.636	13.285
34	16.675	14.950
35	18.765	14.013
36	19.568	15.984
37	19.204	14.751
38	21.996	13.784
39	18.037	12.352
40	14.294	2.013
41	14.870	1.876
42	17.749	14.885
43	17.910	11.284
44	17.323	9.022

APPENDIX E: CT Scan Data

THESNO	5TH PERCENTILE EM1 UNIT	MEDIAN EMI UNIT	MEDIAN TO LOWEST EMI UNIT
1	435	420	15
2	433	410	23
3	429	405	24
4	444	425	19
5	441	415	26
6	409	380	29
7	-	-	-
8	461	435	26
9	452	430	22
10	430	395	35
11	-	-	-
12	432	415	15
13	418	385	33
14	-	-	-
15	-	-	-
16	433	410	23
17	443	385	58
18	-	-	-
19	-	-	-
20	-	-	-
21	-	-	-
22	-	-	-
23	-	-	-
24	-	-	-
25	414	395	19
26	-	-	-
27	-	-	-
28	-	-	-
29	437	425	12
30	449	430	19
31	413	385	28
32	-	-	-
33	-	-	-
34	413	395	18
35	451	425	26
36	449	430	19
37	436	420	16
38	-	-	-
39	423	400	23
40	474	415	59
41	470	450	20
42	430	410	20
43	432	410	22
44	466	445	21

APPENDIX F: Carbon Monoxide Transfer Data (S.D. = Standard Deviation which is rounded to the nearest whole number)

THESNO	TCO	S.D. OF TCO	KCO	S.D. OF KCO
1	4.76	2	0.77	1
2	8.27	0	1.22	0
3	6.59	0	1.26	0
4	-	-	-	-
5	8.70	0	1.33	0
6	-	1	-	0
7	6.48	2	1.09	1
8	-	-	-	-
9	-	-	-	-
10	7.97	1	-	-
11	-	-	-	-
12	7.75	0	1.58	0
13	9.55	0	1.57	0
14	-	-	-	-
15	9.12	0	1.42	0
16	7.39	0	1.62	0
17	5.50	2	0.86	2
18	7.10	0	1.08	1
19	4.02	3	0.68	2
20	3.62	2	0.64	2
21	6.23	1	0.97	1
22	6.51	0	1.52	0
23	10.40	0	1.71	0
24	9.43	0	1.88	0
25	8.87	0	1.87	0
26	5.59	1	1.59	0
27	5.73	1	1.05	0
28	5.88	1	1.21	2
29	-	-	-	-
30	-	-	-	-
31	4.82	1	1.32	0
32	5.68	1	1.42	1
33	9.68	0	1.61	0
34	5.64	1	1.46	1
35	7.75	0	1.30	0
36	9.53	0	1.72	0
37	6.85	0	1.24	0
38	-	-	-	-
39	7.63	0	1.30	0
40	2.72	3	0.41	3
41	3.06	2	0.54	2
42	4.54	1	1.44	0
43	-	-	-	-
44	3.34	2	.87	3

APPENDIX G: Forced Expiratory Volume in One Second and Total Lung Capacity Data

THESNO	$FEV_{1.0}$ ABSOLUTE (litres)	$FEV_{1.0}$ % PREDICTED	TLC ABSOLUTE (litres)	TLC % PREDICTED
1	2.55	85	7.41	115
2	3.55	111	7.13	109
3	2.15	83	7.28	130
4	1.90	59	9.37	135
5	3.05	92	10.77	151
6	1.85	97	4.04	112
7	2.65	70	6.64	86
8	2.10	66	9.48	137
9	1.75	88	6.16	143
10	3.25	88	6.83	97
11	1.40	74	-	-
12	2.10	68	7.93	136
13	2.55	75	8.01	119
14	1.80	82	-	-
15	2.90	94	7.89	129
16	2.10	116	4.93	114
17	3.45	108	8.26	127
18	3.75	121	8.43	131
19	2.10	62	10.31	145
20	1.40	47	8.86	128
21	1.65	52	11.50	166
22	1.35	47	8.02	136
23	3.20	110	7.87	135
24	2.05	79	5.54	93
25	2.15	74	6.96	110
26	1.40	67	4.77	108
27	2.55	98	7.35	122
28	1.55	67	7.29	148
29	2.65	83	8.94	131
30	1.75	52	8.53	133
31	1.95	72	4.88	81
32	2.00	90	5.62	134
33	2.70	87	8.57	128
34	1.65	79	4.97	116
35	2.45	84	8.05	132
36	1.50	54	9.08	149
37	2.60	90	6.80	110
38	1.70	81	5.40	117
39	3.10	107	7.39	109
40	1.65	53	10.09	148
41	2.65	98	7.01	113
42	1.65	72	4.80	94
43	2.45	123	-	-
44	1.00	53	5.21	149

APPENDIX H: Single Breath Nitrogen Washout Test Data

CASE NO	CLOSING VOLUME (litres)	CLOSING VOLUME VITAL CAPACITY (%)	SLOPE OF PHASE III
1	1.53	39	2.95
2	-	-	-
3	-	-	-
4	1.19	27	-
5	0.77	16	2.26
6	-	-	-
7	-	-	-
8	1.85	36	2.21
9	0.95	24	-
10	-	-	-
11	-	-	-
12	0.80	20	3.82
13	0.83	20	1.71
14	-	-	-
15	0.91	22	3.38
16	0.98	29	0.38
17	1.11	26	1.41
18	1.47	26	0.84
19	0.83	22	4.65
20	1.95	48	4.41
21	-	-	-
22	0.83	30	4.82
23	0.83	17	1.43
24	0.51	17	3.04
25	.64	16	4.83
26	.37	22	5.33
27	1.14	26	4.93
28	0.83	26	5.08
29	0.43	10	-
30	0.64	21	6.40
31	-	-	-
32	-	-	-
33	0.19	5	1.83
34	0.70	25	2.68
35	0.51	13	3.14
36	0.53	12	3.98
37	0.73	20	3.96
38	-	-	-
39	1.27	27	0.40
40	-	-	-
41	1.29	28	3.48
42	0.65	25	4.92
43	-	-	-
44	-	-	-

APPENDIX I

Proof that contour length relates to surface density(s) as given by:

A1 $S = \frac{4}{\pi} m$ (Equation 2.7, Williams, 1981)

where m is the contour length per unit area, e.g. mm/mm2.

The relationship between surface density and mean linear intercept determined by Campbell and Tomkeieff (1952) and Hennig (1956) is

A2 $S = \frac{2V}{\bar{L}_3}$ (Equation 5.1, Aherne and Dunnill, 1982)

where V = volume and L_3 is the mean linear intercept which is given by:

A3 $\bar{L}_3 = \frac{nL}{I}$ (Equation 5.2, Aherne and Dunnill, 1982)

where nL is the total length of test line and I, the number of intersections

A4 $S = \frac{2V}{nL} I$

Aherne also shows the relationship between measured perimeter and number of intercepts to be:

A5 $L = \frac{d}{2} \bar{N}int$ (Equation 13.5, Aherne and Dunhill, 1982)

where d is distance between test lines and $\bar{N}int$ is the mean number of intercepts and is equivalent to I in equation **A4**

A5 re-expressed gives:

A6 $I = \frac{2L}{d\pi}$ which substituted in **A4** gives

A7 $S = \frac{2V}{nL} \times \frac{21}{d} = \sqrt{\frac{4}{\pi}} \times \frac{L}{nLd}$

Diagrammatically L, the length of the test line and d, the distance between test lines are related.

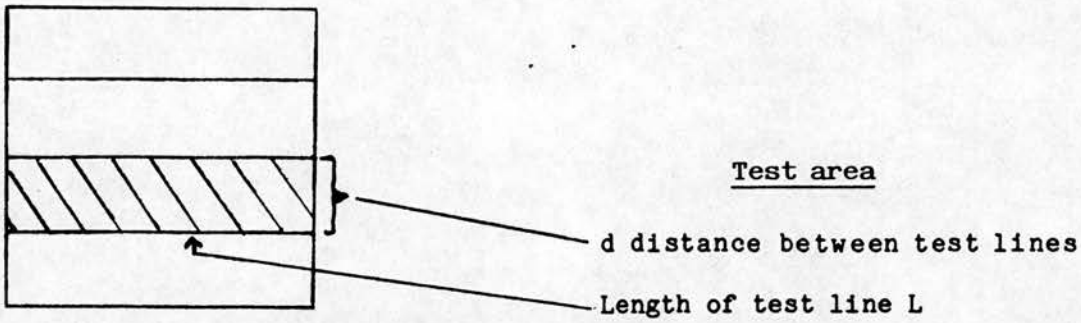

L times d obviously gives the area enclosed by these two parameters and therefore ΣLd or nLd, the number of test lines gives the total test area. Equation A7 then becomes:

$$A8 \qquad S = V \frac{4L}{a}$$

where $\frac{L}{a}$ gives the contour length per unit area, i.e. m. Hence:

$$A9 \qquad S = V \frac{4}{\pi} m$$

Removal of V gives equation A1, i.e. the surface density expressed as surface area per unit volume.

APPENDIX J: Rational for theoretical lumen area equation

The area A of a circle is commonly given as:

$$A = \pi r^2 \qquad \textbf{A10}$$

while the circumference (C) is:

$$C = 2\pi r \qquad \textbf{A11}$$

Knowing only the circumference we wish to calculate the spherical area. To do this we first solve for r in equation **A11**:

$$r = \frac{C}{2\pi} \qquad \textbf{A12}$$

Substituting for r in **A10** using **A12** gives:

$$A = \pi \left(\frac{C}{2\pi} \right)^2 \qquad \textbf{A13}$$

This in its simplest form becomes

$$A = \frac{C^2}{4\pi}$$

Thus one can calculate spherical lumen area (A) having measured the internal circumference. This parameter has been termed theoretical lumen area in this thesis.